The Effect of Blue Light on Unicellular Organisms at Transcriptome Level

by

Mehmet Tardu

A Dissertation Submitted to the
Graduate School of Sciences and Engineering
in Partial Fulfillment of the Requirements for
the Degree of

Doctor of Philosophy

in

Computational Science and Engineering

September 7, 2016

The Effect of Blue Light on Unicellular Organisms at Transcriptome Level

Koç University

Graduate School of Sciences and Engineering

This is to certify that I have examined this copy of a doctoral dissertation by

Mehmet Tardu

and have found that it is complete and satisfactory in all respects,
and that any and all revisions required by the final
examining committee have been made.

Committee Members:

_____

Prof. İ. Halil Kavaklı

_____

Prof. Attila Gürsoy

_____

Asst. Prof. Funda Şar

_____

Prof. Gül Cevahir Öz

_____

Prof. Mahmut Çalışkan

Date: _____

I dedicated this thesis to my family and my beloved wife, Merve, for their constant support and unconditional love.

ABSTRACT

The ability of light perception is crucial for the survival of most organisms that enables them to adjust their physiology and metabolism to the changing environmental conditions. Light, in contrast, is also a threat to any living organism owing to the deleterious effects it can have on nucleic acids, lipids and proteins. Therefore, the capacity to sense and respond to light is widespread among prokaryotes and eukaryotes to survive and adapt themselves as a result of selective pressure of the solar irradiation. This dissertation concentrates on the analysis of light regulated pathways in unicellular organisms, *Vibrio cholerae* and *Cyanidioschyzon merolae*, via transcriptome profiling.

C. merolae is one of the most primitive of photosynthetic eukaryotes. Since it is an extremophile, it is conceivable to study the effect of light on this organism to see how it adapts itself to different environmental conditions and to establish an evolutionary conserved global light response between algae and land plants. Therefore, we decided to investigate the direct effect of red and blue lights at the transcriptional level as well as to verify known blue light receptor genes and the involved transduction pathway using next generation RNA-sequencing approach. Our results indicated that transcriptional regulations of 35 % of the total genes, including the genes encodes 46 % of transcription factors, were regulated by blue and red lights in *C. merolae*. Unexpectedly, although there are yet no identified red light photoreceptors, 22 % of the total genes (1116) were regulated by the red light; 521 genes were solely red-light responsive. Transcriptional modulation due to light exposure does not arise from photo-oxidative stress. Blue light dependent regulation of three cryptochromes (*CmPHR2, CmPHR3* and *CmPHR7*) implies a potential role in light-dependent transcriptional regulation in *C. merolae*. In spite of absences of any red light photoreceptors, a great impact of the red light on

the biological processes suggests the importance of the retrograde signaling in this organism.

Secondly, we investigated the effect of the BL in a non-phototrophic bacteria *Vibrio cholerae* by using genetics and transcriptome profiling. Genome-wide analysis revealed that the transcription of 6.3% of the genes were regulated by BL in *V. cholerae*. To understand signaling mechanisms, we generated several knockout cell lines and subjected to genome-wide analysis under BL conditions. Studies with a double mutant confirm an anti-sigma factor (ChrR) and a novel putative metalloregulatory-like protein (MerR) are responsible for the genome-wide regulation to BL response in *V. cholerae*. We further showed that BL enhances ROS production, possibly generated through the oxidative phosphorylation pathway. These results demonstrate that *V. cholerae* responds to BL with a novel mechanism to produce an appropriate response against photo-oxidative stress. This response regulates the transcription of genes involved in cellular protection, DNA repair, and carbon metabolism. Outside its host, *V. cholerae* can survive for extended periods in natural aquatic environments. Therefore, the regulation of light response for *V. cholerae* is a critical cellular process for its survival. Collectively, all these data reveal that light is important not only for phototrophs but also non-phototrophs to regulate their metabolical and related physiological pathways through elegant and complex signaling cascades.

ÖZETÇE

Canlılar, çevrelerindeki ışığı algılayarak metabolizmalarını ve fizyolojilerini bulundukları ortama uyum sağlayacak şekilde optimize ederler. Bununla beraber, ışık bütün canlılarda bulunan nükleik asitler, lipidler ve proteinler üzerinde zararlı etkilere de sebep olabilir. Güneş ışınlarının bu etkileri nedeniyle prokaryot ve ökaryot hücrelerde hayatta kalma stratejisi olarak ve metabolizmalarını adapta etmek amacıyla ışığı algılama ve tepki kapasitesi çok yaygınlaşmıştır. Bu tez çalışmasında, RNA dizileme yöntemi kullanılarak tek hücreli canlılarda (*Vibrio cholerae* ve *Cyanidioschyzon merolae*) ışığın etkilediği yolaklar hesapsal yöntemler yardımıyla belirlenmiştir.

C. merolae en ilkel fotosentetik ökaryotlardan biridir. Hem bir ekstremofil olması hem yosunlar ve kara bitkileri arasındaki evrimsel geçiş açısından önemli olması nedeniyle, ışığın değişen çevre koşullarında canlılık üzerindeki etkisini araştırmak için iyi bir model organizma olarak düşünülmektedir. Bu yüzden, biz bu canlıda kırmızı ve mavi ışık etkisini RNA dizileme yöntemini kullanarak inceledik. Sonuç olarak, bu canlının sahip olduğu 5103 genin % 35'i ve 155 transkripsiyon faktörün % 46'sının mavi ve kırmızı ışık tarafından düzenlendiği bulunmuştur. Bu canlıda herhangi bir kırmızı ışık fotoreseptörü bulunmamasına rağmen, kırmızı ışığın toplam genlerin % 22'sini düzenlemesi beklenmedik bir sonuç olarak not düşülmüştür. Işığın canlılar üzerindeki etkilerinden birinin de foto-oksidatif stres olduğu bilinmektedir. Yapılan analizler sonucunda *C. merolae* hücrelerinin gen transkripsiyonu düzeyinde verdiği ışık tepkisinin foto-oksidatif stres kaynaklı olmadığı tespit edilmiştir. Mavi ışık tarafından gen transkripsiyonu düzenlenen 3 kriptokrom geninin ise (*CmPHR2, CmPHR3* ve *CmPHR7*), mavi ışığa bağlı bazı genlerin transkripsiyonunu düzenlediğini tahmin etmekteyiz. Ayrıca kırmızı ışık etkisindeki gen transkripsiyonlarındaki değişimin

retrograd sinyal iletim mekanizmaları ile alakalı olabileceğine dair güçlü bir kanıt olarak düşünülebilir.

İkinci çalışma olarak, gen nakavt ve RNA dizileme yöntemlerini kullanarak fototrof olmayan bir bakteri olan *V. cholerae*'da ışığın gen transkripsiyonu üzerine etkisini araştırdık. Genom düzeyinde yapılan analizlerde genlerin % 6,3'ünün (222 gen) transkripsiyonunun mavi ışık tarafından düzenlendiği ortaya çıkmıştır. Bulunan bir diğer sonuç ise, bu düzenlemenin foto-oksidatif stres sonucu üretilen reaktif oksijen türevleri tarafından olduğu tespit edilmiştir. Elde edilen nakavt hücre hatları sayesinde 222 genin transkripsiyonunu düzenleyen mekanizma tam olarak ortaya çıkarılmıştır. Buna göre, anti-sigma faktörü olan ChrR (VC2301) ve metalo-regülatör proteini olan MerR'in (VCA0056), hücresel koruma, DNA onarımı ve karbon metabolizmasında rol oynayan genlerin transkripsiyonunu düzenlediği bulunmuştur. Konak hücresi dışında doğal su ortamında uzun süreler ışığa maruz kalarak yaşayabilen bu canlının hayatta kalabilme stratejisi olarak gen düzeyinde böyle bir düzenlemeyi yaptığı düşünülmektedir.

ACKNOWLEDGMENTS

Firstly, I would like to express my sincere gratitude to my advisor Prof. İ. Halil Kavaklı for the continuous support of my PhD study and related research, for his patience, motivation, and immense knowledge whilst allowing me the room to work in my own way. I would like to thank him for encouraging my research and for allowing me to grow as a research scientist. His guidance helped me in all the time of research and writing of this thesis. One simply could not wish for a better or friendlier supervisor.

I also have to thank the members of my PhD committee, Professors Attila Gürsoy and Funda Şar for their helpful scientific advice and suggestions about my PhD study. I thank all the previous and present members of the Kavaklı lab group for the stimulating discussions, and for all the fun we have had in the last six years. I would also like to thank my friend Fatih Rahim, who supported me in writing, and incented me to strive towards my goal. I also thank to Dr. İbrahim Barış, Dr. Cihan Aydın, Şeref Gül, Ehsan Sarayloo, Derya Kabacaoğlu, Haşimcan Öner, Derya Yarparvar, Selma Bulut, Sibel Çal, Berke Gürkan, Eylem Külköylüoğlu, Çağlar Berkel, Bengisu Seferoğlu, Hande Asımgil, Dila Atak and Uğur Meriç Dikbaş. I thank to TUBITAK (TBAG-110T938 and TBAG-105T417) for funding this study.

A special thanks to my family. Words cannot express how grateful I am to my brothers, my sisters, my mother, and father for all of the sacrifices that you've made on my behalf. At the end, I would like express appreciation to my beloved wife, Merve, for her support, encouragement and quiet patience. Her tolerance of my occasional vulgar moods is a testament in itself of her unyielding devotion and love.

TABLE OF CONTENTS

List of Tables **xiii**

List of Figures **xv**

Nomenclature **xxiv**

Chapter 1: Introduction **1**

Chapter 2: Literature Review **3**

2.1 Blue light photoreceptors 5

2.1.1 Cryptochrome/photolyase family members 6

2.1.2 Phototropins and LOV domains 18

2.1.3 BLUF proteins 21

2.1.4 Blue light induced photo-oxidative stress 23

2.2 Red light photoreceptors 24

2.2.1 Phytochromes 24

2.3 Other photoreceptor families 28

2.3.1 UV-B photoreceptor 28

2.3.2 Rhodopsins 30

Chapter 3: Genome-wide response of *Vibrio cholerae* to blue light via two different signaling mechanisms **33**

3.1 Background 33

3.2 Materials and Methods 36

3.2.1 Growth conditions and light experiments 36

3.2.2 Assessment of photo-oxidative stress 36
3.2.3 Construction of *V. cholerae* deletion mutants 38
3.2.4 Preparation of cDNA library for RNA-seq 40
3.2.5 Transcriptome analysis 42
3.2.6 GO term and KEGG pathway enrichment analyses 43
3.2.7 Hierarchical clustering and heatmap generation 43
3.2.8 Validation of RNA-seq results using qRT-PCR 43
3.3 Results and Discussion 45
3.3.1 Mapping and coverage of RNA-seq data 46
3.3.2 Validation of DEGs identified in RNA-seq using qRT-PCR . . 48
3.3.3 Blue light regulated pathways as determined by GO term and KEGG pathway enrichment analyses 50
3.3.4 Cryptochrome -DASHes of *V. cholerae* are not blue light photoreceptors 54
3.3.5 Blue light induces genome-wide transcriptional modulation due to photo-oxidative stress 55
3.3.6 ChrR and SigmaE regulate gene expression in a blue light-dependent manner 57
3.3.7 Blind phenotype of $\Delta ChrR\Delta MerR$ double-knockout mutant in BL response 61
3.3.8 Blue light prompts *V. cholerae* to produce ROS by oxidative phosphorylation 63

Chapter 4: RNA-Seq analysis of the transcriptional response to blue and red light in the extremophilic red alga, *Cyanidioschyzon merolae* 68

4.1 Background 68
4.2 Materials and Methods 70

4.2.1 Growth conditions and light experiments 70
4.2.2 Assessment of photo-oxidative stress 71
4.2.3 Preparation of the cDNA Library for RNA-Seq 71
4.2.4 Transcriptome analysis 72
4.2.5 GO term and KEGG enrichment analysis 73
4.2.6 Validation of RNA-seq results using qRT-PCR 74
4.3 Results and Discussion 76
4.3.1 Mapping and coverage of RNA-seq data 76
4.3.2 Identification of novel transcripts and differentially expressed genes 79
4.3.3 GO classification and KEGG pathway enrichment analyses reveal the metabolic pathways regulated by blue light and red light . 83
4.3.4 Blue and red light exposure significantly alters the transcription of genes in carbon metabolism, amino acid biosynthesis and pigment biosynthesis 88
4.3.5 Blue light- and red light-elicited expression of transcription factor genes 90
4.3.6 BL and RL up-regulate translation via regulation of tRNA biosynthesis pathway and ribosome biogenesis pathway, respectively 92
4.3.7 Photolyase gene transcription is enhanced by BL or RL 95
4.3.8 Effect of BL on the transcription of the cryptochrome genes . 95
4.3.9 Transcriptional modulation due to BL exposure does not arise from oxidative stress 96

Chapter 5: Conclusion **99**

Bibliography **104**

Appendix A: Appendix **142**

LIST OF TABLES

3.1 Primer sequences used in construction of *V. cholerae* deletion mutants. 38
3.2 Primer sequences used in qRT-PCR. 45
3.3 Bacterial strains and plasmids used in this study. 47
3.4 Mapping results of RNA-seq reads to *V. cholerae* genome. 47
3.5 Significantly up-(UR) and down-regulated (DR) KEGG pathways in wild-type cells under BL ($p<0.05$). 53
3.6 Significantly up- and down-regulated KEGG pathways in $\Delta ChrR$ mutants under blue light ($p<0.05$). 61

4.1 qRT-PCR oligonucleotide primer sequences. 75
4.2 Mapping of RNA-seq reads to the *C. merolae* 10D genome. 77
4.3 Percentage of mapped reads to the regions on the *C. merolae* 10D genome. 80
4.4 Significantly up-regulated (UR) and down-regulated (DR) KEGG pathways specific to only BL ($p<0.05$). 86
4.5 Significantly up-regulated (UR) and down-regulated (DR) KEGG pathways specific to RL ($p<0.05$). 87
4.6 Significantly up-regulated (UR) and down-regulated (DR) KEGG pathways under BRL ($p<0.05$). 88
4.7 Differentially regulated genes encoding proteins involved in tRNA biosynthesis pathway (KEGG id: cme00970) under BL. 93
4.8 Differentially regulated genes encoding proteins involved in ribosome biosynthesis pathway (KEGG id: cme03010) under RL. 94

A.1 Expression values of 222 Statistically significant DEGs at dark and blue light conditions in wild type and mutant *V. cholerae* cells. 143
A.2 Annotation of the hypthetical genes in *V. cholerae* using Annocript pipeline (E-value < 105) 150
A.3 Identification of the putative SigmaE-dependent promoter motif in the upstream region of genes controlled by SigmaE 151
A.4 Annotation of the hypthetical genes in *C. merolae* using Annocript pipeline (E-value < 105) 154
A.5 List of differentially expressed genes under blue light in *C. merolae* (q-value < 0.01 and the absolute value of $|\log_2$ fold change$| \geq 1$). . . 155
A.6 List of differentially expressed genes under red light in *C. merolae* (q-value < 0.01 and the absolute value of $|\log_2$ fold change$| \geq 1$). . . 194

LIST OF FIGURES

2.1 The spectral sensitivity of sensory photoreceptors ranges from the UV to the near-infrared region of the electromagnetic spectrum (280-750 nm). The figure is adapted from [Ziegler and Möglich, 2015, Tilbrook et al., 2013]. 4

2.2 Biological photoreceptors as light-activated switches. The figure is adapted from [Kennis and Mathes, 2013] 4

2.3 Phylogenetic tree of the cryptochrome/photolyase family (CPF). The unrooted phylogenetic tree of the CPF members was inferred using the neighbor joining method. The optimal tree with the sum of branch length=10.04 is shown. Bootstraps of 1000 replicates are expressed in percentage. The figure is adapted from [Öztürk et al., 2008]. 7

2.4 Repair mechanism of photolyases. First folate absorbs a photon in blue light wavelength and then transfers the energy to flavin. Finally, the excited electron breaks the cyclobutane ring and comes back to flavin. The figure is adapted from [Sancar, 2003]. 9

2.5 Schematic representation of the cryptochrome/photolyase family (CPF) proteins. Depending on the type of CPF, the length of proteins ranges from 500 to 700 amino acids. All CPF members contain an N-terminal α/β domain and an α-helical domain where FAD is associated. In addition, most CRYs have C-terminal extensions ranging in size from 50 to 250 amino acids. The figure is adapted from [Hoang et al., 2008]. 10

2.6 The roles of insect Type I and Type II cryptochromes (CRYs) in circadian oscillatory mechanisms of Drosophila and monarch butterfly, *Danaus plexippus*. Type I CRYs (DmCRY and DpCRY1) in both organisms act as a circadian photoreceptors. However, Type II CRY (DpCRY2) only involves in the light-independent regulation of circadian clock. The figure is adapted from [Chaves et al., 2011]. 14

2.7 Schematic outline of the molecular mechanism that contributes to the generation of circadian rhythms. CLOCK and BMAL1 make a heterodimer which bind to the E-boxes (CACGTG) in the promoters of the Per and Cry genes, as well as in the promoters of the other clock-controlled genes. The Cry and Per proteins dimerize and, after a time lag, enter to the nucleus and inhibit CLOCK-BMAL1-activated transcription of their own genes as well as of those of clock-controlled genes, thus generating an oscillatory pattern of gene expression. A second feedback loop is formed by the action of RORα and REV-ERBα proteins on BMAL1 transcription; these nuclear receptors activate (RORα) and repress (REV-ERBα) transcription through their competitive action on response elements (ROREs) on the BMAL1 promoter. The figure is adapted from [Golombek et al., 2014, Hirano et al., 2013]. 16

2.8 Phototropin structure and function. **(A)** Diagram illustrating the range of phototropin-induced responses in higher plants. Phot1 and phot2 are activated by blue light and overlap in function to mediate several responses. **(B)** Protein structures of phototropin photoreceptors. Domain structure of these proteins along with their respective chromophores are indicated. The figure is adapted from [Christie, 2007]. 19

2.9 LOV-domain structure and photochemistry. **(A)** FMN chromophore structure within the LOV domain under dark and light conditions. **(B)** Mechanism of LOV-domain photochemistry after blue light exposure. The figure is adapted from [Christie, 2007]. 20
2.10 **(A)** BLUF domain of Slr1694 in dark- and light-adapted states illustrating the modulation of the protein in response to light condition. **(B)** The visible absorbance spectrum changes shifts by about 10-15 nm to the red upon illumination. The figure is adapted from [Kennis and Mathes, 2013]. 22
2.11 Functioning of Phytochrome (PHY) system. PHY acts as a molecular switch in response to red (RL) and far-red light (FRL). It occurs in two reversible conformations. The biologically-inactive form of PHY (Pr) is converted to the biologically active form Pfr under illumination with RL (660 nm). FRL (730 nm) and darkness convert the molecule back to the inactive form. 25
2.12 **(A)** Domain structures of phytochrome (PHY) photoreceptors in prokaryotes and plants. **(B)** The model showing PHY action in the transcriptional response control in plants. PHYs directly associate with downstream gene promoters by interaction with various sets of phytochrome-interacting factors (PIFs), transcription factors (TF) and coregulators (C), thus facilitating differential regulation of plant growth, development, and stress responses, which in total represent an integrated response to light. The figure is adapted from [Hughes, 2013, Wang and Wang, 2015]. 26
2.13 Schematic illustration of UV-B perception, signaling and responses in *Arabidopsis*. The figure is adapted from [Tilbrook et al., 2013]. 30
2.14 Action mechanism of rhodopsins. The figure is adapted from [Möglich et al., 2010]. 32

3.1 Flow-chart of ROS measurement protocol. 37
3.2 Flow-chart of RNA-seq analysis. 41
3.3 Comparison of gene transcript levels between replicates of dark- and blue-light-treated samples. Correlation plot for transcript-level RPKM values between replicates of wild-type cells treated with dark or BL. Pearson R^2 values for correlation are included as an insert in plot. . . 48
3.4 Validation of RNA-seq data by qRT-PCR. RNA-seq results of selected 21 DEGs (Set 2) were compared with qRT-PCR results. Blue bars with standard errors represent relative transcript levels ($\log_2$ fold) determined by qRT-PCR from three independent biological replicates. Green bars represent transcript levels determined using RNA-seq. 49
3.5 Effect of blue light (BL) and red light (RL) on expression levels of differentially expressed genes (DEGs). Transcript levels of selected 21 DEGs (Set 2) were determined after exposure of wild-type cells to BL and RL. Blue (BL exposure) and red (RL exposure) bars with standard errors represent relative mRNA expression levels ($\log_2$ fold) determined by qRT-PCR from three independent biological replicates. n = 6, $\star$ p < 0.05, Student's t-test. 50
3.6 Gene Ontology (GO) term network analysis of all differentially expressed genes (Set1 DEGs). Functional enrichment analysis was performed for all DEGs with the BINGO plug-in in Cytoscape. Assigned GO terms were used to classify functions of DEGs based on **(A)** biological processes, **(B)** molecular functions, and **(C)** cellular components. Overrepresented categories were determined using a hypergeometric test with a significance threshold $p<0.05$ after Benjamini and Hochberg false discovery rate corrections 52

3.7 Heatmap display of expression values of differentially expressed genes in wild-type and $\Delta cry1\Delta cry2\Delta phr$ knockout (TKO) cells. Expression levels are represented by color: green, lowest expression level; yellow, moderate expression level; red, highest expression level. Extreme values in color gradient are 3 to 12 in $\log_2$ scale. 55

3.8 Time-dependent reactive oxygen species (ROS) accumulation after blue light (BL) exposure. Cells were exposed to BL (50 μmoles $m^{-2}s^{-1}$) for 45 min. Samples were taken at 7, 25, 45, and 60 min after BL exposure and total ROS amount were measured using 2',7'-dichlorofluorescin diacetate (DCF-DA). Fold change was calculated between dark- and BL-treated samples at indicated times. 56

3.9 Heatmap display of expression values of differentially expressed genes in in wild-type, $\Delta ChrR$, and $\Delta ChrR\Delta MerR$ knockout (DKO) cells under dark and blue-light conditions. Expression levels are represented by color: green, lowest expression level; yellow, moderate expression level; red, highest expression level. Extreme values in color gradient are 3 to 12 in $\log_2$ scale. 58

3.10 Effect of blue light (BL) on wild-type, Δ*ChrR*, and Δ*SigmaE* cells. **(A)** Transcript levels of selected 21 DEGs were determined after exposing cells to BL. Blue bars (fold change in wild-type cells), green bars (fold change in Δ*ChrR* mutant) and red bars (fold change in Δ*SigmaE* mutant) with standard errors represent relative mRNA expression levels ($\log_2$ fold) determined by qRT-PCR from three independent biological replicates. n = 6, $\star$ p < 0.05, Student's t-test. **(B)** Putative σ^E- dependent promoter motif identified in upstream region of genes controlled by σ^E. Sequence of σ^E- binding motif (TGATC-N16-18-CGTAW, where W is A or T) derived from upstream of *SigmaE* (VC2302) was used to search upstream regions (-300 to +5 relative to predicted translation start site, +1) of all putative σ^E- dependent genes, allowing for two substitutions. Co-ordinate represents the position of 3'-end nucleotide of putative σ^E-binding motif relative to translation start site (+1). . . 60

3.11 Reactive oxygen species (ROS) accumulation in wild-type and mutant cells after blue light (BL) exposure. Cells were exposed to BL (50 μmoles $m^{-2}s^{-1}$) for 45 min, then samples were collected 45 min later and total ROS amount was measured using 2',7' dichlorofluorescein. Fold change was calculated between dark- and BL-treated samples at indicated times. 63

3.12 Reactive oxygen species (ROS) accumulation under blue light (BL) after chemical treatments and expression analysis of 2,4-dinitrophenol (DNP)-treated wild-type cells. **(A)** Samples were treated with 20 mM malonate (M), 100 μM rotenone (R), or 500 μM DNP for 60 min in darkness, then cells were exposed to BL (50 μmoles $m^{-2}s^{-1}$) for 45 min. Fold change was calculated between dark- and BL- treated samples, and then percentage change for each treatment was calculated after setting amount of ROS in wild-type cells at 100%. Error bar: ±SD, n=6, $\star$ p < 0.05, Student's t-test. **(B)** Transcript levels of selected DEGs were quantified by qRT-PCR after wild-type cells were treated with DNP. Blue (non-treated wild-type cells) and red (DNP-treated wild-type cells) bars with standard errors represent relative mRNA levels ($\log_2$ fold) determined by qRT-PCR from three independent biological replicates. Error bar: ±SD, n=6, $\star$ p < 0.05, Student's t-test. 65

3.13 Model summarizing blue-light-mediated gene regulation pathway in *V. cholerae*. Blue light (BL) excites succinate dehydrogenase (complex II) in electron transport chain, which interacts with molecular oxygen to generate ROS. ROS inactivates ChrR, the anti-σ^E factor. Dissociated σ^E associates with core RNAP, and corresponding RNAP holoenzyme activates Pσ^E, promoter of the regulatory ChrR-σ^E operon. σ^E regulates expression levels of 159 genes. Also, ROS interacts with MerR, which initiates a second cascade in BL-mediated gene regulation pathway. MerR suppresses or enhances expression levels of 63 genes includes its own gene. Ovals depict protein factors, short arrows show genes or operons, solid arrows and blunt-ended lines indicate positive and negative regulation, respectively. 67

4.1 Comparison of gene transcript levels between replicates of dark-, blue-light- and red-light-treated samples. Correlation plot for transcript-level FPKM values between replicates of cells treated with dark, blue light and red light. Pearson R^2 values for correlation are included as an insert in plot. 78

4.2 Visualization of aligned reads and coverage plot on chromosome 1 of *C. merolae* cells treated with dark and blue light. Aligned reads are uniformly mapped to gene loci of chromosome 1 (102 total gene loci). 79

4.3 Numbers of differentially expressed genes (DEGs) under blue and red light conditions. **(A)** A Venn diagram was generated to identify blue light (BL) and red light (RL) specific DEGs, and common DEGs within BL or RL treated cells. **(B)** There are 445 DEGs up-regulated and 238 DEGs down-regulated only specific to BL. BLR up-regulates 285 DEGs and down-regulates 236 DEGs. There are 116 DEGs up-regulated and 479 DEGs down-regulated only specific to RL. 81

4.4 RNA-seq results of selected 36 DEGs were validated with qRT-PCR results with three independent biological replicates (Error bar: ±SD, n=6, $\star$ $p < 0.05$, Student's t-test). Y axis indicates transcript abundance changes ($\log_2$ fold) and x axis represents gene IDs. **(A)** DEGs belong to only blue light (BL) condition. **(B)** DEGs belong to either blue or red light condition. **(C)** DEGs belong to red light (RL) condition. . . 82

4.5 Gene Ontology (GO) term network analysis of all differentially expressed genes (DEGs) under light conditions. Functional enrichment analysis was performed for all DEGs with the BINGO plug-in in Cytoscape. Assigned GO terms were used to classify functions of DEGs based on biological processes, **(A)** Represents the only blue light affected biological processes. **(B)** Represents the only red light affected biological processes. **(C)** Represents commonly regulated biological processes both by BL and RL. Overrepresented categories were determined using a hypergeometric test with a significance threshold $p<0.05$ after Benjamini and Hochberg false discovery rate corrections. 85

4.6 Heatmap display of fold changes of differentially expressed transcription factor (TF) genes in **(A)** Only blue light (BL) condition, **(B)** Either blue or red light condition, and **(C)** Red light (RL) condition. Expression levels are represented by color: blue, lowest fold change (down-regulated with respect to dark kept cells); red, highest fold change (up-regulated with respect to dark kept cells). Extreme values in color gradient are -5 to 5 in $\log_2$ scale. 91

4.7 Reactive oxygen species (ROS) measurement after light exposure and the effect of H_2O_2 on the regulation of light-induced gene expression. **(A)** ROS amount in the dark kept (Control), blue light (BL) and red light (RL) exposed cells was measured using 2',7' dichlorofluorescein. Y axis represents the fluorescence unit (FU). **(B)** Expression analysis of the selected 14 DEGs using qRT-PCR upon treatment of the cells with H2O2. Blue (indicates blue light exposure) and orange (indicates H_2O_2 treatment) bars with standard errors represent the relative mRNA expression levels ($\log_2$ fold) determined using qRT-PCR from three independent biological replicates. n = 6, $\star$ $p < 0.05$, Student's t-test. 98

NOMENCLATURE

8-HDF	8-hydroxy-7,8-didemethyl-5-deazariboflavin
BER	Base excision repair
BL	Blue light
BLUF	Blue light using FAD
BMAL1	Brain and muscle Arnt-like protein-1
CCT	C-terminal extension of CRY
CFA	Cyclopropane-fatty-acyl-phospholipid
CLOCK	Circadian locomotor output cycles kaput
CPD	Cyclobutane pyrimidine dimers
CPF	Cryptochrome/photolyase family
CRY	Cryptochrome
CYC	CYCLE
DCF-DA	2',7' dichlorofluorescein diacetate
DEGs	Differentially expressed genes
DNP	2,4-dinitrophenol
dsDNA	Double stranded DNA
ETC	Electron transport chain
FAD	Flavin adenine dinucleotide
FDR	False discovery rate
FMN	Flavin mononucleotide
FPKM	Fragments per kilobases of exons per million mapped read
FRL	Far-red light
GO	Gene ontology

KEGG	Kyoto Encyclopedia of Genes and Genomes
KO	Knockout
LOV	light,oxygen and voltage
MA	Allen's medium
MTHF	Methenyltetrahydrofolate
MYB	Myeloblastosis
NER	Nucleotide excision repair
NPH1	Nonphototropic Hypocotyl 1
PAS	Per, ARNT, Sim
PER	Period
PHOT	Phototrophins
PHR	Photolyase homology region
PHY	Phytochrome
qRT-PCR	Quantitative real-time PCR
RL	Red light
ROS	Reactive oxygen species
RPKM	Reads per kilobase of transcript per million mapped reads
RUP1	Repressor of uv-b photomorphogenesis 1
SigmaE	σ^E
ssDNA	Single stranded DNA
TFs	Transcription factors
TIM	Timeless
Trp	Tryptophan
UV	Ultra violet

Chapter 1

INTRODUCTION

The ability of light perception is crucial for the survival of most organisms that enables them to adjust their physiology and metabolism to the changing environmental conditions. Light, in contrast, is also a threat to any living organism owing to the deleterious effects it can have on nucleic acids, lipids and proteins. Light can cause direct photochemical damage and can damage cellular components through the photosensitizing effect of tetrapyrrole- and flavin derived pigments. Therefore, the capacity to sense and respond to light is widespread among prokaryotes and eukaryotes to survive and adapt themselves as a result of selective pressure of the solar irradiation.

Since, the intensity and the duration of the light quite varies depending on the ecosystem, organisms may sense intensity changes of light through the proteins called photoreceptors to perceive and respond properly to the temporal, spatial and spectral variability of light and to produce appropriate response to regulate their growth, development and other physiological variables accordingly. Photoreceptors are chromoproteins that undergo fast alteration from dark to signaling states upon light absorption by the prosthetic groups called chromophores. The signaling state initiates signal transduction *in vivo* that allows organisms to gain information about their external world and thus to adjust their physiology and metabolism by eliciting a biological response where the light is converted into biochemical signals, like protein-protein interaction and inactivation of kinases. There are different types of photoreceptor families that can sense different ranges of wavelengths in the visible spectrum. These are mainly grouped as blue light, red/far-red light and other types of photoreceptor

families such as UVB and rhodopsins.

This dissertation focuses on the genome-wide characterization of blue light regulated genes in a non-phototrophic prokaryote, *Vibrio cholerae*, and in an extremophilic phototrophic eukaryote, *Cyanidioschyzon merolae*, via RNA-sequencing. Results indicated that *V. cholerae* respond to blue light with a novel signaling mechanism to produce an appropriate response against photo-oxidative stress at transcriptome level. Blue light dependent regulation of three cryptochromes (*CmPHR2, CmPHR3* and *CmPHR7*) implies a potential role in light-dependent transcriptional regulation in *C. merolae*. In spite of absences of any red light photoreceptors in *C. merolae*, a great impact of the red light on the biological processes suggests the importance of the retrograde signaling in this organism.

The outline of this dissertation is as follows:

Chapter 2 provides pertinent background and literature review on different types of photoreceptor families.

Chapter 3 covers the genome-wide response of *Vibrio cholerae* to blue light via two different signaling mechanisms.

Chapter 4 presents the RNA-seq analysis of the transcriptional response to blue and red light in an extremophilic red alga, *Cyanidioschyzon merolae*.

Chapter 5 comprehends the results that are put forward in this dissertation and the major conclusions about the topics as well as the future directions.

Chapter 2

LITERATURE REVIEW

Our knowledge about light perception and signaling has been greatly increased in the last two decades thanks to a combination of classical genetic and physiological analyses with genomic, biochemical, and phylogenetic studies. These approaches have clearly showed that in spite of the wide diversity of living organisms, the number of photoreceptors can be classified into a limited number of families regarding their function, spectrum range, types of chromophore and domain that they use, structure of protein and output signals that they produce [Björn, 2015].

In the following subsections, photoreceptors will be classified according to the spectrum range which they can sense. There are different types of photoreceptor families that can sense different ranges of wavelengths in the visible spectrum which are mainly grouped as blue light (BL) and red/far-red light (RL) photoreceptors, and other photoreceptor types, such as UV-B photoreceptor and rhodopsins (**Figure 2.1**). Most biological photoreceptors can be described as light-activated switches, which thermally recover to the dark-adapted state. Upon transition from a dark-adapted state to a light-adapted state, the photosensory part of the protein modulates the activity of the cognate effector component (**Figure 2.2**). Light perception by these photoreceptors triggers many biological processes in different organisms such as phototaxis [Choi et al., 1999, Hellingwerf et al., 2002], phototropism [Baskin and Iino, 1987, Sakai et al., 2001], cell cycle regulation [Nishida et al., 2005], photosynthesis [Masuda and Bauer, 2002, Braatsch et al., 2004, Metz et al., 2012], pigment biosynthesis [Nelson et al., 1989, Ehling-Schulz et al., 1997, Chory et al., 1996], pathogenicity and motility [Gomelsky and Hoff, 2011, Purcell and Crosson, 2008, Río-Álvarez et al., 2014].

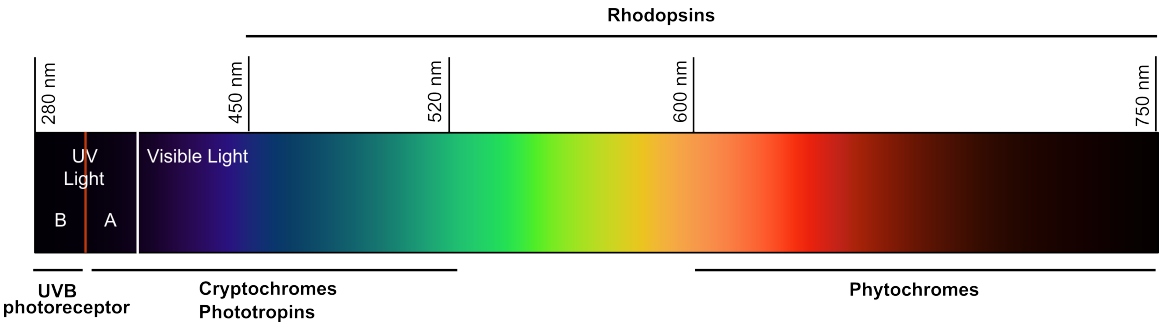

Figure 2.1: The spectral sensitivity of sensory photoreceptors ranges from the UV to the near-infrared region of the electromagnetic spectrum (280-750 nm). The figure is adapted from [Ziegler and Möglich, 2015, Tilbrook et al., 2013].

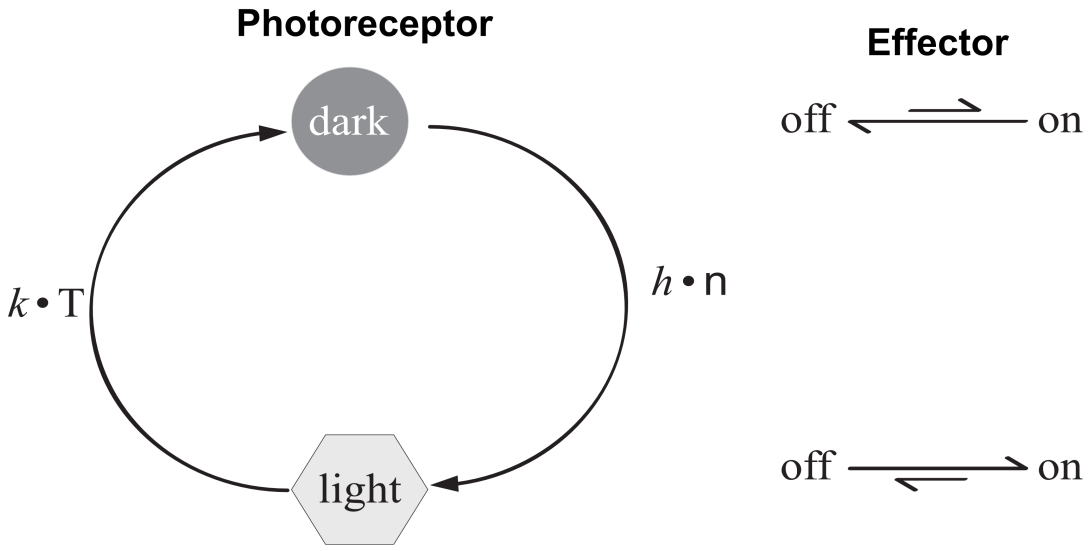

Figure 2.2: Biological photoreceptors as light-activated switches. The figure is adapted from [Kennis and Mathes, 2013]

2.1 Blue light photoreceptors

The ability to perceive and respond to BL (400-500 nm) seems to be ubiquitous in most living organisms. Almost 200 years ago, scientists first started to study the responses of plants to light of different colors. The earliest report is a paper written by Sebastiano Poggioli at 1817 describing the effects of red and violet light on the leaves of plant *Mimosa pudica* [Schäfer and Nagy, 2006]. He used a prism to refract light into spectral colors and postulated that certain colors of light, specifically violet light, might be more favorable for the growth of plants. In addition, he also reported that violet light was more effective than red in inducing changes in the position of the leaves of *Raphanus rusticanus* [Schäfer and Nagy, 2006]. After these breakthrough observations, a BL response was also documented as early as 1881 by Darwin when he discovered what is now known as the BL-induced phototropic response in plants [Darwin and Darwin, 1897]. However, BL receptors mediating phototropism and other photoresponses in plants have remained elusive until recently.

On the basis of molecular genetic studies, it has been revealed that BL photoreceptors mediate phototropism, hypocotyls elongation, stomatal opening, and expression of specific genes in the early development of plants [Ahmad and Cashmore, 1993, Kaufman, 1993, Short and Briggs, 1994, Liscum and Hangarter, 1994]. In addition, the effects of light quality and quantity have been extensively researched not only in plants but also in aquatic organisms because both change with depth and during the day. Among the various light spectra, only BL, along with ultraviolet (UV) radiation, can reach significant depths ($\sim$1500 m) in freshwater and marine ecosystems [Häder et al., 1998]. Therefore, most marine organisms, including algae and bacteria, have different types of BL photoreceptors. Based on the chromophore type following types of photoreceptors have been characterized so far; cryptochrome/photolyase family (CPF) members, phototropins (PHOT), and proteins containing BLUF (BL using FAD) domains to sense the BL [Christie, 2007, Losi and Gärtner, 2008, Losi et al., 2002, van der Horst et al., 2007].

2.1.1 Cryptochrome/photolyase family members

The CPF is a large and diverse gene family that encodes BL photoreceptors found in the biological kingdoms, from archaebacteria to mammals. Photolyases and CRYs are the two major classes of CPF. Although, photolyases and CRYs are structurally similar proteins, their functions are different depending on organisms. Since, photolyases are enzymes that utilize light energy for repair of UV-damaged DNA, CRYs function as signaling molecules that regulate diverse biological and physiological responses such as entrainment of circadian rhythms in animals and growth and development in plants. Based on phylogenetic analyses, CPF was divided into five subfamilies (**Figure 2.3**): CPD photolyase, (6-4) photolyase, plant CRYs, animal CRYs and CRY-DASH [Partch and Sancar, 2005]. The structural biology of DNA photolyases and cryptochromes has been extensively discussed in several reviews [Essen, 2006, Lin and Shalitin, 2003, Lin and Todo, 2005, Müller and Carell, 2009]. I will focus here on the characteristics of CRYs as photoreceptors directly relevant to mechanisms of light perception and signaling.

2.1.1.1 Photolyases

Photolyases, monomeric flavoproteins of 450-600 amino acids, possess an amino terminal photolyase homology region (PHR region) and widely found in microbes including Archaea and yeast [Sancar, 1994]. They catalyze blue/UV-A light-dependent repair of DNA damage resulting from exposure to high-energy short-wavelength UV light (UV-B and UV-C). There are two types of structurally related DNA photolyases, one that repairs CPDs and another that repairs pyrimidine-pyrimidine (6-4) photoproducts [Sancar, 1994]. Interestingly, it has been found that 75% of UV-induced DNA lesions are CPDs [Britt, 1996] and the enzyme, that repairs one, is not able to repair the other; however both have similar sequences, structures and reaction mechanisms [Sancar, 2003].

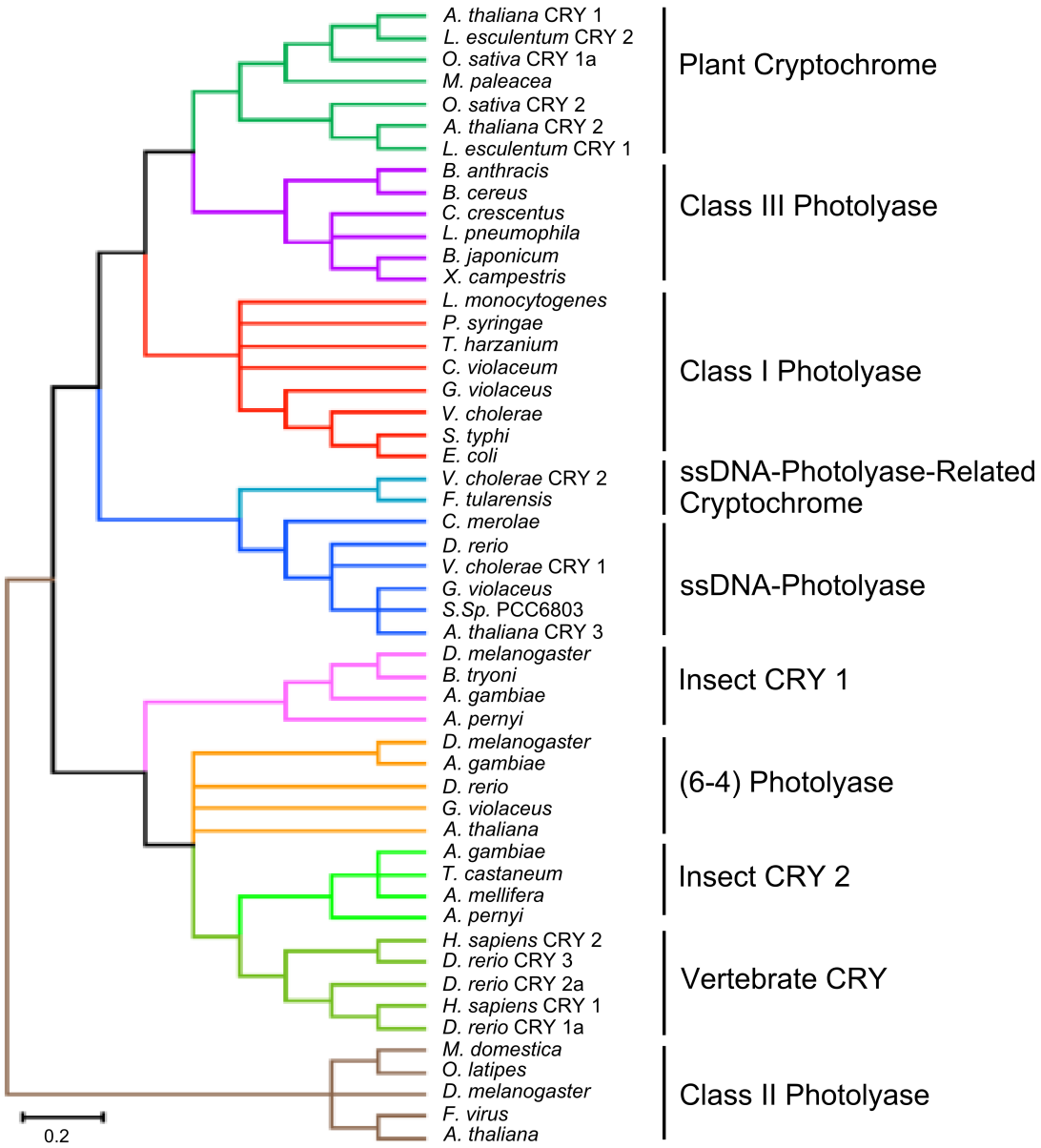

Figure 2.3: Phylogenetic tree of the cryptochrome/photolyase family (CPF). The unrooted phylogenetic tree of the CPF members was inferred using the neighbor joining method. The optimal tree with the sum of branch length=10.04 is shown. Bootstraps of 1000 replicates are expressed in percentage. The figure is adapted from [Öztürk et al., 2008].

Photolyases can be classified according to their primary amino acid sequences. To date, there are three subfamilies identified in photolyase family which can repair CPD lesions, however the kingdoms they exist are mostly different. Class-I photolyases are mostly found in microbial organisms while class-II photolyases are identified mostly in higher organisms, such as animals and plants [Essen, 2006]. In recent studies, phylogenetic and biochemical analysis revealed another class, named as class-III type photolyase, which is mostly found in bacteria and is likely to be the ancestor of plant CRYs [Brudler et al., 2003, Öztürk et al., 2008, Worthington et al., 2003].

Photolyases bound to two chromophore/cofactors non-covalently. The first chromophore is always FAD (flavin adenine dinucleotide), which is responsible for specifically binding to UV induced lesions and catalysis [Sancar et al., 1987b, Payne and Sancar, 1990]. The second chromophore is either MTHF (methenyltetrahydrofolate) or 8-HDF (8-hydroxy-7,8-didemethyl-5- deazariboflavin), that both increase DNA repair activity to 10-100 fold under low light conditions [Jorns et al., 1987, Sancar et al., 1987b, Sancar et al., 1987a].

It has been demonstrated that after purification of the photolyase, FAD is found in different chemical states *in vitro*, fully oxidized (FAD_{ox}), fully reduced ($FADH^{-}$), and radical form ($FADH^{0}$) [Kim and Sancar, 1991], with $FADH^{-}$ being the active form of FAD during the course of catalysis. The role of $FADH^{-}$ during catalysis is defined as follow. The reaction mechanism of photolyases has been well characterized for CPD repair [Sancar, 2003, Thompson and Sancar, 2002]. Briefly, photolyase binds to DNA with low specificity by ionic interactions with the backbone of the damaged DNA strand. The dimer is then 'flipped out' into the center cavity of the protein, which brings it into proximity with the flavin. This interaction between the substrate and enzyme enhances the specificity to photolyase, and results in stable enzyme-substrate complex [Jordan et al., 1989, Jorns et al., 1985]. During the course of catalysis (**Figure 2.4**), second photo-antenna folate (or deazaflavin) absorbs a photon in BL

wavelength, and gets excited to a high-energy state with a lifetime of 0.5 ns (MTHF) or 2.0 ns (8-HDF). Fluorescence resonance energy transfer occurs from the folate to the flavin ($FADH^-$) with a measured of the quantum yield of 0.8 [Kim et al., 1992]. Then, electron transfer occurs from the flavin to the Pyr<>Pyr and the cyclobutane ring is broken. Finally, the electron is transferred back to $FADH^0$ to regenerate the active form of flavin ($FADH^-$) [Kim et al., 1992]. The (6-4) photolyase was not fully characterized yet, but, it is expected to function with a similar mechanism as CPD photolyase.

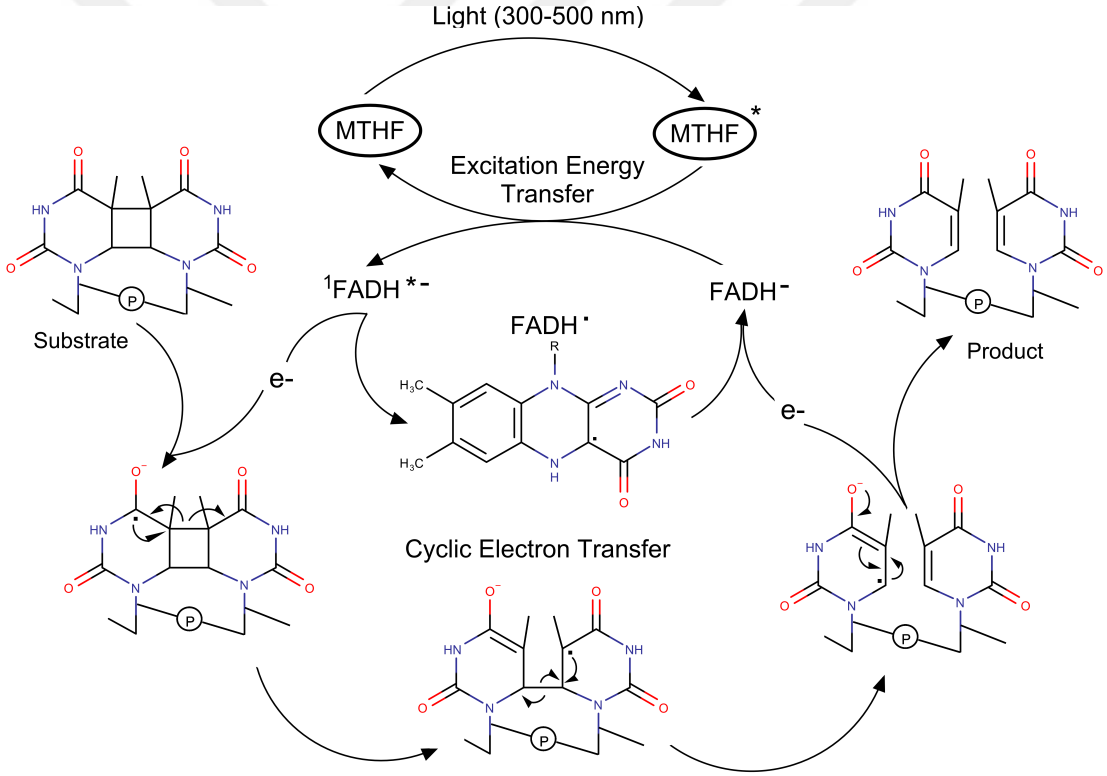

Figure 2.4: Repair mechanism of photolyases. First folate absorbs a photon in blue light wavelength and then transfers the energy to flavin. Finally, the excited electron breaks the cyclobutane ring and comes back to flavin. The figure is adapted from [Sancar, 2003].

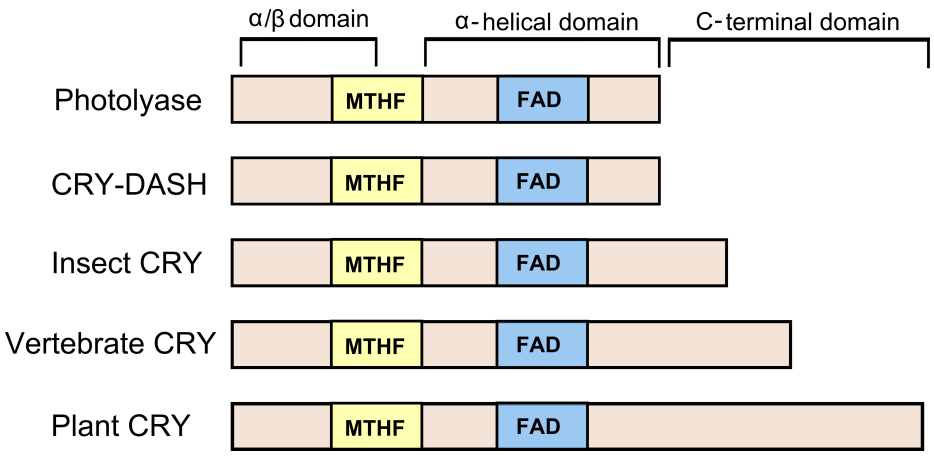

Figure 2.5: Schematic representation of the cryptochrome/photolyase family (CPF) proteins. Depending on the type of CPF, the length of proteins ranges from 500 to 700 amino acids. All CPF members contain an N-terminal α/β domain and an α-helical domain where FAD is associated. In addition, most CRYs have C-terminal extensions ranging in size from 50 to 250 amino acids. The figure is adapted from [Hoang et al., 2008].

2.1.1.2 Cryptochromes

CRYs are flavoproteins whose photosensory domains and primary amino acid sequences are closely related to DNA photolyases. Although they show 25-40% sequence similarity to (6-4) photolyases, typically lack their DNA repair activity [Lin and Todo, 2005] except CRY-DASH proteins [Selby and Sancar, 2006]. Structurally, the main difference between photolyases and CRYs is the presence of 50-250 amino acids length, unstructured C-terminal extension (CCT) of CRYs (**Figure 2.5**). This unstructured C-terminal tail of CRYs is thought to act as an effector domain and to have important roles in nuclear localization, protein stability, post-translational modification, signal transduction, and protein-protein interactions [Lin and Shalitin, 2003, Lin and Todo, 2005].

2.1.1.2.1 Plant cryptochrome Flavoproteins with an action spectrum that overlaps with BL responses of plants are the most probable candidates to study the

BL-dependent metabolic regulations, and physiological and behavioural responses. CRYs were first identifed in the plant kingdom from the isolation and characterization of mutants with altered responses to BL. Subsequently, the protein was identified in bacteria, animals and different species of plants. A clear role as a BL receptor was first demonstrated for *Arabidopsis thaliana* (hereafter *Arabidopsis*) CRY proteins. Particularly, the first gene was identified from the *Arabidopsis hy4* mutant, which had an impaired inhibition of hypocotyl elongation when grown under BL [Ahmad and Cashmore, 1993]. HY4 protein was showing homology to bacterial photolyase protein which binds to FAD but it was unable to repair DNA, hence renamed as cryptochrome1 (AtCRY1) that functions as a BL photoreceptor and mediates BL-dependent responses in plants such as triggering developmental processes, de-etiolation and flower induction [Li and Yang, 2007, Shalitin et al., 2003]. Later on, two other members of CPF in *Arabidopsis* (AtCRY2 and AtCRY3) were identified and characterized. AtCRY1 and AtCRY2 proteins are classified as plant type CRYs and act primarily in the nucleus [Wu and Spalding, 2007, Yu et al., 2007a]. They are composed of a PHR domain and a CCT region (**Figure 2.5**). Interestingly, it has been found that AtCRY3 was belonging to a different cryptochrome class named as CRY-DASH, which contains a shorter N-terminal extension of the PHR domain and probably functions in chloroplasts and mitochondria [Kleine et al., 2003]. CRY-DASH of some organisms have been reported to possess both DNA-repairing enzyme activity and photosensory activity [Brudler et al., 2003, Selby and Sancar, 2006, Coesel et al., 2009]. In the later sections, CRY-DASH proteins will be discussed in more details.

The CCT domain of AtCRY1 and AtCRY2 proteints is approximately 181 and 112 residues in length, respectively, and is thought to act as an effector domain [Yang et al., 2000, Lin and Shalitin, 2003, Sancar, 2000, Sancar, 2003]. Despite the CCT domain appears intrinsically unstructured, it may go into conformational change upon photo-excitation, most likely by light-induced folding [Burney et al., 2009, Partch et al., 2005, Yang et al., 2000, Yang et al., 2001]. It has been stated that BL-dependent

phosphorylation of CRYs triggers electrostatic repelling of the CCT domain from the surface of the negatively charged PHR domain of CRY [Burney et al., 2009, Partch et al., 2005, Yang et al., 2000, Yang et al., 2001] which results with separation of the two domains to change the interaction between CRYs and their signaling partners, such as CIB1 and COP proteins [Yang et al., 2000, Wang et al., 2001, Yang et al., 2001, Yu et al., 2007b, Yu et al., 2009].

Arabidopsis CRYs were mostly studied plant photoreceptors to understand the role of BL regulated metabolic and physiological pathways. Now, it is well known that AtCRY1 and AtCRY2 proteins regulate many aspects of plant growth and development including entrainment of the circadian clock [Somers et al., 1998, Yanovsky et al., 2001], stomatal opening and guard cell development [Mao et al., 2005, Kang et al., 2009], root growth [Usami et al., 2004, Canamero et al., 2006], plant height [Weller et al., 2001], fruit and ovule size [El-Assal et al., 2004], apical meristem activity [López-Juez et al., 2008], programmed cell death [Danon et al., 2006], the high-light and osmotic stress responses [Weston et al., 2000, Kleine et al., 2007, Xu et al., 2009], shade avoidance [Keller et al., 2011] and responses to viral and bacterial pathogens [Wu and Yang, 2010, Jeong et al., 2010].

2.1.1.2.2 Animal cryptochrome Animal CRYs are phylogenetically divided into two classes: one contains light-sensitive *Drosophila*-type CRY (DmCRY1) and the other includes a presumed light-insensitive vertebrate-type CRY (DpCRY2) [Rubin et al., 2006, Yuan et al., 2007]. *Drosophila* species only possess *cry1*, mosquitoes and butterflies have both genes, and hymenopteran insects and *Tribolium castaneum* have lost *cry1* [Rubin et al., 2006, Yuan et al., 2007, Zhu et al., 2005]. DmCRY1 is a BL sensor that plays a major role in photic entrainment in *Drosophila* [Tomioka and Matsumoto, 2010, Collins et al., 2006]. It was first shown when a mutant allele, *cry* ^{b}, of the flies exhibited attenuated rhythmic behavioral photoresponses and strongly reduced synchronization to light/ dark cycles [Stanewsky et al., 1998].

Circadian clock is important for the timing of the regulation of key biological activities in insects. For instance, the date of egg hatching and adult exclusion, the seasonal timing of adult development, and time-compensated sun compass navigation are some of the circadian clock mediated biological developmental regulations in insects [Yuan et al., 2007]. In **Figure 2.6**, functional differences of insect Type I (*DmCRY*) and light-insentive type II (*DpCRY2*) in the circadian clock of both insects are shown schematically. Briefly, circadian clock proteins CLOCK and CYCLE (CYC) forms a heterodimer and binds to the E-box promoter of *Period (Per)*, *Timeless (Tim)* and *Cry* genes. After transcription, the proteins are localized in the cytoplasm. At dark, PER-TIM heterodimer passes to the nucleus and prevents the binding of CYC-CLOCK transcription factors to the E-box sequence of their own promoters. However, in the light, the Type I CRY interacts with TIM in a light-dependent manner. The interaction results in the ubiquitylation of TIM and proteosomal degradation of both TIM and CRY proteins. TIM degradation leads to the transcriptional de-repression of *Per* and *Tim* genes and also allows the circadian clock to reset itself [Ceriani et al., 1999]. On the other hand, insect CRY2 is a crucial transcriptional repressor in the circadian clock, which shows no light-sensitivity in culture [Yuan et al., 2007, Ikeno et al., 2011]. It behaves much like vertebrate CRY. Unlike DmCRY, monarch butterfly DpCRY2 represses CLOCK-CYC-mediated transcription and it does not undergo light-dependent proteosomal degradation [Yuan et al., 2007].

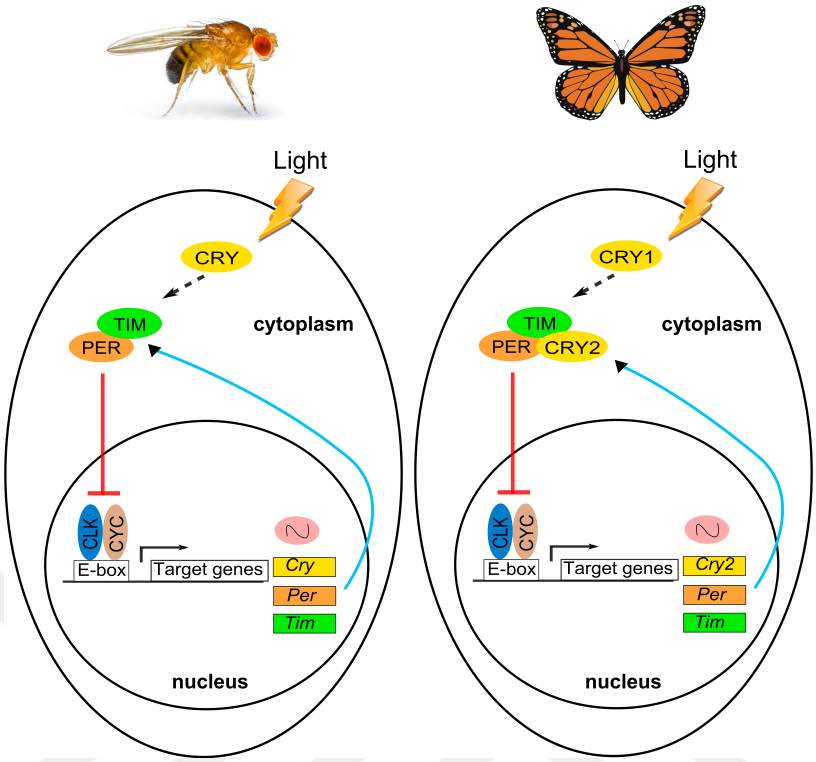

Figure 2.6: The roles of insect Type I and Type II cryptochromes (CRYs) in circadian oscillatory mechanisms of Drosophila and monarch butterfly, *Danaus plexippus*. Type I CRYs (DmCRY and DpCRY1) in both organisms act as a circadian photoreceptors. However, Type II CRY (DpCRY2) only involves in the light-independent regulation of circadian clock. The figure is adapted from [Chaves et al., 2011].

In mammals, circadian clock mechanism includes several proteins that take place in positive and negative transcriptional/translational feedback loops (**Figure 2.7**). Positive feedback loop; BMAL1 (brain and muscle Arnt-like protein-1) and CLOCK (circadian locomotor output cycles kaput) proteins are the transcription factors that contain two basic helix-loop-helix domains and bind to E-box elements in the *Per, Cry*, and other clock controlled genes [Gekakis et al., 1998, Hogenesch et al., 1998, King et al., 1997]. The mammalian PERIOD (PER) and CRY proteins act as negative regulators of transcription driven by the BMAL1/CLOCK heterodimer [Van Der Horst et al.,

1999, Vitaterna et al., 1999, Kume et al., 1999]. PER and CRY form heterodimers and interact with casein kinase Iε (CKIε). Afterthat, they translocate into nucleus where CRY acts as a negative regulator of BMAL1/CLOCK-driven transcription [Vielhaber et al., 2001]. This basic molecular clock is present in all tissues, but the peripheral clocks are synchronized to the master clock originating from the suprachiasmatic nucleus (pacemaker), which is a region of the brain in the hypothalamus responsible for controlling circadian rhythm, through humoral and neural signals.

Post-translational modifications also affect the stability, subcellular localization, and function of CRY in circadian clock mechanism. Both CRY1 and CRY2 can be ubiquitinylated by FBXL21 ubiquitin ligase and directed to proteasome for degradation [Hirano et al., 2013]. Also, acetylation of CRY is another modification that affects the stability of those proteins [Chaves et al., 2011]. hCRY1 and hCRY2 are able to carry out autophosphorylation but the correlation of auto-phosphorylation activity with light and the redox states of FAD as well as its role in signaling are still unknown [Öztürk et al., 2007].

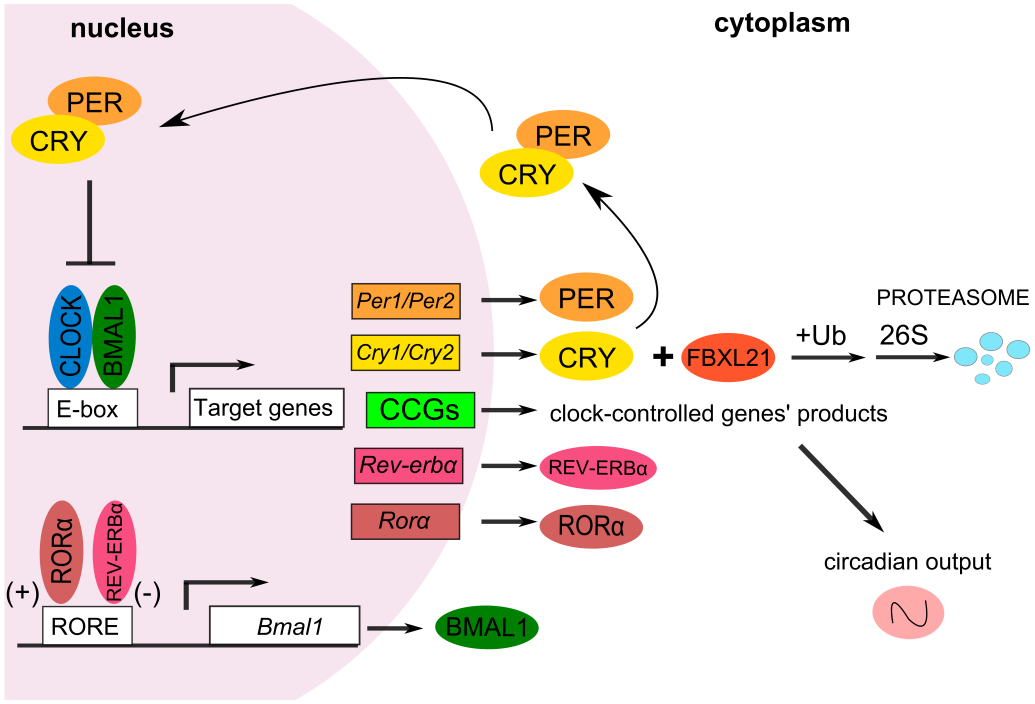

Figure 2.7: Schematic outline of the molecular mechanism that contributes to the generation of circadian rhythms. CLOCK and BMAL1 make a heterodimer which bind to the E-boxes (CACGTG) in the promoters of the Per and Cry genes, as well as in the promoters of the other clock-controlled genes. The Cry and Per proteins dimerize and, after a time lag, enter to the nucleus and inhibit CLOCK-BMAL1-activated transcription of their own genes as well as of those of clock-controlled genes, thus generating an oscillatory pattern of gene expression. A second feedback loop is formed by the action of RORα and REV-ERBα proteins on BMAL1 transcription; these nuclear receptors activate (RORα) and repress (REV-ERBα) transcription through their competitive action on response elements (ROREs) on the BMAL1 promoter. The figure is adapted from [Golombek et al., 2014, Hirano et al., 2013].

2.1.1.2.3 CRY-DASH The sequence similarity among some CRYs and photolyases is very high and hence only the sequence assessment is not sufficient enough to discover whether a recently indetified CPF member is a CRY or a photolyase. In the absence of genetic data, a recently discovered member of the family is assigned to the photolyase sub-group if it possesses repair activity and it is called a CRY if it lacks repair function. This assignment by default sometimes can cause to errors.

Until a decade ago, CRYs were thought to exist only in higher eukaryotes. However, Brudler et al, for the first time, classified a new type of CRY, called CRY-DASH, in unicellular cyanobacteria *Synechocystis* [Brudler et al., 2003]. After this study, several CRY-DASHs are also reported in other organisms [Veluchamy and Rollins, 2008, Daiyasu et al., 2004, Kleine et al., 2003, Selby and Sancar, 2006]. CRY-DASH proteins, were originally called CRYs because no photolyase activity could be detected in these enzymes by conventional assays [Brudler et al., 2003, Worthington et al., 2003]. However, later work revealed that CRY-DASH proteins are in fact photolyases with high specificity for Pyr<>Pyr in ssDNA and are now designated as ssDNA-photolyase [Selby and Sancar, 2006]. Additionally, CPF proteins including CRY-DASHes isolated from fungi, diatom and algae performing dual functions were observed. CRY-DASHes of *Aspergillus nidulans* were found to regulate sexual development and to repair ssDNA [Bayram et al., 2008]. In a fungi, *Sclerotinia sclerotiorum*, CRY-DASH protein was revealed to mediate UV-A specific development [Veluchamy and Rollins, 2008]. Additionally, PHL1 proteins of *Cercospora zeae-maydis* and *Trichoderma atroviride* involve in the gene regulation and also exhibit DNA photorepair activity [Berrocal-Tito et al., 2007, Bluhm and Dunkle, 2008]. Presently, a universal role for CRY-DASH has been clearly defined despite its *in vitro* DNA repair ability. Therefore, the biological role and the signaling mechanism of CRY-DASH are needed to be more elucidated by the identification of its signaling partners and the biological responses it causes.

Last but not the least, studying CRYs of simple unicellular organisms could be more effective to understand functional divergence of CRY from photolyase in terms of the evolution of structure-function relationship. The studies investigating the role of CRYs in unicells revealed that those proteins not only percept light but also involve in various pathways depending on the organism itself. A genome-wide study in a photosynthetic organism, *Prochlorococcus* ME4, showed that the expression levels of genes related to photosynthesis are directly dependent on BL suggesting that the actual sensing of high light is mediated via BL photoreceptors in this organism [Steglich et al.,

2006]. Another study with *Rhodobacter sphaeroides* reported that Cry-B protein acts as a transcription factor and regulates the expression levels of photosynthetic genes depending on BL [Hendrischk et al., 2009]. Additionally, stress induced transcription factor *Sigma38* and its cognate partner *ChrR* expression levels were also affected by BL in the same organism.

2.1.2 Phototropins and LOV domains

Phototropins are flavo-photoreceptor proteins that mediate phototropism responses in higher plants. Along with cryptochromes they allow plants to respond and regulate their growth in response to the BL. Genetic analysis using *Arabidopsis* has been instrumental in identifying the molecular nature of the phototropins and establishing their roles as BL receptors. *Arabidopsis* contains two phototropins designated as phot1 and phot2 [Briggs and Christie, 2002]. They have also been found in other plant species [Elliott et al., 2004, Kanegae et al., 2000, Kinoshita et al., 2001]. They mediate chloroplast accumulation movement [Sakai et al., 2001, Kagawa and Wada, 2000], phototropism [Huala et al., 1997], stomatal opening [Kinoshita et al., 2001], and cotyledon [Ohgishi et al., 2004] and leaf expansion [Sakamoto and Briggs, 2002] in plants. Phototropins have also been implicated in controlling BL-induced leaf movements [Inoue et al., 2005]. While only phot2 mediates chloroplast avoidance movement [Kagawa et al., 2004], phot1 plays an important role in mediating the rapid inhibition of hypocotyl growth and promoting the destabilization of specific transcripts under high BL intensities [Folta et al., 2003, Folta and Kaufman, 2003]. A summary of the known phototropin regulated responses found in higher plants is represented in **Figure 2.8A**.

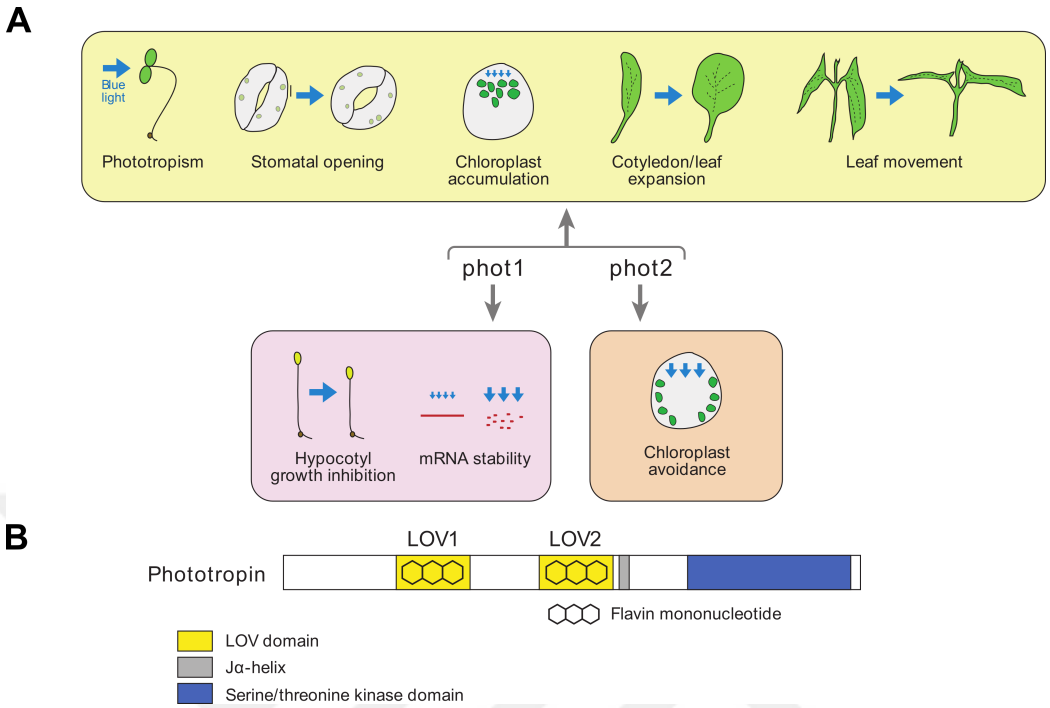

Figure 2.8: Phototropin structure and function. **(A)** Diagram illustrating the range of phototropin-induced responses in higher plants. Phot1 and phot2 are activated by blue light and overlap in function to mediate several responses. **(B)** Protein structures of phototropin photoreceptors. Domain structure of these proteins along with their respective chromophores are indicated. The figure is adapted from [Christie, 2007].

A phototropin was first cloned as a BL receptor responsible for phototropic bending, using an *Arabidopsis* mutant impaired in phototropism [Huala et al., 1997]. These mutants were absent in the light-dependent phosphorylation of a 120 kD protein that appeared related to phototropism. The cloned gene, initially named *NPH1* (Nonphototropic Hypocotyl 1), contained two repeated LOV domains in the photosensory N-terminus and a Ser/Thr protein kinase domain in the C-terminus (**Figure 2.8B**) [Huala et al., 1997, Briggs and Christie, 2002]. The gene later was renamed *PHOT1*. After that, a *PHOT1* homolog (*NPH1-like 1*) has been cloned from *Arabidopsis* and was renamed *PHOT2* [Jarillo et al., 1998, Briggs and Christie, 2002]. Phot1 went through autophosphorylation in response to BL in insect cells and indicated to be an autophosphorylating receptor kinase [Arabidopsis, 1998, Christie et al., 1999].

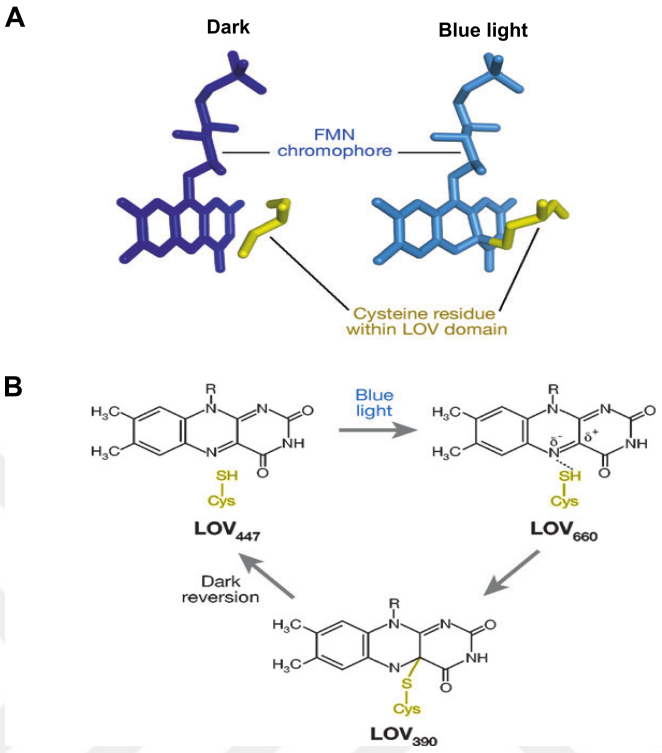

Figure 2.9: LOV-domain structure and photochemistry. **(A)** FMN chromophore structure within the LOV domain under dark and light conditions. **(B)** Mechanism of LOV-domain photochemistry after blue light exposure. The figure is adapted from [Christie, 2007].

The N-terminal domain of the phototropins possesses two very similar domains of ∼110 amino acids designated LOV1 and LOV2. LOV domains are members of the large and diverse superfamily of PAS (Per, ARNT, Sim) domains associated with cofactor binding and mediating protein interactions [Taylor and Zhulin, 1999]. LOV domains bind the cofactor flavin mononucleotide (FMN) and function as BL sensors for the proteins [Christie et al., 1999, Salomon et al., 2000]. Schematic representation of LOV-domain photochemistry can be seen in **Figure 2.9**. Briefly, in darkness, the FMN chromophore is noncovalently bound within the LOV domain, forming a species that absorbs maximally at 447 nm (LOV447). Light drives the production of a highly reactive triplet-state flavin (LOV660) that leads to formation of a covalent bond

between the C(4a) carbon of the FMN chromophore and a conserved cysteine residue within the LOV domain (LOV390). The photoreaction process is fully reversible in darkness.

2.1.3 BLUF proteins

BLUF is a recently identified photoreceptor protein domain that senses BL using a novel FAD chromophore [Gomelsky and Klug, 2002]. It is involved in sensing BL using FAD and is similar to the flavin-binding PAS domains and CRYs. BLUF family members are found mainly in prokaryotes but also in eukaryotic unicellular microbes. They have first been revealed to be responsible for photoprotective reactions such as phototaxis [Iseki et al., 2002], but later on have also been found to control lifestyle decisions, for instance virulence and biofilm formation [Tschowri et al., 2009, Gomelsky and Hoff, 2011].

BLUF photoreceptors are modular photoreceptors with approximately 150 amino acid containing receptor domain forming a ferredoxin-like $\beta\alpha\beta\beta\alpha\beta$ fold (**Figure 2.10A**) [Yuan et al., 2006, Jung et al., 2005, Kita et al., 2005]. Many BLUF domains are part of larger proteins C-terminally attached to enzymes as effector domains, which are involved in second messenger synthesis or breakdown. The activity of these effectors is modulated by the BLUF domain in response to light conditions [Stierl et al., 2011, Barends et al., 2009]. The signal cascade in a BLUF domain can be summarized as follows [Kennis and Mathes, 2013]: light absorption by the flavin moiety results in hydrogen bond rearrangements between the flavin and the conserved methionine (or tryptophan) residues and leads to a conformational alteration involving the β5 strand and this induces further structural changes in the C-terminal α-helices of the BLUF domain, which in turn result in the interaction between the BLUF domain and a specific, but as yet unknown, downstream component. Main characteristic of BLUF domain is the 10-15 nm red shift in the absorption spectrum of the flavin after light

exposure (**Figure 2.10B**). Once the signaling state is formed, the photoactivated state returns to the dark state in a light-independent reaction that occurs in seconds to minutes, depending on the BLUF domain.

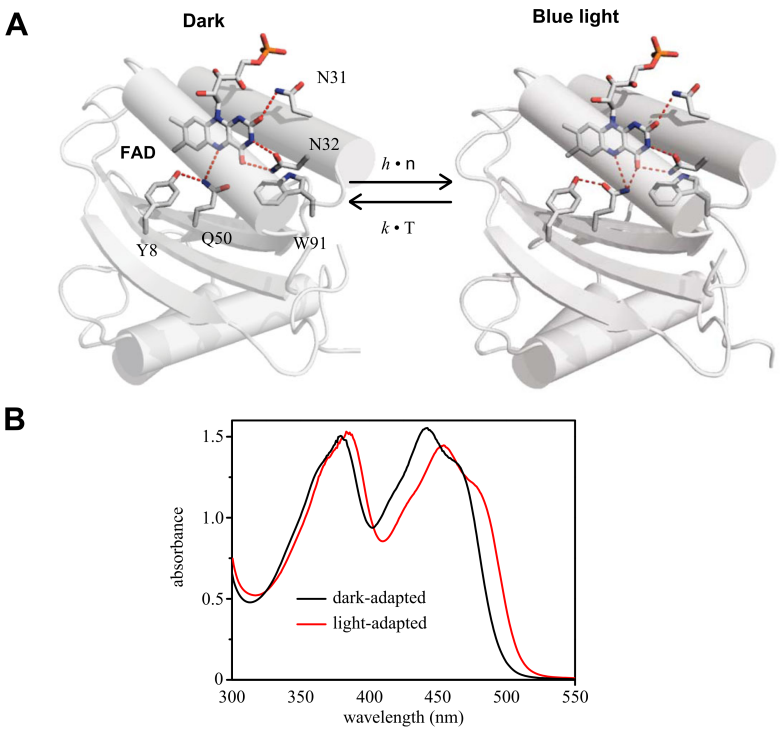

Figure 2.10: (A) BLUF domain of Slr1694 in dark- and light-adapted states illustrating the modulation of the protein in response to light condition. **(B)** The visible absorbance spectrum changes shifts by about 10-15 nm to the red upon illumination. The figure is adapted from [Kennis and Mathes, 2013].

Up to now, more than 50 members of the BLUF family proteins have been found where their physiological functions and spectroscopic properties are determined [Jung et al., 2005]. BLUF proteins that have been well characterized so far are; AppA and BlrB from phototrophic bacteria *R. sphaeroides* [Braatsch et al., 2002, Jung et al., 2005], YcgF from *Escherichia coli* (functions as BL regulated phosphodiesterase [Hasegawa et al., 2006]), PAC from *Euglena gracilis* (BL receptor for photophobic response [Iseki et al., 2002]), Slr1694 from cyanobacterium *Synechocystis*

(negative phototaxis, [Okajima et al., 2005]) and Tll0078 from thermophilic unicellular cyanobacterium *Thermosynechococcus elongates* BP-1 [Kita et al., 2005]. Because of its unique properties in the light signal transmission as a photoreceptor, a deep understanding of the BLUF photoactivation mechanisms may enable us to rationally customize and design novel tools for optogenetics and synthetic biology with optimized activities and sensitivities for their corresponding application.

2.1.4 Blue light induced photo-oxidative stress

Many key biological processes are dependent on molecular oxygen (O_2). A consequence of the use of O_2 in bioenergetic or other metabolic pathways is the formation of reactive oxygen species (ROS). In addition, various environmental stimuli, including high-fluence BL, result also in ROS generation. These molecules can act as signaling molecules to regulate a number of developmental processes and stress responses including bacteria and plants [Elías-Arnanz et al., 2011, Anthony et al., 2005, Ziegelhoffer and Donohue, 2009, Danon et al., 2006, Gadjev et al., 2006]. For example, photosynthetic bacteria capture light to convert it into chemical bond energy or electrochemical potential for cellular energy requirements. In these, as well as in non-phototrophic bacteria, light can also cause photo-oxidative stress. This occurs because absorption of light energy by photosynthetic pigments (chlorophyll) or other photosensitizer molecules such as tetrapyrroles (porphyrins and heme) and flavins generates excited states that enable the formation of singlet oxygen and other ROS that readily modify biomolecules leading to cellular toxicity [Ziegelhoffer and Donohue, 2009].

The LOV- and BLUF-domain containing proteins absorb BL and initiate photo-oxidative stress via the production of (ROS) in phototrophic and non-phototrophic bacteria [Anthony et al., 2004, Avila-Perez et al., 2006, Fuangthong et al., 2001, Lourenço and Gomes, 2009]. Studies on the photosynthetic bacterium *R. sphaeroides* have shown

that BL mediates its effect through a BLUF protein, AppA, to regulate the transcription of genes related to photosynthesis [Braatsch et al., 2002, Braatsch et al., 2004]. Further studies on this organism have revealed that light causes bacteriochlorophyll-a to produce singlet oxygen [Uchoa et al., 2008]. The production of singlet oxygen marks the photo-oxidative stress response, which is mediated by the release of the extracytoplasmic factor SigmaE from its inhibitory anti-sigma factor ChrR [Anthony et al., 2004, Newman et al., 2001].

Such mechanisms also exist in non-phototrophic bacteria enabling them to regulate pigment biosynthesis, pathogenicity, biofilm formation, and motility under BL stress [Elías-Arnanz et al., 2011, Purcell and Crosson, 2008, Río-Álvarez et al., 2014]. For example, the Gram-negative bacterium *Myxococcus xanthus* regulates carotenoid synthesis in a BL-dependent manner [Burchard and Dworkin, 1966]. In *M. Xanthus*, protoporphyrin IX absorbs BL and mediates its effect through the CarB operon to regulate carotenoid production via sigma and anti-sigma factors [Browning et al., 2003, Hodgson, 1993].

2.2 Red light photoreceptors

2.2.1 Phytochromes

One superfamily of photoreceptors includes the phytochromes (PHYs, meaning plant color), which absorb in the red/far-red part of the spectrum [Rockwell et al., 2006]. These receptors were first discovered in plants 60 years ago [Butler et al., 1959], but have more recently been found in a broad spectrum of eukaryotic and prokaryotic organisms.

PHYs are reversibly transformed by red light (RL) and far-red light (FRL) between conformations with different absorption spectra [Sharrock, 2008]. The light-sensing

part in all PHYs is the covalently attached bilin chromophore. After the synthesis of PHY in the cytoplasm, it binds chromophore. Under complete darkness condition, bilin attached PHY holoprotein folds into a stable, RL-absorbing conformation, called Pr. Absorption of RL by Pr converts the protein to the FRL-absorbing conformation, called Pfr. Absorption of FRL by Pfr converts the conformation back to Pr (**Figure 2.11**). Pfr is the physiologically-active form of the protein; exposure to RL yields physiological activity in the plant. Exposure to RL converts the Pfr to the inactive Pr form, inhibiting PHY activity [Sharrock, 2008]. Collectively, the two forms represent the PHY system.

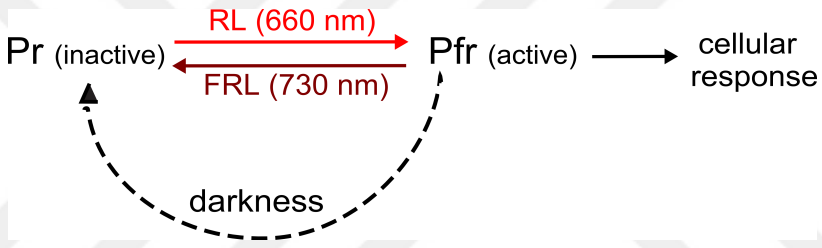

Figure 2.11: Functioning of Phytochrome (PHY) system. PHY acts as a molecular switch in response to red (RL) and far-red light (FRL). It occurs in two reversible conformations. The biologically-inactive form of PHY (Pr) is converted to the biologically active form Pfr under illumination with RL (660 nm). FRL (730 nm) and darkness convert the molecule back to the inactive form.

As shown in **Figure 2.12A**, the plant PHY holoprotein comprises an N-terminal sensory module carrying a covalently attached linear bilin chromophore in the GAF domain and a C-terminal module responsible for dimer formation [Wang and Wang, 2015]. Phytochrome C-terminal domains mediate the transmission of photosensory signals perceived by the N-terminal region to signal transduction pathways within the cell. The N-terminal region exhibits similarities to the transmitter modules of two component sensor histidine protein kinases, and indeed most prokaryotic PHY are such kinases, their activity being suppressed by light. On the other hand, plant PHYs have fully lost histidine kinase activity. Additionally, the tandem PAS domains

typical of plant PHYs are missing in prokaryotic PHYs.

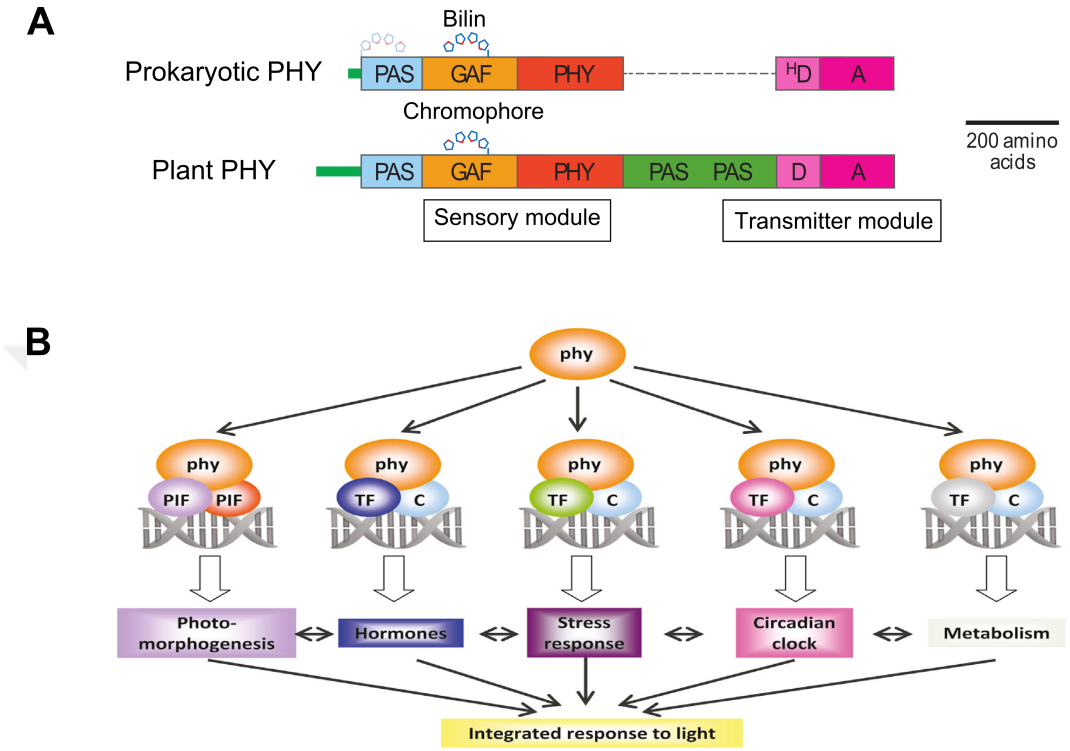

Figure 2.12: **(A)** Domain structures of phytochrome (PHY) photoreceptors in prokaryotes and plants. **(B)** The model showing PHY action in the transcriptional response control in plants. PHYs directly associate with downstream gene promoters by interaction with various sets of phytochrome-interacting factors (PIFs), transcription factors (TF) and coregulators (C), thus facilitating differential regulation of plant growth, development, and stress responses, which in total represent an integrated response to light. The figure is adapted from [Hughes, 2013, Wang and Wang, 2015].

PHYs regulate many metabolic and physiological pathways in plants (**Figure 2.12B**) such as control of seed germination, control of cell growth and division, chloroplast development, seedling photo-morphogenesis, shade avoidance, stress response, circadian rhythm, phototropism and flowering [Möglich et al., 2010, Rockwell et al., 2006, Franklin and Quail, 2010, Hughes, 2013]. In cyanobacteria and eubacteria, PHYs function in the regulation of phototaxis, pigmentation, and synthesis of the

photosynthetic apparatus [Rockwell et al., 2006, Karniol et al., 2005]. In fungi, PHYs have roles in the control of sexual development and mycotoxin production [Sharrock, 2008]. Unlike plant PHY proteins, localization of the fungal PHYs was firstly observed in the cytosol, regardless of the light conditions [Froehlich et al., 2005, Blumenstein et al., 2005]. Because of their biological significance, PHYs have been a major focus in plant research. PHY photochemistry, function and its associated signal transduction mechanisms have been researched extensively, mostly on the model flowering plant *Arabidopsis* [Möglich et al., 2010, Rockwell et al., 2006, Franklin and Quail, 2010, Chen and Chory, 2011].

Arabidopsis possesses five members of PHY gene family designated phytochrome A (phyA) to phyE. Among these, phyA is light-labile which rapidly degraded upon light illumination and abundant in etiolated seedlings, while other four phytochromes (phyB to phyE) are light-stable, with phyB being the predominant phytochrome in light-grown plants [Sharrock and Clack, 2002]. PhyA is responsible for sensing FR as well as mediating early R responses, whereas phyB to phyE play predominant roles under sustained R or white light conditions [Tepperman et al., 2006, Kami et al., 2010]. Although a complete signal transduction pathway for a plant phytochrome response has not yet been described, both cytosolic and nuclear mechanisms are implicated. There is strong evidence that plant PHYs have Serine/Threonine kinase activity [Rockwell et al., 2006]. Supportively, upon movement to the nucleus, PHYs bind to a subfamily of plant basic helix-loop-helix (bHLH) transcription factors [Quail, 2000]. Following the interaction with PHY, several bHLH proteins are rapidly phosphorylated and degraded, suggesting that rapid Phy signaling mechanism comprises targeted turnover of transcriptional regulators [Huq, 2006]. In summary, the PHY dependent 'light switch' has been discovered in many of its details over the past decade and much more information is on the way.

2.3 Other photoreceptor families

2.3.1 UV-B photoreceptor

UV-B comprises one of the three classes of ultraviolet radiation and is positioned between UV-A (315-400 nm) and UV-C (100-280 nm) in the electromagnetic spectrum. UV-B can cause damage to macromolecules, including DNA, and generate reactive oxygen species [Brown et al., 2005]. Thus, UV-B is a potential abiotic stress factor for any organism exposed to sunlight, and particularly for photosynthetic organisms such as plants [Christie et al., 2012]. UV-B resistance 8 (UVR8) protein, also known as UV-B photoreceptor, is responsible for sensing ultraviolet light in the range 280-315 nm and initiating the plant stress response. It is a β-propeller protein with 7 blade-shaped β-sheets [Wu et al., 2012]. It shares sequence similarity with the mammalian proteins involved in modulating chromatin condensation, such as the human RCC1 gene product [Kliebenstein et al., 2002]. UVR8 is thought to be a unique photoreceptor as it doesn't contain a prosthetic chromophore but its light-sensing ability is intrinsic to the molecule. Tryptophan (Trp) residue 285 has been proposed to act the UV-B sensor, while other Trp residues have been also seen to be involved (Trp233 > Trp337 > Trp94) although *in vivo* data suggests that Trp285 and Trp233 are most important [Voityuk et al., 2014].

UVR8 was first identified as a crucial mediator of a plant's response to UV-B in *Arabidopsis* containing a mutation in this protein. This plant was found to have a hypersensitivity to UV-B which damages DNA [Britt et al., 1993]. Later on, distinct responses to UV-B irradiation have also been reported for other plant species [Kendrick and Kronenberg, 2012, Ballaré et al., 1995, Frohnmeyer et al., 1999, D'surney et al., 1993].

Briefly the action mechanism of UVR8 photoreceptors is as follow. In the dark

state, UVR8 forms a homodimer that is localized in the cytosol and is held together via a complex salt bridge network [Christie et al., 2012], but UV-B exposure leads to the dissociation of UVR8 dimer to its respective monomers and translocation to the nucleus takes place [Cloix and Jenkins, 2008]. Activation of UVR8 leads to interaction with the E3 ubiquitin ligase COP1 and stabilization of the bZIP transcription factor HY5 that relays the UV-B signal resulting in the alterations of transcript levels (**Figure 2.13**). Among the collection of UV-B-responsive genes are those that encode proteins that function in UV-B-induced photo-morphogenesis and acclimation. These include proteins involved in UV protection (production of sunscreen pigments, such as phenylpropanoids), scavenging of reactive oxygen species (antioxidants), DNA damage repair (photolyases) and hypocotyl growth inhibition. Also, the WD40-repeat proteins repressor of UV-B photomorphogenesis 1 (RUP1) and RUP2 are induced upon UV-B, which facilitate negative feedback of the UV-B signalling pathway by directly inactivating UVR8.

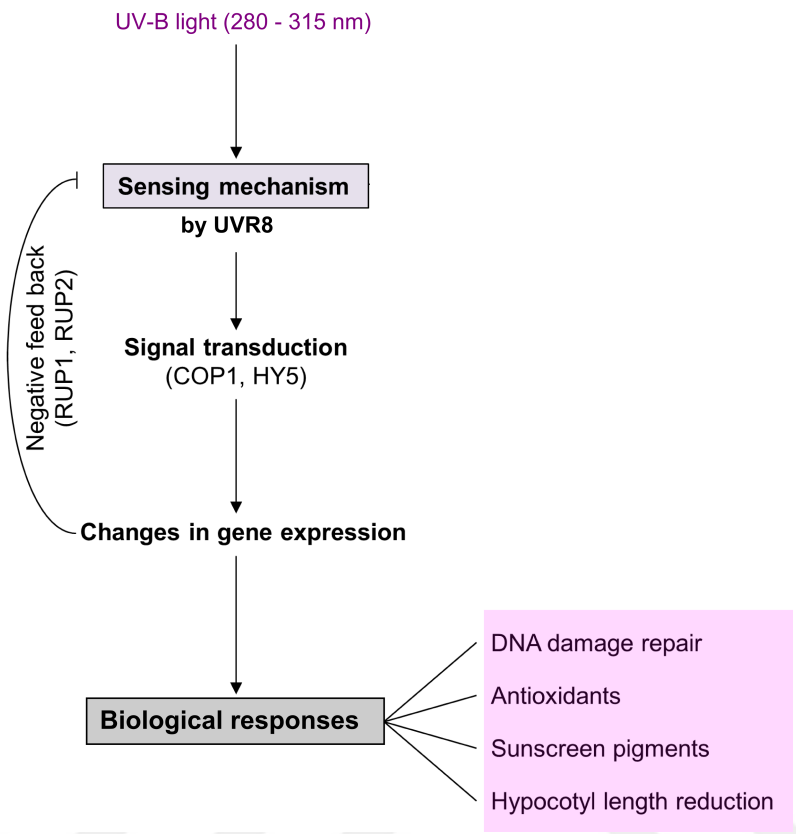

Figure 2.13: Schematic illustration of UV-B perception, signaling and responses in *Arabidopsis*. The figure is adapted from [Tilbrook et al., 2013].

Despite the studies in the last 30 years revealed that UV-B has regulatory effects on plant growth, morphology, and biochemical content, there are still much remains to be learned about the physiological role of UVR8 and its interaction partners, the molecular mechanism of UVR8 photoreception, how the UVR8 protein initiates signaling, and how UVR8 regulates transcription of its target genes.

2.3.2 Rhodopsins

Rhodopsin, is a G-coupled sensory protein that converts light into an electrical signal. It is present in a wide range of organisms, from vertebrates to bacteria [Oesterhelt and

Stoeckenius, 1973, Bogomolni and Spudich, 1982, Foster et al., 1984]. Rhodopsin was firstly discovered in 1876 by German physiologist Franz Christian Boll, who observed that the normally reddish purple frog retina turned pale in bright light [Daroff and Aminoff, 2014]. The fading of colour was later noticed to the destruction of rhodopsin, by a process known as bleaching. In many seeing animals, including humans, it is required for vision in dim light and is located in the retina of the eye specifically, within the tightly packed disks that make up the outer segment of the retinas photoreceptive rod cells, which are specially adapted for vision under low-light conditions [Ernst et al., 2013].

Vertebrates have two kinds of photoreceptor cells, called rods and cones because of their distinctive shapes. Cones are functional in bright light and they are responsible for color vision, while rods function in dim light but do not distinguish color. A human retina includes approximately 3 million cones and 100 million rods [Ernst et al., 2013]. Surprisingly, a rod cell can react to a single photon, and the brain needs fewer than 10 such responses to register the sensation of a flash of light. Some bacteria have proton pumps called bacteriorhodopsins, proteorhodopsins, and xanthorhodopsins to carry out phototrophy [Bryant and Frigaard, 2006]. Like animal visual pigments, these include a retinal chromophore and possess seven transmembrane α-helices; however, they are not coupled to a G-protein. Prokaryotic halorhodopsins are chloride ion pumps which are activated by light [Bryant and Frigaard, 2006]. Additionally, unicellular flagellate algae contain channelrhodopsins that act as light-gated cation channels. Many other prokaryotic and eukaryotic organisms (such as fugi, *Neurospora*) possess rhodopsin ion pumps or sensory rhodopsins of yet unknown function [Brown, 2004].

In contrast to the other water soluble photoreceptor family proteins, rhodopsins are integral membrane proteins. Light is perceived via a retinal chromophore that is covalently bound to a lysine residue as a protonated Schiff base [Möglich et al., 2010]. Rhodopsin possesses two chromoproteins which are opsin and 11-cis-retinal (11-cis-

retinaldehyde), a pigmented molecule derived from vitamin A. In **Figure 2.14**, the action mechanism of rhodopsins can be seen. Briefly, the chromophore of rhodopsins adopts the all-trans conformation in its dark-adapted state D470. Upon BL absorption around 470 nm, the retinal moiety isomerizes to the 13-cis form [Hegemann et al., 1991, Lawson et al., 1991]. The initial photoexcited state P500 interconverts to the P510 state within 200 μs through an intermediate with a deprotonated Schiff base. Based on electrophysiological experiments, P510 is the major signaling, ion-conducting state [Ernst et al., 2008]. P510 thermally relaxes to the ground state through a spectroscopically silent intermediate denoted N with time constants of 20 and 100 ms, respectively.

Figure 2.14: Action mechanism of rhodopsins. The figure is adapted from [Möglich et al., 2010].

Chapter 3

GENOME-WIDE RESPONSE OF *VIBRIO CHOLERAE* TO BLUE LIGHT VIA TWO DIFFERENT SIGNALING MECHANISMS

3.1 Background

The ability of light perception is crucial for the survival of most organisms that enables them to adjust their physiology and metabolism to the changing environmental conditions. Light, in contrast, is also a threat to any living organism owing to the deleterious effects it can have on nucleic acids, lipids and proteins [Attia, 2010]. Therefore, the capacity to sense and respond to light is widespread among prokaryotes and eukaryotes to survive and adapt themselves as a result of the selective pressure of solar irradiation.

Since, the intensity and the duration of light quite varies depending on the ecosystem, organisms may sense intensity changes of light through the proteins called photoreceptors to produce appropriate response and to regulate their growth, development and other physiological variables accordingly [Galvao and Fankhauser, 2015, Hegemann, 2008, Losi and Gartner, 2012, Montgomery, 2007, Rockwell et al., 2006, Sancar, 2000]. In the UV-VIS spectrum, only blue light (BL) and ultraviolet (UV) radiation, can reach significant depths in freshwater and marine ecosystems [Häder et al., 1998]. Therefore, most marine organisms, including phototrophic bacteria and non-phototrophic bacteria, have different types of BL photoreceptors. These photoreceptors include phototropins, cryptochromes, and proteins containing BLUF

(BL using FAD) domains and LOV (Light, Oxygen and Voltage) domains to sense the light [Christie, 2007, Losi and Gärtner, 2008, Losi et al., 2002, van der Horst et al., 2007]. The LOV- and BLUF-domain-containing proteins absorb BL and initiate photo-oxidative stress via the production of reactive oxygen species (ROS) in phototrophic and non-phototrophic bacteria [Anthony et al., 2004, Avila-Perez et al., 2006, Fuangthong et al., 2001, Lourenço and Gomes, 2009, Ondrusch and Kreft, 2011, Paget et al., 2001, Storz and Imlay, 1999].

In photosynthetic bacteria, the presence of oxygen can be very harmful to the organisms due to excessively generated ROS under light condition. Studies on the photosynthetic bacterium *Rhodobacter sphaeroide* have shown that BL mediates its effect through a BLUF protein, AppA, to regulate the transcription of genes related to photosynthesis [Braatsch et al., 2002, Braatsch and Klug, 2004]. Further studies on this organism have revealed that light causes bacteriochlorophyll a to produce singlet oxygen [Uchoa et al., 2008]. The production of singlet oxygen marks the photo-oxidative stress response, which is mediated by the release of the extracytoplasmic factor SigmaE from its inhibitory anti-sigma factor ChrR [Anthony et al., 2004, Newman et al., 2001].

Such mechanisms also exist in non-phototrophic bacteria enabling them to regulate pigment biosynthesis, pathogenicity, biofilm formation, and motility under BL stress [Elías-Arnanz et al., 2011, Gomelsky and Hoff, 2011, Purcell and Crosson, 2008, Río-Álvarez et al., 2014]. For example, the Gram-negative bacterium *Myxococcus xanthus* regulates carotenoid synthesis in a BL-dependent manner [Burchard and Dworkin, 1966]. In *M. xanthus*, protoporphyrin IX absorbs BL and mediates its effect through the CarB operon to regulate carotenoid production via sigma and anti-sigma factors [Browning et al., 2003, Hodgson, 1993]. In fact, genome sequencing studies have shown that there are diverse putative BL photoreceptors in many different non-phototrophic bacteria [Losi and Gärtner, 2008, Losi and Gartner, 2011, Losi and Gartner, 2012, Losi et al., 2014, van der Horst et al., 2007], indicating that different microorganisms may

respond similarly to BL.

Vibrio cholerae O1 biovar El Tor N1696 (hereafter abbreviated as *V. cholerae*) is a Gram-negative facultative human pathogen that colonizes the human intestine. Outside its host, it can survive for extended periods in natural aquatic environments. Therefore, the regulation of light response for *V. cholerae* is a critical cellular process for its survival. Genome sequencing of *V. cholerae* revealed three *phr* genes that encode photolyase/cryptochrome proteins as the sole BL photoreceptors, indicating that BL may regulate gene expression in this organism [Heidelberg et al., 2000, Selby and Sancar, 2006, Worthington et al., 2003]. Therefore, in the present study, we used molecular genetics and transcriptomics approaches to investigate possible BL response mechanisms in *V. cholerae* and to explore how cells produce an appropriate BL response at the genome-wide level.

Here, we report that *V. cholerae* responds to BL by regulating the transcript levels of 6.3% of its total genes by a novel mechanism. Our findings indicate that BL-induced transcriptional regulation is not mediated by any putative photoreceptors but instead it is mediated by the photo-oxidative stress induced ROS generation after BL exposure. Subsequent studies with the uncoupling reagent 2,4-dinitrophenol revealed that BL exposure results in ROS production through oxidative phosphorylation. Further inhibition studies using rotenone and malonate indicated that the source of ROS production is complex II (succinate dehydrogenase) within the ETC. To identify how ROS mediates the photo-oxidative stress response, we generated knockout cell lines by deleting candidate genes that may play a role in transmitting the effect of increased ROS level. Genome-wide studies of the knockout cell lines indicated that both an anti-sigma factor (ChrR, VC2301) and a putative metalloregulatory-like protein (MerR, VCA0056) mediate the effect of ROS through two separate signaling cascades to control the genome-wide gene expression in *V. cholerae*. Analyses of differentially expressed genes (DEGs) showed that BL strongly affects the transcription of genes related to

cellular protection, carbon metabolism and DNA repair.

3.2 Materials and Methods

3.2.1 Growth conditions and light experiments

Cultures of *V. cholerae* and *Escherichia coli* were grown in LuriaBertani (LB) broth (1% tryptone, 0.5% yeast extract, and 1% NaCl) at 37^0C with agitation (250 rpm). Antibiotics were added at the following concentrations unless otherwise noted: streptomycin, 100 μg/ml, ampicillin, 100 μg/ml, and kanamycin, 50 μg/ml. For blue light (BL) experiments, *V. cholerae* cells were inoculated into 5 mL streptomycin-supplemented LB and grown overnight in complete darkness. Then, the dark-grown cells were diluted (1:50) in 15 mL streptomycin-supplemented LB and grown until OD_{600}=0.8-1.0. After that, the cells were harvested by centrifugation at 7000xg for 5 min, washed once with PBS and then resuspended in 15 mL PBS buffer. Cells were then exposed to BL 50 μmoles $m^{-2}s^{-1}$, fluorescent black light source, each 20 W; General Electric, Cleveland, OH, USA)for 45 min. BL intensity was measured by a UVX Digital Radiometer (UVP, San Gabriel, CA, USA) at 365 nm. For red light (RL) experiments, dark-kept cells were exposed to red light (50 μmoles $m^{-2}s^{-1}$, red LED light source P10, Hangzhou Zhejiang, China) for 45 min. RL intensity was measured by the Thorlabs PM100 console system (Thorlabs, Newton, NJ, USA) at 630 nm.

3.2.2 Assessment of photo-oxidative stress

The fluorogenic dye 2',7' dichlorofluorescein diacetate (DCF-DA) was used to detect total ROS production. After DCF-DA diffuses into the cell, it is deacetylated by cellular esterases into a non-fluorescent compound that is subsequently oxidized by ROS into 2',7' dichlorofluorescein (DCF) [Gomes et al., 2005]. This ROS measurement

method is summarized in **Figure 3.1**. Briefly, a cell culture grown overnight in the dark was diluted (1:50) with 15 mL streptomycin-supplemented LB and grown until OD_{600}=0.8. The cells were harvested by centrifugation at 7000xg for 5 min, washed once with PBS, and later on resuspended in 15 mL PBS buffer. Cells were then incubated with 10 μM DCF-DA in the dark for 60 min and subsequently exposed to BL (50 μmoles $m^{-2}s^{-1}$) for 45 min. After BL exposure, DCF fluorescence was detected and analyzed using an Fluoroskan Ascent microplate reader (Thermo Scientific, Waltham, MA, USA) at maximum excitation and emission spectra of 485 and 535 nm, respectively. The fold change of ROS between dark- and BL-treated cells was calculated. The same experiment was performed in the presence of 100 μM rotenone, 500 μM 2,4-dinitrophenol (DNP), and 20 mM malonate.

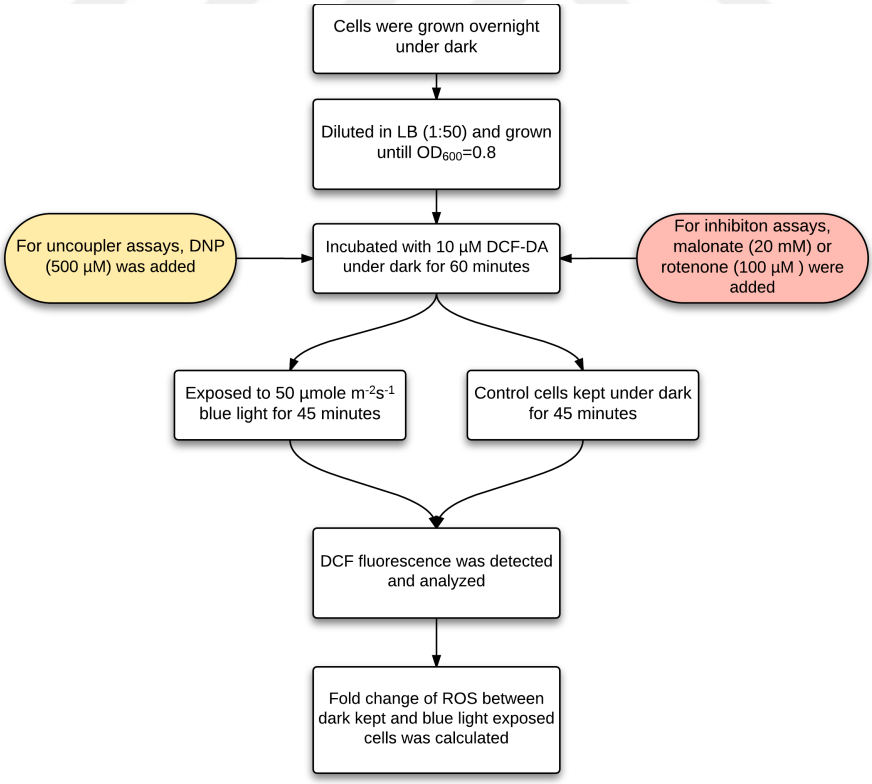

Figure 3.1: Flow-chart of ROS measurement protocol.

3.2.3 Construction of V. cholerae deletion mutants

We used the PCR method described in [Fong et al., 2006] to generate an in-frame deletion mutant of each of the target genes using the primers listed in **Table 3.1**. Briefly, P1 primer sets for each target gene were used to amplify approximately 500-bp 5' flanking sequences (including ∼150 bp of the coding sequence) and P2 primer sets were used to amplify approximately 500-bp of the 3' regions (including ∼150 bp of the coding sequence). The two PCR products were joined using the splicing overlap extension technique, and the resulting PCR product that lacked most of the internal coding sequence of the gene was digested with SacI and XbaI and cloned into the similarly digested pGP704-sacB28 suicide vector [Casper-Lindley and Yildiz, 2004]. The *E. coli* SM10λpir strain [Simon et al., 1983] was used to maintain the pGP704-sacB28 plasmid carrying the deletion construct. Biparental mating was carried out between recipient wild-type *V. cholerae* [Heidelberg et al., 2000] and the *E. coli* SM10λpir strain harboring the deletion construct. Ampicillin-resistant *V. cholerae* strains resulting from a single homologous recombination were identified, grown without ampicillin, and then subjected to 10% sucrose selection. Strains with the properties of a double recombination event (ampicillin-sensitive and sucrose-resistant) were identified and further analyzed by PCR with the flanking primers to confirm that the gene was successfully deleted.

Table 3.1: Primer sequences used in construction of *V. cholerae* deletion mutants.

Primer ID	**Primer Sequence**
VC1814_P1_F	AACTCTAGATTGAGTAAAAAAATTGGCCTG
VC1814_P1_R	GTGCTTCCACTGTAAAAAGGAGAGGGAGATCGTTTCTAC
VC1814_P2_F	GTAGAAACGATCTCCCTCTCCTTTTTACAGTGGAAGCAC
VC1814_ P2_R	TATGAGCTCTCATGATGAGCTTTCCTTATTTTG
VC1814_Flank_F	TCGATGGGTAGCAGGACATCGTATCCG

continued on next page!

Table 3.1 – continued from previous page

Primer ID	Primer Sequence
VC1814_Flank_R	CTTTACTTGCTGTATGCAGTACGCCG
VC1392_P1_F	GGAATCTAGAATGGAAAAGATCAATCTGGT
VC1392_P1_R	TAAGCTGTCAAACATGAGAACCAATCGGATGTGACGATCA
VC1392_P2_F	ACGGATTCAC CACTCCAAGA CATGACAGCG AAGGGCAGTT
VC1392_ P2_R	AGCTAGATCTTTAATCCATCTCCGGTTGACGCTTG
VC1392_Flank_F	CTCGGTAATAGGCAGAAAG
VC1392_Flank_R	GCTAGCTTGGCTTGGCGCGATG
VC2301_P1_F	AACTCTAGACACAGGCTTTTGCTCTGGTATTTAG
VC2301_P1_R	GACCATCATGCTGCATAAAGTAACTCACCAAGTTCTGCCTC
VC2301_P2_F	GAGGCAGAACTTGGTGAGTTACTTTATGCAGCATGATGGTC
VC2301_P2_R	TATGAGCTCTAGCCTTTGTTTCCTTCCTGAC
VC2301_Flank_F	ATCTCGACACGTGAACAATTTGCTTG
VC2301_Flank_R	TCACCTTGCTTGGCAGCTTAGTC
VC2302_P1_F	AACTCTAGAAATGCAAACGAATTATCT
VC2302_P1_R	TCGAGCATGTCGGCCACATCGCCTGTGTGTCCCTGCTTTTA
VC2302_P2_F	TAAAAGCAGGGACACACAGGCGATGTGGCCGACATGCTCGA
VC2302_P2_R	TATGAGCTCGTAATGACCATTTTCAT
VC2302_Flank_F	GTGAGTGATCGACGAATGAACTCT
VC2302_Flank_R	AGCATAAAGAAGAGTTACCGCCT
VCA0056_P1_F	CAACTCTAGAATGGTTTGTGATGAAAAACG
VCA0056_P1_R	GCCCATAACCAAGCATTCCCAGCGCCGTAAGAAGTGTTTC
VCA0056_P2_F	GAAACACTTCTTACGGCGCTGGGAATGCTTGGTTATGGGC
VCA0056_P2_R	TATCGAGCTCCTAAGATTGTAGCTGTTGTA
VCA0056_Flank_F	CCTGATGGCACATAACCCACAG
VCA0056_Flank_R	AGCAGACCATATTATCCCTTGT

3.2.4 Preparation of cDNA library for RNA-seq

The cDNA library preparation method is summarized in **Figure 3.2**. Briefly, total RNA was extracted from dark-grown and BL-exposed cell cultures (500 μl of culture with OD_{600}=1.0) using TRIzol reagent (Invitrogen, Carlsbad, CA, USA) according to the manufacturer's instructions. After quality and quantity measurements using a 2100 BioAnalyzer (Agilent, Palo Alto, CA, USA), the RNA was treated with RNase-free DNase I (Thermo Scientific, Waltham, MA, USA) at a concentration of 1 U/μg to remove residual genomic DNA. To remove the rRNA, 2.5 μg total RNA was treated with a Ribo-Zero bacterial rRNA removal kit (Illumina, San Diego, CA, USA) following the manufacturers instructions. The rRNA-depleted RNA pellets obtained after the ethanol precipitation step were re-suspended in 10 μl RNase free water, and then samples were fragmented using a TruSeq mRNA sample preparation kit (Illumina, USA). The cleaved short RNA fragments were used for first-strand cDNA synthesis using random hexamer primers, and then the second strand was synthesized using DNA polymerase I and RNase H. The double-stranded cDNAs were purified with AMPure XP beads (Beckman Coulter, Brea, CA, USA) and eluted with resuspension buffer followed by 3'-end adenine nucleotide addition. Finally, sequencing adaptors were ligated to the fragments and cDNA fragments were enriched by PCR amplification. Enriched cDNA libraries were used for cluster generation and sequencing. Paired-end sequencing of the cDNA libraries (dark- and BL-treated) of wild-type and knockout *V. cholerae* cells was performed in duplicate (biological replicates) using the Illumina MiSeq sequencing platform (Illumina).

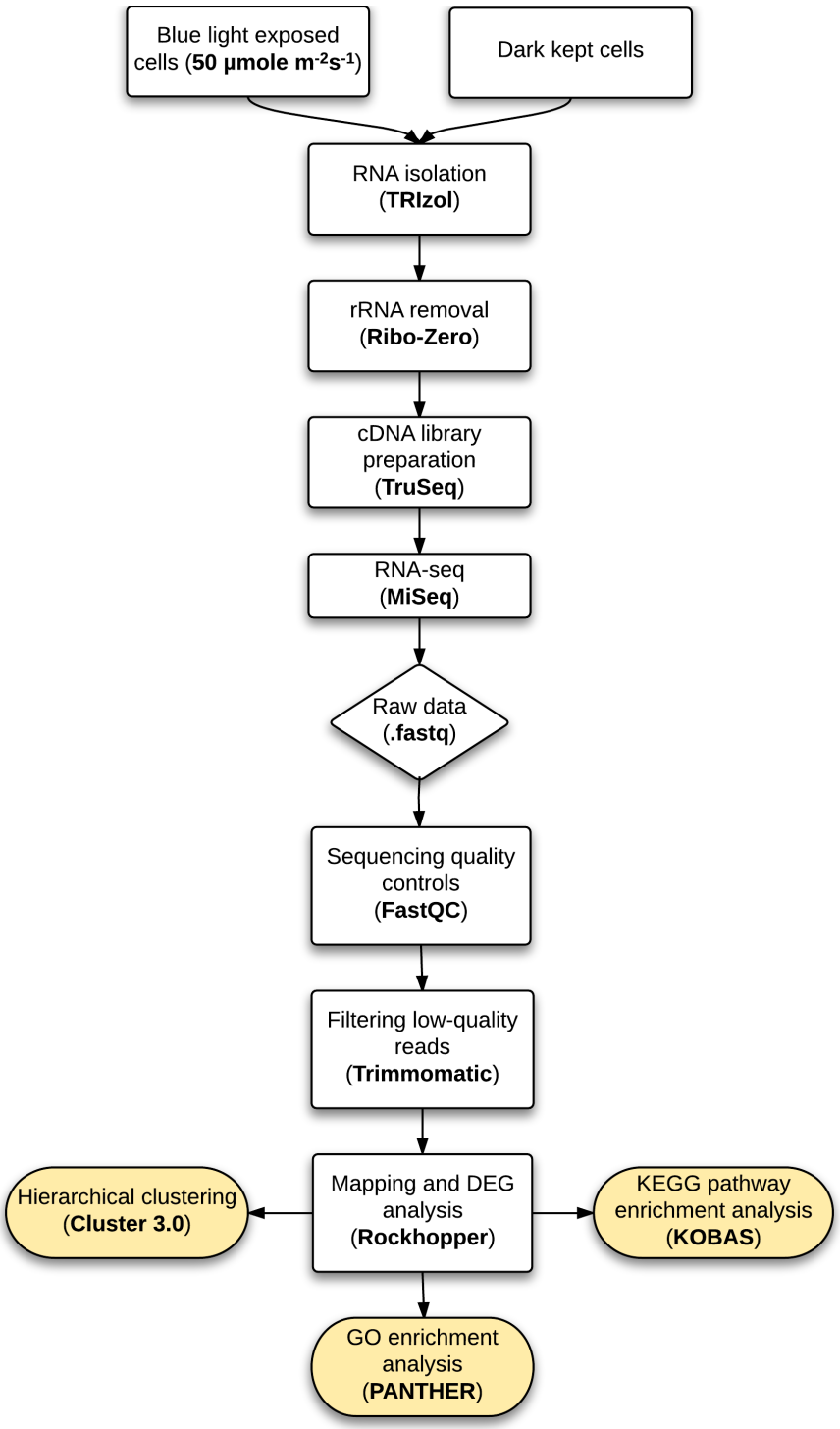

Figure 3.2: Flow-chart of RNA-seq analysis.

3.2.5 Transcriptome analysis

All sequence data were at 2x75-bp length. The high-quality reads were saved in fastq files and deposited at the GEO database at NCBI under the accession number: GSE79911 (`http://www.ncbi.nlm.nih.gov/geo/query/acc.cgi?token=mhwraiymxvsxnkn&acc=GSE79911`). The processing of fluorescent images into sequences, base calling, and quality value calculations were performed by the Illumina data processing pipeline (v1.5). For quality control, reads with adaptor contamination and low-quality bases (quality score < Q30) were removed using Trimmomatic (v0.35). All the downstream analyses were based on high-quality, clean data.

The RNA-seq data were analyzed with Rockhopper [McClure et al., 2013]. A summary of the analytical methods is provided below. Reads were aligned to the *V. cholerae* O1 biovar El Tor str. N16961 genome with the following parameters: minimum seed length 0.33, allowed mismatches 15%. After aligning the sequencing reads to the genome, reads from each experiment were normalized by upper quartile normalization [Bullard et al., 2010]. A Pearson's correlation analysis was conducted to obtain the transcript-level R^2 value between replicates. We used the q-value < 0.01 (false discovery rate) and the absolute value of $|\log_2$ fold change$| \geq 1$ as the threshold to judge significant differences in gene expression.

To annotate the hypothetical DEGs, we used the custom pipeline Annocript [Musacchia et al., 2015] (`https://github.com/frankMusacchia/Annocript/tree/master/GUIDE`). We used Swiss-Prot (SP) and UniRef90 [Suzek et al., 2007] (version: August 2015) databases for blastp searches with the following parameters: word_size=4; e-value=10^{-5} ; num_descriptions=5; num_alignments=5; threshold=18. For each sequence, the best hit was chosen. The domain composition of putative proteins in the Conserved Domains Database [Marchler-Bauer et al., 2013] was determined by Rpsblast with the following parameters: e-value=10^{-5} ; num_descriptions=20; num_alignments=20.

3.2.6 GO term and KEGG pathway enrichment analyses

To functionally categorize the DEGs, a GO term enrichment analysis was conducted using the PANTHER classification system [Mi et al., 2013] (`http://www.pantherdb.org/`) with Bonferroni multiple correction testing. After GO term functional enrichment analysis, the correlations were analyzed to construct a network using the BiNGO plug-in (v2.44) (`http://apps.cytoscape.org/apps/bingo`) [Maere et al., 2005] in Cytoscape (v2.8.3) (`http://www.cytoscape.org/`) [Shannon et al., 2003]. KOBAS (v2.0) (`http://kobas.cbi.pku.edu.cn`) was used to test for the statistical enrichment of differentially expressed genes in KEGG pathways. Fisher's exact test was used to calculate p-values, and pathways with a p-value < 0.05 were designated as being significantly enriched in DEGs.

3.2.7 Hierarchical clustering and heatmap generation

For the heatmap display, the expression values of DEGs in dark and BL conditions were $\log_2$ transformed, and hierarchical clustering was performed on genes and arrays using the Euclidean distance similarity metric with the centroid linkage clustering method. Heatmaps were generated and visualized using Cluster3.0 (v1.52) and Java Treeview (v1.1.6r4), respectively.

3.2.8 Validation of RNA-seq results using qRT-PCR

Twenty-one representative BL-responsive genes (VC0837, VC0943, VC1118, VC1248, VC1263, VC1359, VC1392, VC1484, VC1570, VC1643, VC1814, VC1922, VC2088, VC2301, VCA0055, VCA0615, VCA0782, VCA0798, VCA0809, VCA0957, VCA1087) were selected for validation by qRT-PCR. Total RNA was extracted using TRIzol reagent (Invitrogen, Carlsbad, CA, USA) according to the manufacturers instructions. After DNase I treatment, 1 μg total RNA was used for first-strand cDNA synthesis using random hexamer oligos. The qRT-PCRs were performed with Luminaris HiGreen

qRT-PCR Master Mix (Thermo Scientific, Waltham, MA, USA) on the CFX Connect Real-Time PCR Detection System (Biorad, Hercules, CA, USA) using gene-specific primers (**Table 3.2**), with *gapdh* (VC2000) as the internal reference gene. The amplification program was as follows: 95^0C for 10 min; 40 cycles of 95 ^{0}C for 2 s, 56^0C for 10 s, and 72^0C for 10 s, followed by a thermal denaturing step to generate the melting curves. All reactions were performed in biological triplicate (each triplicate with two technical replicates), and the results were expressed relative to the transcript level of *gapdh* in each sample using the $2^{-\Delta\Delta CT}$ method [Livak and Schmittgen, 2001]. The mRNA expression data were analyzed using IBM SPSS ver. 20.0 (SPSS Inc., Chicago, IL, USA). All relative mRNA expression data are presented as mean ± S.D. (n = 6).

Table 3.2: Primer sequences used in qRT-PCR.

Gene ID	Forward primer	Reverse primer
VC2000	GGTCAAGACATCGTTTCTAACGC	GTTGAAGATGGGATGATGTTTTG
VC0837	TCCACATGCAGAAACAGGAG	TTGCCACTAGGCTGATATGG
VC0943	TCAAGAACATGCCGACAGAG	TCTTGAATGCGCTGGCTATC
VC1118	GCCGCACATCGCATCGAAGGG	GTGGCTCACGCCTTTCACATC
VC1248	CTCTGCCAATGCCCTAAAAG	CTTTGGGTAGGGTTTGGTTG
VC1263	AACATGGCGGAAGTAAGAGC	ACATCGCCCGTTAAACACTC
VC1359	GAAGGCATGACCATGTTGTG	TCTGTGTACGATCCGATTGC
VC1392	ATTACAGCGAACGACACTGG	CTCAGCAATACGTGCAAAGC
VC1484	GAAAGAGCTCAATCGCAAGG	TTTCTAGCATCACGCCAACC
VC1570	TTGGTTGGTGCTCAAAACCG	AAACCAACGTTCTGCGACTG
VC1643	GGTTTCAAAGGCTTGACAGG	CCAGCACGAATCGTATGTTG
VC1814	AAACACAATGGGGCGAAG	GCTTGATAGGGCAAAAGTGG
VC1922	TTGTTGGCAGAGCATACAGG	CATCCACCAAACCGTATTCC
VC2088	CCGGATGTCGATAACAAACC	GCATCCAACACCATCATGTC
VC2301	GATTCGATTGTGGCCTTGCC	ACGCGCTAAGACTTTGGGAA
VCA0055	GGAGCAAAAGTACGCTTCGATG	GTGAGTAACTCTCTAACGCTG
VCA0615	CCGCTCAACTCGAGTTACATTG	TCATGCAATAGCGCAAACCG
VCA0782	GATTCAAGCGGGAGAAAGTG	GGCTTCATCATCCAGTTGTG
VCA0798	CCGGATCTCATCCGTTATTG	GGCTCAATTGAAAGGTCAGC
VCA0809	GTACGTTCGCCATCACATTC	AGATCCAGATGCCATACGTG
VCA0957	TTCTAATGACCACGCACAGC	TGTGGTCGACCTTGTTCATC
VCA1087	GCATGATCACCGATTCACC	CCGCTTGCTCAAGGTATTTC

3.3 Results and Discussion

To identify the pathways affected solely by BL in *V. cholerae*, wild type and knockout cells were irradiated with 50 μmoles $m^{-2}s^{-1}$ BL as previously described [Pandhal et al.,

2007]. Total RNAs from dark- and BL-treated cells were isolated followed by rRNA depletion, mRNA selection, and library preparation. The quality of the library was assessed and then the samples were sequenced using the Illumina MiSeq platform.

3.3.1 Mapping and coverage of RNA-seq data

The bacterial strains and plasmids used in this study are listed in **Table 3.3**. After sequencing and de-multiplexing, RNA-seq data were aligned to the *V. cholerae* reference genome [Gomes et al., 2005] and gene expression values were calculated using Rockhopper [McClure et al., 2013]. An overview of the sequencing and mapping data for wild-type and mutant cells is shown in **Table 3.4**. To evaluate reproducibility among biological replicates, a Pearson's correlation test was performed on the expression values. There was a strong correlation between biological replicates for each condition based on the calculated Pearson's correlation coefficients (R^2 >0.95) (**Figure 3.3**). This finding confirmed that there was consensus among the replicates in each condition, which allowed us to perform further differential gene expression analyses.

Table 3.3: Bacterial strains and plasmids used in this study.

Strain or plasmid	Relevant genotype	Source
E.coli strains		
SM10-λpir	Kan^R, thi^{-1}, thr, leu, tonA, lacY, recA::RP4-2-Tc::Mu, pir	[de Lorenzo and Timmis, 1994]
V. cholerae strains		
MT_VC_0001	*V. cholerae* O1 biovar El Tor N16961, wild-type, Str^R	[Yildiz et al., 2004]
MT_VC_0002	ΔVCA0056 (*MerR*)	This study
MT_VC_0003	ΔVCA0057 (*phr*), Kan^R	[Casper-Lindley and Yildiz, 2004]
MT_VC_0004	ΔVC1392 (*cry2*), Tet^R	This study
MT_VC_0005	ΔVC1814 (*cry1*)	This study
MT_VC_0006	ΔVC2301 (*ChrR*)	This study
MT_VC_0007	ΔVC2302 (*SigmaE*)	This study
MT_VC_0453	ΔVC1392ΔVC1814ΔVCA0057 (*cry1,cry2,phr*), Kan^R, Tet^R	This study
MT_VC_0062	ΔVC2301ΔVCA0056 (*ChrR, MerR*)	This study
Plasmids		
pGP704-*sacB28*	pGP704 derivative, *mob/oriT sacB*, Amp^R	[Casper-Lindley and Yildiz, 2004]
pMT-0003	pGP704-*sacB28*::ΔVC1392, Amp^R	This study
pMT-0004	pGP704-*sacB28*::ΔVC1814, Amp^R	This study
pMT-0005	pGP704-*sacB28*::ΔVC2301, Amp^R	This study
pMT-0006	pGP704-*sacB28*::ΔVC2302, Amp^R	This study
pMT-0007	pGP704-*sacB28*::ΔVCA0056, Amp^R	This study

Table 3.4: Mapping results of RNA-seq reads to *V. cholerae* genome.

Sample	# of clean reads	Mapped percentage	Q30
WT BL (-)	5,853,433	97%	
WT BL (+)	4,709,718	96%	
Δ*ChrR* (-)	3,128,595	94%	
Δ*ChrR* (+)	3,089,688	95%	96.40%
Δ*ChrR*Δ*Mer*R (-)	5,805,656	89%	
Δ*ChrR*Δ*Mer*R (+)	5,662,305	89%	
Δ*cry1*Δ*cry2*Δ*phr* (-)	7,146,681	97%	
Δ*cry1*Δ*cry2*Δ*phr* (+)	6,842,177	97%	

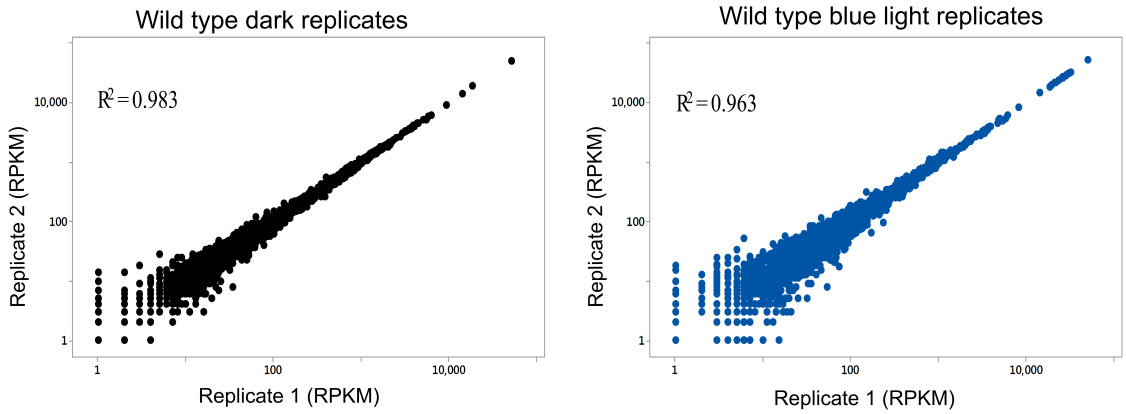

Figure 3.3: Comparison of gene transcript levels between replicates of dark- and blue-light-treated samples. Correlation plot for transcript-level RPKM values between replicates of wild-type cells treated with dark or BL. Pearson R^2 values for correlation are included as an insert in plot.

To identify DEGs in response to BL, we calculated the difference in the number of mapped reads per kilobase of exon per million mapped reads (RPKM) between dark- and BL-treated samples. The number of DEGs was determined using Rockhopper. In total, 222 (6.3%) DEGs were identified with $\mid \log_2$ fold change $\mid \geq 1$ and a false discovery rate (FDR) < 0.01, in response to BL (**Appendix Table A.1**). Of those genes, 81 genes were down-regulated and 141 genes were up-regulated. Further analysis of the 222 DEGs (designated as Set1) revealed that 117 were grouped under 57 operons and the rest were controlled by separate promoters

3.3.2 Validation of DEGs identified in RNA-seq using qRT-PCR

A total of 21 representative up- and down-regulated DEGs, designated as Set2 DEGs, were selected to validate the RNA-seq results. Among the selected DEGs, 12 were from 12 different operons while nine were not grouped into operons. Firstly, cells were exposed to BL and total RNAs were isolated from each sample. After conversion of the total RNA into cDNAs, qRT-PCR was performed using appropriate primers. A

comparison of qRT-PCR data (fold changes calculated with respect to *gapdh* gene) and RNA-seq data indicated that the data obtained using both methods were statistically comparable (**Figure 3.4**).

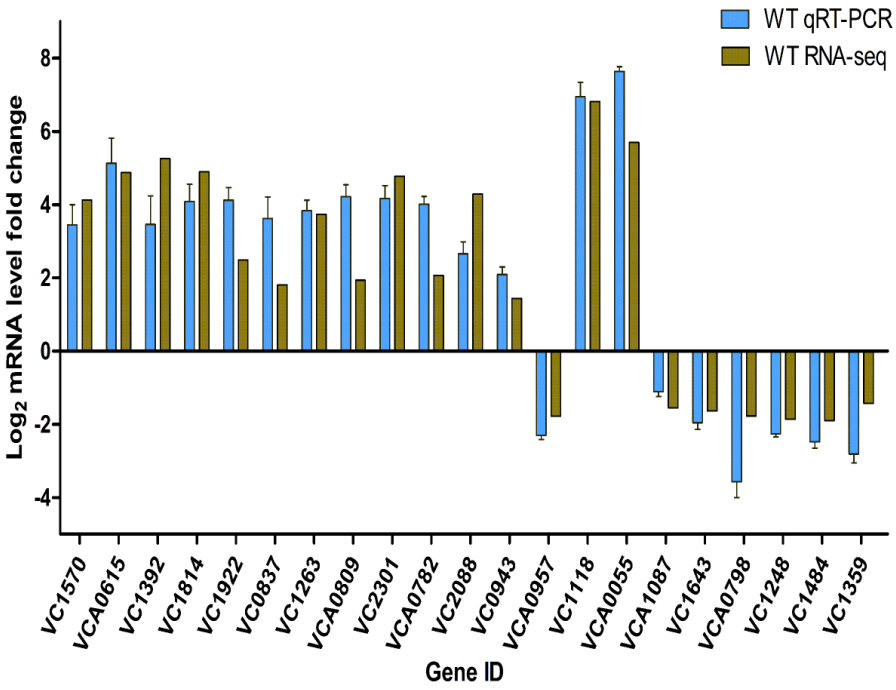

Figure 3.4: Validation of RNA-seq data by qRT-PCR. RNA-seq results of selected 21 DEGs (Set 2) were compared with qRT-PCR results. Blue bars with standard errors represent relative transcript levels ($\log_2$ fold) determined by qRT-PCR from three independent biological replicates. Green bars represent transcript levels determined using RNA-seq.

To determine whether such genome-wide regulation in *V. cholerae* is specific to BL, cells were also grown under red light (RL) condition. After preparation of cDNAs from RL- and dark-treated cells, the transcriptional levels of Set2 DEGs were measured by qRT-PCR. As shown in **Figure 3.5**, RL did not significantly affect the transcription of these genes, suggesting that these DEGs are specifically responsive to BL.

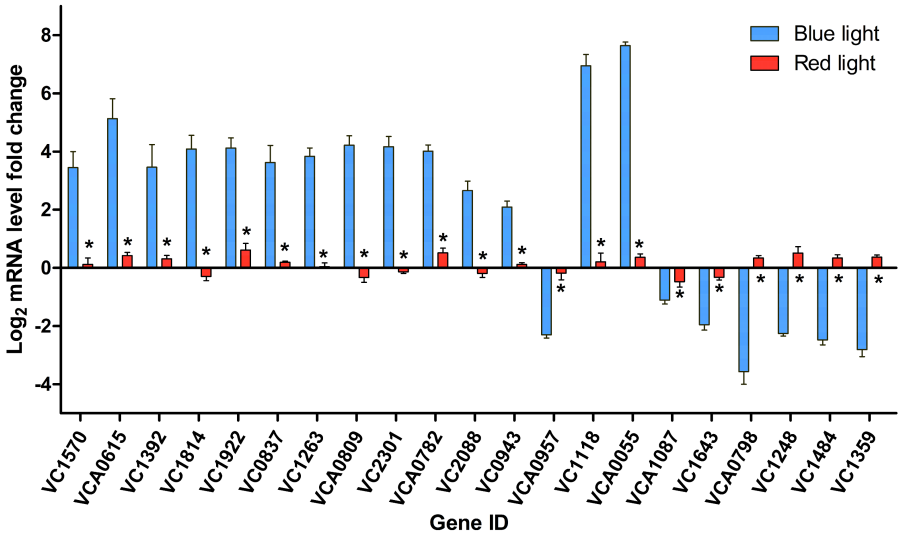

Figure 3.5: Effect of blue light (BL) and red light (RL) on expression levels of differentially expressed genes (DEGs). Transcript levels of selected 21 DEGs (Set 2) were determined after exposure of wild-type cells to BL and RL. Blue (BL exposure) and red (RL exposure) bars with standard errors represent relative mRNA expression levels ($\log_2$ fold) determined by qRT-PCR from three independent biological replicates. n = 6, $\star$ $p < 0.05$, Student's t-test.

3.3.3 Blue light regulated pathways as determined by GO term and KEGG pathway enrichment analyses

To functionally categorize DEGs in cells exposed to BL, a GO term enrichment analysis was performed using the PANTHER classification tool [Mi et al., 2013]. The assigned GO terms were used to classify functions of the DEGs based on biological processes, molecular functions, and cellular components.

To define the biological functions of Set1 DEGs, GO and KEGG analyses were carried out. Forty-five significantly enriched GO terms ($p<0.05$) were identified, including single-organism metabolic process (61 genes), oxidation-reduction process (32

genes), metabolic process (83 genes), cellular respiration (13 genes), aerobic respiration (10 genes), tricarboxylic acid cycle (nine genes), carboxylic acid metabolic process (27 genes), single-organism process (72 genes), chemotaxis (nine genes), response to chemical (10 genes), catalytic activity (70 genes), DNA photolyase activity (four genes), and plasma membrane (21 genes). Then, a GO term network was constructed using Cytoscape with the BINGO plug-in [Maere et al., 2005]. As shown in the results of the GO term network analysis in **Figure 3.6A**, metabolic processes were significantly ($p<0.05$) linked to cellular respiration, fatty acid oxidation, cofactor metabolic processes, and organic acid metabolic processes. Additionally, a molecular function network analysis indicated that genes related to FAD binding, DNA repair, oxido-reductase activity, and electron carrier activity were significantly ($p<0.05$) linked (**Figure 3.6B**). Together, these results indicated that the respiratory chain complex, plasma membrane, and succinate dehydrogenase complex cellular components play a significant ($p<0.05$) role in the BL response of *V. cholerae* (**Figure 3.6C**).

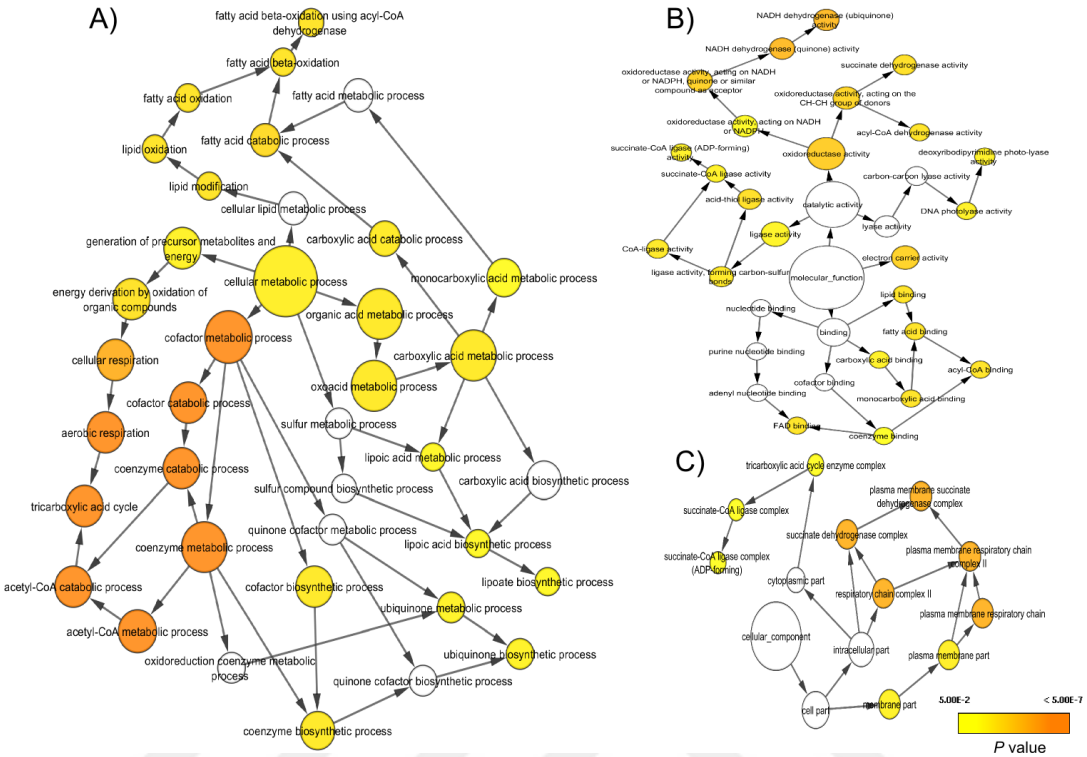

Figure 3.6: Gene Ontology (GO) term network analysis of all differentially expressed genes (Set1 DEGs). Functional enrichment analysis was performed for all DEGs with the BINGO plug-in in Cytoscape. Assigned GO terms were used to classify functions of DEGs based on **(A)** biological processes, **(B)** molecular functions, and **(C)** cellular components. Overrepresented categories were determined using a hypergeometric test with a significance threshold $p<0.05$ after Benjamini and Hochberg false discovery rate corrections

After the GO term analysis of the Set1 DEGs in response to BL, a KEGG pathway enrichment analysis was performed to identify the metabolic or signal transduction pathways that were highly regulated under BL. Of the Set1 DEGs, 145 were assigned to 14 significantly enriched pathways (**Table 3.5**) and the remaining DEGs were categorized as hypothetical genes. The following pathways were found to be significantly ($p<0.05$) up-regulated under BL: citrate cycle (TCA cycle), butanoate metabolism, geraniol degradation, C5-branched dibasic acid metabolism, propanoate metabolism, lysine degradation, oxidative phosphorylation, carbon metabolism, fatty acid degradation, and biosynthesis of secondary metabolites. The following pathways

were found to be significantly ($p<0.05$) down-regulated under BL: bacterial chemotaxis, two-component system, glyoxylate and dicarboxylate metabolism, and ABC transporters. Since most of the GO and KEGG assignments and distributions were related to energy metabolism, biosynthesis of secondary metabolites, DNA repair, and bacterial chemotaxis, our results indicated that the DEGs were involved in a wide range of regulatory functions in *V. cholerae*. Among the Set1 DEGs, 77 were categorized as hypothetical proteins in the current KEGG database, highlighting that our understanding of the molecular mechanism of the BL response in *V. cholerae* is incomplete. We used the Annocript pipeline [Musacchia et al., 2015] to annotate these 77 hypothetical DEGs. Annocript successfully annotated 28 DEGs as being involved in ROS inactivation, based on data at the Swiss-Prot (SP) and UniRef90 databases [Suzek et al., 2007] (**Appendix Table A.2**). These results indicated that some of these hypothetical genes encode putative glutaredoxin (VC2044) and thioredoxin-dependent thiol peroxidase (VC2160) proteins, which protect cells from photo-oxidative stress.

Table 3.5: Significantly up-(UR) and down-regulated (DR) KEGG pathways in wild-type cells under BL ($p<0.05$).

KEGG pathway name	**KEGG pathway ID**	**# of DEGs**	**# of total genes**	**p-value**	**up- or down-regulated**
Citrate cycle (TCA cycle)	vch00020	9	24	5.97E-06	UR
Butanoate metabolism	vch00650	7	27	2.48E-03	UR
Geraniol degradation	vch00281	3	5	8.20E-03	UR
C5-Branched dibasic acid metabolism	vch00660	4	11	8.42E-03	UR
Propanoate metabolism	vch00640	5	19	9.87E-03	UR
Lysine degradation	vch00310	3	7	1.61E-02	UR
Oxidative phosphorylation	vch00190	6	34	2.37E-02	UR
Carbon metabolism	vch01200	11	90	2.65E-02	UR
Fatty acid degradation	vch00071	3	9	2.72E-02	UR
Biosynthesis of secondary metabolites	vch01110	23	248	3.07E-02	UR
Bacterial chemotaxis	vch02030	10	67	8.79E-03	DR
Two-component system	vch02020	9	146	3.23E-04	DR
ABC transporters	vch02010	7	126	2.88E-03	DR
Glyoxylate and dicarboxylate metabolism	vch00630	2	22	4.79E-02	DR

3.3.4 Cryptochrome -DASHes of V. cholerae are not blue light photoreceptors

A class of the cryptochrome/photolyase family (CPF) called CRY-DASH, found in algea, bacteria, plants, and animals [Brudler et al., 2003], was originally classified as cryptochrome since no photolyase activity could be detected *in vitro* and *in vivo* with photolyase complementation assays [Asimgil and Kavakli, 2012, Hitomi et al., 2000, Kleine et al., 2003, Worthington et al., 2003]. VcCRY1 (CRY-DASH) from *V. cholerae* was co-purified with RNA which indicates its affinity towards single stranded nucleic acids [Worthington et al., 2003]. Subsequent studies showed that CRY-DASH proteins have photolyase activity, and specifically repair CPD photoproducts in single-stranded DNA (ssDNA) rather than double-stranded DNA (dsDNA). Therefore, they are called ssDNA photolyases [Selby and Sancar, 2006]. Previous studies have shown that both cryptochrome and photolyase regulate several genes in response to BL, in organisms ranging from fungi to plants [Ahmad and Cashmore, 1993, Bayram et al., 2008, Berrocal-Tito et al., 2007, Berrocal-Tito et al., 1999]. In addition, DEG analysis showed that operons containing genes in the CPF (VC1392, VC1814 and VCA0057) were highly up- regulated after BL exposure, raises possibility of the CPF in BL reception and genome-wide regulation. Therefore, we generated a triple-knockout mutant ($\Delta cry1\Delta cry2\Delta phr$) to investigate the roles of CPF in BL regulation. The triple mutant cells were exposed to BL and then RNA-seq was performed. Analyses of the RNA-seq data from wild-type and triple mutant cells revealed that the same genes (Set1 DEGs) were up- and down-regulated under both dark and BL conditions, as shown in the heat map (**Figure 3.7**). This result indicated that cryptochrome/photolyase genes are not involved in BL-mediated gene expression in *V. cholerae*.

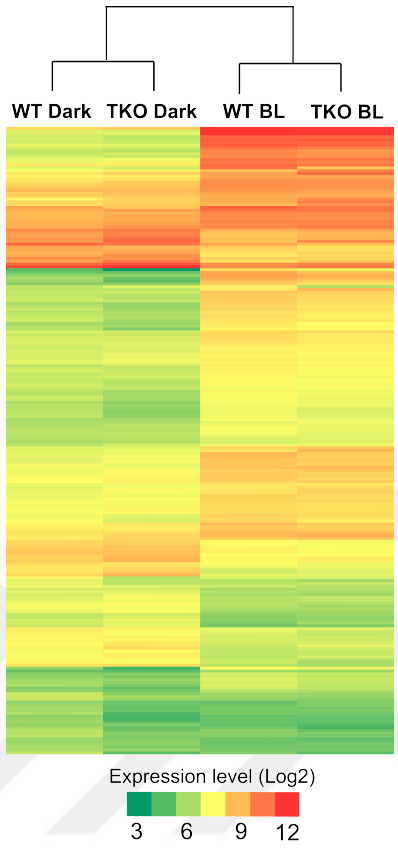

Figure 3.7: Heatmap display of expression values of differentially expressed genes in wild-type and Δ*cry1*Δ*cry2*Δ*phr* knockout (TKO) cells. Expression levels are represented by color: green, lowest expression level; yellow, moderate expression level; red, highest expression level. Extreme values in color gradient are 3 to 12 in $\log_2$ scale.

3.3.5 Blue light induces genome-wide transcriptional modulation due to photo-oxidative stress

Various environmental stimuli, including high-fluence BL, result in ROS generation. These molecules can act as signaling molecules to regulate a number of developmental processes and stress responses in bacteria [Anthony et al., 2005, Elías-Arnanz et al., 2011, Ziegelhoffer and Donohue, 2009]. We performed a series of experiments to determine whether *V. cholerae* produces ROS under BL conditions or not. Cells

were exposed to BL for various time periods and total ROS were measured using the fluorogenic dye 2',7' dichlorofluorescein diacetate (DCF-DA). There was a gradual increase in intracellular ROS levels over time, and ROS production was saturated after 45 min of BL exposure (**Figure 3.8**). The results showed that BL induced the formation of ROS, which caused oxidative stress in *V. cholerae*. This phenomenon, the so-called photo-oxidative stress response, has been observed in many different organisms including phototrophic and non-phototrophic bacteria [Seib et al., 2006, Ziegelhoffer and Donohue, 2009] such as *R. sphaeroides* [Anthony et al., 2005], *M. xanthus* [Gorham et al., 1996], *Pseudomanas aeruginosa* [Orlandi et al., 2015], and *Caulobacter crescentus* [Lourenço and Gomes, 2009].

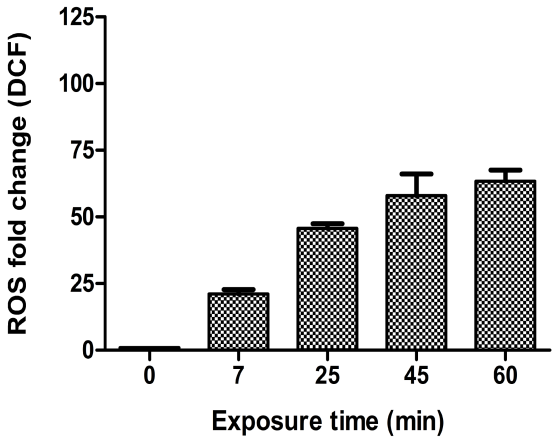

Figure 3.8: Time-dependent reactive oxygen species (ROS) accumulation after blue light (BL) exposure. Cells were exposed to BL (50 μmoles $m^{-2}s^{-1}$) for 45 min. Samples were taken at 7, 25, 45, and 60 min after BL exposure and total ROS amount were measured using 2',7'-dichlorofluorescin diacetate (DCF-DA). Fold change was calculated between dark- and BL-treated samples at indicated times.

3.3.6 ChrR and SigmaE regulate gene expression in a blue light-dependent manner

To identify the genes mediating BL regulation in *V. cholerae* at the genome-wide level, we analyzed the operons that were most strongly responsive to BL. Studies on *R. sphaeroides* [Anthony et al., 2005] and *C. crescentus* [Lourenço and Gomes, 2009] have indicated that the effect of light-generated ROS is mediated by anti-sigma ChrR and its cognate partner SigmaE (σ^E), and in turn, genome-wide regulation of specific genes occurs in a BL-dependent manner. We identified a highly up-regulated putative ChrR operon consisting of *ChrR* (VC2301), *SigmaE* (VC2302) and a hypothetical gene (VC2303). To investigate the role of ChrR in the photo-oxidative response, we generated a Δ*ChrR V. cholerae* mutant. Dark- and BL-treated Δ*ChrR* cells were subjected to RNA-seq to identify DEGs. Analysis of the RNA-seq results indicated that 159 DEGs (Set 3 DEGs) out of the Set1 DEGs identified in wild-type cells were no longer regulated in the Δ*ChrR* mutant, while the remaining 63 of the Set1 DEGs were still up- and down-regulated. In the Δ*ChrR* mutant, the mRNA expression levels of these Set3 DEGs were elevated in the dark, so their expression level did not change after BL exposure (WT BL vs. Δ*ChrR* Dark in **Figure 3.9**). This finding indicated that the *ChrR* gene suppresses the transcription of Set3 DEGs.

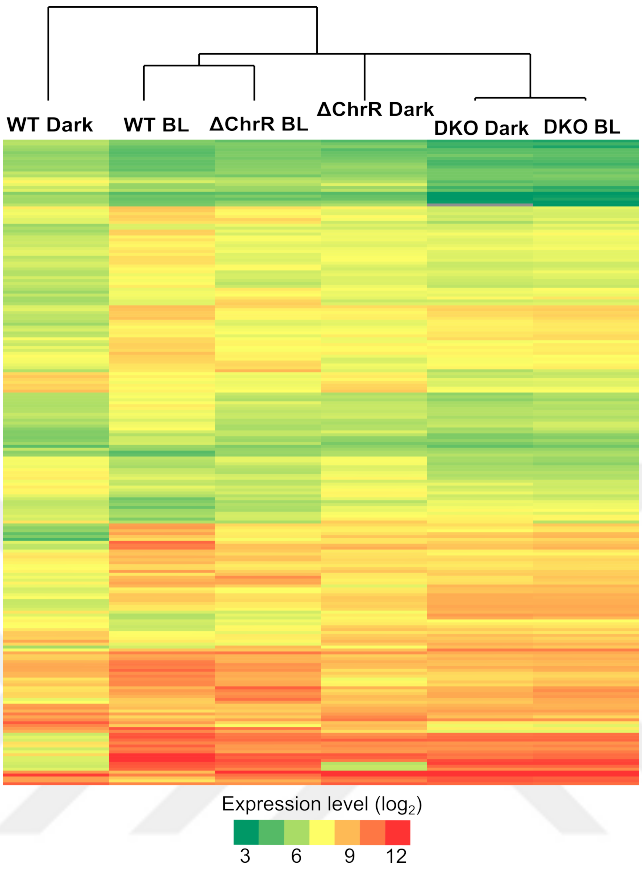

Figure 3.9: Heatmap display of expression values of differentially expressed genes in in wild-type, $\Delta ChrR$, and $\Delta ChrR\Delta MerR$ knockout (DKO) cells under dark and blue-light conditions. Expression levels are represented by color: green, lowest expression level; yellow, moderate expression level; red, highest expression level. Extreme values in color gradient are 3 to 12 in $\log_2$ scale.

A number of studies have shown that ChrR and σ^E work together to regulate the genome-wide BL transcription response in various organisms [Braatsch et al., 2004, Glaeser et al., 2011, Ziegelhoffer and Donohue, 2009]. Since we observed that some DEGs were controlled by ChrR, we investigated whether it works with its cognate partner σ^E, whose transcription is controlled by the same operon. We therefore generated the $\Delta SigmaE$ *V. cholerae* mutant and subjected it to a BL treatment. We prepared cDNA from the total RNA and measured the transcript levels of selected

DEGs out of the 159 genes that were not regulated in the Δ*ChrR* mutant by qRT-PCR. Like in Δ*ChrR* cells, Set2 DEGs in Δ*SigmaE* cells were not differentially regulated in response to BL (**Figure 3.10A**). However, the transcript levels of the Set2 DEGs in BL-treated Δ*SigmaE* cells were similar to those in dark-treated wild-type cells. These results indicated that ChrR and σ^E work together in the response to BL, where σ^E activates the transcription of the Set3 DEGs. These results showed that in the dark, ChrR binds to and suppresses σ^E. Upon exposure of cells to BL, σ^E released from its cognate partner ChrR and σ^E binds to either the operon or to the promoter regions of genes regulated by photo-oxidative stress, as shown in other organisms [Anthony et al., 2005, Gorham et al., 1996, Orlandi et al., 2015]. We also analyzed the upstream regions of the Set3 DEGs whose transcriptional regulation depended on ChrR and σ^E by using the 'dna pattern' tool at the RSA website (`http://rsat.ulb.ac.be/rsat`) to find consensus σ^E-binding sequences [Thomas-Chollier et al., 2008]. The following promoter sequence recognizable by the σ^E factor was deduced: TGATC-N18-CGTAT [Newman et al., 1999]. This consensus sequence was found (**Figure 3.10B**) in the upstream of 31 operons and 29 genes (**Appendix Table A.3**), implying that they were regulated by activated σ^E in *V. cholerae*.

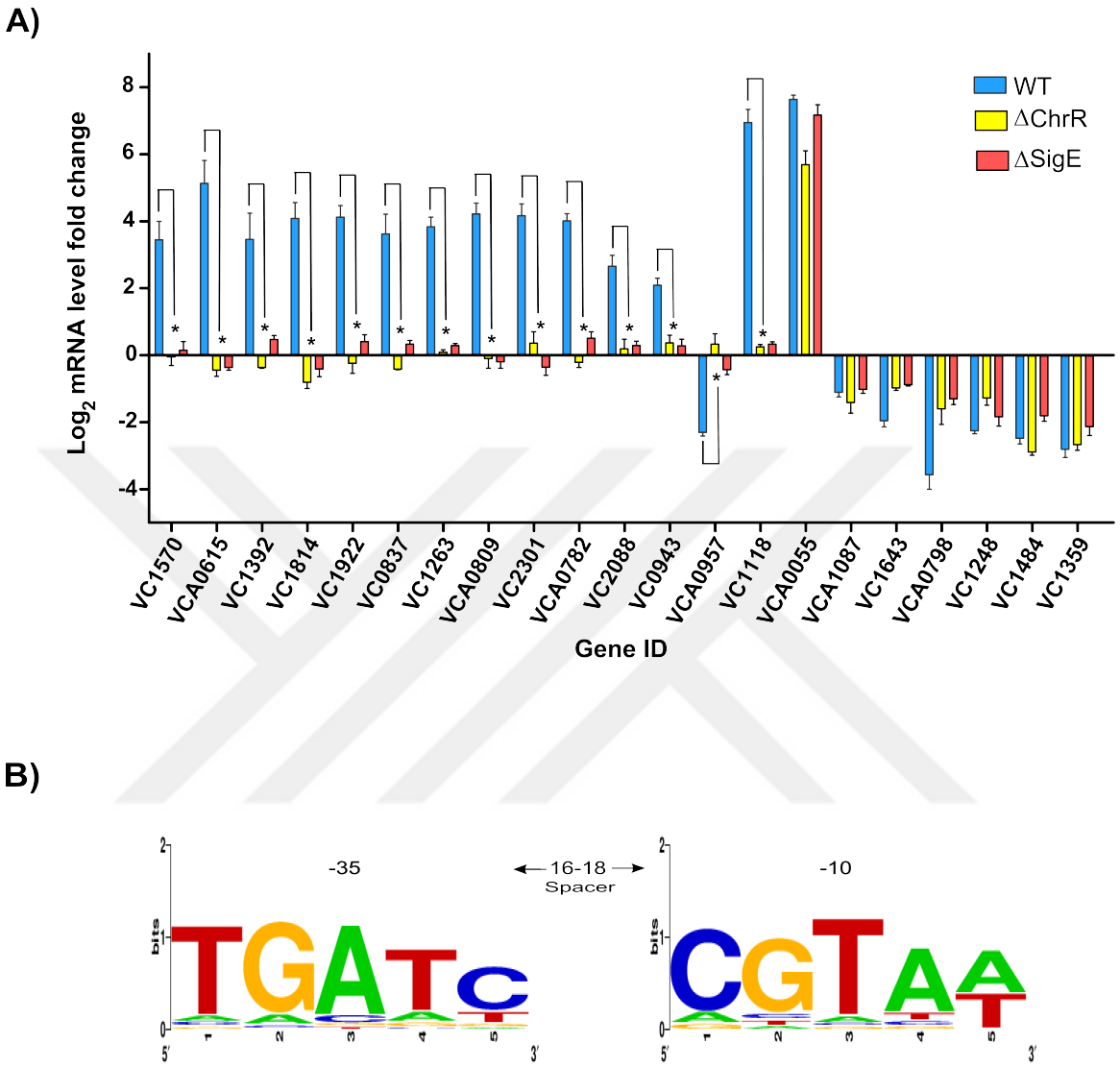

Figure 3.10: Effect of blue light (BL) on wild-type, Δ*ChrR*, and Δ*SigmaE* cells. **(A)** Transcript levels of selected 21 DEGs were determined after exposing cells to BL. Blue bars (fold change in wild-type cells), green bars (fold change in Δ*ChrR* mutant) and red bars (fold change in Δ*SigmaE* mutant) with standard errors represent relative mRNA expression levels ($\log_2$ fold) determined by qRT-PCR from three independent biological replicates. n = 6, $\star$ p < 0.05, Student's t-test. **(B)** Putative σ^E- dependent promoter motif identified in upstream region of genes controlled by σ^E. Sequence of σ^E- binding motif (TGATC-N16-18-CGTAW, where W is A or T) derived from upstream of *SigmaE* (VC2302) was used to search upstream regions (-300 to +5 relative to predicted translation start site, +1) of all putative σ^E- dependent genes, allowing for two substitutions. Co-ordinate represents the position of 3'-end nucleotide of putative σ^E-binding motif relative to translation start site (+1).

A KEGG pathway enrichment analysis was carried out to identify the metabolic pathways of genes that were strongly regulated in response to BL in the Δ*ChrR* mutant. Out of 63 DEGs, 22 were assigned to 11 significantly enriched pathways and 18 were categorized as hypothetical genes. Comparison of the affected pathways between the Δ*ChrR* mutant and wild-type cells revealed that geraniol degradation, fatty acid degradation, propanoate metabolism, and butanoate metabolism pathways (**Table 3.6**) were still significantly regulated in response to BL in the Δ*ChrR* mutant.

Table 3.6: Significantly up- and down-regulated KEGG pathways in Δ*ChrR* mutants under blue light ($p<0.05$).

KEGG pathway name	**KEGG pathway ID**	**# of DEGs**	**# of total genes**	**p-value**	**up- or down-regulated**
Geraniol degradation	vch00281	3	5	4.91E-04	UR
Fatty acid degradation	vch00071	3	9	1.81E-03	UR
Propanoate metabolism	vch00640	3	19	1.09E-02	UR
Fatty acid metabolism	vch01212	3	19	1.09E-02	UR
Valine, leucine and isoleucine degradation	vch00280	2	9	2.21E-02	UR
Butanoate metabolism	vch00650	3	27	2.54E-02	UR
C5-Branched dibasic acid metabolism	vch00660	2	11	3.05E-02	UR
Histidine metabolism	Vch00340	2	14	4.44E-02	UR
Bacterial chemotaxis	vch02030	8	67	2.20E-11	DR
Two-component system	vch02020	7	146	6.32E-11	DR
ABC transporters	vch02010	6	126	2.50E-04	DR

3.3.7 Blind phenotype of ΔChrRΔMerR double-knockout mutant in BL response

As mentioned above, the RNA-seq data from the Δ*ChrR* mutant cells indicated that an additional gene was responsible for regulating 63 genes under BL condition. To identify this gene, we examined the transcript levels of the DEGs in Δ*ChrR* cells. We found that *MerR-like* (VCA0056) gene was highly regulated together with *phr* (VCA0057) gene, which are found as an operon. Proteins from the MerR family of transcriptional

regulators (originally described as proteins involved in mercury resistance) are known to mediate light-induced carotenoid synthesis in both *Streptomyces coelicolor* and in *M. xanthus* [Takano et al., 2006a, Takano et al., 2006b]. To investigate the possible role of MerR in the BL response of *V. cholerae*, we generated $\Delta ChrR\Delta MerR$ double-knockout (KO) mutant and performed RNA-seq analyses of these cells under both dark and BL conditions. After analyzing DEGs in the double KO cells, we observed a light-blind phenotype (**Figure 3.9**). This result indicated that putative MerR-like protein in *V. cholerae* play a role in transmission the effect of the BL. We further analyzed the RNA-seq data from the double KO cells to understand the role of MerR in the transcriptional regulation of DEGs. The transcript levels of some of the DEGs were comparable to those in dark-treated wild-type cells (**Figure 3.9**), while those of other DEGs were comparable to those in BL-treated wild-type cells. These data suggested that MerR may act as a suppressor or an enhancer of those 63 genes. In this second ROS-mediated signaling cascade, upon exposure of cells to BL, MerR releases from its promoter and binds to the promoter regions of those 63 DEGs and results in down- and up-regulation. To verify that ROS was still produced in these mutants, the cells were exposed to BL and the ROS production was measured. As shown in **Figure 3.11**, ROS were produced in comparable amounts in all of the mutants. Based on these results, we concluded that ChrR and MerR together regulate gene expression in response to photo-oxidative stress by BL-generated ROS through two separate signaling cascades.

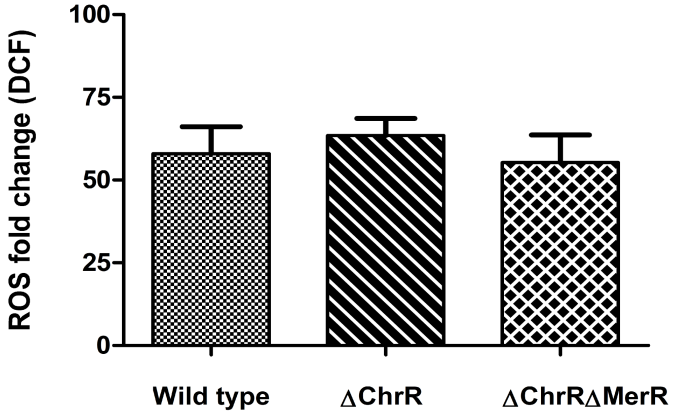

Figure 3.11: Reactive oxygen species (ROS) accumulation in wild-type and mutant cells after blue light (BL) exposure. Cells were exposed to BL (50 μmoles $m^{-2}s^{-1}$) for 45 min, then samples were collected 45 min later and total ROS amount was measured using 2',7' dichlorofluorescein. Fold change was calculated between dark- and BL-treated samples at indicated times.

3.3.8 Blue light prompts V. cholerae to produce ROS by oxidative phosphorylation

Both GO and KEGG pathway analyses of the DEGs in wild-type cells provided insights into the main biological processes and pathways related to catabolic reactions. Among these pathways, "propanoate metabolism" and "fatty acid degradation" catabolize imported nutrients into products that are the initial substrates for "citrate cycle (TCA cycle)", "butanoate metabolism" and "C5-Branched dibasic acid metabolism". These catabolic pathways provide NADH and $FADH_2$ as substrates for the oxidative phosphorylation (electron transport) pathway that produces ATP under aerobic conditions [Hatefi, 1985]. These results indicated that BL prompts *V. cholerae* to produce energy by cellular respiration.

Several studies have shown that the oxidative phosphorylation pathway is the major source of ROS produced in various organisms [Drose, 2013, Li et al., 2013b, Seib

et al., 2006]. Therefore, we hypothesized that ROS production was initiated from oxidative phosphorylation upon exposure of *V. cholerae* cells to BL. To investigate this hypothesis, we treated cells with the uncoupling reagent 2,4-dinitrophenol (DNP), a protonophore that uncouples oxidative phosphorylation and results in decreased total ROS production [Brand, 2000, Liu and Chen, 1997, Mailloux and Harper, 2012, Miwa and Brand, 2003]. The cells were treated with uncoupler DNP in the presence and the absence of BL, and then total ROS production was measured. Cells were incubated with DNP for 60 min in the dark and then irradiated with BL. As seen in **Figure 3.12A**, ROS production was significantly ($p<0.05$) lower in DNP-treated cells compared to untreated control cells after BL exposure. We conducted qRT-PCR analyses to quantify the transcript levels of Set2 DEGs in the DNP-treated cells, using *gapdh* as the reference gene. The transcript levels of the selected Set2 DEGs differed significantly after BL exposure between the untreated and DNP-treated cells (**Figure 3.12B**). These results revealed that BL causes ROS production through oxidative phosphorylation and results in genome-wide gene regulation in *V. cholerae*.

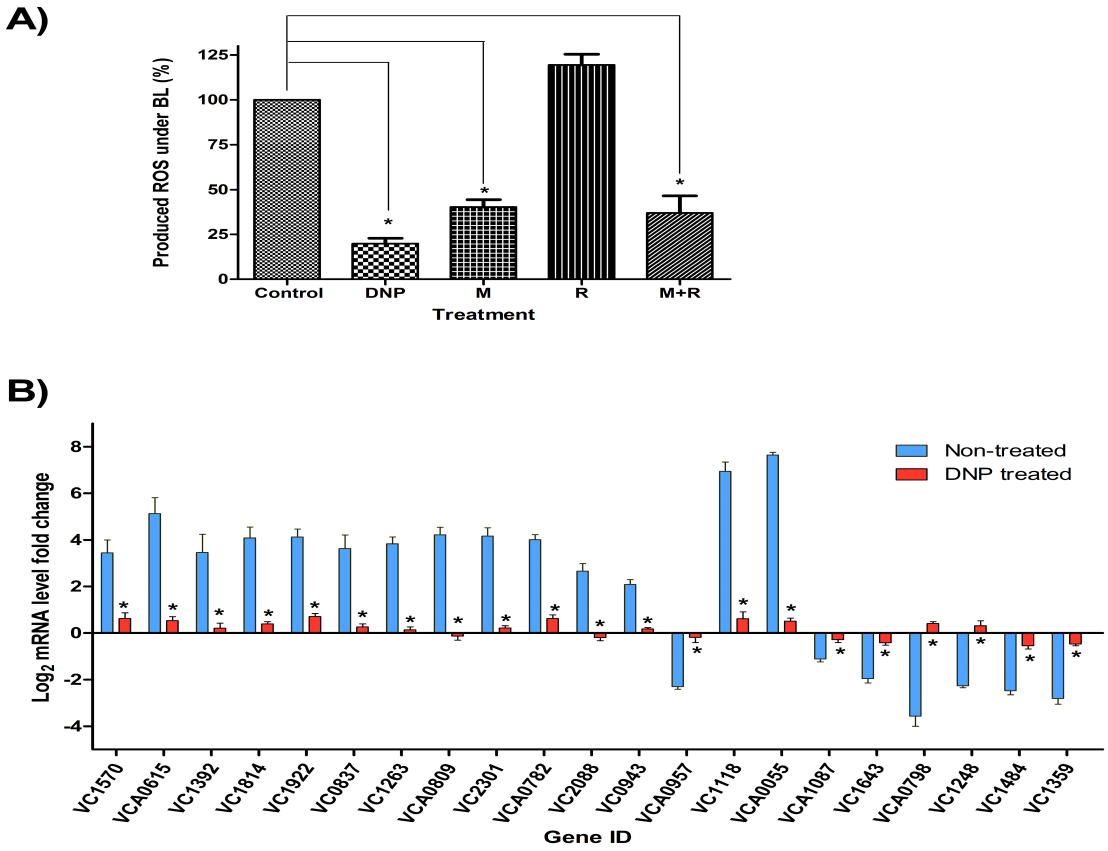

Figure 3.12: Reactive oxygen species (ROS) accumulation under blue light (BL) after chemical treatments and expression analysis of 2,4-dinitrophenol (DNP)-treated wild-type cells. **(A)** Samples were treated with 20 mM malonate (M), 100 μM rotenone (R), or 500 μM DNP for 60 min in darkness, then cells were exposed to BL (50 μmoles $m^{-2}s^{-1}$) for 45 min. Fold change was calculated between dark- and BL-treated samples, and then percentage change for each treatment was calculated after setting amount of ROS in wild-type cells at 100%. Error bar: $\pm$SD, n=6, $\star$ $p < 0.05$, Student's t-test. **(B)** Transcript levels of selected DEGs were quantified by qRT-PCR after wild-type cells were treated with DNP. Blue (non-treated wild-type cells) and red (DNP-treated wild-type cells) bars with standard errors represent relative mRNA levels ($\log_2$ fold) determined by qRT-PCR from three independent biological replicates. Error bar: $\pm$SD, n=6, $\star$ $p < 0.05$, Student's t-test.

In addition, analyses of Set1 DEGs and the GO term network revealed that genes encoding components of complex I and II were highly up-regulated under BL. The transcript levels of genes encoding all six subunits (components of the complex I)

of Na^+-translocating NADH-quinone reductase (Na^+-NQR) (VC2290-VC2295) were up-regulated in response to BL. A previous study showed that Na^+-NQR represents a major source of extracellular singlet oxygen production in *V. cholerae* cells [Lin et al., 2007]. Also BL exposure resulted in increased transcript levels of genes encoding the succinate dehydrogenase ironsulfur subunit (VC2088), the succinate dehydrogenase flavoprotein subunit (VC2089), the succinate dehydrogenase hydrophobic membrane anchor protein (VC2090), and the succinate dehydrogenase cytochrome b556 large membrane subunit (VC2091). Succinate dehydrogenase (complex II) is a flavin-containing enzyme that functions in the TCA cycle as well as in complex II of the electron transport chain (ETC). It catalyzes the oxidation of succinate to fumarate and the reduction of ubiquinone to ubiquinol, thereby linking the TCA cycle to the ETC [Cecchini, 2003]. This protein was shown to be the major source of ROS production resulting in oxidative stress [Seib et al., 2006].

To identify the source of BL-induced ROS production in the respiratory chain, we inhibited various components of the respiratory chain. Rotenone inhibits electron transfer (taken from NADH) from the Fe-S center of complex I (NADH dehydrogenase complex) to ubiquinone, whereas malonate inhibits electron transfer (taken from $FADH_2$) from complex II (succinate dehydrogenase complex) to ubiquinone. Therefore, after cells were treated with rotenone or malonate, ROS production was measured under both dark and BL conditions. As seen in **Figure 3.12A**, ROS production was reduced by 50% in the malonate-treated cells, while ROS production in the rotenone-treated cells was statistically comparable to that in control cells in response to BL. However, ROS was still produced in the malonate-treated cells, implying that there are electron inputs from other proteins to the respiratory chain. The Set1 DEGs and GO term network analyses indicated that genes encoding acyl CoA dehydrogenase (VC1740 and VC2231), which participates in β-oxidation of fatty acids, were up-regulated under BL. Acyl-CoA dehydrogenase produces $FADH_2$, and then electrons from $FADH_2$ are transferred to ubiquinone, the site of ROS production by Q-oxidoreductase (**Figure**

3.13) [Seib et al., 2006]. Therefore, it is possible that the remaining 50% of ROS were produced by ubiquinone after β-oxidation of fatty acids. Taken together, these results show that BL regulates gene transcription at a genome-wide level by increasing ROS production via the respiratory chain from succinate dehydrogenase, and possibly from ubiquinone.

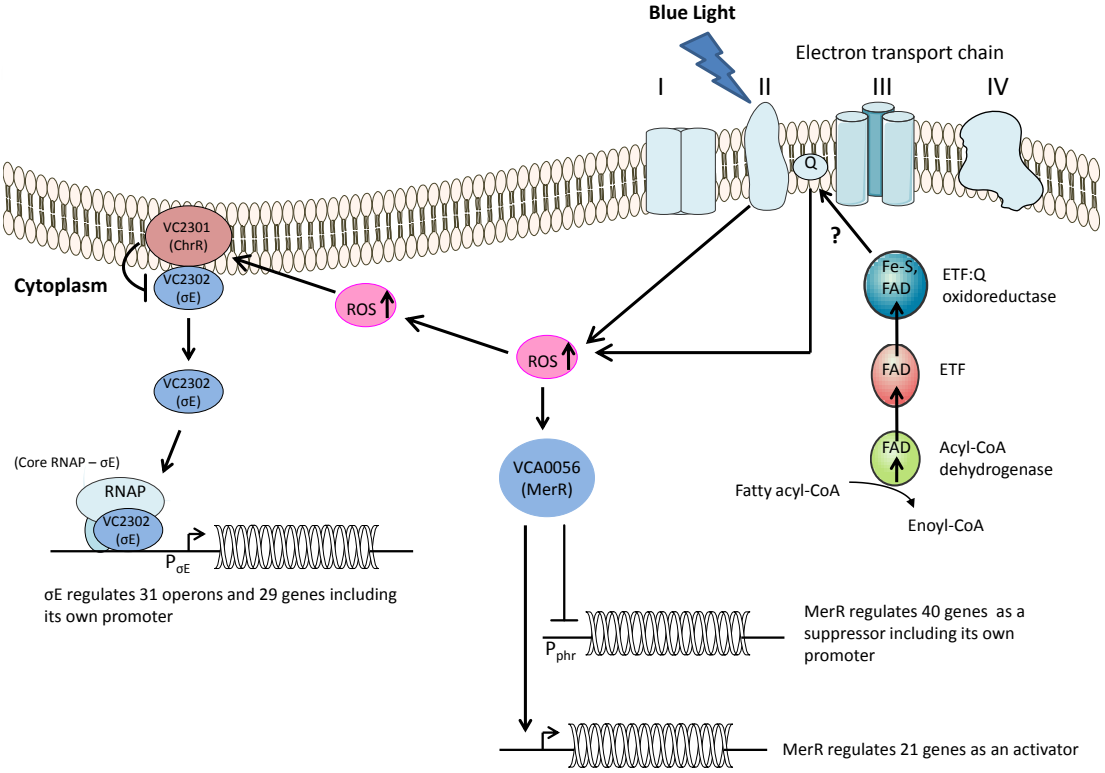

Figure 3.13: Model summarizing blue-light-mediated gene regulation pathway in *V. cholerae*. Blue light (BL) excites succinate dehydrogenase (complex II) in electron transport chain, which interacts with molecular oxygen to generate ROS. ROS inactivates ChrR, the anti-σ^E factor. Dissociated σ^E associates with core RNAP, and corresponding RNAP holoenzyme activates Pσ^E, promoter of the regulatory ChrR-σ^E operon. σ^E regulates expression levels of 159 genes. Also, ROS interacts with MerR, which initiates a second cascade in BL-mediated gene regulation pathway. MerR suppresses or enhances expression levels of 63 genes includes its own gene. Ovals depict protein factors, short arrows show genes or operons, solid arrows and blunt-ended lines indicate positive and negative regulation, respectively.

Chapter 4

RNA-SEQ ANALYSIS OF THE TRANSCRIPTIONAL RESPONSE TO BLUE AND RED LIGHT IN THE EXTREMOPHILIC RED ALGA, *CYANIDIOSCHYZON MEROLAE*

4.1 Background

Algae are essentially autotrophic organisms that have evolved diverse adaptation strategies to survive in a wide range of terrestrial and aquatic habitats. Algae show wide variations in morphological, ecological, and biochemical traits, which indicate the presence of different genes among this group of organisms. This extremely wide diversity indicates that algae have developed different strategies to respond to different environmental stimuli [Delwiche and Cooper, 2015]. Among the various stimuli, light is one of the main environmental cues that affects the physiology and behavior of many organisms. Since the intensity and the duration of light quite vary depending on the ecosystem, algae may detect changes in the intensity of light to produce appropriate responses to regulate their growth, development, and other physiological variables accordingly [Fortunato et al., 2015, Kianianmomeni and Hallmann, 2014].

Although the effects of light have been extensively studied at the physiological and molecular levels in plants and green algae [Hegemann, 2008, Talarico and Maranzana, 2000], few studies have investigated the direct effect of light on red algae at the genome-wide level. Several studies have suggested that light regulates several physiological parameters in the red alga *Cyanidioschyzon merolae*. In this organism, organelle

division is closely related to the cell cycle, and organelles divide synchronously with the light/dark cycle [Nishida et al., 2005]. These processes are cyclic and are likely to be controlled by a circadian clock entrained by photoreceptors [Terui et al., 1995]. A plastid DNA microarray showed that four sigma factor genes in *C. merolae* were differentially regulated upon illumination with white light [Minoda et al., 2005]. In addition, *C. merolae* has no genes encoding photoreceptors other than those in the cryptochrome/photolyase gene family (CPF) (Matsuzakiet al. 2004; [Asimgil and Kavakli, 2012]. Characterization of CPF members in this organism showed that it contains three cryptochrome-DASHs, one (6-4) photolyase, and three plant-like cryptochromes [Asimgil and Kavakli, 2012]. Collectively, these findings suggest that light is a very important factor that tightly regulates gene expression to control photomorphogenic responses through transcription factors in this primitive organism.

In this study, we selected the red alga *C. merolae* to investigate the effects of specific light qualities (blue and red light) on transcription at the genome-wide level. We chose this organism for the following reasons: firstly, because it has the smallest and most compact genome (∼16 MB) among photosynthetic eukaryotes [Matsuzaki et al., 2004, Nozaki et al., 2007]. Secondly, *C. merolae* has only CPF photoreceptors, which makes it an ideal organism to study the role of CPFs in photoreception. Thirdly, *C. merolae* has been shown to alter its pigment composition, growth, and energy transfer patterns under different light spectra [Ueno et al., 2015]. Finally, complete sequences are available for the *C. merolae* genome and those of its organelles [Matsuzaki et al., 2004, Nozaki et al., 2007].

In this study, analyses of RNA-seq data indicated that 35% (1799 genes) of the total genes in *C. merolae* were regulated by blue (BL) and red light (RL). Further analysis revealed a light-specific genome-wide transcriptional regulation. Our results showed that BL solely regulates transcription of 683 genes (13% of total genes) while RL solely regulates the transcription of 521 genes (10%). The remaining 595 genes

(12%) were commonly regulated both by BL and RL. Gene ontology (GO) term and Kyoto Encyclopedia of Genes and Genomes (KEGG) pathway enrichment analysis revealed that genes with roles in photosynthesis, tRNA and ribosome biosynthesis, pigment biosynthesis and carbon metabolic pathways were regulated by RL. Consistent with its role in global gene regulation, cryptochrome genes (*CmPHR2, CmPHR3* and *CmPHR7*) were differentially regulated by BL, suggesting that they have a potential role in light-dependent transcriptional regulation in *C. merolae*.

4.2 Materials and Methods

4.2.1 Growth conditions and light experiments

C. merolae 10D cells were grown in 2xAllens medium (2xMA) at pH 2.3 [Minoda et al., 2004]. Fifty-mL flasks containing *C. merolae* cultures were shaken under continuous light (100 μmoles $m^{-2}s^{-1}$) at 42^0C. For the blue light (BL) experiments, exponentially growing cells were sub-cultured to OD_{750}=0.6 (3x10^7 cells/ml) in 50 mL of 2xMA and then placed into complete darkness for 36 hours by covering the tubes with aluminum foil. Then, the cells were exposed to BL (15 μmoles $m^{-2}s^{-1}$, fluorescent black light source with 20W/each, General Electric, USA) for 30 minutes. BL intensity was measured with a UVX Digital Radiometer (UVP, USA) at 365 nm. For red light (RL) experiments, dark kept cells were exposed to RL (15 μmoles $m^{-2}s^{-1}$, red led light source model P10, NJ, CHINA) for 30 minutes. RL intensity was measured by Thorlabs PM100 console system (Thorlabs, USA) at 630 nm. To assess the effect of reactive oxygen species (ROS), cells grown under complete darkness were treated with 600 μM hydrogen peroxide (H_2O_2) for 45 minutes.

4.2.2 Assessment of photo-oxidative stress

The fluorogenic dye 2',7' dichlorofluorescein diacetate (DCF-DA) was used to detect total ROS production. After DCF-DA diffuses into the cell, it is deacetylated by cellular esterases into a non-fluorescent compound that is subsequently oxidized by ROS into 2',7' dichlorofluorescein (DCF) [Gomes et al., 2005]. Briefly, exponentially growing cells were sub-cultured to OD_{750}=0.6 in 50 mL of 2xMA and then placed into complete darkness for 36 hours by covering the tubes with aluminum foil. After that, cells were harvested by centrifugation at 7000xg for 5 minutes, washed once with PBS and resuspended in 15 mL PBS buffer. Cells were then incubated with 10 μM DCF-DA in the dark for 60 min and then exposed to BL (15 μmoles $m^{-2}s^{-1}$) for 30 min. After BL exposure, DCF fluorescence was detected and analyzed using an Fluoroskan Ascent microplate reader (Thermo Scientific, Waltham, MA, USA) at maximum excitation and emission spectra of 485 and 535 nm, respectively. ROS fold change between dark kept and light exposed cells was calculated.

4.2.3 Preparation of the cDNA Library for RNA-Seq

Total RNA was extracted from dark-grown and BL-exposed 5 mL cell cultures using the TRIzol reagent (Invitrogen, USA) according to the manufacturer's instructions. The quality and quantity of RNA samples were assessed using Nanodrop 2000 spectrophotometer (Thermo Scientific, USA) and 2100 BioAnalyzer (Agilent, Palo Alto, CA, USA). Only the RNA samples with $OD_{260/280}$ between 1.8 and 2.2, 28S:18S $\geq$ 1 and the RNA integrity number (RIN) $\geq$ 8 were used for library construction. After quality and quantity measurements, the RNA was treated with RNase-free DNase I (Thermo Scientific, Waltham, MA, USA) at a concentration of 1 U/μg to remove residual genomic DNA. Next, mRNAs were purified from 1 μg of total RNA using oligo (dT) magnetic beads and fragmented using fragmentation buffer with the TruSeq mRNA Sample Preparation Kit (Illumina, USA). The cleaved short RNA fragments were subjected to first-strand cDNA synthesis using random hexamer-primers,

and the second strand was synthesized using DNA polymerase I and RNase H. The double-stranded cDNAs were purified with AMPure XP beads (Beckman Coulter, USA), eluted with resuspension buffer and then subjected to 3'-end adenine nucleotide addition. Finally, sequencing adaptors were ligated to the fragments, and the cDNA fragments were enriched by PCR amplification. Enriched cDNA libraries were used for cluster generation and sequencing. Paired-end sequencing was performed for the two cDNA libraries (two biological replicates) for each condition using the Illumina MiSeq sequencing platform (Illumina, USA).

4.2.4 Transcriptome analysis

All sequence data were at 2x75-bp length. The high quality reads were saved in fastq files and deposited in the Gene Expression Omnibus (GEO) database at NCBI with the accession number GSE83828 (`http://www.ncbi.nlm.nih.gov/geo/query/acc.cgi?token=angloimifjybhav&acc=GSE83828`). The processing of fluorescent images into sequences, base calling, and quality value calculations were performed by the Illumina data processing pipeline (v1.5). For quality control, reads with adaptor contamination and low-quality bases (quality score $<$ Q30) were removed using Trimmomatic (v0.35). All the downstream analyses were based on high-quality, clean data.

The TopHat-cufflink-cuffmerge-cuffcompare-cuffdiff pipeline was used to discover novel transcripts and to identify differentially expressed genes (DEGs) [Trapnell et al., 2012]. TopHat (v2.0.5) was used to align reads to the *C. merolae* 10D reference genome. Following TopHat alignment, Qualimap software (v2.1) was used to evaluate the coverage of the alignment data [Garcia-Alcalde et al., 2012] and a Pearson's correlation analysis was conducted to obtain the transcript-level R^2 value between replicates. After mapping, cufflink-cuffmerge-cuffcompare (v2.2) tuxedo pipeline was used to assemble transcripts with default parameters. To annotate the hypothetical DEGs, we used the custom pipeline Annocript [Musacchia et al., 2015] (`https://github.com/`

`frankMusacchia/Annocript/tree/master/GUIDE`). We used Swiss-Prot (SP) and UniRef90 [Suzek et al., 2007] (version: August 2015) databases for blastp searches with the following parameters: word_size=4; e-value=10^{-5} ; num_descriptions=5; num_alignments=5; threshold=18. For each sequence, the best hit was chosen. The domain composition of putative proteins in the Conserved Domains Database [Marchler-Bauer et al., 2013] was determined by Rpsblast with the following parameters: e-value=10^{-5} ; num_descriptions=20; num_alignments=20.

Cuffdiff was used for differential expression testing between darkness and light conditions (BL and RL). Fragments per kilobases of exons per million mapped read (FPKM) and fold changes were calculated using the Cuffdiff command from the Cufflinks suite. Quartile library normalization and pooled dispersion estimation methods were performed for the differential expression analysis. We used a minimum alignment count of 10, false discovery rate (FDR) < 0.01 and the absolute value of $\mid \log_2$ fold change $\mid \geq 1$ as the threshold to judge significant differences in gene expression.

4.2.5 GO term and KEGG enrichment analysis

To functionally categorize the DEGs, a GO term enrichment analysis was conducted using the PANTHER classification system [Mi et al., 2013] (`http://www.pantherdb.org/`) with Bonferroni multiple correction testing. After GO term functional enrichment analysis, the correlations were analyzed to construct a network using the BiNGO plug-in (v2.44) (`http://apps.cytoscape.org/apps/bingo`) [Maere et al., 2005] in Cytoscape (v2.8.3) (`http://www.cytoscape.org/`) [Shannon et al., 2003]. KOBAS (v2.0) (`http://kobas.cbi.pku.edu.cn`) was used to test for the statistical enrichment of differentially expressed genes in KEGG pathways. Fisher's exact test was used to calculate p-values, and pathways with a p-value < 0.05 were designated as being significantly enriched in DEGs.

4.2.6 Validation of RNA-seq results using qRT-PCR

A total of following 36 representative light response-relevant genes were selected for the validation of RNA-seq results by qRT-PCR; CmPHR2, CmPHR3, CmPHR7, CMV081C, CMN328C, CMJ212C, CML205C, CMI244C, CMO210C, CMF012C, CMI050C, CMJ042C, CMO306C, CME023C, CMS308C, CMK188C, CMB093C, CMK115C, CMS128C, CML323C, CML196C, CMV159C, CMS311C, CMN234C, CMV209C, CMG066C, CMI129C, CML245C, CMR291C, CMT305C, CMI244C, CmSIG1, CmSIG2, CmSIG3, CmSIG4, CME194C. Total RNA was extracted using the TRIzol reagent according to the manufacturer's instructions (Invitrogen, USA). After DNase I treatment, 1 μg of total RNA was used for first-strand cDNA synthesis using random hexamer oligos. qRT-PCR was performed with the Luminaris HiGreen qRT-PCR Master Mix (Thermo Scientific, USA) on the Light Cycler 1.5 (Roche Diagnostics, Germany). qRT-PCR was performed with gene-specific primers (**Table 4.1**). *CMM193C* gene was used as an internal reference gene. This gene is the red algal homologue of the constitutively expressed gene TIP-41-like (At4g34270) in *A. thaliana* [Czechowski et al., 2005]. The amplification programs were performed according to the following protocol: 95^0C for 5 min; 40 cycles of 95^0C for 2 s, 57^0C for 10 s, and 72^0C for 10 s, followed by a thermal denaturing step to generate the melting curves. All reactions were performed in biological triplicates (each triplicate with two technical replicates), and the results were expressed relative to the transcript level of *CMM193C* in each sample using the $2^{-\Delta\Delta CT}$ method [Livak and Schmittgen, 2001]. The mRNA expression data were analyzed using IBM SPSS ver. 20.0 (SPSS Inc., Chicago, IL, USA). All relative mRNA expression data are presented as mean $\pm$ S.D. (n = 6).

Table 4.1: qRT-PCR oligonucleotide primer sequences.

Gene ID	**Forward primer (5' to 3')**	**Reverse primer (5' to 3')**
CMM193C	TCACGCAAAACAACATCCAT	TCAACAGCGTTGAATCGAAG
CmPHR2	TGCAGCATCTCATTTTCAGC	CGGGTACGGTAGGTCTTCAA
CmPHR3	GCTGTGTACTGGAATCGGGT	CTATTCGCTTAGGTGCAGGC
CmPHR7	GAAGCAGATGACAACGACGA	ACATGTTTTTCAGGAACGCC
CMV081C	ATCTTGCCTTAGGTGCTTGG	ACCCATGCTATTTGCTGGAG
CMN328C	ACTTCTCCCTGCGACAAATG	ATGCATAGATTGGCCAGGAG
CMJ212C	ACGGCTGCAAACAAGAACTC	AGGAAAGCGATCAAGTCTGC
CML205C	TGTCAGCGCTGTTGATAAGG	CTCTTCAGCGTGCATTTCAG
CMI244C	TTCAACTGGTTGCACCTTGC	AAAACGATCCGACCACTTGG
CMO210C	TTCCTCACTTTGGTGTGCTG	AACGACTCGCTCAACCATTC
CMF012C	TCTACGTCACCTGCCATTTG	CGAGCATTTCTTCCTCCTTG
CMI050C	CATTCACTCGCGTCATTCAC	TAAGTCCGGGAACTTGATCG
CMJ042C	GCGCACTCGAATCTTGTGAT	ATGAGCGGCAGTTTTGATGC
CMO306C	TCACCTTCAAGCTCACATCG	ATGAGAAAGCGAGCAACGTC
CME023C	TGCCAAGCACATGATTCTCG	TTGGCGATTGTCACATTGGG
CMS308C	AGGAGGACTTTTGCGATGAG	ATGGTTGCTCTGGATGAAGC
CMK188C	AAGAATGTTCTGGCCGAGTG	CCTCGCCTTTGTATGCTTTC
CMB093C	TCGCAAGCATGTCATCTCTG	AGATCGCGCACAACCATATG
CMK115C	TTTGCGTTAACGGAGCTTGG	AGTTTGGCAAACACCACTGC
CMS128C	TGAACGCACATCGCTACATG	ATCAAGCGGCGATCCAAATC
CML323C	TTTTGGGGTCGCACTTTAGC	ACGCCGCGATATTTTGATCC
CML196C	TACAATTCGAGGGCAGAAGG	AAACCGAGGTCGATGTGTTC
CMV159C	AATGCAGCAGACGTACAAGG	CCGCTGCTCTTACTCTCAAT
CMS311C	TGCGTGACAATATCGAGGAC	GTTGAGGCCATGATCTTTCC

continued on next page!

Table 4.1 – continued from previous page

Gene ID	Forward primer (5' to 3')	Reverse primer (5' to 3')
CMN234C	TCAGTGGAAGCGTATGCAAG	CGATGATACCCTGCTTTGTG
CMV209C	AGTATGGGCCGCAGATTTAG	CTGGCATGATCACATTGTTG
CMG066C	TAGACAGGCATGCAACAAGC	TGGACAGCGTTGATAAGTGC
CMI129C	ATCCGACGATTTGTGAGGAC	TATTCTTTCGGCGACGACTC
CML245C	TGGATATGCTGCTGGAGTTG	GATGCAGCACTTGGTGATTG
CMR291C	TGAAGCGCTCCTTCAAACTC	AGGAATTGCGTCCAGTGTTC
CMT305C	TGCGATCAACAAGAGTCAGG	CAAACAGGAGCCTTTGAAGC
CMI244C	TGAGAATGGATCTGCAGTGG	ATTGTCCGAACGTGTTCCTC
CmSIG1	CACGTCCATGACACGATTTC	CTTTCGCAGATTTCGTCCTC
CmSIG2	ATGCGTGAAGATGTCGAGTG	CGAAATGCCGTACCTCAAAC
CmSIG3	TATCGTTCGGCTTCCTGTTC	ACAGATATCCGCTTCGGTTG
CmSIG4	TGAAGTGCAGCAGATGGAAC	ACGTCATCACTTTGGCCTTC
CME194C	AAAGGCCGAAGCACATACAC	TACCACAAAACACCGTCTCG

4.3 Results and Discussion

To identify the pathways affected by BL and RL, cells were subjected to low dose BL and RL (15 μmoles $m^{-2}s^{-1}$) as previously described [Pandhal et al., 2007]. Total RNAs were isolated from dark-, blue- and red-light treated cells, followed by mRNA selection, and library preparation. Library quality was assessed and then the samples were sequenced using the Illumina MiSeq platform.

4.3.1 Mapping and coverage of RNA-seq data

After sequencing and de-multiplexing, RNA-seq data were mapped to the *C. merolae* 10D reference genome [Matsuzaki et al., 2004] using TopHat [Trapnell et al., 2012].

For all analyses, we used only data from reads that uniquely mapped to the reference genome and excluded all multi-mappers. An overview of the sequencing and mapping data is shown in **Table 4.2**. To evaluate reproducibility among biological replicates, a Pearson's correlation test was performed on the expression values. There was a strong correlation between biological replicates for each condition based on the calculated Pearson's correlation coefficients (R^2 >0.95) (**Figure 4.1**). This finding confirmed that there was consensus among the replicates in each condition, which allowed us to perform further differential gene expression analyses.

Table 4.2: Mapping of RNA-seq reads to the *C. merolae* 10D genome.

Sample	# of clean reads	Mapped percentage	Multiple alignment	Q30
Blue light (-) duplicate 1	1,707,508	93.9%	2.9%	
Blue light (-) duplicate 2	1,224,029	93.7%	3.4%	
Blue light (+) duplicate 1	1,021,924	94.1%	3.3%	
Blue light (+) duplicate 2	762,229	93.7%	2.1%	98.4%
Red light (-) duplicate 1	4,479,820	91.9%	4.5%	
Red light (-) duplicate 2	1,651,434	91.7%	11.4%	
Red light (+) duplicate 1	2,471,037	92.7%	2.9%	
Red light (+) duplicate 2	2,173,690	92.4%	2.9%	

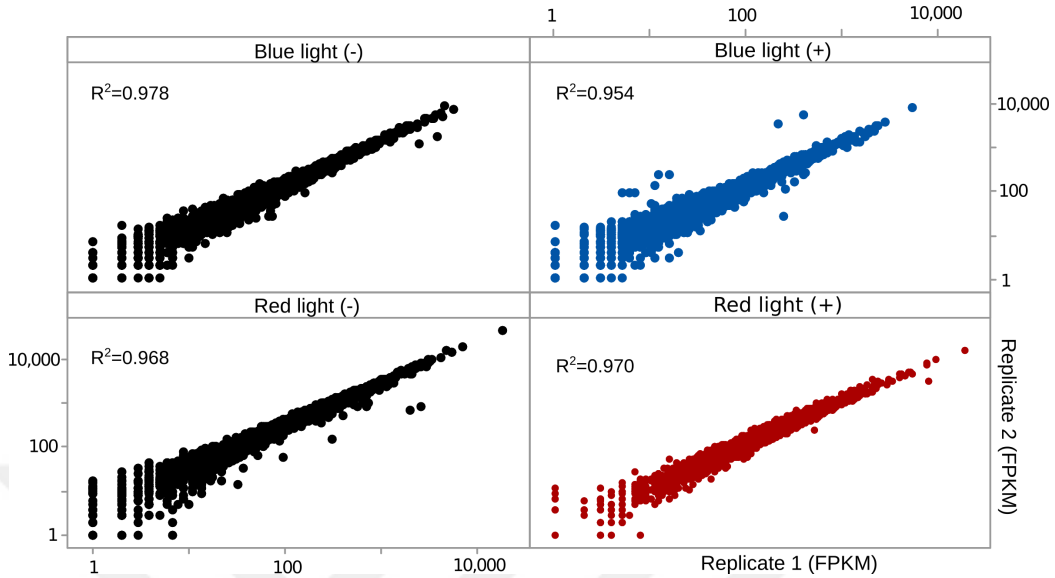

Figure 4.1: Comparison of gene transcript levels between replicates of dark-, blue-light- and red-light-treated samples. Correlation plot for transcript-level FPKM values between replicates of cells treated with dark, blue light and red light. Pearson R^2 values for correlation are included as an insert in plot.

We used the Integrated Genome Viewer (IGV) browser to visualize the coverage of the RNA-seq data throughout the *C. merolae* genome. Our analysis is illustrated by using an example of the coverage plots for chromosome 1, which is 421 kb in length (**Figure 4.2**). Aligned reads were uniformly mapped in the gene loci of chromosome 1 (102 total gene loci) under all conditions.

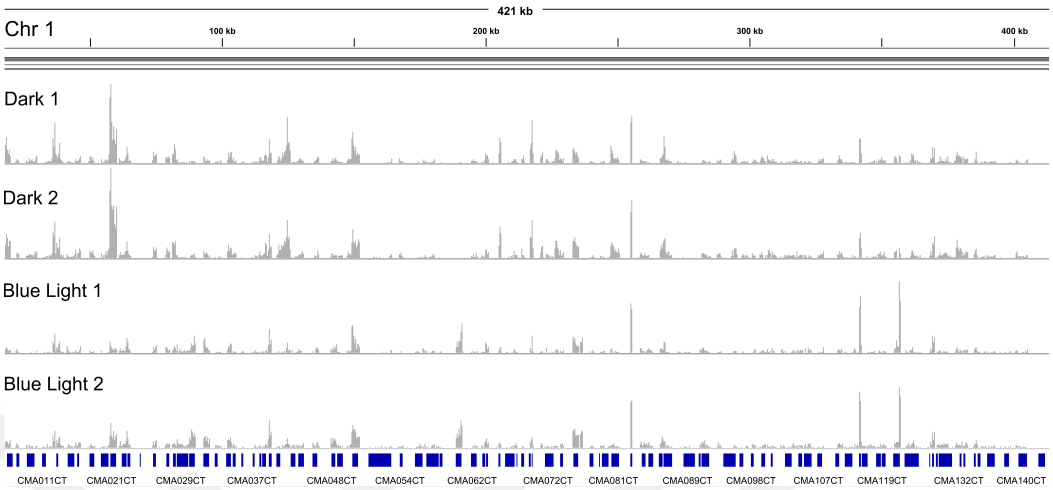

Figure 4.2: Visualization of aligned reads and coverage plot on chromosome 1 of *C. merolae* cells treated with dark and blue light. Aligned reads are uniformly mapped to gene loci of chromosome 1 (102 total gene loci).

4.3.2 Identification of novel transcripts and differentially expressed genes

Qualimap (v2.1) [Garcia-Alcalde et al., 2012] was used to assess the alignment of the reads throughout the genome. Among the RNA-seq reads, 52% to 62% mapped within the annotated exonic regions and 38% to 47% mapped within the intergenic regions for each condition (**Table 4.3**). The high number of mapped reads within the intergenic region allowed us to perform additional analyses to determine whether the sequences might encode novel transcripts. Therefore, cufflink (v2.2) [Trapnell et al., 2012] was used to assemble the TopHat-aligned reads. The analysis revealed 167 candidate novel transcripts. We used the Annocript pipeline [Musacchia et al., 2015] to annotate these transcripts, resulting in the annotation of 22 novel transcripts (**Appendix Table A.4**). This result suggested that some transcriptionally active regions are currently unannotated and that the Ensembl annotation might require extension or revision.

Table 4.3: Percentage of mapped reads to the regions on the *C. merolae* 10D genome.

Condition	Exonic	Intergenic	Intronic
Blue light (-) duplicate 1	52.67%	47.22%	0.11%
Blue light (-) duplicate 2	55.27%	44.61%	0.12%
Blue light (+) duplicate 1	56.56%	43.29%	0.15%
Blue light (+) duplicate 2	58.34%	41.50%	0.16%
Red light (-) duplicate 1	61.63 %	38.20%	0.17%
Red light (-) duplicate 2	61.34%	38.47%	0.18%
Red light (+) duplicate 1	59.32%	40.38%	0.3%
Red light (+) duplicate 2	57.91%	41.79%	0.3%

To identify differentially expressed genes (DEGs) under BL and RL, the FPKM values for each gene were compared among the samples treated with BL, RL, and complete darkness. The number of DEGs in both conditions was determined using the Cuffdiff tool [Trapnell et al., 2012] with the following settings: minimum alignment count of 10; $|\log_2$ fold change $| \geq 1$; and a stringent FDR of <0.01 . The results indicated that 1799 DEGs (35%) were regulated by BL and RL. The 1799 DEGs were classified into three categories: BL-regulated, RL-regulated, and either BL- or RL-(BRL) regulated. Comparative analysis of the DEGs between BL and RL conditions revealed that 683, 595 and 521 genes are regulated by only BL, only RL, and BRL, respectively (**Figure 4.3A**). A total of 36 representative light response-relevant genes were selected for qRT-PCR validation of the RNA-seq results. The qRT-PCR and RNA-seq results revealed similar expression patterns for each gene, indicating that the RNA-seq results were reliable and that the results obtained using both methods were comparable (**Figure 4.4**).

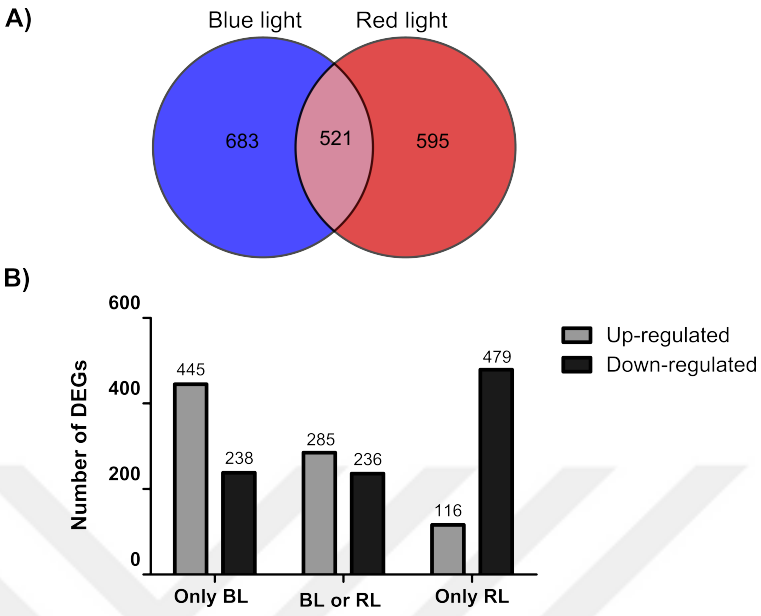

Figure 4.3: Numbers of differentially expressed genes (DEGs) under blue and red light conditions. **(A)** A Venn diagram was generated to identify blue light (BL) and red light (RL) specific DEGs, and common DEGs within BL or RL treated cells. **(B)** There are 445 DEGs up-regulated and 238 DEGs down-regulated only specific to BL. BLR up-regulates 285 DEGs and down-regulates 236 DEGs. There are 116 DEGs up-regulated and 479 DEGs down-regulated only specific to RL.

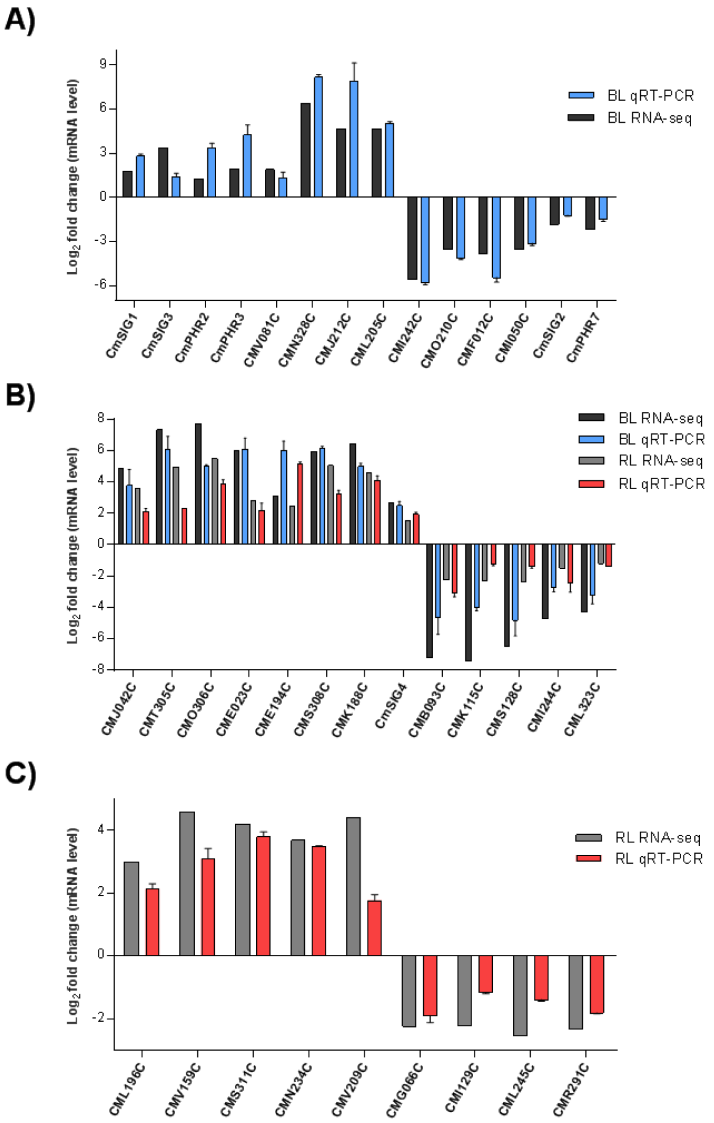

Figure 4.4: RNA-seq results of selected 36 DEGs were validated with qRT-PCR results with three independent biological replicates (Error bar: ±SD, n=6, $\star$ $p < 0.05$, Student's t-test). Y axis indicates transcript abundance changes ($\log_2$ fold) and x axis represents gene IDs. **(A)** DEGs belong to only blue light (BL) condition. **(B)** DEGs belong to either blue or red light condition. **(C)** DEGs belong to red light (RL) condition.

We calculated the number of up- and down-regulated DEGs in the BL-only, RL-

only, and BRL samples (**Figure 4.3B**). In the BL exposed cells, 1204 (23.6%) DEGs were identified (**Appendix Table A.5**), of which 730 genes were up-regulated and 474 were down-regulated. In the RL-only sample, 1116 (21.9%) DEGs were identified in response to RL (**Appendix Table A.6**), of which 406 genes were up-regulated and 710 were down-regulated. All of these results indicated that *C. merolae* responds to both BL and RL to regulate its transcription at the genome-wide level. This pattern of regulation differs from those observed in other algae. For example, a recent genome-wide study with RNA-seq on the kelp *Saccharina japonica* revealed that RL regulated many more genes than did BL [Wang et al., 2013]. In *S. japonica*, 69% of total DEGs were regulated by the RL while the remaining 31% DEGs were regulated by BL [Wang et al., 2013]. Another study on *Synechocystis* sp. PCC 6803 indicated that RL greatly affected genome-wide regulation, where 15% DEGs were regulated by RL [Hubschmann et al., 2005].

4.3.3 GO classification and KEGG pathway enrichment analyses reveal the metabolic pathways regulated by blue light and red light

To functionally categorize the DEGs in cells exposed to BL and RL, a GO term enrichment analysis was performed using the PANTHER classification system [Mi et al., 2013]. After GO term functional enrichment analysis, the correlations were analyzed to construct a network using the BiNGO plug-in (v2.44) [Maere et al., 2005] in Cytoscape (v2.8.3) [Shannon et al., 2003]. The assigned GO terms were used to classify functions of the DEGs based on biological processes, molecular functions and cellular components.

The most significantly enriched ($p<0.05$) GO terms are presented in **Figure 4.5**. Under the GO biological processes category, the three main processes solely regulated by BL were cellular ketone metabolic process (50 genes) organic acid metabolic process (48 genes), and cellular amino acid metabolic process (37 genes) (**Figure**

4.5A). In addition, BL significantly affected the number of DEGs participating in nuclear import and localization (nine genes). The three main GO biological processes that specifically changed under RL (**Figure 4.5B**) were cellular metabolic process (47 genes), cellular biosynthetic process (37 genes), and cellular protein metabolic process (23 genes). Several common GO biological processes were affected by BRL (**Figure 4.5C**): cellular metabolic process (142 genes), primary metabolic process (122 genes), carbohydrate metabolic process (42 genes), and cellular nitrogen compound biosynthetic process (34 genes). In addition, BRL affected photosynthetic electron transport system in photosystem I, and photosynthesis. Collectively, these data showed that some biological processes were regulated in a light-specific manner whereas some processes were regulated by either BL or RL. Both lights particularly affected the transcriptional levels of genes involved in photosynthesis.

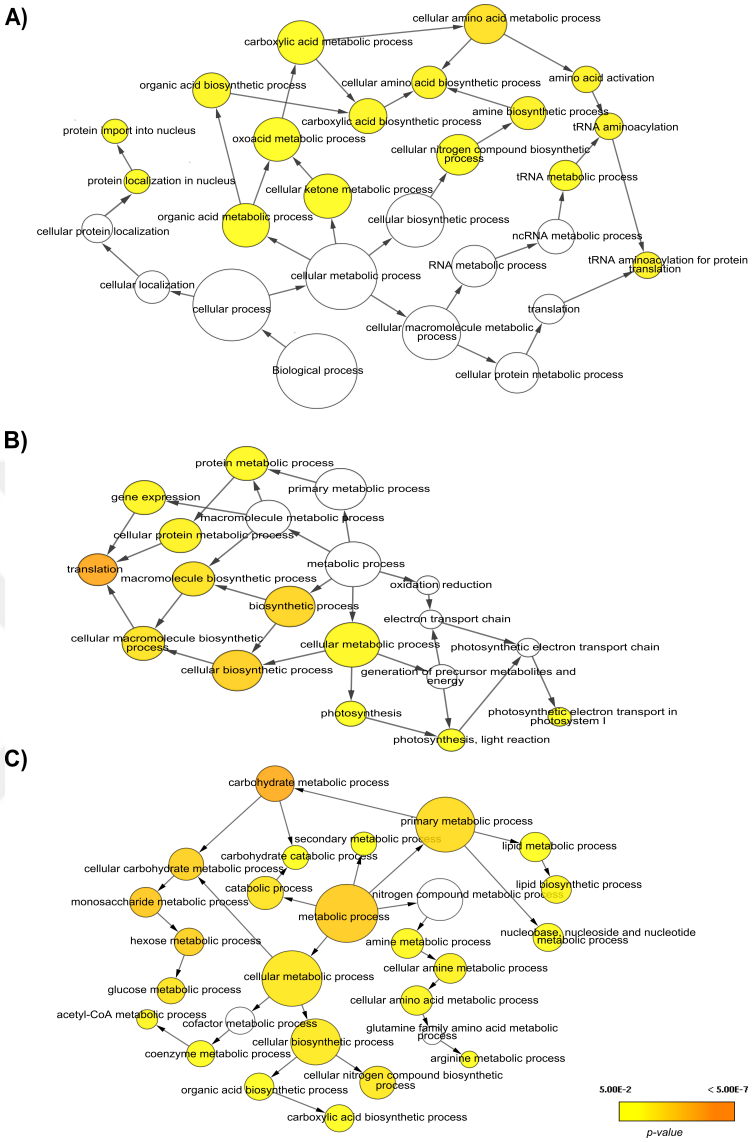

Figure 4.5: Gene Ontology (GO) term network analysis of all differentially expressed genes (DEGs) under light conditions. Functional enrichment analysis was performed for all DEGs with the BINGO plug-in in Cytoscape. Assigned GO terms were used to classify functions of DEGs based on biological processes, **(A)** Represents the only blue light affected biological processes. **(B)** Represents the only red light affected biological processes. **(C)** Represents commonly regulated biological processes both by BL and RL. Overrepresented categories were determined using a hypergeometric test with a significance threshold $p<0.05$ after Benjamini and Hochberg false discovery rate corrections.

After the GO term analysis of the DEGs in response to BL, RL and BRL, a

pathway enrichment analysis was performed to identify the metabolic or signal transduction pathways that were significantly regulated based on KEGG orthology. Under BL, biosynthesis of amino acids, secondary metabolites, and aminoacyl-tRNA, and 2-oxocarboxylic acid metabolism were significantly ($p<0.05$) up-regulated, while tryptophan metabolism, DNA replication and phenylalanine metabolism were significantly ($p<0.05$) down-regulated (**Table 4.4**). Analysis of DEGs revealed several pathways are solely affected by RL (**Table 4.5**). Following pathways were significantly ($p<0.05$) up-regulated by RL: ribosome, carbon fixation in photosynthetic organisms, and photosynthesis-antenna proteins. Conversely, the following pathways were found to be significantly ($p<0.05$) down-regulated: tryptophan metabolism, DNA replication and phenylalanine metabolism.

Table 4.4: Significantly up-regulated (UR) and down-regulated (DR) KEGG pathways specific to only BL ($p<0.05$).

KEGG pathway name	**KEGG pathway ID**	**# of DEGs**	**# of total genes**	**p-value**	**up- or down-regulated**
Biosynthesis of amino acids	cme01230	24	111	5,87E-03	UR
Aminoacyl-tRNA biosynthesis	cme00970	12	41	7,20E-03	UR
2-Oxocarboxylic acid metabolism	cme01210	8	26	2,11E-02	UR
Lysine biosynthesis	cme00300	4	8	2,96E-02	UR
Biosynthesis of secondary metabolites	cme01110	43	285	4,38E-02	UR
Tryptophan metabolism	cme00380	3	10	1,22E-02	DR
DNA replication	cme03030	5	32	1,29E-02	DR
Phenylalanine metabolism	cme00360	3	11	1,50E-02	DR

Table 4.5: Significantly up-regulated (UR) and down-regulated (DR) KEGG pathways specific to RL ($p<0.05$).

KEGG pathway name	**KEGG pathway ID**	**# of DEGs**	**# of total genes**	**p-value**	**up- or down-regulated**
Ribosome	cme03010	20	108	3,50E-03	UR
Carbon fixation in photosynthetic organisms	cme00710	4	28	3,16E-02	UR
Photosynthesis - antenna proteins	cme00196	2	6	3,47E-02	UR
Ubiquitin mediated proteolysis	cme04120	13	40	1,00E-06	DR
Nucleotide excision repair	cme03420	8	39	6,48E-03	DR
Basal transcription factors	cme03022	6	23	6,80E-03	DR
RNA degradation	cme03018	8	44	1,19E-02	DR
Phosphatidylinositol signaling system	cme04070	4	13	1,68E-02	DR
Glutathione metabolism	cme00480	5	26	3,66E-02	DR
Protein processing in endoplasmic reticulum	cme04141	8	56	3,78E-02	DR
Mismatch repair	cme03430	4	19	4,70E-02	DR

Although cells are exposed to BL and RL separately in these experiments, our analysis indicated that both BL and RL regulated some common pathways (**Table 4.6**). The following pathways were found to be significantly ($p<0.05$) up-regulated under both BL and RL: alanine, aspartate and glutamate metabolism, carbon metabolism, citrate cycle (TCA cycle), biosynthesis of amino acids, biosynthesis of secondary metabolites and vitamin B6 metabolism. The following pathways were significantly ($p<0.05$) down-regulated by both BL and RL: valine, leucine and isoleucine degradation, peroxisome, butanoate metabolism, fatty acid degradation, lysine degradation and fatty acid metabolism.

Table 4.6: Significantly up-regulated (UR) and down-regulated (DR) KEGG pathways under BRL ($p<0.05$).

KEGG pathway name	KEGG pathway ID	# of DEGs	# of total genes	p-value	up- or down-regulated
Alanine, aspartate and glutamate metabolism	cme00250	9	20	2,18E-03	UR
Carbon metabolism	cme01200	23	95	2,36E-03	UR
Citrate cycle (TCA cycle)	cme00020	8	26	2,22E-02	UR
Biosynthesis of amino acids	cme01230	21	111	3,45E-02	UR
Biosynthesis of secondary metabolites	cme01110	45	285	3,83E-02	UR
Vitamin B6 metabolism	cme00750	3	5	4,38E-02	UR
Valine, leucine and isoleucine degradation	cme00280	8	20	1,39E-05	DR
Peroxisome	cme04146	5	24	1,85E-03	DR
Butanoate metabolism	cme00650	3	10	6,96E-03	DR
Fatty acid degradation	cme00071	3	10	6,96E-03	DR
Lysine degradation	cme00310	2	8	3,77E-02	DR
Fatty acid metabolism	cme01212	3	21	3,83E-02	DR

4.3.4 Blue and red light exposure significantly alters the transcription of genes in carbon metabolism, amino acid biosynthesis and pigment biosynthesis

Genes involved in carbon metabolism (specifically in glycolysis, carbon fixation and the TCA cycle) were up-regulated in either BL- or RL-exposed cells. The up-regulated genes encoded key enzymes in the TCA cycle (citrate synthase, isocitrate dehydrogenase, and malate dehydrogenase), glycolysis (pyruvate kinase), and carbon fixation (3-phosphoglycerate kinase), enzymes involved in the regeneration of the ribulose 1,5-bisphosphate (ribose 5-phosphate isomerase and the ribulose-1,5 bisphosphate carboxylase/oxygenase large subunit N-methyltransferase) and other enzymes involved in these pathways. Transcription of genes encoding enzymes involved in amino acid biosynthesis was elevated under BRL, consistent with the results of previous studies [Figueroa et al., 1995, Korbee et al., 2005, Li et al., 2013a]. Specifically, BRL resulted in significantly up-regulated transcription of genes encoding enzymes involved

in the biosynthesis of alanine, aspartate, methionine, glutamine, leucine, serine and lysine. Our results showed that BL regulates 45 genes in amino acid biosynthesis pathways whereas RL regulates only 21 genes involved in amino acid biosynthesis. Therefore, compared with RL, BL more extensively up-regulated amino acid-related genes.

The BRL treatment highly regulated biosynthetic pathways of secondary metabolites including terpenoids, porphyrin, chlorophyll, phenylpropanoids, anthocyanins, carotenoids, and pantothenate, as well as CoA. The products of these pathways are pigments that either participate in photosynthesis or act in defense against reactive oxygen species (ROS). Thus, exposure of *C. merolae* to BL or RL results in an increase in pigment production that not only increases the photosynthetic capacity of the organism but also protects it against the harmful effects of excess light. In this study, BL regulated 88 genes involved in secondary metabolite pathways while RL regulated only 45 genes in these pathways. Although both BL and RL regulated the transcription of genes involved in pigment biosynthesis, BL light was more effective than RL since it regulated many more genes involved in pigment biosynthesis. Taken together, our results suggest that the detection of both BL and RL by this organism is crucial for its ability to orchestrate the transcription of genes involved in carbon metabolism, amino acid biosynthesis, and pigment biosynthesis.

Interestingly, both glycerophospholipid and phospholipid metabolism were down-regulated under BRL conditions. Key enzymes in these pathways, such as long-chain-fatty-acid CoA ligase (CMT459C), diacylglycerol kinase (CMK069C) and acyltransferases (CMJ049C, CMA042C), were down-regulated by BRL. This result indicated that carbohydrates were available in the presence of either BL or RL, enabling *C. merolae* to produce different types of membrane phospholipids to cope with light stress. This pattern of regulation appears to be conserved in higher plants. An integrative analysis of transcriptomic and lipidomic data showed that the membrane composition

in *Arabidopsis thaliana* changed under various light conditions [Szymanski et al., 2014]. The transcription of genes encoding the key enzymes (DAG-kinase, phosphatide cytidylyltransferase and inositol monophosphatase) in the phosphatidylinositol signaling system that regulates Ca^{2+} levels in chloroplasts were also down-regulated in *A. thaliana* [Szymanski et al., 2014]. The Ca^{2+} level regulates the activity of chloroplastic enzymes and decreases in the presence of light, which favors reactions in the Calvin-Benson cycle [Roh et al., 1998, Sai and Johnson, 2002]. A decrease in the Ca^{2+} levels was shown to result in the activation of enzymes in the Calvin-Benson cycle, an increase in the production of 3-phosphoglyceric acid and, consequently, an increase in the photosynthetic capacity of the organism [Burgos et al., 2011].

In summary, our results showed that BL and RL enhance both carbon metabolism and photosynthesis and reduce lipid metabolism in *C. merolae*, thereby potentially orchestrating carbon flow in different metabolic pathways to define energy and carbon availability. A recent genome-wide study on the pico-alga *Ostreococcus tauri* revealed that several genes were differentially expressed during the day/night cycle [Monnier et al., 2010]. Additionally, a recent genome-wide study based on RNA-seq analysis of the kelp *S. japonica* revealed that RL has a stronger effect than BL to differentially regulate the majority of genes involved in photosynthesis [Wang et al., 2013].

4.3.5 Blue light- and red light-elicited expression of transcription factor genes

We identified 155 genes encoding transcription factors (TFs) in *C. merolae* using the Plant Transcription Factor Database (PlnTFDB) [Perez-Rodriguez et al., 2010]. The DEG analysis revealed that BL and RL regulated the expression levels of 71 (46%) TFs. The transcript levels of 22, 28 and 21 TF genes were differentially regulated by BL, RL and BRL, respectively (**Figure 4.6**). Among these significantly light-regulated TFs, were 16 myeloblastosis family (MYB)-related TFs. As seen in **Figure 4.6**, RL regulated 13 MYB-related TF genes while BL regulated eight MYB-related TF

genes. This result indicated that, compared with BL, RL significantly up-regulates MYB-related TFs in *C. merolae*.

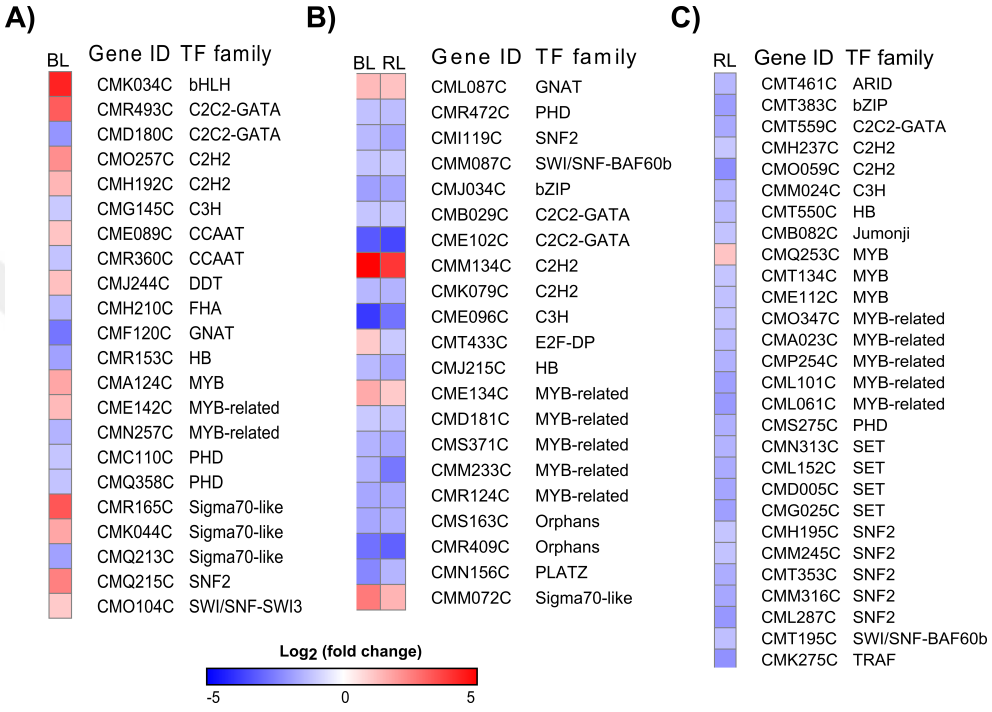

Figure 4.6: Heatmap display of fold changes of differentially expressed transcription factor (TF) genes in **(A)** Only blue light (BL) condition, **(B)** Either blue or red light condition, and **(C)** Red light (RL) condition. Expression levels are represented by color: blue, lowest fold change (down-regulated with respect to dark kept cells); red, highest fold change (up-regulated with respect to dark kept cells). Extreme values in color gradient are -5 to 5 in $\log_2$ scale.

MYB TFs can form multiple complexes with other proteins to regulate many physiological variables in plants, including cell wall synthesis, cell death, the circadian clock, responses to abiotic and biotic stress, hormone signaling, and the biosynthesis of specialized metabolites [Pireyre and Burow, 2015]. A previous study on *A. thaliana* showed that MYB-related TF transcript levels were regulated by either BL or RL [Jiao et al., 2003, Wang et al., 1997]. Interestingly, the transcript levels of four Sigma70-like

TFs genes were altered under BL and RL conditions. Under BL, *CmSIG1 (CMK044C)* and *CmSIG3 (CMR165C)* were up-regulated while *CmSIG2 (CMQ213C)* was down-regulated. The transcriptional level of *CmSIG4 (CMM072C)* was affected by BL or RL. In a previous microarray profiling study in *C. merolae*, it was shown that white light regulates the transcription of these four sigma factor genes [Minoda et al., 2005]. In another study, sigma factors were proposed to control the plastid transcriptome in *C. merolae* [Kanesaki et al., 2012]. Moreover, Yagi et al., 2012, also suggested that the photoregulation of the expression of SIG factors may contribute to the light-dependent activation of some plastid-encoded, RNA-associated, plant-specific factors [Yagi and Shiina, 2014].

Interestingly, the transcript levels of genes encoding splicing factors were also regulated by BL in *C. merolae*. The splicing machinery in *C. merolae* was recently elucidated in detail [Stark et al., 2015]; the authors showed that only 27 introns are present. Thus, it would be interesting to study the effect of BL on the splicing machinery in this primitive photosynthetic organism.

4.3.6 BL and RL up-regulate translation via regulation of tRNA biosynthesis pathway and ribosome biogenesis pathway, respectively

The BL treatment increased the transcript levels of 12 genes encoding enzymes in the aminoacyl-tRNA biosynthesis pathway, including tRNA ligases and synthetases (**Table 4.7**). The RL treatment regulated the levels of 20 genes encoding components of the ribosome biosynthesis pathway including the small and large subunits of the 40S and 60S ribosomal proteins (**Table 4.8**). Similar findings were reported for the brown algae *Saccharina latissima*, in which high levels of photosynthetically active radiation up-regulated genes encoding components of the aminoacyl-tRNA biosynthesis pathway [Heinrich et al., 2012]. [Heinrich et al., 2012]. In the cyanobacterium *Synechocystis* sp. PCC 6803, ired light was shown to up-regulate the transcript levels of 45 genes

related to translation [Hubschmann et al., 2005]. patterns seem to be conserved in *A. thaliana*, as well. It has been shown that the mRNA levels of most of the cytoplasmic ribosomal genes were elevated after light exposure, indicating there is a large demand for cytoplasmic protein translation during the dark/light transition [Ma et al., 2001].

Table 4.7: Differentially regulated genes encoding proteins involved in tRNA biosynthesis pathway (KEGG id: cme00970) under BL.

Gene ID	**Uniprot ID**	**Protein names**	**Log2 (fold change)**
CMJ218C	M1VHH8	Aspartate-tRNA ligase	1.53
CMP205C	M1VA00	Leucine-tRNA ligase	1.26
CMS024C	M1VBH7	Prolyl-tRNA synthetase	1.14
CMQ336C	M1VGD5	Leucyl-tRNA ligase	1.82
CMP345C	M1VKC6	Valine-tRNA ligase	1.75
CMK097C	M1V5D6	Serine-tRNA ligase	1.18
CMG043C	M1UQ03	Tryptophane-tRNA ligase	1.88
CMH090C	M1V4Z4	Cysteine-tRNA ligase	1.09
CMS289C	M1V798	Glutamine-tRNA ligase	1.03
CMJ139C	M1VHD6	Tyrosine-tRNA ligase	1.33
CMC054C	M1UNL8	Glycine-tRNA ligase	1.45
CMS208C	M1UWY0	Threonine-tRNA ligase	1.03

Table 4.8: Differentially regulated genes encoding proteins involved in ribosome biosynthesis pathway (KEGG id: cme03010) under RL.

Gene ID	Entry	Protein names	Log2 (fold change)
CMP012C	M1V626	60S ribosomal protein L34	3.33
CMS189C	M1VHI3	40S ribosomal protein S3a	3.19
CML196C	M1V5J8	60S ribosomal protein L11	3.01
CMK273C	M1V5G2	60S ribosomal protein L23A	2.78
CMJ170C	M1V845	60S ribosomal protein L38	2.65
CMT410C	M1VCU1	40S ribosomal protein SA	2.35
CMH065C	M1UQG7	60S ribosomal protein L14	2.30
CMN125C	M1VEB6	40S ribosomal protein S27A	2.10
CMT154C	M1VCD4	40S ribosomal protein S6	1.93
CMB018C	M1V6E4	60S ribosomal protein L18	1.90
CMH071C	M1V7H2	60S ribosomal protein L5	1.86
CMP007C	M1VFE4	40S ribosomal protein S16	1.84
CMJ289C	M1V5B6	60S ribosomal protein L32	1.74
CMA082C	M1V6B9	40S ribosomal protein S2	1.67
CMQ463C	M1UW23	60S ribosomal protein L17	1.63
CMP179C	M1V9Z0	60S ribosomal protein L29	1.50
CMH046C	M1V4Y0	40S ribosomal protein S14	1.49
CMG157C	M1UQ70	60S ribosomal protein L26	1.48
CMD140C	Q6Q765	60S ribosomal protein L27A	1.35
CMG118C	M1VBF0	60S acidic ribosomal protein P2	1.26

4.3.7 Photolyase gene transcription is enhanced by BL or RL

Either BL or RL down-regulated genes involved in nucleotide excision repair (NER) and base excision repair (BER) pathways in *C. merolae*. Interestingly, our results indicated that a putative photolyase (CMN022C) gene was up-regulated under both BL and RL, presumably to increase photolyase expression and facilitate the repair of photoproducts on DNA [Partch and Sancar, 2005]. This result indicated that CMN022C may be able to absorb both BL and RL, and/or it may be functionally related to a signaling pathway under the control of an as-yet-unidentified *C. merolae* RL photoreceptor.

The green alga, *Chlamydomonas reinhardtii* was shown to have a photolyase responsive to both BL and RL [Beel et al., 2012]. Previous studies showed that BL increased the transcription of photolyase genes to more rapidly and efficiently repair photoproducts compared with the NER pathway [Berrocal-Tito et al., 1999, Suter et al., 2000]. A similar study showed that white light up-regulated some genes involved in DNA repair (*recA, phrA, uvrA, ruvC,* and *umuC*) in *Prochlorococcus marinus* [Kolowrat et al., 2010]. Taken together, these results indicate that BL and RL up-regulated the transcription of photolyase genes, whose products participate in direct repair, and down-regulated genes encoding components of the NER and BER pathways.

4.3.8 Effect of BL on the transcription of the cryptochrome genes

The differential expression analysis revealed that only three cryptochrome genes were differentially regulated under BL while none was affected by RL. Under BL, the transcript levels of *CMJ130C (CmPHR2)* and *CMM076C (CmPHR3)* were significantly elevated, whereas that *CMQ453C (CmPHR7)* was significantly decreased. The transcript levels of these three genes were validated by qRT-PCR (**Figure 4.4**).

The plant-like cryptochrome CmPHR3 is highly homologous to the tomato CRY2.

Lopez et al. [Lopez et al., 2012] showed that the tomato CRY2 profoundly altered molecular pathways related to photosynthesis, starch biosynthesis, sucrose biosynthesis, and secondary metabolite pathways [Korbee et al., 2005, Lopez et al., 2012]. Because the CmPHR3 protein shares high homology with the tomato CRY2, they are presumed to have similar functions; thus, CmPHR3 might regulate carbon metabolism, pigment biosynthesis and the photosynthetic capacity of this alga. Another plant-like cryptochrome (CmPHR7) in *C. merolae*, is highly homologous to the *C. reinhardtii* cryptochrome CPH1. A study revealed that both the mRNA and protein levels of CPH1 in synchronized *C. reinhardtii* cells were increased in the dark; this effect disappeared when the cells were subjected to low intensity BL [Reisdorph and Small, 2004]. Another study reported that the absence of CPH1 in this organism increased its sensitivity to clock resetting following BL pulses [Forbes-Stovall et al., 2014]. CPH1 in *C. reinhardtii* was shown to function as a negative rather than a positive modulator of circadian clock resetting. Therefore, CmPHR7 may play a similar role in *C. merolae*.

Our findings indicated that the transcription of plant-like CRYs was significantly altered after BL exposure. This result indicated that CRYs may a role in BL photoreception to orchestrate the genome-wide transcription of genes involved in different BL-regulated metabolic pathways.

4.3.9 Transcriptional modulation due to BL exposure does not arise from oxidative stress

Various environmental stimuli, including high-fluence BL, result in the generation of ROS. These substances act as signaling molecules to regulate a number of developmental processes and stress responses in many organisms [Danon et al., 2006, Figueroa et al., 1995, Gadjev et al., 2006, Mittler et al., 2004]. To determine whether *C. merolae* produces ROS under BL or RL conditions, ROS were quantified using the fluorogenic dye 2',7' dichlorofluorescein diacetate (DCF-DA). The amount of ROS was comparable

among control cells (dark-kept), BL-exposed, and RL-exposed cells (**Figure 4.7A**). Additionally, although low-fluence (15 μmoles $m^{-2}s^{-1}$) light was used in this study, we investigated whether ROS contributed to differential gene expression by treating cells with H_2O_2. Initially, we performed a series of experiments in which cells were incubated with various concentrations of H_2O_2 for 45 min before measuring the transcript level of *catalase (CMI050C)* gene, which is known to increase in response to H_2O_2 [Gadjev et al., 2006]. The expression level of textitcatalase was saturated after incubation with 600 μM for 45 min in complete darkness. Next, the cells were grown under these conditiosn and the expression levels of the selected 14 DEGs were tested using qRT-PCR; CMI050C was used as a positive control [Guan and Scandalios, 2000]. The qRT-PCR results revealed that the transcript level of *catalase* gene increased by 6-fold whereas the transcript level of the other tested genes did not change significantly (**Figure 4.7B**). This result confirmed that the identified DEGs were related to the BL response and not to oxidative stress.

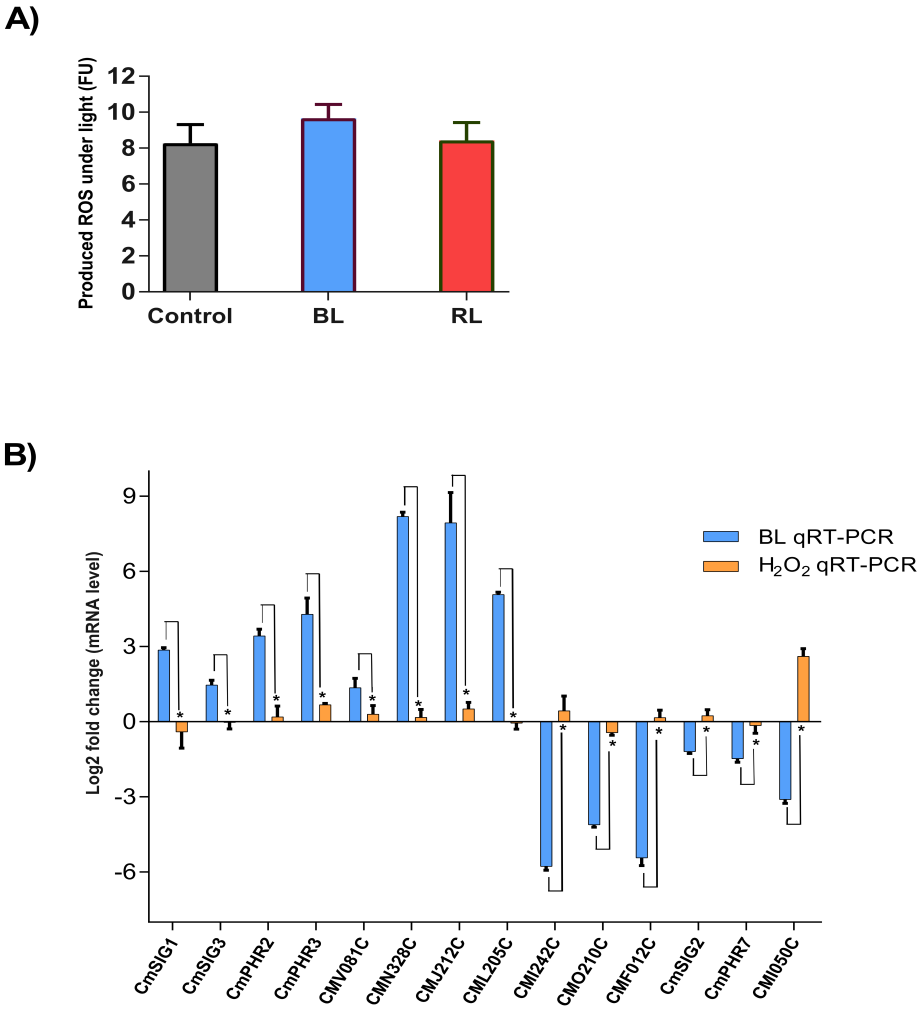

Figure 4.7: Reactive oxygen species (ROS) measurement after light exposure and the effect of H_2O_2 on the regulation of light-induced gene expression. **(A)** ROS amount in the dark kept (Control), blue light (BL) and red light (RL) exposed cells was measured using 2',7' dichlorofluorescein. Y axis represents the fluorescence unit (FU). **(B)** Expression analysis of the selected 14 DEGs using qRT-PCR upon treatment of the cells with H2O2. Blue (indicates blue light exposure) and orange (indicates H_2O_2 treatment) bars with standard errors represent the relative mRNA expression levels ($\log_2$ fold) determined using qRT-PCR from three independent biological replicates. n = 6, $\star$ $p < 0.05$, Student's t-test.

Chapter 5

CONCLUSION

The ability of light perception is crucial for the survival of most organisms that enables them to adjust their physiology and metabolism to the changing environmental conditions. Light, in contrast, is also a threat to any living organism owing to the deleterious effects it can have on nucleic acids, lipids and proteins [Attia, 2010]. Therefore, the capacity to sense and respond to light is widespread among prokaryotes and eukaryotes to survive and adapt themselves as a result of the selective pressure of solar irradiation.

Since, the intensity and the duration of light quite varies depending on the ecosystem, organisms may sense intensity changes of light through the proteins called photoreceptors to produce appropriate response and to regulate their growth, development and other physiological variables accordingly [Galvao and Fankhauser, 2015, Hegemann, 2008, Losi and Gartner, 2012, Montgomery, 2007, Rockwell et al., 2006, Sancar, 2000]. In the UV-VIS spectrum, only blue light (BL) and ultraviolet (UV) radiation, can reach significant depths in freshwater and marine ecosystems [Häder et al., 1998]. Therefore, most marine organisms, including phototrophic bacteria and non-phototrophic bacteria, have different types of BL photoreceptors. These photoreceptors include phototropins, cryptochromes, and proteins containing BLUF (BL using FAD) domains and LOV (Light, Oxygen and Voltage) domains to sense the light [Christie, 2007, Losi and Gärtner, 2008, Losi et al., 2002, van der Horst et al., 2007].

V. cholerae is an enteric bacterium and is therefore insulated from light in its

host. However, when it is in its natural aquatic environment or is being transmitted through water and foodstuff to its host, it may be exposed to sunlight which contains photoreactivating near UV-visible light and harmful UV light [Selby and Sancar, 2006, Worthington et al., 2003]. Light is important not only for phototrophic organisms, but also for non-phototrophic organisms to regulate their cellular signaling and pigment biosynthesis pathways, biofilm formation, and pathogenesis [Elías-Arnanz et al., 2011, Gomelsky and Kaplan, 1997, Purcell and Crosson, 2008, Takano et al., 2006b]. To explore the effect of BL on *V. cholerae* at the genome-wide level, we exposed cells to BL and then conducted RNA-seq analyses. After observing a global response to BL, we decided to identify the mechanism that enables *V. cholerae* to produce such a response. Studies with wild-type and mutant cells revealed that the cells produce ROS upon exposure to BL (**Figure 3.8** and **Figure 3.11**) and its effect is mediated by the transcription factors ChrR-σ^E and MerR (**Figure 3.9**). Based on these findings, we propose a new working model for this organism (**Figure 3.13**). Briefly, BL induces the production of ROS from succinate dehydrogenase (complex II) in the ETC. Then, ROS may cause the dissociation of σ^E from ChrR. The dissociated σ^E binds to the Pσ^E region and recruits RNA polymerase to initiate the transcription of 159 genes. In addition, ROS regulates the binding properties of MerR to DNA, initiating a second cascade in the BL-mediated gene regulation pathway. Our RNA seq results suggested that MerR acts as a suppressor or enhancer to regulate the expression levels of 63 genes, including its own encoding gene.

Analysis of the Set1 DEGs indicated that the genes induced by photo-oxidative stress in this organism encode proteins with protective and repair functions. The cellular molecules affected by ROS reactions include membrane lipids, proteins, and nucleic acids [Ryter and Tyrrell, 1998]. Lipid peroxidation by ROS leads to the loss of cell integrity [Girotti and Kriska, 2004], and cell leakage that affects essential cell membrane processes such as transport and energy generation. In *V. cholerae*, a putative gene (VC1122) encoding cyclopropane-fatty-acyl-phospholipid synthase

(CFA synthase) was highly regulated upon exposure to BL. This enzyme catalyzes the cyclopropane ring formation of bacterial phospholipids using S-adenosylmethionine as the substrate. It has been shown that modification of the membrane by CFA synthase protects the cell against ROS and thereby minimizes its susceptibility to further damage [Grogan and Cronan, 1986, Grogan and Cronan, 1997]. It is possible that the putative CFA synthase modifies the plasma membrane to protect the cell against the harmful effects of ROS.

ROS is known to oxidize thiol-containing proteins and macromolecules; therefore, cellular redox systems enable microorganisms to reverse such damage via the activities of thioredoxins and glutaredoxins [Carmel-Harel and Storz, 2000, Kim et al., 2002]. The transcript levels of genes encoding glutaredoxin (VC2044) and a thioredoxin-dependent thiol peroxidase (VC2160) were up-regulated in *V. cholerae* under BL. Furthermore, the presence of BL is an indicator of UV-light as well. To avoid the harmful effects of UV light, photo-oxidative stress increases the transcript levels of *phr* genes, whose products are involved in genome repair. Such regulation has been demonstrated in other organisms [Bayram et al., 2008, Berrocal-Tito et al., 1999]. All of these results indicate that the photo-oxidative stress generated in response to BL enables *V. cholerae* to regulate the transcription of genes related to cellular protection, DNA repair, and carbon metabolism. Since the ROS assay used in this study measures all types of ROS, further experiments yet to be done to identify which type of ROS is causing photo-oxidative stress in this organism.

C. merolae has noteworthy properties that allow us to study the origin of eukaryotic cells, primary endosymbiosis between cyanobacteria and eukaryotic hosts, and secondary endosymbiosis between red algae and their hosts. Small and compact genomes of *C. merolae* provide information on the basic and essential genes that support the lives of photosynthetic eukaryotes, including higher plants. Thus *C. merolae* provides an excellent opportunity for addressing fundamental traits (for example, light

adaptation, photosynthesis, multiplication, and differentiation) using transcriptomic and proteomic analyses. Light has significant effect on the growth and development of *C. merolae*, but there are limited reports on the light mediated physiological responses and molecular mechanism. *C. merolae* has only CPF photoreceptors, which makes it an ideal organism to study the role of CPFs in photoreception [Asimgil and Kavakli, 2012, Matsuzaki et al., 2004]. Moreover, *C. merolae* has been shown to alter its pigment composition, growth, and energy transfer patterns under different light spectra [Ueno et al., 2015]. Thus, we aimed to investigate the effect of BL and RL at the transcriptional level, and to understand the role of known light receptor genes in this organism.

To understand these physiological changes at the molecular level, we used the RNA-seq approach to reveal the genes that were differentially regulated by BL and RL in *C. merolae*. Our results showed that there is light-specific transcriptional regulation in this organism. The results of this study showed that different pathways (i.e., photopigment production, DNA repair, and carbon, amino acid and lipid metabolisms) were co-regulated by RL- and BL via the transcriptional regulation of genes encoding key enzymes in these pathways. The data provided in this study can be combined with other functional data to construct gene networks and elucidate the responses to BL and RL. Additionally, our data may be used to identify the signal transduction pathways that orchestrate the co-regulation of metabolism and transcription factors that bind to light-responsive DNA elements in the *C. merolae* genome.

Genome-wide studies have shown that there is no gene encoding a RL receptor in *C. merolae* [Asimgil and Kavakli, 2012, Matsuzaki et al., 2004]. In light of this, it is interesting to note that RL greatly affected gene transcription in this organism. Such regulation may occur through the retrograde signaling and/or by triggering, as reported for many plant and algae species [Kleine and Leister, 2016, Lepisto et al., 2012, Tanaka and Hanaoka, 2012]. The finding that many genes were commonly regulated by

BRL (**Table 4.6**) also supports the impact of retrograde signaling on genome-wide regulation in this organism, as suggested previously [Tanaka and Hanaoka, 2012]. The transcriptional regulation of plant-like CRYs in *C. merolae* suggested that CRYs have a potential role in BL photoreception and in the orchestration of genome-wide transcriptional regulation. In summary, the results of this study demonstrate that BL and RL regulate 35% of all genes in *C. merolae*, allowing it to adjust its metabolism accordingly and to gain an adaptive response in extreme environmental conditions.

BIBLIOGRAPHY

[Ahmad and Cashmore, 1993] Ahmad, M. and Cashmore, A. R. (1993). Hy4 gene of a. thaliana encodes a protein with characteristics of a blue-light photoreceptor. *Nature*.

[Anthony et al., 2004] Anthony, J. R., Newman, J. D., and Donohue, T. J. (2004). Interactions between the rhodobacter sphaeroides ecf sigma factor, sigma(e), and its anti-sigma factor, chrr. *Journal of Molecular Biology*, 341(2):345–360.

[Anthony et al., 2005] Anthony, J. R., Warczak, K. L., and Donohue, T. J. (2005). A transcriptional response to singlet oxygen, a toxic byproduct of photosynthesis. *Proceedings of the National Academy of Sciences of the United States of America*, 102(18):6502–6507.

[Arabidopsis, 1998] Arabidopsis, N. (1998). a flavoprotein with the properties of a photoreceptor for phototropism christie jm; reymond p; powell gk; bernasconi p; raibekas aa; liscum e; briggs wr. *Science (New York, NY)*, 282(5394):1698–701.

[Asimgil and Kavakli, 2012] Asimgil, H. and Kavakli, I. H. (2012). Purification and characterization of five members of photolyase/cryptochrome family from cyanidioschyzon merolae. *Plant Science*, 185-186:190–8.

[Attia, 2010] Attia, S. M. (2010). Deleterious effects of reactive metabolites. *Oxid Med Cell Longev*, 3(4):238–53.

[Avila-Perez et al., 2006] Avila-Perez, M., Hellingwerf, K. J., and Kort, R. (2006). Blue light activates the sigmab-dependent stress response of bacillus subtilis via ytva. *J Bacteriol*, 188(17):6411–4.

[Ballaré et al., 1995] Ballaré, C. L., Barnes, P. W., and Flint, S. D. (1995). Inhibition of hypocotyl elongation by ultraviolet-b radiation in de-etiolating tomato seedlings. i. the photoreceptor. *Physiologia Plantarum*, 93(4):584–592.

[Barends et al., 2009] Barends, T. R., Hartmann, E., Griese, J. J., Beitlich, T., Kirienko, N. V., Ryjenkov, D. A., Reinstein, J., Shoeman, R. L., Gomelsky, M., and Schlichting, I. (2009). Structure and mechanism of a bacterial light-regulated cyclic nucleotide phosphodiesterase. *Nature*, 459(7249):1015–1018.

[Baskin and Iino, 1987] Baskin, T. I. and Iino, M. (1987). An action spectrum in the blue and ultraviolet for phototropism in alfalfa. *Photochemistry and photobiology*, 46(1):127–136.

[Bayram et al., 2008] Bayram, Ö., Biesemann, C., Krappmann, S., Galland, P., and Braus, G. H. (2008). More than a repair enzyme: Aspergillus nidulans photolyase-like crya is a regulator of sexual development. *Molecular biology of the cell*, 19(8):3254–3262.

[Beel et al., 2012] Beel, B., Prager, K., Spexard, M., Sasso, S., Weiss, D., Muller, N., Heinnickel, M., Dewez, D., Ikoma, D., Grossman, A. R., Kottke, T., and Mittag, M. (2012). A flavin binding cryptochrome photoreceptor responds to both blue and red light in chlamydomonas reinhardtii. *Plant Cell*, 24(7):2992–3008.

[Berrocal-Tito et al., 1999] Berrocal-Tito, G., Sametz-Baron, L., Eichenberg, K., Horwitz, B. A., and Herrera-Estrella, A. (1999). Rapid blue light regulation of a trichoderma harzianum photolyase gene. *Journal of Biological Chemistry*, 274(20):14288–14294.

[Berrocal-Tito et al., 2007] Berrocal-Tito, G. M., Esquivel-Naranjo, E. U., Horwitz, B. A., and Herrera-Estrella, A. (2007). Trichoderma atroviride phr1, a fungal photolyase responsible for dna repair, autoregulates its own photoinduction. *Eukaryotic cell*, 6(9):1682–1692.

[Björn, 2015] Björn, L. O. (2015). Photoreceptive proteins and their evolution. In *Photobiology*, pages 169–176. Springer.

[Bluhm and Dunkle, 2008] Bluhm, B. and Dunkle, L. (2008). Phl1 of cercospora zeae-maydis encodes a member of the photolyase/cryptochrome family involved in uv protection and fungal development. *Fungal Genetics and Biology*, 45(10):1364–1372.

[Blumenstein et al., 2005] Blumenstein, A., Vienken, K., Tasler, R., Purschwitz, J., Veith, D., Frankenberg-Dinkel, N., and Fischer, R. (2005). The aspergillus nidulans phytochrome fpha represses sexual development in red light. *Current Biology*, 15(20):1833–1838.

[Bogomolni and Spudich, 1982] Bogomolni, R. A. and Spudich, J. L. (1982). Identification of a third rhodopsin-like pigment in phototactic halobacterium halobium. *Proceedings of the National Academy of Sciences*, 79(20):6250–6254.

[Braatsch et al., 2002] Braatsch, S., Gomelsky, M., Kuphal, S., and Klug, G. (2002). A single flavoprotein, appa, integrates both redox and light signals in rhodobacter sphaeroides. *Molecular microbiology*, 45(3):827–836.

[Braatsch and Klug, 2004] Braatsch, S. and Klug, G. (2004). Orf90, a gene required for photoreactivation in rhodobacter capsulatus sb1003 encodes a cyclobutane pyrimidine dimer photolyase. *Photosynthesis Research*, 79(2):167–177.

[Braatsch et al., 2004] Braatsch, S., Moskvin, O. V., Klug, G., and Gomelsky, M. (2004). Responses of the rhodobacter sphaeroides transcriptome to blue light under semiaerobic conditions. *Journal of bacteriology*, 186(22):7726–7735.

[Brand, 2000] Brand, M. D. (2000). Uncoupling to survive? the role of mitochondrial inefficiency in ageing. *Exp Gerontol*, 35(6-7):811–20.

[Briggs and Christie, 2002] Briggs, W. R. and Christie, J. M. (2002). Phototropins 1 and 2: versatile plant blue-light receptors. *Trends in plant science*, 7(5):204–210.

[Britt et al., 1993] Britt, A., Chen, J., Wykoff, D., and Mitchell, D. (1993). A uv-sensitive mutant of arabidopsis defective in the repair of pyrimidine-pyrimidinone (6-4) dimers. *Science*, 261(5128):1571–1574.

[Britt, 1996] Britt, A. B. (1996). Dna damage and repair in plants. *Annual review of plant biology*, 47(1):75–100.

[Brown et al., 2005] Brown, B. A., Cloix, C., Jiang, G. H., Kaiserli, E., Herzyk, P., Kliebenstein, D. J., and Jenkins, G. I. (2005). A uv-b-specific signaling component orchestrates plant uv protection. *Proceedings of the National Academy of Sciences of the United States of America*, 102(50):18225–18230.

[Brown, 2004] Brown, L. S. (2004). Fungal rhodopsins and opsin-related proteins: eukaryotic homologues of bacteriorhodopsin with unknown functions. *Photochemical & Photobiological Sciences*, 3(6):555–565.

[Browning et al., 2003] Browning, D. F., Whitworth, D. E., and Hodgson, D. A. (2003). Light-induced carotenogenesis in myxococcus xanthus: functional characterization of the ecf sigma factor carq and antisigma factor carr. *Molecular microbiology*, 48(1):237–251.

[Brudler et al., 2003] Brudler, R., Hitomi, K., Daiyasu, H., Toh, H., Kucho, K.-i., Ishiura, M., Kanehisa, M., Roberts, V. A., Todo, T., Tainer, J. A., et al. (2003). Identification of a new cryptochrome class: structure, function, and evolution. *Molecular cell*, 11(1):59–67.

[Bryant and Frigaard, 2006] Bryant, D. A. and Frigaard, N.-U. (2006). Prokaryotic photosynthesis and phototrophy illuminated. *Trends in microbiology*, 14(11):488–496.

[Bullard et al., 2010] Bullard, J. H., Purdom, E., Hansen, K. D., and Dudoit, S. (2010).

Evaluation of statistical methods for normalization and differential expression in mrna-seq experiments. *Bmc Bioinformatics*, 11.

[Burchard and Dworkin, 1966] Burchard, R. P. and Dworkin, M. (1966). Light-induced lysis and carotenogenesis in myxococcus xanthus. *Journal of bacteriology*, 91(2):535–545.

[Burgos et al., 2011] Burgos, A., Szymanski, J., Seiwert, B., Degenkolbe, T., Hannah, M. A., Giavalisco, P., and Willmitzer, L. (2011). Analysis of short-term changes in the arabidopsis thaliana glycerolipidome in response to temperature and light. *Plant J*, 66(4):656–68.

[Burney et al., 2009] Burney, S., Hoang, N., Caruso, M., Dudkin, E. A., Ahmad, M., and Bouly, J.-P. (2009). Conformational change induced by atp binding correlates with enhanced biological function of arabidopsis cryptochrome. *FEBS letters*, 583(9):1427–1433.

[Butler et al., 1959] Butler, W. L., Norris, K., Siegelman, H., and Hendricks, S. (1959). Detection, assay, and preliminary purification of the pigment controlling photoresponsive development of plants. *Proceedings of the National Academy of Sciences*, 45(12):1703–1708.

[Canamero et al., 2006] Canamero, R. C., Bakrim, N., Bouly, J.-P., Garay, A., Dudkin, E. E., Habricot, Y., and Ahmad, M. (2006). Cryptochrome photoreceptors cry1 and cry2 antagonistically regulate primary root elongation in arabidopsis thaliana. *Planta*, 224(5):995–1003.

[Carmel-Harel and Storz, 2000] Carmel-Harel, O. and Storz, G. (2000). Roles of the glutathione- and thioredoxin-dependent reduction systems in the escherichia coli and saccharomyces cerevisiae responses to oxidative stress. *Annu Rev Microbiol*, 54:439–61.

[Casper-Lindley and Yildiz, 2004] Casper-Lindley, C. and Yildiz, F. H. (2004). Vpst is a transcriptional regulator required for expression of vps biosynthesis genes and the development of rugose colonial morphology in vibrio cholerae o1 el tor. *Journal of Bacteriology*, 186(5):1574–1578.

[Cecchini, 2003] Cecchini, G. (2003). Function and structure of complex ii of the respiratory chain. *Annu Rev Biochem*, 72:77–109.

[Ceriani et al., 1999] Ceriani, M. F., Darlington, T. K., Staknis, D., Más, P., Petti, A. A., Weitz, C. J., and Kay, S. A. (1999). Light-dependent sequestration of timeless by cryptochrome. *Science*, 285(5427):553–556.

[Chaves et al., 2011] Chaves, I., Pokorny, R., Byrdin, M., Hoang, N., Ritz, T., Brettel, K., Essen, L.-O., van der Horst, G. T., Batschauer, A., and Ahmad, M. (2011). The cryptochromes: blue light photoreceptors in plants and animals. *Annual review of plant biology*, 62:335–364.

[Chen and Chory, 2011] Chen, M. and Chory, J. (2011). Phytochrome signaling mechanisms and the control of plant development. *Trends in cell biology*, 21(11):664–671.

[Choi et al., 1999] Choi, J.-S., Chung, Y.-H., Moon, Y.-J., Kim, C., Watanabe, M., Song, P.-S., Joe, C.-O., Bogorad, L., and Park, Y. M. (1999). Photomovement of the gliding cyanobacterium synechocystis sp. pcc 6803. *Photochemistry and photobiology*, 70(1):95–102.

[Chory et al., 1996] Chory, J., Chatterjee, M., Cook, R., Elich, T., Fankhauser, C., Li, J., Nagpal, P., Neff, M., Pepper, A., Poole, D., et al. (1996). From seed germination to flowering, light controls plant development via the pigment phytochrome. *Proceedings of the National Academy of Sciences*, 93(22):12066–12071.

[Christie, 2007] Christie, J. M. (2007). Phototropin blue-light receptors. *Annu. Rev. Plant Biol.*, 58:21–45.

[Christie et al., 2012] Christie, J. M., Arvai, A. S., Baxter, K. J., Heilmann, M., Pratt, A. J., OHara, A., Kelly, S. M., Hothorn, M., Smith, B. O., Hitomi, K., et al. (2012). Plant uvr8 photoreceptor senses uv-b by tryptophan-mediated disruption of cross-dimer salt bridges. *Science*, 335(6075):1492–1496.

[Christie et al., 1999] Christie, J. M., Salomon, M., Nozue, K., Wada, M., and Briggs, W. R. (1999). Lov (light, oxygen, or voltage) domains of the blue-light photoreceptor phototropin (nph1): binding sites for the chromophore flavin mononucleotide. *Proceedings of the National Academy of Sciences*, 96(15):8779–8783.

[Cloix and Jenkins, 2008] Cloix, C. and Jenkins, G. I. (2008). Interaction of the arabidopsis uv-b-specific signaling component uvr8 with chromatin. *Molecular plant*, 1(1):118–128.

[Coesel et al., 2009] Coesel, S., Mangogna, M., Ishikawa, T., Heijde, M., Rogato, A., Finazzi, G., Todo, T., Bowler, C., and Falciatore, A. (2009). Diatom ptcpf1 is a new cryptochrome/photolyase family member with dna repair and transcription regulation activity. *EMBO reports*, 10(6):655–661.

[Collins et al., 2006] Collins, B., Mazzoni, E. O., Stanewsky, R., and Blau, J. (2006). Drosophila cryptochrome is a circadian transcriptional repressor. *Current biology*, 16(5):441–449.

[Czechowski et al., 2005] Czechowski, T., Stitt, M., Altmann, T., Udvardi, M. K., and Scheible, W.-R. (2005). Genome-wide identification and testing of superior reference genes for transcript normalization in arabidopsis. *Plant physiology*, 139(1):5–17.

[Daiyasu et al., 2004] Daiyasu, H., Ishikawa, T., Kuma, K.-i., Iwai, S., Todo, T., and

Toh, H. (2004). Identification of cryptochrome dash from vertebrates. *Genes to Cells*, 9(5):479–495.

[Danon et al., 2006] Danon, A., Coll, N. S., and Apel, K. (2006). Cryptochrome-1-dependent execution of programmed cell death induced by singlet oxygen in arabidopsis thaliana. *Proceedings of the National Academy of Sciences*, 103(45):17036–17041.

[Daroff and Aminoff, 2014] Daroff, R. B. and Aminoff, M. J. (2014). *Encyclopedia of the neurological sciences*. Academic press.

[Darwin and Darwin, 1897] Darwin, C. and Darwin, F. (1897). *The power of movement in plants*. Appleton.

[de Lorenzo and Timmis, 1994] de Lorenzo, V. and Timmis, K. N. (1994). Analysis and construction of stable phenotypes in gram-negative bacteria with tn5- and tn10-derived minitransposons. *Methods Enzymol*, 235:386–405.

[Delwiche and Cooper, 2015] Delwiche, C. F. and Cooper, E. D. (2015). The evolutionary origin of a terrestrial flora. *Current Biology*, 25(19):R899–R910.

[Drose, 2013] Drose, S. (2013). Differential effects of complex ii on mitochondrial ros production and their relation to cardioprotective pre- and postconditioning. *Biochimica Et Biophysica Acta-Bioenergetics*, 1827(5):578–587.

[D'surney et al., 1993] D'surney, S., Tschaplinski, T., Edwards, N., and Shugart, L. (1993). Biological responses of two soybean cultivars exposed to enhanced uvb radiation. *Environmental and Experimental Botany*, 33(3):347–356.

[Ehling-Schulz et al., 1997] Ehling-Schulz, M., Bilger, W., and Scherer, S. (1997). Uv-b-induced synthesis of photoprotective pigments and extracellular polysaccharides in the terrestrial cyanobacterium nostoc commune. *Journal of Bacteriology*, 179(6):1940–1945.

[El-Assal et al., 2004] El-Assal, S., Alonso-Blanco, C., Hanhart, C., and Koornneef, M. (2004). Pleiotropic effects of the arabidopsis cryptochrome 2 allelic variation underlie fruit trait-related qtl. *Plant Biology*, 6(04):370–374.

[Elías-Arnanz et al., 2011] Elías-Arnanz, M., Padmanabhan, S., and Murillo, F. J. (2011). Light-dependent gene regulation in nonphototrophic bacteria. *Current opinion in microbiology*, 14(2):128–135.

[Elliott et al., 2004] Elliott, R. C., Platten, J. D., Watson, J. C., and Reid, J. B. (2004). Phytochrome regulation of pea phototropin. *Journal of plant physiology*, 161(3):265–270.

[Ernst et al., 2013] Ernst, O. P., Lodowski, D. T., Elstner, M., Hegemann, P., Brown, L. S., and Kandori, H. (2013). Microbial and animal rhodopsins: structures, functions, and molecular mechanisms. *Chemical reviews*, 114(1):126–163.

[Ernst et al., 2008] Ernst, O. P., Murcia, P. A. S., Daldrop, P., Tsunoda, S. P., Kateriya, S., and Hegemann, P. (2008). Photoactivation of channelrhodopsin. *Journal of Biological Chemistry*, 283(3):1637–1643.

[Essen, 2006] Essen, L.-O. (2006). Photolyases and cryptochromes: common mechanisms of dna repair and light-driven signaling? *Current opinion in structural biology*, 16(1):51–59.

[Figueroa et al., 1995] Figueroa, F. L., Aguilera, J., Jimenez, C., Vergara, J. J., Robles, M. D., and Niell, F. X. (1995). Growth, pigment synthesis and nitrogen assimilation in the red alga porphyra sp (bangiales, rhodophyta) under blue and red light. *Scientia Marina*, 59:9–20.

[Folta and Kaufman, 2003] Folta, K. M. and Kaufman, L. S. (2003). Phototropin 1 is required for high-fluence blue-light-mediated mrna destabilization. *Plant molecular biology*, 51(4):609–618.

[Folta et al., 2003] Folta, K. M., Lieg, E. J., Durham, T., and Spalding, E. P. (2003). Primary inhibition of hypocotyl growth and phototropism depend differently on phototropin-mediated increases in cytoplasmic calcium induced by blue light. *Plant Physiology*, 133(4):1464–1470.

[Fong et al., 2006] Fong, J. C., Karplus, K., Schoolnik, G. K., and Yildiz, F. H. (2006). Identification and characterization of rbma, a novel protein required for the development of rugose colony morphology and biofilm structure in vibrio cholerae. *J Bacteriol*, 188(3):1049–59.

[Forbes-Stovall et al., 2014] Forbes-Stovall, J., Howton, J., Young, M., Davis, G., Chandler, T., Kessler, B., Rinehart, C. A., and Jacobshagen, S. (2014). Chlamydomonas reinhardtii strain cc-124 is highly sensitive to blue light in addition to green and red light in resetting its circadiari clock, with the blue-light photoreceptor plant cryptochrome likely acting as negative modulator. *Plant Physiology and Biochemistry*, 75:14–23.

[Fortunato et al., 2015] Fortunato, A. E., Annunziata, R., Jaubert, M., Bouly, J. P., and Falciatore, A. (2015). Dealing with light: The widespread and multitasking cryptochrome/photolyase family in photosynthetic organisms. *Journal of Plant Physiology*, 172:42–54.

[Foster et al., 1984] Foster, K. W., Saranak, J., Patel, N., Zarilli, G., Okabe, M., Kline, T., and Nakanishi, K. (1984). A rhodopsin is the functional photoreceptor for phototaxis in the unicellular eukaryote chlamydomonas. *Nature*.

[Franklin and Quail, 2010] Franklin, K. A. and Quail, P. H. (2010). Phytochrome functions in arabidopsis development. *Journal of experimental botany*, 61(1):11–24.

[Froehlich et al., 2005] Froehlich, A. C., Noh, B., Vierstra, R. D., Loros, J., and Dunlap, J. C. (2005). Genetic and molecular analysis of phytochromes from the filamentous fungus neurospora crassa. *Eukaryotic Cell*, 4(12):2140–2152.

[Frohnmeyer et al., 1999] Frohnmeyer, H., Loyall, L., Blatt, M. R., and Grabov, A. (1999). Millisecond uv-b irradiation evokes prolonged elevation of cytosolic-free ca2+ and stimulates gene expression in transgenic parsley cell cultures. *The Plant Journal*, 20(1):109–117.

[Fuangthong et al., 2001] Fuangthong, M., Atichartpongkul, S., Mongkolsuk, S., and Helmann, J. D. (2001). Ohrr is a repressor of ohra, a key organic hydroperoxide resistance determinant in bacillus subtilis. *Journal of bacteriology*, 183(14):4134–4141.

[Gadjev et al., 2006] Gadjev, I., Vanderauwera, S., Gechev, T. S., Laloi, C., Minkov, I. N., Shulaev, V., Apel, K., Inzé, D., Mittler, R., and Van Breusegem, F. (2006). Transcriptomic footprints disclose specificity of reactive oxygen species signaling in arabidopsis. *Plant Physiology*, 141(2):436–445.

[Galvao and Fankhauser, 2015] Galvao, V. C. and Fankhauser, C. (2015). Sensing the light environment in plants: photoreceptors and early signaling steps. *Curr Opin Neurobiol*, 34C:46–53.

[Garcia-Alcalde et al., 2012] Garcia-Alcalde, F., Okonechnikov, K., Carbonell, J., Cruz, L. M., Gotz, S., Tarazona, S., Dopazo, J., Meyer, T. F., and Conesa, A. (2012). Qualimap: evaluating next-generation sequencing alignment data. *Bioinformatics*, 28(20):2678–9.

[Gekakis et al., 1998] Gekakis, N., Staknis, D., Nguyen, H. B., Davis, F. C., Wilsbacher, L. D., King, D. P., Takahashi, J. S., and Weitz, C. J. (1998). Role of the clock protein in the mammalian circadian mechanism. *Science*, 280(5369):1564–1569.

[Girotti and Kriska, 2004] Girotti, A. W. and Kriska, T. (2004). Role of lipid hydroperoxides in photo-oxidative stress signaling. *Antioxid Redox Signal*, 6(2):301–10.

[Glaeser et al., 2011] Glaeser, J., Nuss, A. M., Berghoff, B. A., and Klug, G. (2011). Singlet oxygen stress in microorganisms. *Adv Microb Physiol*, 58:141–73.

[Golombek et al., 2014] Golombek, D. A., Bussi, I. L., and Agostino, P. V. (2014). Minutes, days and years: molecular interactions among different scales of biological timing. *Philosophical Transactions of the Royal Society of London B: Biological Sciences*, 369(1637):20120465.

[Gomelsky and Hoff, 2011] Gomelsky, M. and Hoff, W. D. (2011). Light helps bacteria make important lifestyle decisions. *Trends in microbiology*, 19(9):441–448.

[Gomelsky and Kaplan, 1997] Gomelsky, M. and Kaplan, S. (1997). Molecular genetic analysis suggesting interactions between appa and ppsr in regulation of photosynthesis gene expression in rhodobacter sphaeroides 2.4.1. *Journal of Bacteriology*, 179(1):128–134.

[Gomelsky and Klug, 2002] Gomelsky, M. and Klug, G. (2002). Bluf: a novel fad-binding domain involved in sensory transduction in microorganisms. *Trends in biochemical sciences*, 27(10):497–500.

[Gomes et al., 2005] Gomes, A., Fernandes, E., and Lima, J. L. F. C. (2005). Fluorescence probes used for detection of reactive oxygen species. *Journal of Biochemical and Biophysical Methods*, 65(2-3):45–80.

[Gorham et al., 1996] Gorham, H. C., McGowan, S. J., Robson, P. R., and Hodgson, D. A. (1996). Light-induced carotenogenesis in myxococcus xanthus: light-dependent membrane sequestration of ecf sigma factor carq by anti-sigma factor carr. *Mol Microbiol*, 19(1):171–86.

[Grogan and Cronan, 1997] Grogan, D. W. and Cronan, J. E., J. (1997). Cyclopropane ring formation in membrane lipids of bacteria. *Microbiol Mol Biol Rev*, 61(4):429–41.

[Grogan and Cronan, 1986] Grogan, D. W. and Cronan, J. E. (1986). Characterization of escherichia-coli mutants completely defective in synthesis of cyclopropane fatty-acids. *Journal of Bacteriology*, 166(3):872–877.

[Guan and Scandalios, 2000] Guan, L. M. and Scandalios, J. G. (2000). Hydrogen-peroxide-mediated catalase gene expression in response to wounding. *Free Radic Biol Med*, 28(8):1182–90.

[Häder et al., 1998] Häder, D.-P., Kumar, H., Smith, R., and Worrest, R. (1998). Effects on aquatic ecosystems. *Journal of Photochemistry and photobiology B: Biology*, 46(1):53–68.

[Hasegawa et al., 2006] Hasegawa, K., Masuda, S., and Ono, T.-a. (2006). Light induced structural changes of a full-length protein and its bluf domain in ycgf (blrp), a blue-light sensing protein that uses fad (bluf). *Biochemistry*, 45(11):3785–3793.

[Hatefi, 1985] Hatefi, Y. (1985). The mitochondrial electron-transport and oxidative-phosphorylation system. *Annual Review of Biochemistry*, 54:1015–1069.

[Hegemann, 2008] Hegemann, P. (2008). Algal sensory photoreceptors. *Annu Rev Plant Biol*, 59:167–89.

[Hegemann et al., 1991] Hegemann, P., Gärtner, W., and Uhl, R. (1991). All-trans retinal constitutes the functional chromophore in chlamydomonas rhodopsin. *Biophysical journal*, 60(6):1477.

[Heidelberg et al., 2000] Heidelberg, J. F., Eisen, J. A., Nelson, W. C., Clayton, R. A., Gwinn, M. L., Dodson, R. J., Haft, D. H., Hickey, E. K., Peterson, J. D., Umayam, L., Gill, S. R., Nelson, K. E., Read, T. D., Tettelin, H., Richardson, D., Ermolaeva, M. D., Vamathevan, J., Bass, S., Qin, H. Y., Dragoi, I., Sellers, P., McDonald, L., Utterback, T., Fleishmann, R. D., Nierman, W. C., White, O., Salzberg, S. L., Smith, H. O., Colwell, R. R., Mekalanos, J. J., Venter, J. C., and Fraser, C. M.

(2000). Dna sequence of both chromosomes of the cholera pathogen vibrio cholerae. *Nature*, 406(6795):477–483.

[Heinrich et al., 2012] Heinrich, S., Valentin, K., Frickenhaus, S., John, U., and Wiencke, C. (2012). Transcriptomic analysis of acclimation to temperature and light stress in saccharina latissima (phaeophyceae). *Plos One*, 7(8).

[Hellingwerf et al., 2002] Hellingwerf, K., Hendriks, J., and Gensch, T. (2002). On the configurational and conformational changes in photoactive yellow protein that leads to signal generation in ectothiorhodospira halophila. *Journal of biological physics*, 28(3):395–412.

[Hendrischk et al., 2009] Hendrischk, A.-K., Frühwirth, S. W., Moldt, J., Pokorny, R., Metz, S., Kaiser, G., Jäger, A., Batschauer, A., and Klug, G. (2009). A cryptochrome-like protein is involved in the regulation of photosynthesis genes in rhodobacter sphaeroides. *Molecular microbiology*, 74(4):990–1003.

[Hirano et al., 2013] Hirano, A., Yumimoto, K., Tsunematsu, R., Matsumoto, M., Oyama, M., Kozuka-Hata, H., Nakagawa, T., Lanjakornsiripan, D., Nakayama, K. I., and Fukada, Y. (2013). Fbxl21 regulates oscillation of the circadian clock through ubiquitination and stabilization of cryptochromes. *Cell*, 152(5):1106–1118.

[Hitomi et al., 2000] Hitomi, K., Okamoto, K., Daiyasu, H., Miyashita, H., Iwai, S., Toh, H., Ishiura, M., and Todo, T. (2000). Bacterial cryptochrome and photolyase: characterization of two photolyase-like genes of synechocystis sp pcc6803. *Nucleic Acids Research*, 28(12):2353–2362.

[Hoang et al., 2008] Hoang, N., Schleicher, E., Kacprzak, S., Bouly, J.-P., Picot, M., Wu, W., Berndt, A., Wolf, E., Bittl, R., and Ahmad, M. (2008). Human and drosophila cryptochromes are light activated by flavin photoreduction in living cells. *PLoS Biol*, 6(7):e160.

[Hodgson, 1993] Hodgson, D. A. (1993). Light-induced carotenogenesis in myxococcus xanthus: genetic analysis of the carr region. *Molecular microbiology*, 7(3):471–488.

[Hogenesch et al., 1998] Hogenesch, J. B., Gu, Y.-Z., Jain, S., and Bradfield, C. A. (1998). The basic-helix–loop–helix-pas orphan mop3 forms transcriptionally active complexes with circadian and hypoxia factors. *Proceedings of the National Academy of Sciences*, 95(10):5474–5479.

[Huala et al., 1997] Huala, E., Oeller, P. W., Liscum, E., Han, I.-S., Larsen, E., and Briggs, W. R. (1997). Arabidopsis nph1: a protein kinase with a putative redox-sensing domain. *Science*, 278(5346):2120–2123.

[Hubschmann et al., 2005] Hubschmann, T., Yamamoto, H., Gieler, T., Murata, N., and Borner, T. (2005). Red and far-red light alter the transcript profile in the cyanobacterium synechocystis sp. pcc 6803: impact of cyanobacterial phytochromes. *FEBS Lett*, 579(7):1613–8.

[Hughes, 2013] Hughes, J. (2013). Phytochrome cytoplasmic signaling. *Plant Biology*, 64(1):377.

[Huq, 2006] Huq, E. (2006). Degradation of negative regulators: a common theme in hormone and light signaling networks? *Trends in plant science*, 11(1):4–7.

[Ikeno et al., 2011] Ikeno, T., Katagiri, C., Numata, H., and Goto, S. (2011). Causal involvement of mammalian-type cryptochrome in the circadian cuticle deposition rhythm in the bean bug riptortus pedestris. *Insect molecular biology*, 20(3):409–415.

[Inoue et al., 2005] Inoue, S.-i., Kinoshita, T., and Shimazaki, K.-i. (2005). Possible involvement of phototropins in leaf movement of kidney bean in response to blue light. *Plant physiology*, 138(4):1994–2004.

[Iseki et al., 2002] Iseki, M., Matsunaga, S., Murakami, A., Ohno, K., Shiga, K., Yoshida, K., Sugai, M., Takahashi, T., Hori, T., and Watanabe, M. (2002). A

blue-light-activated adenylyl cyclase mediates photoavoidance in euglena gracilis. *Nature*, 415(6875):1047–1051.

[Jarillo et al., 1998] Jarillo, J., Ahmad, M., and Cashmore, A. (1998). Phr2: A novel arabidopsis gene related to the blue-light photoreceptor/photolyase family. *Plant Physiol*, 117:719.

[Jeong et al., 2010] Jeong, R.-D., Chandra-Shekara, A., Barman, S. R., Navarre, D., Klessig, D. F., Kachroo, A., and Kachroo, P. (2010). Cryptochrome 2 and phototropin 2 regulate resistance protein-mediated viral defense by negatively regulating an e3 ubiquitin ligase. *Proceedings of the National Academy of Sciences*, 107(30):13538–13543.

[Jiao et al., 2003] Jiao, Y., Yang, H., Ma, L., Sun, N., Yu, H., Liu, T., Gao, Y., Gu, H., Chen, Z., Wada, M., Gerstein, M., Zhao, H., Qu, L. J., and Deng, X. W. (2003). A genome-wide analysis of blue-light regulation of arabidopsis transcription factor gene expression during seedling development. *Plant Physiol*, 133(4):1480–93.

[Jordan et al., 1989] Jordan, S. P., Alderfer, J. L., Chanderkar, L. P., and Jorns, M. S. (1989). Reaction of escherichia coli and yeast photolyases with homogeneous short-chain oligonucleotide substrates. *Biochemistry*, 28(20):8149–8153.

[Jorns et al., 1987] Jorns, M., Baldwin, E., Sancar, G., and Sancar, A. (1987). Action mechanism of escherichia coli dna photolyase. ii. role of the chromophores in catalysis. *Journal of Biological Chemistry*, 262(1):486–491.

[Jorns et al., 1985] Jorns, M. S., Sancar, G. B., and Sancar, A. (1985). Identification of oligothymidylates as new simple substrates for e. coli dna photolyase and their use in a rapid spectrophotometric enzyme assay. *Biochemistry*, 24(8):1856–1861.

[Jung et al., 2005] Jung, A., Domratcheva, T., Tarutina, M., Wu, Q., Ko, W.-h., Shoeman, R. L., Gomelsky, M., Gardner, K. H., and Schlichting, I. (2005). Structure of

a bacterial bluf photoreceptor: insights into blue light-mediated signal transduction. *Proceedings of the National Academy of Sciences of the United States of America*, 102(35):12350–12355.

[Kagawa et al., 2004] Kagawa, T., Kasahara, M., Abe, T., Yoshida, S., and Wada, M. (2004). Function analysis of phototropin2 using fern mutants deficient in blue light-induced chloroplast avoidance movement. *Plant and Cell Physiology*, 45(4):416–426.

[Kagawa and Wada, 2000] Kagawa, T. and Wada, M. (2000). Blue light-induced chloroplast relocation in arabidopsis thaliana as analyzed by microbeam irradiation. *Plant and Cell Physiology*, 41(1):84–93.

[Kami et al., 2010] Kami, C., Lorrain, S., Hornitschek, P., and Fankhauser, C. (2010). Chapter two-light-regulated plant growth and development. *Current topics in developmental biology*, 91:29–66.

[Kanegae et al., 2000] Kanegae, H., Tahir, M., Savazzini, F., Yamamoto, K., Yano, M., Sasaki, T., Kanegae, T., Wada, M., and Takano, M. (2000). Rice nph1 homologues, osnph1a and osnph1b, are differently photoregulated. *Plant and Cell Physiology*, 41(4):415–423.

[Kanesaki et al., 2012] Kanesaki, Y., Imamura, S., Minoda, A., and Tanaka, K. (2012). External light conditions and internal cell cycle phases coordinate accumulation of chloroplast and mitochondrial transcripts in the red alga cyanidioschyzon merolae. *DNA Research*, 19(3):289–303.

[Kang et al., 2009] Kang, C.-Y., Lian, H.-L., Wang, F.-F., Huang, J.-R., and Yang, H.-Q. (2009). Cryptochromes, phytochromes, and cop1 regulate light-controlled stomatal development in arabidopsis. *The Plant Cell*, 21(9):2624–2641.

[Karniol et al., 2005] Karniol, B., Wagner, J. R., Walker, J. M., and Vierstra, R. D.

(2005). Phylogenetic analysis of the phytochrome superfamily reveals distinct microbial subfamilies of photoreceptors. *Biochemical Journal*, 392(1):103–116.

[Kaufman, 1993] Kaufman, L. S. (1993). Transduction of blue-light signals. *Plant physiology*, 102(2):333.

[Keller et al., 2011] Keller, M. M., Jaillais, Y., Pedmale, U. V., Moreno, J. E., Chory, J., and Ballaré, C. L. (2011). Cryptochrome 1 and phytochrome b control shade-avoidance responses in arabidopsis via partially independent hormonal cascades. *The Plant Journal*, 67(2):195–207.

[Kendrick and Kronenberg, 2012] Kendrick, R. E. and Kronenberg, G. H. (2012). *Photomorphogenesis in plants*. Springer Science & Business Media.

[Kennis and Mathes, 2013] Kennis, J. T. and Mathes, T. (2013). Molecular eyes: proteins that transform light into biological information. *Interface focus*, 3(5):20130005.

[Kianianmomeni and Hallmann, 2014] Kianianmomeni, A. and Hallmann, A. (2014). Algal photoreceptors: in vivo functions and potential applications. *Planta*, 239(1):1–26.

[Kim et al., 1992] Kim, S. T., Heelis, P. F., and Sancar, A. (1992). Energy transfer (deazaflavin. fwdarw. fadh2) and electron transfer (fadh2. fwdarw. t. ltbbrac.. rtbbrac. t) kinetics in anacystis nidulans photolyase. *Biochemistry*, 31(45):11244–11248.

[Kim and Sancar, 1991] Kim, S. T. and Sancar, A. (1991). Effect of base, pentose, and phosphodiester backbone structures on binding and repair of pyrimidine dimers by escherichia coli dna photolyase. *Biochemistry*, 30(35):8623–8630.

[Kim et al., 2002] Kim, S. Y., Kim, E. J., and Park, J. W. (2002). Yeast thioredoxin peroxidase expression enhances the resistance of escherichia coli to oxidative stress induced by singlet oxygen. *Redox Rep*, 7(2):79–84.

[King et al., 1997] King, D. P., Zhao, Y., Sangoram, A. M., Wilsbacher, L. D., Tanaka, M., Antoch, M. P., Steeves, T. D., Vitaterna, M. H., Kornhauser, J. M., Lowrey, P. L., et al. (1997). Positional cloning of the mouse circadian clockgene. *Cell*, 89(4):641–653.

[Kinoshita et al., 2001] Kinoshita, T., Doi, M., Suetsugu, N., Kagawa, T., Wada, M., and Shimazaki, K.-i. (2001). Phot1 and phot2 mediate blue light regulation of stomatal opening. *Nature*, 414(6864):656–660.

[Kita et al., 2005] Kita, A., Okajima, K., Morimoto, Y., Ikeuchi, M., and Miki, K. (2005). Structure of a cyanobacterial bluf protein, tll0078, containing a novel fad-binding blue light sensor domain. *Journal of molecular biology*, 349(1):1–9.

[Kleine et al., 2007] Kleine, T., Kindgren, P., Benedict, C., Hendrickson, L., and Strand, Å. (2007). Genome-wide gene expression analysis reveals a critical role for cryptochrome1 in the response of arabidopsis to high irradiance. *Plant Physiology*, 144(3):1391–1406.

[Kleine and Leister, 2016] Kleine, T. and Leister, D. (2016). Retrograde signaling: Organelles go networking. *Biochim Biophys Acta*, 1857(8):1313–25.

[Kleine et al., 2003] Kleine, T., Lockhart, P., and Batschauer, A. (2003). An arabidopsis protein closely related to synechocystis cryptochrome is targeted to organelles. *The Plant Journal*, 35(1):93–103.

[Kliebenstein et al., 2002] Kliebenstein, D. J., Lim, J. E., Landry, L. G., and Last, R. L. (2002). Arabidopsis uvr8 regulates ultraviolet-b signal transduction and tolerance and contains sequence similarity to human regulator of chromatin condensation 1. *Plant Physiology*, 130(1):234–243.

[Kolowrat et al., 2010] Kolowrat, C., Partensky, F., Mella-Flores, D., Le Corguille, G., Boutte, C., Blot, N., Ratin, M., Ferreol, M., Lecomte, X., Gourvil, P., Lennon,

J. F., Kehoe, D. M., and Garczarek, L. (2010). Ultraviolet stress delays chromosome replication in light/dark synchronized cells of the marine cyanobacterium prochlorococcus marinus pcc9511. *BMC Microbiol*, 10:204.

[Korbee et al., 2005] Korbee, N., Figueroa, F. L., and Aguilera, J. (2005). Effect of light quality on the accumulation of photosynthetic pigments, proteins and mycosporine-like amino acids in the red alga porphyra leucosticta (bangiales, rhodophyta). *Journal of Photochemistry and Photobiology B-Biology*, 80(2):71–78.

[Kume et al., 1999] Kume, K., Zylka, M. J., Sriram, S., Shearman, L. P., Weaver, D. R., Jin, X., Maywood, E. S., Hastings, M. H., and Reppert, S. M. (1999). mcry1 and mcry2 are essential components of the negative limb of the circadian clock feedback loop. *Cell*, 98(2):193–205.

[Lawson et al., 1991] Lawson, M., Zacks, D., Derguini, F., Nakanishi, K., and Spudich, J. (1991). Retinal analog restoration of photophobic responses in a blind chlamydomonas reinhardtii mutant. evidence for an archaebacterial like chromophore in a eukaryotic rhodopsin. *Biophysical journal*, 60(6):1490.

[Lepisto et al., 2012] Lepisto, A., Toivola, J., Nikkanen, L., and Rintamaki, E. (2012). Retrograde signaling from functionally heterogeneous plastids. *Front Plant Sci*, 3:286.

[Li and Yang, 2007] Li, Q.-H. and Yang, H.-Q. (2007). Cryptochrome signaling in plants. *Photochemistry and Photobiology*, 83(1):94–101.

[Li et al., 2013a] Li, X., Kim, Y. B., Uddin, M. R., Lee, S., Kim, S. J., and Park, S. U. (2013a). Influence of light on the free amino acid content and gamma-aminobutyric acid synthesis in brassica juncea seedlings. *Journal of Agricultural and Food Chemistry*, 61(36):8624–8631.

[Li et al., 2013b] Li, X. Y., Fang, P., Mai, J. T., Choi, E. T., Wang, H., and Yang, X. F. (2013b). Targeting mitochondrial reactive oxygen species as novel therapy for inflammatory diseases and cancers. *Journal of Hematology*, 6.

[Lin and Shalitin, 2003] Lin, C. and Shalitin, D. (2003). Cryptochrome structure and signal transduction. *Annual Review of Plant Biology*, 54(1):469–496.

[Lin and Todo, 2005] Lin, C. and Todo, T. (2005). The cryptochromes. *Genome biology*, 6(5):1.

[Lin et al., 2007] Lin, P. C., Turk, K., Hase, C. C., Fritz, G., and Steuber, J. (2007). Quinone reduction by the na+-translocating nadh dehydrogenase promotes extracellular superoxide production in vibrio cholerae. *J Bacteriol*, 189(10):3902–8.

[Liscum and Hangarter, 1994] Liscum, E. and Hangarter, R. (1994). Mutational analysis of blue-light sensing in arabidopsis. *Plant, Cell & Environment*, 17(5):639–648.

[Liu and Chen, 1997] Liu, Y. and Chen, G. H. (1997). Model of energy uncoupling for substrate-sufficient culture. *Biotechnol Bioeng*, 55(3):571–6.

[Livak and Schmittgen, 2001] Livak, K. J. and Schmittgen, T. D. (2001). Analysis of relative gene expression data using real-time quantitative pcr and the 2(t)(-delta delta c) method. *Methods*, 25(4):402–408.

[Lopez et al., 2012] Lopez, L., Carbone, F., Bianco, L., Giuliano, G., Facella, P., and Perrotta, G. (2012). Tomato plants overexpressing cryptochrome 2 reveal altered expression of energy and stress-related gene products in response to diurnal cues. *Plant Cell Environ*, 35(5):994–1012.

[López-Juez et al., 2008] López-Juez, E., Dillon, E., Magyar, Z., Khan, S., Hazeldine, S., de Jager, S. M., Murray, J. A., Beemster, G. T., Bögre, L., and Shanahan, H.

(2008). Distinct light-initiated gene expression and cell cycle programs in the shoot apex and cotyledons of arabidopsis. *The Plant Cell*, 20(4):947–968.

[Losi and Gärtner, 2008] Losi, A. and Gärtner, W. (2008). Bacterial bilin-and flavin-binding photoreceptors. *Photochemical & Photobiological Sciences*, 7(10):1168–1178.

[Losi and Gartner, 2011] Losi, A. and Gartner, W. (2011). Old chromophores, new photoactivation paradigms, trendy applications: flavins in blue light-sensing photoreceptors. *Photochem Photobiol*, 87(3):491–510.

[Losi and Gartner, 2012] Losi, A. and Gartner, W. (2012). The evolution of flavin-binding photoreceptors: an ancient chromophore serving trendy blue-light sensors. *Annu Rev Plant Biol*, 63:49–72.

[Losi et al., 2014] Losi, A., Mandalari, C., and Grtner, W. (2014). From plant infectivity to growth patterns: The role of blue-light sensing in the prokaryotic world. *Plants*, 3(1):70.

[Losi et al., 2002] Losi, A., Polverini, E., Quest, B., and Gärtner, W. (2002). First evidence for phototropin-related blue-light receptors in prokaryotes. *Biophysical journal*, 82(5):2627–2634.

[Lourenço and Gomes, 2009] Lourenço, R. F. and Gomes, S. L. (2009). The transcriptional response to cadmium, organic hydroperoxide, singlet oxygen and uv-a mediated by the σe–chrr system in caulobacter crescentus. *Molecular microbiology*, 72(5):1159–1170.

[Ma et al., 2001] Ma, L., Li, J., Qu, L., Hager, J., Chen, Z., Zhao, H., and Deng, X. W. (2001). Light control of arabidopsis development entails coordinated regulation of genome expression and cellular pathways. *Plant Cell*, 13(12):2589–607.

[Maere et al., 2005] Maere, S., Heymans, K., and Kuiper, M. (2005). Bingo: a cytoscape plugin to assess overrepresentation of gene ontology categories in biological networks. *Bioinformatics*, 21(16):3448–9.

[Mailloux and Harper, 2012] Mailloux, R. J. and Harper, M. E. (2012). Mitochondrial proticity and ros signaling: lessons from the uncoupling proteins. *Trends Endocrinol Metab*, 23(9):451–8.

[Mao et al., 2005] Mao, J., Zhang, Y.-C., Sang, Y., Li, Q.-H., and Yang, H.-Q. (2005). A role for arabidopsis cryptochromes and cop1 in the regulation of stomatal opening. *Proceedings of the National Academy of Sciences of the United States of America*, 102(34):12270–12275.

[Marchler-Bauer et al., 2013] Marchler-Bauer, A., Zheng, C., Chitsaz, F., Derbyshire, M. K., Geer, L. Y., Geer, R. C., Gonzales, N. R., Gwadz, M., Hurwitz, D. I., Lanczycki, C. J., Lu, F., Lu, S., Marchler, G. H., Song, J. S., Thanki, N., Yamashita, R. A., Zhang, D., and Bryant, S. H. (2013). Cdd: conserved domains and protein three-dimensional structure. *Nucleic Acids Res*, 41(Database issue):D348–52.

[Masuda and Bauer, 2002] Masuda, S. and Bauer, C. E. (2002). Appa is a blue light photoreceptor that antirepresses photosynthesis gene expression in rhodobacter sphaeroides. *Cell*, 110(5):613–623.

[Matsuzaki et al., 2004] Matsuzaki, M., Misumi, O., Shin, I. T., Maruyama, S., Takahara, M., Miyagishima, S. Y., Mori, T., Nishida, K., Yagisawa, F., Nishida, K., Yoshida, Y., Nishimura, Y., Nakao, S., Kobayashi, T., Momoyama, Y., Higashiyama, T., Minoda, A., Sano, M., Nomoto, H., Oishi, K., Hayashi, H., Ohta, F., Nishizaka, S., Haga, S., Miura, S., Morishita, T., Kabeya, Y., Terasawa, K., Suzuki, Y., Ishii, Y., Asakawa, S., Takano, H., Ohta, N., Kuroiwa, H., Tanaka, K., Shimizu, N., Sugano, S., Sato, N., Nozaki, H., Ogasawara, N., Kohara, Y., and Kuroiwa, T.

(2004). Genome sequence of the ultrasmall unicellular red alga cyanidioschyzon merolae 10d. *Nature*, 428(6983):653–7.

[McClure et al., 2013] McClure, R., Balasubramanian, D., Sun, Y., Bobrovskyy, M., Sumby, P., Genco, C. A., Vanderpool, C. K., and Tjaden, B. (2013). Computational analysis of bacterial rna-seq data. *Nucleic Acids Research*, 41(14).

[Metz et al., 2012] Metz, S., Haberzettl, K., Frühwirth, S., Teich, K., Hasewinkel, C., and Klug, G. (2012). Interaction of two photoreceptors in the regulation of bacterial photosynthesis genes. *Nucleic acids research*, page gks243.

[Mi et al., 2013] Mi, H., Muruganujan, A., Casagrande, J. T., and Thomas, P. D. (2013). Large-scale gene function analysis with the panther classification system. *Nat Protoc*, 8(8):1551–66.

[Minoda et al., 2005] Minoda, A., Nagasawa, K., Hanaoka, M., Horiuchi, M., Takahashi, H., and Tanaka, K. (2005). Microarray profiling of plastid gene expression in a unicellular red alga, cyanidioschyzon merolae. *Plant Mol Biol*, 59(3):375–85.

[Minoda et al., 2004] Minoda, A., Sakagami, R., Yagisawa, F., Kuroiwa, T., and Tanaka, K. (2004). Improvement of culture conditions and evidence for nuclear transformation by homologous recombination in a red alga, cyanidioschyzon merolae 10d. *Plant Cell Physiol*, 45(6):667–71.

[Mittler et al., 2004] Mittler, R., Vanderauwera, S., Gollery, M., and Van Breusegem, F. (2004). Reactive oxygen gene network of plants. *Trends Plant Sci*, 9(10):490–8.

[Miwa and Brand, 2003] Miwa, S. and Brand, M. D. (2003). Mitochondrial matrix reactive oxygen species production is very sensitive to mild uncoupling. *Biochem Soc Trans*, 31(Pt 6):1300–1.

[Möglich et al., 2010] Möglich, A., Yang, X., Ayers, R. A., and Moffat, K. (2010). Structure and function of plant photoreceptors. *Annual review of plant biology*, 61:21–47.

[Monnier et al., 2010] Monnier, A., Liverani, S., Bouvet, R., Jesson, B., Smith, J. Q., Mosser, J., Corellou, F., and Bouget, F. Y. (2010). Orchestrated transcription of biological processes in the marine picoeukaryote ostreococcus exposed to light/dark cycles. *BMC Genomics*, 11:192.

[Montgomery, 2007] Montgomery, B. L. (2007). Sensing the light: photoreceptive systems and signal transduction in cyanobacteria. *Mol Microbiol*, 64(1):16–27.

[Müller and Carell, 2009] Müller, M. and Carell, T. (2009). Structural biology of dna photolyases and cryptochromes. *Current opinion in structural biology*, 19(3):277–285.

[Musacchia et al., 2015] Musacchia, F., Basu, S., Petrosino, G., Salvemini, M., and Sanges, R. (2015). Annocript: a flexible pipeline for the annotation of transcriptomes able to identify putative long noncoding rnas. *Bioinformatics*, 31(13):2199–201.

[Nelson et al., 1989] Nelson, M., Morelli, G., Carattoli, A., Romano, N., and Macino, G. (1989). Molecular cloning of a neurospora crassa carotenoid biosynthetic gene (albino-3) regulated by blue light and the products of the white collar genes. *Molecular and cellular biology*, 9(3):1271–1276.

[Newman et al., 2001] Newman, J. D., Anthony, J. R., and Donohue, T. J. (2001). The importance of zinc-binding to the function of rhodobacter sphaeroides chrr as an anti-sigma factor. *Journal of molecular biology*, 313(3):485–499.

[Newman et al., 1999] Newman, J. D., Falkowski, M. J., Schilke, B. A., Anthony, L. C., and Donohue, T. J. (1999). The rhodobacter sphaeroides ecf sigma factor, sigma(e), and the target promoters cyca p3 and rpoe p1. *J Mol Biol*, 294(2):307–20.

[Nishida et al., 2005] Nishida, K., Yagisawa, F., Kuroiwa, H., Nagata, T., and Kuroiwa, T. (2005). Cell cycle-regulated, microtubule-independent organelle division in cyanidioschyzon merolae. *Molecular biology of the cell*, 16(5):2493–2502.

[Nozaki et al., 2007] Nozaki, H., Takano, H., Misumi, O., Terasawa, K., Matsuzaki, M., Maruyama, S., Nishida, K., Yagisawa, F., Yoshida, Y., Fujiwara, T., Takio, S., Tamura, K., Chung, S. J., Nakamura, S., Kuroiwa, H., Tanaka, K., Sato, N., and Kuroiwa, T. (2007). A 100the hot-spring red alga cyanidioschyzon merolae. *BMC Biol*, 5:28.

[Oesterhelt and Stoeckenius, 1973] Oesterhelt, D. and Stoeckenius, W. (1973). Functions of a new photoreceptor membrane. *Proceedings of the National Academy of Sciences*, 70(10):2853–2857.

[Ohgishi et al., 2004] Ohgishi, M., Saji, K., Okada, K., and Sakai, T. (2004). Functional analysis of each blue light receptor, cry1, cry2, phot1, and phot2, by using combinatorial multiple mutants in arabidopsis. *Proceedings of the National Academy of Sciences of the United States of America*, 101(8):2223–2228.

[Okajima et al., 2005] Okajima, K., Yoshihara, S., Fukushima, Y., Geng, X., Katayama, M., Higashi, S., Watanabe, M., Sato, S., Tabata, S., Shibata, Y., et al. (2005). Biochemical and functional characterization of bluf-type flavin-binding proteins of two species of cyanobacteria. *Journal of biochemistry*, 137(6):741–750.

[Ondrusch and Kreft, 2011] Ondrusch, N. and Kreft, J. (2011). Blue and red light modulates sigb-dependent gene transcription, swimming motility and invasiveness in listeria monocytogenes. *PLoS One*, 6(1):e16151.

[Orlandi et al., 2015] Orlandi, V. T., Bolognese, F., Chiodaroli, L., Tolker-Nielsen, T., and Barbieri, P. (2015). Pigments influence the tolerance of pseudomonas aeruginosa pao1 to photodynamically induced oxidative stress. *Microbiology*, 161(12):2298–309.

[Öztürk et al., 2008] Öztürk, N., Kao, Y.-T., Selby, C. P., Kavaklı, I. H., Partch, C. L., Zhong, D., and Sancar, A. (2008). Purification and characterization of a type iii photolyase from caulobacter crescentus. *Biochemistry*, 47(39):10255–10261.

[Öztürk et al., 2007] Öztürk, N., Song, S.-H., Özgür, S., Selby, C. P., Morrison, L., Partch, C., Zhong, D., and Sancar, A. (2007). Structure and function of animal cryptochromes. In *Cold Spring Harbor Symposia on Quantitative Biology*, volume 72, pages 119–131. Cold Spring Harbor Laboratory Press.

[Paget et al., 2001] Paget, M. S. B., Molle, V., Cohen, G., Aharonowitz, Y., and Buttner, M. J. (2001). Defining the disulphide stress response in streptomyces coelicolor a3(2): identification of the sigma(r) regulon. *Molecular Microbiology*, 42(4):1007–1020.

[Pandhal et al., 2007] Pandhal, J., Wright, P. C., and Biggs, C. A. (2007). A quantitative proteomic analysis of light adaptation in a globally significant marine cyanobacterium prochlorococcus marinus med4. *J Proteome Res*, 6(3):996–1005.

[Partch et al., 2005] Partch, C. L., Clarkson, M. W., Özgür, S., Lee, A. L., and Sancar, A. (2005). Role of structural plasticity in signal transduction by the cryptochrome blue-light photoreceptor. *Biochemistry*, 44(10):3795–3805.

[Partch and Sancar, 2005] Partch, C. L. and Sancar, A. (2005). Photochemistry and photobiology of cryptochrome blue-light photopigments: The search for a photocycle. *Photochemistry and Photobiology*, 81(6):1291–1304.

[Payne and Sancar, 1990] Payne, G. and Sancar, A. (1990). Absolute action spectrum of e-fadh2 and e-fadh2-mthf forms of escherichia coli dna photolyase. *Biochemistry*, 29(33):7715–7727.

[Perez-Rodriguez et al., 2010] Perez-Rodriguez, P., Riano-Pachon, D. M., Correa, L. G., Rensing, S. A., Kersten, B., and Mueller-Roeber, B. (2010). Plntfdb: updated

content and new features of the plant transcription factor database. *Nucleic Acids Res*, 38(Database issue):D822–7.

[Pireyre and Burow, 2015] Pireyre, M. and Burow, M. (2015). Regulation of myb and bhlh transcription factors: A glance at the protein level. *Mol Plant*, 8(3):378–388.

[Purcell and Crosson, 2008] Purcell, E. B. and Crosson, S. (2008). Photoregulation in prokaryotes. *Current opinion in microbiology*, 11(2):168–178.

[Quail, 2000] Quail, P. H. (2000). Phytochrome-interacting factors. In *Seminars in cell & developmental biology*, volume 11, pages 457–466. Elsevier.

[Reisdorph and Small, 2004] Reisdorph, N. A. and Small, G. D. (2004). The cph1 gene of chlamydomonas reinhardtii encodes two forms of cryptochrome whose levels are controlled by light-induced proteolysis. *Plant Physiol*, 134(4):1546–54.

[Río-Álvarez et al., 2014] Río-Álvarez, I., Rodríguez-Herva, J. J., Martínez, P. M., González-Melendi, P., García-Casado, G., Rodríguez-Palenzuela, P., and López-Solanilla, E. (2014). Light regulates motility, attachment and virulence in the plant pathogen pseudomonas syringae pv tomato dc3000. *Environmental microbiology*, 16(7):2072–2085.

[Rockwell et al., 2006] Rockwell, N. C., Su, Y.-S., and Lagarias, J. C. (2006). Phytochome structure and signaling mechanisms. *Annual review of plant biology*, 57:837.

[Roh et al., 1998] Roh, M. H., Shingles, R., Cleveland, M. J., and McCarty, R. E. (1998). Direct measurement of calcium transport across chloroplast inner-envelope vesicles. *Plant Physiol*, 118(4):1447–54.

[Rubin et al., 2006] Rubin, E. B., Shemesh, Y., Cohen, M., Elgavish, S., Robertson, H. M., and Bloch, G. (2006). Molecular and phylogenetic analyses reveal mammalian-like clockwork in the honey bee (apis mellifera) and shed new light on the molecular evolution of the circadian clock. *Genome Research*, 16(11):1352–1365.

[Ryter and Tyrrell, 1998] Ryter, S. W. and Tyrrell, R. M. (1998). Singlet molecular oxygen (o-1(2)): A possible effector of eukaryotic gene expression. *Free Radical Biology and Medicine*, 24(9):1520–1534.

[Sai and Johnson, 2002] Sai, J. Q. and Johnson, C. H. (2002). Dark-stimulated calcium ion fluxes in the chloroplast stroma and cytosol. *Plant Cell*, 14(6):1279–1291.

[Sakai et al., 2001] Sakai, T., Kagawa, T., Kasahara, M., Swartz, T. E., Christie, J. M., Briggs, W. R., Wada, M., and Okada, K. (2001). Arabidopsis nph1 and npl1: blue light receptors that mediate both phototropism and chloroplast relocation. *Proceedings of the National Academy of Sciences*, 98(12):6969–6974.

[Sakamoto and Briggs, 2002] Sakamoto, K. and Briggs, W. R. (2002). Cellular and subcellular localization of phototropin 1. *The Plant Cell*, 14(8):1723–1735.

[Salomon et al., 2000] Salomon, M., Christie, J. M., Knieb, E., Lempert, U., and Briggs, W. R. (2000). Photochemical and mutational analysis of the fmn-binding domains of the plant blue light receptor, phototropin. *Biochemistry*, 39(31):9401–9410.

[Sancar, 1994] Sancar, A. (1994). Structure and function of dna photolyase. *Biochemistry*, 33(1):2–9.

[Sancar, 2000] Sancar, A. (2000). Cryptochrome: the second photoactive pigment in the eye and its role in circadian photoreception. *Annual review of biochemistry*, 69(1):31–67.

[Sancar, 2003] Sancar, A. (2003). Structure and function of dna photolyase and cryptochrome blue-light photoreceptors. *Chemical reviews*, 103(6):2203–2238.

[Sancar et al., 1987a] Sancar, G., Jorns, M. S., Payne, G., Fluke, D., Rupert, C., and Sancar, A. (1987a). Action mechanism of escherichia coli dna photolyase.

iii. photolysis of the enzyme-substrate complex and the absolute action spectrum. *Journal of Biological Chemistry*, 262(1):492–498.

[Sancar et al., 1987b] Sancar, G. B., Smith, F. W., Reid, R., Payne, G., Levy, M., and Sancar, A. (1987b). Action mechanism of escherichia coli dna photolyase. i. formation of the enzyme-substrate complex. *Journal of Biological Chemistry*, 262(1):478–485.

[Schäfer and Nagy, 2006] Schäfer, E. and Nagy, F. (2006). *Photomorphogenesis in plants and bacteria: function and signal transduction mechanisms*. Springer Science & Business Media.

[Seib et al., 2006] Seib, K. L., Wu, H. J., Kidd, S. P., Apicella, M. A., Jennings, M. P., and McEwan, A. G. (2006). Defenses against oxidative stress in neisseria gonorrhoeae: a system tailored for a challenging environment. *Microbiol Mol Biol Rev*, 70(2):344–61.

[Selby and Sancar, 2006] Selby, C. P. and Sancar, A. (2006). A cryptochrome/photolyase class of enzymes with single-stranded dna-specific photolyase activity. *Proceedings of the National Academy of Sciences*, 103(47):17696–17700.

[Shalitin et al., 2003] Shalitin, D., Yu, X., Maymon, M., Mockler, T., and Lin, C. (2003). Blue light–dependent in vivo and in vitro phosphorylation of arabidopsis cryptochrome 1. *The Plant Cell*, 15(10):2421–2429.

[Shannon et al., 2003] Shannon, P., Markiel, A., Ozier, O., Baliga, N. S., Wang, J. T., Ramage, D., Amin, N., Schwikowski, B., and Ideker, T. (2003). Cytoscape: a software environment for integrated models of biomolecular interaction networks. *Genome Res*, 13(11):2498–504.

[Sharrock, 2008] Sharrock, R. A. (2008). The phytochrome red/far-red photoreceptor superfamily. *Genome biology*, 9(8):1.

[Sharrock and Clack, 2002] Sharrock, R. A. and Clack, T. (2002). Patterns of expression and normalized levels of the five arabidopsis phytochromes. *Plant Physiology*, 130(1):442–456.

[Short and Briggs, 1994] Short, T. W. and Briggs, W. R. (1994). The transduction of blue light signals in higher plants. *Annual review of plant biology*, 45(1):143–171.

[Simon et al., 1983] Simon, R., Priefer, U., and Puhler, A. (1983). A broad host range mobilization system for invivo genetic-engineering - transposon mutagenesis in gram-negative bacteria. *Bio-Technology*, 1(9):784–791.

[Somers et al., 1998] Somers, D. E., Devlin, P. F., and Kay, S. A. (1998). Phytochromes and cryptochromes in the entrainment of the arabidopsis circadian clock. *Science*, 282(5393):1488–1490.

[Stanewsky et al., 1998] Stanewsky, R., Kaneko, M., Emery, P., Beretta, B., Wager-Smith, K., Kay, S. A., Rosbash, M., and Hall, J. C. (1998). The cryb mutation identifies cryptochrome as a circadian photoreceptor in drosophila. *Cell*, 95(5):681–692.

[Stark et al., 2015] Stark, M. R., Dunn, E. A., Dunn, W. S., Grisdale, C. J., Daniele, A. R., Halstead, M. R., Fast, N. M., and Rader, S. D. (2015). Dramatically reduced spliceosome in cyanidioschyzon merolae. *Proc Natl Acad Sci U S A*.

[Steglich et al., 2006] Steglich, C., Futschik, M., Rector, T., Steen, R., and Chisholm, S. W. (2006). Genome-wide analysis of light sensing in prochlorococcus. *Journal of bacteriology*, 188(22):7796–7806.

[Stierl et al., 2011] Stierl, M., Stumpf, P., Udwari, D., Gueta, R., Hagedorn, R., Losi, A., Gärtner, W., Petereit, L., Efetova, M., Schwarzel, M., et al. (2011). Light modulation of cellular camp by a small bacterial photoactivated adenylyl cyclase,

bpac, of the soil bacterium beggiatoa. *Journal of Biological Chemistry*, 286(2):1181–1188.

[Storz and Imlay, 1999] Storz, G. and Imlay, J. A. (1999). Oxidative stress. *Current Opinion in Microbiology*, 2(2):188–194.

[Suter et al., 2000] Suter, B., Wellinger, R. E., and Thoma, F. (2000). Dna repair in a yeast origin of replication: contributions of photolyase and nucleotide excision repair. *Nucleic Acids Res*, 28(10):2060–8.

[Suzek et al., 2007] Suzek, B. E., Huang, H., McGarvey, P., Mazumder, R., and Wu, C. H. (2007). Uniref: comprehensive and non-redundant uniprot reference clusters. *Bioinformatics*, 23(10):1282–8.

[Szymanski et al., 2014] Szymanski, J., Brotman, Y., Willmitzer, L., and Cuadros-Inostroza, A. (2014). Linking gene expression and membrane lipid composition of arabidopsis. *Plant Cell*, 26(3):915–28.

[Takano et al., 2006a] Takano, H., Asker, D., Beppu, T., and Ueda, K. (2006a). Genetic control for light-induced carotenoid production in non-phototrophic bacteria. *Journal of Industrial Microbiology and Biotechnology*, 33(2):88–93.

[Takano et al., 2006b] Takano, H., Beppu, T., and Ueda, K. (2006b). The cara/litr-family transcriptional regulator: Its possible role as a photosensor and wide distribution in non-phototrophic bacteria. *Bioscience Biotechnology and Biochemistry*, 70(9):2320–2324.

[Talarico and Maranzana, 2000] Talarico, L. and Maranzana, G. (2000). Light and adaptive responses in red macroalgae: an overview. *J Photochem Photobiol B*, 56(1):1–11.

[Tanaka and Hanaoka, 2012] Tanaka, K. and Hanaoka, M. (2012). The early days of plastid retrograde signaling with respect to replication and transcription. *Front Plant Sci*, 3:301.

[Taylor and Zhulin, 1999] Taylor, B. L. and Zhulin, I. B. (1999). Pas domains: internal sensors of oxygen, redox potential, and light. *Microbiology and Molecular Biology Reviews*, 63(2):479–506.

[Tepperman et al., 2006] Tepperman, J. M., Hwang, Y.-S., and Quail, P. H. (2006). phya dominates in transduction of red-light signals to rapidly responding genes at the initiation of arabidopsis seedling de-etiolation. *The Plant Journal*, 48(5):728–742.

[Terui et al., 1995] Terui, S., Suzuki, K., Takahashi, H., Itoh, R., and Kuroiwa, T. (1995). Synchronization of chloroplast division in the ultramicroalga cyanidioschyzon merolae (rhodophyta) by treatment with light and aphidicolin. *Journal of Phycology*, 31(6):958–961.

[Thomas-Chollier et al., 2008] Thomas-Chollier, M., Sand, O., Turatsinze, J. V., Janky, R., Defrance, M., Vervisch, E., Brohee, S., and van Helden, J. (2008). Rsat: regulatory sequence analysis tools. *Nucleic Acids Research*, 36:W119–W127.

[Thompson and Sancar, 2002] Thompson, C. L. and Sancar, A. (2002). Photolyase/cryptochrome blue-light photoreceptors use photon energy to repair dna and reset the circadian clock. *Oncogene*, 21(58).

[Tilbrook et al., 2013] Tilbrook, K., Arongaus, A. B., Binkert, M., Heijde, M., Yin, R., and Ulm, R. (2013). The uvr8 uv-b photoreceptor: perception, signaling and response. *The Arabidopsis Book*, page e0164.

[Tomioka and Matsumoto, 2010] Tomioka, K. and Matsumoto, A. (2010). A comparative view of insect circadian clock systems. *Cellular and Molecular Life Sciences*, 67(9):1397–1406.

[Trapnell et al., 2012] Trapnell, C., Roberts, A., Goff, L., Pertea, G., Kim, D., Kelley, D. R., Pimentel, H., Salzberg, S. L., Rinn, J. L., and Pachter, L. (2012). Differential gene and transcript expression analysis of rna-seq experiments with tophat and cufflinks. *Nat Protoc*, 7(3):562–78.

[Tschowri et al., 2009] Tschowri, N., Busse, S., and Hengge, R. (2009). The bluf-eal protein ycgf acts as a direct anti-repressor in a blue-light response of escherichia coli. *Genes & development*, 23(4):522–534.

[Uchoa et al., 2008] Uchoa, A. F., Knox, P. P., Turchielle, R., Seifullina, N. K., and Baptista, M. S. (2008). Singlet oxygen generation in the reaction centers of rhodobacter sphaeroides. *European Biophysics Journal*, 37(6):843–850.

[Ueno et al., 2015] Ueno, Y., Aikawa, S., Kondo, A., and Akimoto, S. (2015). Light adaptation of the unicellular red alga, cyanidioschyzon merolae, probed by time-resolved fluorescence spectroscopy. *Photosynthesis Research*, 125(1-2):211–218.

[Usami et al., 2004] Usami, T., Mochizuki, N., Kondo, M., Nishimura, M., and Nagatani, A. (2004). Cryptochromes and phytochromes synergistically regulate arabidopsis root greening under blue light. *Plant and Cell Physiology*, 45(12):1798–1808.

[Van Der Horst et al., 1999] Van Der Horst, G. T., Muijtjens, M., Kobayashi, K., Takano, R., Kanno, S.-i., Takao, M., de Wit, J., Verkerk, A., Eker, A. P., van Leenen, D., et al. (1999). Mammalian cry1 and cry2 are essential for maintenance of circadian rhythms. *Nature*, 398(6728):627–630.

[van der Horst et al., 2007] van der Horst, M. A., Key, J., and Hellingwerf, K. J. (2007). Photosensing in chemotrophic, non-phototrophic bacteria: let there be light sensing too. *Trends in microbiology*, 15(12):554–562.

[Veluchamy and Rollins, 2008] Veluchamy, S. and Rollins, J. A. (2008). A cry-dash-

type photolyase/cryptochrome from sclerotinia sclerotiorum mediates minor uv-a-specific effects on development. *Fungal Genetics and Biology*, 45(9):1265–1276.

[Vielhaber et al., 2001] Vielhaber, E. L., Duricka, D., Ullman, K. S., and Virshup, D. M. (2001). Nuclear export of mammalian period proteins. *Journal of Biological Chemistry*, 276(49):45921–45927.

[Vitaterna et al., 1999] Vitaterna, M. H., Selby, C. P., Todo, T., Niwa, H., Thompson, C., Fruechte, E. M., Hitomi, K., Thresher, R. J., Ishikawa, T., Miyazaki, J., et al. (1999). Differential regulation of mammalian period genes and circadian rhythmicity by cryptochromes 1 and 2. *Proceedings of the National Academy of Sciences*, 96(21):12114–12119.

[Voityuk et al., 2014] Voityuk, A. A., Marcus, R. A., and Michel-Beyerle, M.-E. (2014). On the mechanism of photoinduced dimer dissociation in the plant uvr8 photoreceptor. *Proceedings of the National Academy of Sciences*, 111(14):5219–5224.

[Wang et al., 2001] Wang, H., Ma, L.-G., Li, J.-M., Zhao, H.-Y., and Deng, X. W. (2001). Direct interaction of arabidopsis cryptochromes with cop1 in light control development. *Science*, 294(5540):154–158.

[Wang and Wang, 2015] Wang, H. and Wang, H. (2015). Phytochrome signaling: time to tighten up the loose ends. *Molecular plant*, 8(4):540–551.

[Wang et al., 2013] Wang, W. J., Wang, F. J., Sun, X. T., Liu, F. L., and Liang, Z. R. (2013). Comparison of transcriptome under red and blue light culture of saccharina japonica (phaeophyceae). *Planta*, 237(4):1123–33.

[Wang et al., 1997] Wang, Z. Y., Kenigsbuch, D., Sun, L., Harel, E., Ong, M. S., and Tobin, E. M. (1997). A myb-related transcription factor is involved in the phytochrome regulation of an arabidopsis lhcb gene. *Plant Cell*, 9(4):491–507.

[Weller et al., 2001] Weller, J. L., Perrotta, G., Schreuder, M. E., Van Tuinen, A., Koornneef, M., Giuliano, G., and Kendrick, R. E. (2001). Genetic dissection of blue-light sensing in tomato using mutants deficient in cryptochrome 1 and phytochromes a, b1 and b2. *The Plant Journal*, 25(4):427–440.

[Weston et al., 2000] Weston, E., Thorogood, K., Vinti, G., and López-Juez, E. (2000). Light quantity controls leaf-cell and chloroplast development in arabidopsis thaliana wild type and blue-light-perception mutants. *Planta*, 211(6):807–815.

[Worthington et al., 2003] Worthington, E. N., Kavakli, İ. H., Berrocal-Tito, G., Bondo, B. E., and Sancar, A. (2003). Purification and characterization of three members of the photolyase/cryptochrome family blue-light photoreceptors from vibrio cholerae. *Journal of Biological Chemistry*, 278(40):39143–39154.

[Wu et al., 2012] Wu, D., Hu, Q., Yan, Z., Chen, W., Yan, C., Huang, X., Zhang, J., Yang, P., Deng, H., Wang, J., et al. (2012). Structural basis of ultraviolet-b perception by uvr8. *Nature*, 484(7393):214–219.

[Wu and Spalding, 2007] Wu, G. and Spalding, E. P. (2007). Separate functions for nuclear and cytoplasmic cryptochrome 1 during photomorphogenesis of arabidopsis seedlings. *Proceedings of the National Academy of Sciences*, 104(47):18813–18818.

[Wu and Yang, 2010] Wu, L. and Yang, H.-Q. (2010). Cryptochrome 1 is implicated in promoting r protein-mediated plant resistance to pseudomonas syringae in arabidopsis. *Molecular plant*, 3(3):539–548.

[Xu et al., 2009] Xu, P., Xiang, Y., Zhu, H., Xu, H., Zhang, Z., Zhang, C., Zhang, L., and Ma, Z. (2009). Wheat cryptochromes: subcellular localization and involvement in photomorphogenesis and osmotic stress responses. *Plant physiology*, 149(2):760–774.

[Yagi and Shiina, 2014] Yagi, Y. and Shiina, T. (2014). Recent advances in the study of chloroplast gene expression and its evolution. *Frontiers in Plant Science*, 5.

[Yang et al., 2001] Yang, H.-Q., Tang, R.-H., and Cashmore, A. R. (2001). The signaling mechanism of arabidopsis cry1 involves direct interaction with cop1. *The Plant Cell*, 13(12):2573–2587.

[Yang et al., 2000] Yang, H.-Q., Wu, Y.-J., Tang, R.-H., Liu, D., Liu, Y., and Cashmore, A. R. (2000). The c termini of arabidopsis cryptochromes mediate a constitutive light response. *Cell*, 103(5):815–827.

[Yanovsky et al., 2001] Yanovsky, M. J., Mazzella, M. A., Whitelam, G. C., and Casal, J. J. (2001). Resetting of the circadian clock by phytochromes and cryptochromes in arabidopsis. *Journal of biological rhythms*, 16(6):523–530.

[Yildiz et al., 2004] Yildiz, F. H., Liu, X. S., Heydorn, A., and Schoolnik, G. K. (2004). Molecular analysis of rugosity in a vibrio cholerae o1 el tor phase variant. *Mol Microbiol*, 53(2):497–515.

[Yu et al., 2007a] Yu, X., Klejnot, J., Zhao, X., Shalitin, D., Maymon, M., Yang, H., Lee, J., Liu, X., Lopez, J., and Lin, C. (2007a). Arabidopsis cryptochrome 2 completes its posttranslational life cycle in the nucleus. *The Plant Cell*, 19(10):3146–3156.

[Yu et al., 2009] Yu, X., Sayegh, R., Maymon, M., Warpeha, K., Klejnot, J., Yang, H., Huang, J., Lee, J., Kaufman, L., and Lin, C. (2009). Formation of nuclear bodies of arabidopsis cry2 in response to blue light is associated with its blue light–dependent degradation. *The Plant Cell*, 21(1):118–130.

[Yu et al., 2007b] Yu, X., Shalitin, D., Liu, X., Maymon, M., Klejnot, J., Yang, H., Lopez, J., Zhao, X., Bendehakkalu, K. T., and Lin, C. (2007b). Derepression of the

nc80 motif is critical for the photoactivation of arabidopsis cry2. *Proceedings of the National Academy of Sciences*, 104(17):7289–7294.

[Yuan et al., 2006] Yuan, H., Anderson, S., Masuda, S., Dragnea, V., Moffat, K., and Bauer, C. (2006). Crystal structures of the synechocystis photoreceptor slr1694 reveal distinct structural states related to signaling. *Biochemistry*, 45(42):12687–12694.

[Yuan et al., 2007] Yuan, Q., Metterville, D., Briscoe, A. D., and Reppert, S. M. (2007). Insect cryptochromes: gene duplication and loss define diverse ways to construct insect circadian clocks. *Molecular Biology and Evolution*, 24(4):948–955.

[Zhu et al., 2005] Zhu, H., Yuan, Q., Froy, O., Casselman, A., and Reppert, S. M. (2005). The two crys of the butterfly. *Current Biology*, 15(23):R953–R954.

[Ziegelhoffer and Donohue, 2009] Ziegelhoffer, E. C. and Donohue, T. J. (2009). Bacterial responses to photo-oxidative stress. *Nature Reviews Microbiology*, 7(12):856–863.

[Ziegler and Möglich, 2015] Ziegler, T. and Möglich, A. (2015). Photoreceptor engineering. *Frontiers in molecular biosciences*, 2.

Appendix A

APPENDIX

Table A.1: Expression values of 222 Statistically significant DEGs at dark and blue light conditions in wild type and mutant *V. cholerae* cells.

Gene ID	Expression Values						Statistical q-value		
	Wt BL (-)	Wt BL (+)	ΔChrR BL (-)	ΔChrR BL (+)	ΔChrRΔMerR BL (-)	ΔChrRΔMerR BL (+)	Wt BL (-) vs Wt BL (+)	ΔChrR BL (-) vs ΔChrR BL (+)	ΔChrRΔMerR BL (-) vs ΔChrRΔMerR BL (+)
VC2303	75	8543	2588	2411	1564	2097	0.0E+00	9.1E-01	1.4E-08
VC1118	75	8485	1502	3706	3947	4282	0.0E+00	6.9E-12	1.9E-02
VC1812	12	744	226	177	333	454	0.0E+00	7.1E-01	3.2E-05
VCA0055	66	3452	43	2717	4653	4680	0.0E+00	0.0E+00	6.7E-01
VC1119	59	3071	1003	1605	1780	1935	0.0E+00	2.4E-04	3.2E-01
VCA0056	60	2997	54	2157	2341	2339	0.0E+00	0.0E+00	4.3E-01
VC1120	86	3453	1305	1784	1986	2079	0.0E+00	9.1E-01	2.1E-01
VC1392	22	844	181	191	185	223	0.0E+00	9.1E-01	1.5E-01
VC2302	259	9722	3034	3138	1833	2089	0.0E+00	9.1E-01	2.2E-02
VC1811	48	1595	591	405	395	532	0.0E+00	6.4E-03	3.8E-02
VC1122	69	2127	2588	2051	2359	2302	0.0E+00	7.3E-01	3.3E-11
VC1814	8	239	208	118	218	268	0.0E+00	1.1E-05	6.7E-03
VCA0615	49	1446	461	409	380	455	0.0E+00	5.9E-01	2.8E-01
VCA0057	82	2327	52	1252	1117	1176	0.0E+00	0.0E+00	6.7E-02
VC2301	81	2226	210	217	306	357	0.0E+00	6.5E-01	9.4E-01
VC1571	33	750	257	268	245	358	0.0E+00	9.9E-01	8.7E-13
VC1121	63	1396	932	917	956	976	0.0E+00	9.7E-01	4.8E-02
VC2088	98	1930	905	708	1379	1567	0.0E+00	1.7E-01	1.0E-03
VC1815	19	358	371	188	392	496	0.0E+00	8.7E-09	1.4E-02
VC1570	26	457	171	155	136	199	0.0E+00	9.0E-01	2.4E-07
VC1263	197	2632	1201	859	1139	1340	0.0E+00	5.3E-02	4.4E-04
VC0149	31	317	97	100	86	108	0.0E+00	7.0E-01	7.9E-07
VC2293	49	399	171	145	203	262	0.0E+00	7.6E-01	6.5E-04
VCA0902	40	303	107	70	115	142	0.0E+00	2.6E-01	1.2E-05
VC2294	46	335	163	149	253	309	0.0E+00	9.2E-01	1.7E-03
VC1123	54	363	331	257	585	592	1.9E-271	2.5E-01	3.7E-01
VC2231	81	536	162	643	216	334	0.0E+00	9.8E-50	2.0E-06
VC2044	56	339	144	140	245	273	5.7E-151	9.6E-01	1.9E-05
VC1923	30	180	86	76	158	188	1.9E-269	9.3E-01	9.2E-01

continued on next page!

Table A.1 – continued from previous page

Gene ID	Expression Values						Statistical q-value		
	Wt BL (-)	Wt BL (+)	ΔChrR BL (-)	ΔChrR BL (+)	ΔChrRΔMerR BL (-)	ΔChrRΔMerR BL (+)	Wt BL (-) vs Wt BL (+)	ΔChrR BL (-) vs ΔChrR BL (+)	ΔChrRΔMerR BL (-) vs ΔChrRΔMerR BL (+)
VC1389	22	131	41	35	31	54	6.4E-51	9.9E-01	1.0E-02
VC1422a	75	434	245	276	275	297	1.4E-106	6.8E-01	4.9E-01
VC1922	231	1298	1006	1208	948	971	0.0E+00	5.4E-01	8.7E-02
VC0987	56	309	163	155	134	183	2.6E-271	9.8E-01	4.5E-05
VC1271	46	241	123	83	76	87	5.0E-169	3.7E-01	2.4E-06
VCA0783	155	812	387	312	300	323	0.0E+00	3.3E-01	4.7E-01
VCA0058	97	503	83	315	505	527	0.0E+00	9.0E-57	7.6E-04
VC0747	209	1050	105	535	248	349	0.0E+00	6.5E-103	4.4E-06
VC0156	37	180	56	63	36	40	8.9E-212	4.4E-01	1.4E-06
VC2292	43	207	90	84	161	210	1.2E-111	9.6E-01	5.9E-06
VC2501	83	384	175	167	309	335	0.0E+00	9.1E-01	4.9E-03
VC2087	56	258	288	185	574	587	0.0E+00	4.3E-03	2.5E-01
VCA0291	42	188	78	493	38	66	3.3E-134	5.2E-205	1.8E-18
VC0666	158	689	185	675	236	287	5.3E-123	1.8E-29	1.1E-08
VCA0782	56	236	124	76	86	94	3.2E-108	1.0E-01	1.2E-05
VC0083	107	444	190	346	163	199	4.2E-174	2.0E-09	2.8E-03
VC0852	110	452	190	1085	216	385	0.0E+00	2.8E-129	7.2E-42
VC0748	303	1230	144	631	358	462	0.0E+00	2.2E-100	8.5E-01
VC1423	44	177	134	126	208	220	2.5E-83	9.5E-01	3.0E-01
VC2242	40	156	57	56	42	38	2.1E-111	8.0E-01	5.2E-01
VC2291	106	410	175	159	161	194	1.5E-116	1.0E+00	1.9E-05
VCA0809	41	158	85	62	85	106	2.6E-114	3.0E-01	1.7E-03
VC0084	69	264	104	151	112	122	3.0E-92	1.5E-02	3.6E-06
VC0944	29	110	96	150	106	114	5.1E-45	2.9E-03	5.9E-06
VC2290	68	257	135	121	141	170	5.1E-135	8.2E-01	2.1E-01
VC1393	48	181	100	59	48	54	4.6E-39	2.4E-01	8.6E-01
VC1191	226	851	248	1351	547	1088	2.0E-144	5.5E-172	1.3E-29
VC2042	58	218	105	118	79	101	2.1E-97	4.4E-01	8.2E-09
VC2759	91	336	422	1927	416	629	2.1E-158	2.3E-59	1.7E-05
VC2091	101	372	279	222	607	592	8.1E-79	6.7E-01	1.7E-02
VC2704	848	3099	407	1766	166	181	0.0E+00	3.5E-105	4.8E-01
VC0082	80	285	113	293	67	90	2.0E-166	4.3E-25	2.9E-06
VC0837	19	67	77	53	35	40	4.5E-38	3.8E-01	2.6E-01
VC1647	18	63	25	32	18	20	2.7E-53	3.8E-01	4.2E-01
VC0749	641	2227	228	1038	399	584	0.0E+00	2.1E-98	3.5E-08

continued on next page!

Table A.1 – continued from previous page

Gene ID	Expression Values						Statistical q-value		
	Wt BL (-)	Wt BL (+)	ΔChrR BL (-)	ΔChrR BL (+)	ΔChrRΔMerR BL (-)	ΔChrRΔMerR BL (+)	Wt BL (-) vs Wt BL (+)	ΔChrR BL (-) vs ΔChrR BL (+)	ΔChrRΔMerR BL (-) vs ΔChrRΔMerR BL (+)
VC1220	32	111	42	35	57	66	3.6E-96	8.0E-01	3.2E-02
VC2092	113	386	412	358	1495	1483	2.1E-180	5.1E-01	5.2E-01
VCA0090	100	337	87	153	61	72	1.1E-106	1.5E-05	1.6E-07
VC0426	96	321	138	175	56	68	1.4E-57	2.3E-01	6.1E-01
VC1810	154	508	234	237	207	248	4.6E-47	9.0E-01	1.1E-01
VCA0313	72	234	100	89	57	62	1.9E-39	9.5E-01	9.0E-01
VC2086	60	195	322	181	672	662	3.1E-78	3.6E-06	1.0E-01
VC2760	39	126	53	89	34	47	9.5E-51	6.7E-03	2.5E-03
VC0750	388	1227	161	658	257	364	5.8E-122	2.8E-47	2.5E-09
VC1816	49	152	177	86	199	259	7.3E-21	3.2E-02	1.6E-04
VC1297	97	298	136	127	164	171	6.3E-122	9.8E-01	1.5E-01
VC1413	21	64	24	29	25	30	1.5E-42	5.3E-01	1.4E-01
VC1255	34	101	87	202	144	203	1.5E-42	5.8E-18	6.1E-06
VC2485	41	121	47	46	31	37	1.9E-42	9.4E-01	2.6E-01
VC2085	75	220	204	125	390	424	5.0E-71	8.3E-04	6.6E-03
VCA0159	509	1449	237	636	247	270	0.0E+00	1.9E-29	5.1E-01
VC2090	125	351	354	225	589	540	2.5E-40	1.0E-01	3.4E-03
VC0636	529	1461	555	545	441	491	2.6E-199	8.9E-01	9.9E-01
VC0085	57	156	100	119	91	104	4.0E-61	2.5E-01	5.5E-02
VC1637	51	139	67	136	64	75	2.0E-19	1.9E-03	7.3E-01
VC0943	28	76	82	103	69	96	2.3E-22	1.8E-01	2.8E-11
VC2287	82	217	60	218	34	55	2.8E-53	5.2E-46	3.3E-14
VC0031	78	206	98	238	153	178	1.7E-72	5.5E-21	8.1E-01
VC1793	11	29	23	19	12	15	1.6E-06	9.7E-01	7.5E-01
VCA0185	42	110	38	56	24	39	8.0E-13	2.5E-01	4.8E-02
VC2089	73	191	265	144	610	613	7.7E-71	8.3E-07	4.5E-01
VC1964	631	1629	453	1001	409	446	0.0E+00	6.4E-11	6.0E-01
VC1885	63	162	85	94	82	96	4.3E-27	6.7E-01	1.5E-02
VC2542	56	144	78	82	96	106	5.5E-43	6.3E-01	5.4E-02
VC1133	33	84	58	287	60	69	5.8E-30	3.5E-108	3.6E-06
VC1303	45	114	78	57	60	62	4.7E-35	4.9E-01	2.2E-04
VC2084	68	172	186	129	413	413	6.5E-35	4.7E-02	2.9E-01
VC0543	280	700	324	979	651	778	4.8E-147	3.1E-28	6.6E-04
VC2540	68	169	79	137	57	61	6.3E-18	2.6E-02	8.8E-01
VC0057	89	220	110	112	81	87	8.2E-17	9.1E-01	8.8E-01

continued on next page!

Table A.1 – continued from previous page

Gene ID	Expression Values						Statistical q-value		
	Wt BL (-)	Wt BL (+)	ΔChrR BL (-)	ΔChrR BL (+)	ΔChrRΔMerR BL (-)	ΔChrRΔMerR BL (+)	Wt BL (-) vs Wt BL (+)	ΔChrR BL (-) vs ΔChrR BL (+)	ΔChrRΔMerR BL (-) vs ΔChrRΔMerR BL (+)
VC0298	111	274	75	256	119	126	4.9E-106	2.8E-58	2.3E-01
VC1740	127	313	302	805	358	607	5.2E-139	1.2E-13	3.7E-21
VCA0186	219	539	228	395	237	238	2.4E-41	1.0E-05	5.8E-04
VC1117	115	283	70	151	116	143	1.4E-47	2.0E-09	1.9E-05
VC2758	205	504	533	2546	537	830	6.6E-150	2.2E-31	1.1E-17
VC0643	76	183	101	99	112	116	2.0E-91	9.7E-01	4.9E-01
VC2300	42	101	96	69	77	84	4.2E-30	2.7E-01	1.2E-03
VC0637	335	805	411	534	558	585	0.0E+00	1.4E-02	2.7E-01
VC1254	40	96	119	195	97	136	2.2E-10	4.5E-02	4.2E-03
VC0396	41	98	52	48	43	48	2.7E-15	9.9E-01	8.9E-01
VC1541	40	95	38	38	23	29	2.3E-22	8.8E-01	5.5E-01
VC2160	59	139	107	102	175	194	1.2E-15	9.8E-01	2.5E-05
VCA0779	44	103	36	43	50	67	1.1E-28	3.5E-01	2.9E-10
VC1096	30	70	17	46	17	22	2.3E-15	2.3E-04	2.5E-01
VC0520	115	268	101	121	254	249	4.5E-14	7.3E-01	9.4E-01
VC0086	615	1427	998	1657	643	649	2.7E-60	1.7E-05	6.6E-01
VC0667	88	204	198	427	338	326	3.2E-37	1.6E-15	6.0E-02
VC2295	72	166	118	112	172	179	3.1E-38	9.9E-01	1.8E-01
VC0030	94	216	109	276	133	158	3.4E-14	2.7E-07	1.1E-01
VC2705	132	300	101	166	143	127	9.9E-87	9.9E-06	2.6E-04
VCA0781	59	134	76	45	55	62	2.7E-52	4.4E-04	3.5E-02
VC0087	175	392	258	409	269	284	5.8E-26	4.2E-05	2.0E-03
VCA0105	564	1252	235	635	86	87	2.8E-55	3.9E-21	5.9E-01
VC0593	34	74	40	41	45	46	8.8E-10	9.8E-01	6.7E-01
VCA1028	48	103	65	57	35	38	2.4E-20	9.8E-01	4.4E-01
VC1065	112	239	82	137	74	67	2.2E-14	8.2E-02	1.3E-01
VCA0538	179	381	165	229	64	88	2.9E-30	2.6E-02	2.4E-03
VC0150	314	663	316	528	437	495	3.7E-87	2.1E-04	5.5E-01
VC1132	40	84	78	324	80	84	1.4E-14	4.3E-68	2.9E-05
VC2741	186	390	217	252	147	149	2.4E-24	3.4E-01	1.2E-04
VC2645	53	111	100	131	89	97	2.7E-19	2.3E-02	3.8E-04
VCA0158	503	1051	333	604	270	309	3.7E-29	1.1E-05	2.8E-06
VC0592	55	114	60	55	43	47	4.4E-16	9.9E-01	4.4E-01
VC0228	20	41	47	52	18	23	4.0E-08	7.3E-01	3.4E-01
VC0039	122	250	191	176	188	235	8.8E-28	9.5E-01	3.8E-03

continued on next page!

Table A.1 – continued from previous page

Gene ID	Expression Values						Statistical q-value		
	Wt BL (-)	Wt BL (+)	ΔChrR BL (-)	ΔChrR BL (+)	ΔChrRΔMerR BL (-)	ΔChrRΔMerR BL (+)	Wt BL (-) vs Wt BL (+)	ΔChrR BL (-) vs ΔChrR BL (+)	ΔChrRΔMerR BL (-) vs ΔChrRΔMerR BL (+)
VC2541	67	137	76	70	64	80	6.8E-15	9.9E-01	3.7E-02
VC0092	263	536	460	1207	651	892	9.7E-43	4.7E-18	6.6E-02
VC0422	128	260	297	206	219	232	1.9E-46	1.1E-02	9.3E-01
VC1358	668	1339	432	864	588	638	2.7E-71	1.0E-07	3.5E-01
VC0005	38	76	64	66	67	73	7.6E-06	9.8E-01	9.6E-01
VC0114	84	168	113	80	77	86	1.9E-14	5.6E-01	3.4E-01
VC1340	34	68	122	478	437	362	1.1E-16	1.4E-79	8.0E-01
VCA0988	78	39	45	28	12	7	3.8E-10	2.5E-01	3.4E-06
VCA0152	181	90	112	68	60	59	1.3E-06	2.7E-01	5.3E-01
VCA0738	109	54	66	44	63	63	1.3E-10	3.0E-01	9.6E-05
VC2357	81	40	180	92	844	760	1.3E-03	5.1E-02	4.0E-03
VC1436	65	32	119	64	100	80	4.3E-03	1.2E-01	1.6E-02
VCA1090	179	88	148	74	44	40	6.0E-11	1.4E-03	1.7E-01
VCA1091	314	154	275	104	74	78	9.6E-15	1.7E-15	2.6E-05
VC1483	49	24	62	41	93	104	2.8E-04	4.5E-01	2.6E-01
VC1605a	1471	714	855	502	552	510	1.7E-21	1.9E-04	2.0E-01
VC2702	301	146	373	171	354	288	4.5E-16	2.6E-10	6.5E-06
VCA0031	266	129	165	109	58	52	9.7E-28	6.4E-03	5.6E-03
VCA0113	31	15	24	23	3	1	3.2E-03	9.8E-01	2.4E-02
VCA1092	280	135	288	113	112	108	5.6E-43	7.8E-19	1.2E-02
VCA0663	52	25	30	26	27	26	8.9E-08	9.4E-01	9.5E-01
VC1361	229	110	220	99	74	78	1.1E-16	8.9E-13	2.4E-04
VC0736	781	375	431	343	521	530	5.2E-74	2.3E-01	2.5E-01
VCA0523	25	12	18	20	8	9	6.9E-05	9.0E-01	9.2E-01
VCA0965	275	132	146	110	86	92	9.4E-22	1.6E-01	7.0E-04
VCA0645	90	43	32	40	16	16	9.5E-06	6.5E-01	7.9E-01
VCA0689	21	10	13	18	11	11	5.3E-03	2.8E-01	8.0E-01
VC0799	21	10	10	11	2	2	1.0E-05	8.7E-01	4.9E-01
VCA0739	40	19	25	16	16	19	1.9E-03	6.9E-01	8.4E-01
VCA0858	150	71	42	49	10	12	2.6E-04	5.7E-01	9.3E-01
VC1247	951	450	586	397	612	557	9.0E-26	3.0E-02	6.8E-04
VC1584	55	26	29	28	7	5	6.4E-06	9.7E-01	2.5E-01
VC2530	2585	1209	2838	1034	2245	2058	1.8E-66	1.4E-22	2.0E-02
VC1311	30	14	16	16	11	10	7.3E-05	9.8E-01	4.1E-01
VC2047	133	62	189	89	180	184	1.0E-08	3.8E-04	4.4E-02

continued on next page!

Table A.1 – continued from previous page

Gene ID	Expression Values						Statistical q-value		
	Wt BL (-)	Wt BL (+)	ΔChrR BL (-)	ΔChrR BL (+)	ΔChrRΔMerR BL (-)	ΔChrRΔMerR BL (+)	Wt BL (-) vs Wt BL (+)	ΔChrR BL (-) vs ΔChrR BL (+)	ΔChrRΔMerR BL (-) vs ΔChrRΔMerR BL (+)
VC1919	807	376	2132	1320	2957	2544	2.6E-19	1.8E-04	9.9E-01
VC0706	967	449	6845	7102	8294	7840	5.3E-23	9.7E-01	9.7E-01
VC1687	41	19	9	12	5	4	1.4E-06	6.0E-01	6.5E-02
VC1861	80	37	130	68	152	149	1.0E-07	1.1E-02	3.6E-03
VCA0789	26	12	23	23	16	17	4.4E-04	9.9E-01	9.4E-01
VCA0619	65	30	90	35	143	131	7.1E-05	9.4E-04	5.6E-01
VCA0231	26	12	24	20	8	7	6.5E-05	8.4E-01	2.6E-01
VCA0935	364	168	189	94	49	58	4.5E-13	1.8E-02	5.7E-01
VCA1086	158	72	113	66	37	37	7.0E-20	2.2E-04	3.3E-04
VCA0201	22	10	38	28	32	34	1.1E-03	6.0E-01	9.3E-01
VCA0221	31	14	28	21	11	10	8.1E-06	6.7E-01	3.9E-01
VC2221	1123	505	1635	728	1062	950	1.9E-17	5.8E-11	8.3E-01
VC1360	147	66	138	54	72	66	2.0E-17	1.4E-08	1.3E-03
VCA0505	27	12	39	26	43	38	2.5E-04	4.5E-01	9.8E-02
VCA0892	126	56	317	140	245	215	1.3E-08	2.5E-05	1.1E-02
VCA0911	34	15	13	19	2	3	6.2E-05	3.1E-01	4.0E-01
VCA0484	25	11	14	19	16	12	4.2E-03	3.0E-01	6.2E-02
VCA0687	87	38	145	42	60	51	1.4E-10	4.4E-18	1.7E-01
VC0183	114	48	113	87	33	28	3.0E-26	2.2E-01	9.2E-02
VCA0912	31	13	14	12	2	4	2.4E-05	9.5E-01	3.2E-01
VCA0034	158	66	166	109	129	126	1.0E-17	4.7E-02	1.3E-02
VC1043	550	226	606	321	776	783	1.1E-81	8.9E-07	1.1E-01
VCA1062	44	18	15	19	7	7	1.0E-10	6.5E-01	9.7E-01
VC0868	32	13	20	18	6	4	4.4E-03	9.4E-01	1.4E-01
VCA0685	682	275	1188	324	419	273	4.0E-85	2.8E-50	2.1E-40
VC1530	53	21	20	26	16	14	3.0E-04	5.1E-01	4.8E-01
VC1644	48	19	44	32	101	92	1.1E-11	6.5E-01	1.8E-01
VC1583	28	11	10	16	11	11	7.8E-06	1.2E-01	9.0E-01
VC0142	344	133	319	182	449	429	3.5E-19	3.3E-02	8.8E-01
VCA1088	141	54	82	41	35	35	1.4E-25	2.7E-03	8.4E-01
VC0184	111	42	119	89	34	28	1.1E-30	2.0E-01	8.9E-02
VC1359	432	161	351	129	124	122	8.9E-43	3.5E-20	1.2E-03
VC0701	137	50	94	46	96	62	9.1E-14	4.5E-02	2.6E-06
VC1298	346	126	205	91	238	202	9.1E-77	1.3E-13	1.5E-09
VC1948	47	17	37	30	0	1	2.6E-05	1.0E+00	2.0E-01

continued on next page!

Table A.1 – continued from previous page

Gene ID	Expression Values						Statistical q-value		
	Wt BL (-)	Wt BL (+)	ΔChrR BL (-)	ΔChrR BL (+)	ΔChrRΔMerR BL (-)	ΔChrRΔMerR BL (+)	Wt BL (-) vs Wt BL (+)	ΔChrR BL (-) vs ΔChrR BL (+)	ΔChrRΔMerR BL (-) vs ΔChrRΔMerR BL (+)
VCA0881	113	39	115	65	28	22	3.1E-15	1.2E-01	3.9E-02
VCA1087	163	56	104	39	43	43	4.2E-16	4.2E-04	6.0E-01
VC1262	123	42	148	71	627	476	2.0E-10	4.2E-02	1.6E-01
VC1707	205	69	116	64	522	566	1.9E-15	1.5E-01	9.8E-04
VC0185	102	34	77	46	35	33	4.2E-25	1.2E-01	8.6E-01
VC1643	151	49	151	69	100	77	1.4E-57	2.1E-12	7.6E-03
VC1249	277	89	318	100	593	532	1.3E-30	2.0E-17	8.1E-04
VCA0798	207	61	398	147	347	324	3.6E-36	1.7E-20	2.5E-03
VCA0957	2819	822	394	269	185	200	0.0E+00	3.3E-02	4.0E-03
VC1325	66	19	172	64	165	145	4.8E-27	1.7E-10	8.0E-01
VCA0880	94	27	81	40	15	12	4.2E-18	5.4E-02	2.5E-01
VC1248	675	186	492	147	418	362	0.0E+00	2.6E-39	7.4E-04
VC1484	5139	1380	6206	2012	18456	17815	0.0E+00	1.3E-31	4.2E-03
VC0076	804	214	1378	583	3141	2806	1.4E-111	4.2E-15	2.9E-01
VCA0831	1289	333	484	120	103	84	3.4E-86	1.3E-16	1.1E-02
VCA0628	56	14	97	37	113	106	6.2E-56	1.2E-13	2.2E-03
VC0169	62	15	92	55	69	61	2.9E-11	2.8E-01	2.4E-01
VC2283	214	42	330	36	177	44	2.4E-157	3.4E-261	9.3E-37

Table A.2: Annotation of the hypthetical genes in *V. cholerae* using Annocript pipeline (E-value < 105)

Transcript ID	Transcript Length (bp)	UniRef90 ID	Length (bp)	E-value	Hit Length (a.a.)	Query coverage (%)	Hit coverage (%)	Description
VC2303	582	A0A085QK30	579	3.00E-138	193	99.5	100	ATP-dependent protease La domain protein
VC1647	1764	A0A085TBV5	1761	0	587	99.8	100	Bacterial extracellular solute-binding s 5 Middle family protein
VCA0523	1170	Q9KM65	1167	0	389	99.7	100	CAI-1 autoinducer synthase
VC1812	420	C2HSR3	393	5.00E-92	131	93.6	100	Cell division inhibitor
VC0114	549	A5F4H7	546	3.00E-101	182	99.5	100	Der GTPase-activating protein YihI
VC0082	1542	Q9KVQ7	1539	0	513	99.8	100	DNA recombination protein RmuC homolog
VCA0090	894	A0A085TBB0	855	0	297	95.6	96	EamA-like transporter family protein
VC1120	1281	A0A085T9Q2	1275	0	425	99.5	100	Flavin containing amine oxidoreductase family protein
VCA0781	2448	A0A085T7Y4	2445	0	815	99.9	100	FtsX-like permease family protein
VC2044	333	D2YDR9	330	2,00E-72	110	99.1	100	Glutaredoxin
VC1096	948	D0IFW4	942	0	314	99.4	100	Glutathione S-transferase omega
VCA0645	381	A0A086SL77	378	5.00E-88	126	99.2	100	Glyoxalase family protein
VC0747	567	Q9KTY3	519	9.00E-123	173	91.5	100	HTH-type transcriptional regulator IscR
VC1311	879	A0A085SHE2	876	5.00E-162	292	99.7	100	Inner membrane transporter rhtA
VCA0058	921	A0A085QGY8	918	0	306	99.7	100	L D-transpeptidase catalytic domain protein
VC0426	384	A0A085SEZ2	381	3.00E-87	127	99.2	100	Membrane protein
VCA0186	378	M5NC05	375	1.00E-76	125	99.2	100	NADH ubiquinone oxidoreductase subunit 2
VC1811	474	A0A085TCR1	471	2.00E-111	157	99.4	100	NYN domain protein
VC0183	2112	A0A0H3Q8W4	2109	0	703	99.9	100	Phage Integrase
VCA0689	348	A0A085QWC3	345	2.00E-75	115	99.1	100	Phasin family protein
VC1605a	234	A0A085SFT6	228	2.00E-50	77	97.4	99	Putative cation transport ATPase
VCA0902	837	A0A085TEU8	834	0	278	99.6	100	Putative lipoprotein
VC0005	258	Q9KVY3	255	5.00E-56	85	98.8	100	Putative membrane protein insertion efficiency factor
VCA0779	1434	A0A085T7Z1	1431	0	478	99.8	100	Pyridine nucleotide-disulfide oxidoreductase family protein
VC0084	624	A0A085QTH5	603	1,00E-133	201	96.6	100	SCP-2 sterol transfer family protein
VC1191	399	A0A085T8I7	396	2,00E-88	132	99.2	100	Superfamily II DNA and RNA helicase
VCA0113	477	A0A085TB81	474	1,00E-110	158	99.4	100	Type VI secretion lipofamily protein
VC1358	672	Q9KSA1	669	7,00E-124	223	99.6	100	Uncharacterized membrane protein VC_1358

Table A.3: Identification of the putative SigmaE-dependent promoter motif in the upstream region of genes controlled by SigmaE

	Position of promoter			
Gene ID	**-35**	**Spacer (16-18)**	**-10**	**Co-ordinate**
VC0039	TGATC	GATAGTTGACCAATTTTG	CGTAA	-27
VC0829	TGCTC	CATTCACAGTAGCTTTT	GGTAA	-87
VC0944	AGCTC	GGTGAAATCGATATCGTG	CGTAT	-189
VC1118	TGATC	CCTTACATTCTGAGTTT	CGTAA	-102
VC1571	TAAAC	CAATCCAGTACCAATGA	CGTAT	-68
VC1814	TGATC	GCTCAATCCCTTTGAC	CGTAT	-41
VC1885	TTATC	AAATCTGTGTAAGAGAA	CGTTT	-83
VC2044	AGATC	CAGCAACGCCAAGTCGAG	CGTAT	-85
VC2085	CGCTC	AAGAGTGACCCTACAAA	CGTAA	-53
VC2091	TGCAC	TCACTTTGATTTTTTATA	CGTAT	-268
VC2159	TGGTC	ATTTTCAGGGTGAGCGCA	CGGAA	-76
VC2242	CGATC	TGGATGCACTGGATCA	CGAAA	-190
VC2295	TGATT	TCTTAGCCTTTCACTC	CGGAT	-242
VC2303	TGATC	GACGAATGAACTCTTTT	CGTAT	-32
VC2542	TGAAC	TGCTGCACTCGCTTTTG	CGTAG	-54
VCA0538	AGATG	GATTGACTAGGCGCAA	CGTAA	-85
VCA0740	TGAAG	ACATGATGAGCAACCATG	CGTAA	-231
VCA0782	TGTTC	CACTAGCTCTTCGGCC	AGTAA	-128
VCA0783	AGATA	CACTTCCCCTTCACTTGG	CGTAT	-126
VCA0910	TGATC	AGCCTGCCACTTGCTG	AGTTT	-33
VC0007	TGACC	ATCCACAGGATCCGCG	CTTAA	-274
VC0142	TAATC	AAAGGGATTTTTTCGG	CTTAT	-92

continued on next page!

Table A.3 – continued from previous page

	Position of promoter			
Gene ID	**-35**	**Spacer (16-18)**	**-10**	**Co-ordinate**
VC0426	TAATC	GGCACTCATCTTCAAT	CGTTT	-128
VC0520	TCATC	AAAATATCAGCATTAA	CGAAT	-23
VC0868	GGATT	GTTGAGCGTACCAACG	CGTAA	-230
VC1262	TATTC	GCCAAGGTACTCGCTG	CGTAA	-119
VC1810	TGATT	GTCAAGTCATGCACAA	AGTAA	-223
VC2485	TGATT	ATTAAGGCTTTTTTAA	AGTAA	-167
VC0113	TGACC	GATGCGGATATCGATAT	CCTAT	-198
VC0169	TGATT	TCACCGCCGCGTGCACAC	CGTGA	-180
VC0227	TGAAT	CGCTTGTACGGCAGCTAT	CGTAT	-156
VC0396	TGATA	AACTTATCGGTTACTTAG	CCTAT	-99
VC0636	TGATC	GAGCGCAATTTCGATTTC	CGCCA	-220
VC0706	TGATC	TAAATCACATTATTTCCG	CGATA	-53
VC0987	TAAAC	TTTTTACCAGAAAGAGA	CGTAA	-22
VC1413	TAATT	TTTGTAAATGAATGCAA	CGTAA	-111
VC1530	TCATG	AATGTTGTGATGCTTTT	CGTAT	-100
VC1541	TGATT	GAGAAGAACCATAAACGC	AGTAT	-127
VC1707	TGAGC	TTTGGCTTATTGATTACG	GGTAT	-238
VC1811	GGATC	AGTGACCGAATGTATCT	CCTAT	-201
VC2501	CGATC	CTAGATGGGATCCAGCA	AGTAA	-54
VC2645	TGGTT	TTTAACATCAAAAACATC	CGTAT	-141
VCA0157	TGCTC	ACGAATGAGCTACCGCT	CGTCA	-218
VCA0231	TGATC	GCAAGCCATAACGCAGA	CTTCT	-40
VCA0505	TGAGC	TAAACGTTTTGTTTCTT	CGTCT	-220
VCA0615	TGATT	CTTTCCTAAAAAGTTTCC	CCTAA	-56
VCA0691	TGATC	AACTTTTATAAAAATACA	CAAAA	-226

continued on next page!

Table A.3 – continued from previous page

	Position of promoter			
Gene ID	**-35**	**Spacer (16-18)**	**-10**	**Co-ordinate**
VCA0738	TGATC	AACTGGAGATTATTTTTC	AGTGA	-102
VCA0789	TGATT	GTGTGAAGCTCAATGCG	CATAA	-132
VCA0809	TGATG	CTTTACTCGGTTTCTAC	CGTGT	-104
VCA0858	TGAGC	TTACTGAACTTCGTCTGT	CGTTA	-37
VCA1028	TGATC	CTCCATACACTTTGTATT	GGTTT	-265
VCA1088	TGAAC	AACTACAAAAGAAGCACG	CATAA	-43
VC0415	TGATC	AAACCACCCAAGGTCGAG	CGCAA	-222
VC1263	TGATC	TTTTCTTTGAAAAAAGG	GGTAT	-37
VC1389	TGAGC	CAATCAGACGCAACGTT	CGTAT	-40
VC1392	TGATA	CTGACCGCTTGGCGTTTA	CGTAA	-178
VC0039	TGATC	GATAGTTGACCAATTTTG	CGTAA	-27
VC1812	TGATC	CTCGAAAAGAGAGTGTG	CGTAA	-10
VCA0779	TGATC	GGCCGAGGATAAGTCCG	CGTAA	-81

Table A.4: Annotation of the hypthetical genes in *C. merolae* using Annocript pipeline (E-value < 105)

Transcript Locus	Transcript Length (bp)	Uniprot ID	Length (bp)	E-value	Hit Length (a.a.)	Query coverage (%)	Hit coverage (%)	Description
chr13_139414_140161_	748	E2A9N3	399	3.00E-20	218	53.34	61.01	Putative uncharacterized protein (Fragment)
chr7_534126_536042_	1917	K7EXP2	540	6.00E-22	429	28.17	41.96	Uncharacterized protein
chr18_715581_716972_-	1392	M1UUI4	375	1.00E-08	340	26.94	37.06	Uncharacterized protein
chr1_287245_289300_-	2056	M1V4S2	576	8.00E-11	305	28.02	64.26	Uncharacterized protein
chr15_352954_355474_	2521	M1V4S2	648	1.00E-15	305	25.70	67.87	Uncharacterized protein
chr3_33302_35103_	1802	M1V772	642	2.00E-08	316	35.63	63.92	Uncharacterized protein
chr20_163945_165734_	1790	M1VBA0	681	3.00E-109	235	38.04	100.00	26S proteasome non-ATPase regulatory subunit 9
chr3_404029_407036_+	3008	M1VC85	1419	0	548	47.17	86.31	GTP-binding protein of Nug1 family
chr7_479013_480594_	1582	M1VCN7	498	4.00E-09	179	31.48	92.18	Uncharacterized protein
chr20_1508708_1510732_	2025	M1VE79	651	3.00E-08	335	32.15	65.37	Uncharacterized protein
chr19_1275224_1276784_	1561	M1VEC8	1317	0	911	84.37	51.26	Similar to trefoil factor
chr6_6135_7726_	1592	M1VFE1	1338	0	901	84.05	52.39	Similar to trefoil factor
chr18_1245329_1247075_+	1747	M1VFE1	1437	0	901	82.26	56.05	Similar to trefoil factor
chr5_218867_219625_-	759	M1VH39	201	5.00E-11	68	26.48	98.53	Transposon
chr1_364793_365289_	497	M1VJL8	477	2.00E-50	600	95.98	26.50	Similar to bacterial putative methyl transferase
chr15_471347_472826_-	1480	M1VJL8	543	2.00E-45	600	36.69	30.17	Similar to bacterial putative methyl transferase
chr4_210184_211812_	1629	M1VJL8	510	4.00E-55	600	31.31	28.50	Similar to bacterial putative methyl transferase
chr20_1125809_1127458_+	1650	M1VJL8	486	5.00E-12	600	29.45	27.33	Similar to bacterial putative methyl transferase
chr4_389118_392097_	2980	M1VJL8	642	6.00E-75	600	21.54	35.83	Similar to bacterial putative methyl transferase
chr4_469600_471919_+	2320	M1VJL8	495	6.00E-37	600	21.34	27.50	Similar to bacterial putative methyl transferase
chr15_740289_743091_	2803	M1VM81	675	0	573	24.08	39.44	Retroelement alive
chr16_62048_65905_	3858	M1VMD2	1608	0	1016	41.68	52.56	Similar to triacylglycerol lipase

Table A.5: List of differentially expressed genes under blue light in *C. merolae* (q-value < 0.01 and the absolute value of $|\log_2$ fold change$| \geq 1$).

	FPKM values			**Statistical cuffdiff values**	
Gene ID	**BL(-)**	**BL (+)**	**$\log_2$ (fold change)**	**p value**	**q value**
CMO306C	4.5	953.2	7.7	1.3E-03	6.4E-03
CMT305C	4.8	776.4	7.3	2.5E-04	1.8E-03
CMP252C	4.8	760.3	7.3	4.5E-04	2.8E-03
CMK188C	11.3	978.7	6.4	5.0E-05	4.5E-04
CMN328C	14.2	1224.7	6.4	5.0E-05	4.5E-04
CME023C	13.2	848.2	6.0	5.0E-05	4.5E-04
CMF098C	25.0	1551.3	6.0	5.0E-05	4.5E-04
CMS308C	41.9	2590.6	6.0	5.0E-05	4.5E-04
CMS455C	6.1	352.7	5.8	5.0E-04	3.1E-03
CME120C	29.0	1548.3	5.7	5.0E-05	4.5E-04
CMD051C	35.5	1862.4	5.7	5.0E-05	4.5E-04
CMT538C	2.8	120.3	5.4	5.0E-05	4.5E-04
CMQ436C	7.8	327.9	5.4	5.0E-05	4.5E-04
CMO111C	31.7	1259.0	5.3	5.0E-05	4.5E-04
CMT162C	21.1	800.2	5.2	5.0E-05	4.5E-04
CMM134C	93.1	3506.1	5.2	5.0E-05	4.5E-04
CMQ317C	2.5	89.8	5.1	1.8E-03	8.3E-03
CMT384C	2.3	81.5	5.1	5.0E-04	3.1E-03
CMH178C	8.8	303.4	5.1	4.5E-04	2.8E-03
CMR346C	28.2	967.3	5.1	5.0E-05	4.5E-04
CMG058C	18.3	594.9	5.0	5.0E-05	4.5E-04
CMQ233C	6.8	219.2	5.0	5.0E-05	4.5E-04
CMJ265C	19.0	596.0	5.0	5.0E-05	4.5E-04

continued on next page!

Table A.5 – continued from previous page

	FPKM values			Statistical cuffdiff values	
Gene ID	**BL(-)**	**BL (+)**	**$\log_2$ (fold change)**	**p value**	**q value**
CMP354C	4.6	141.9	4.9	5.0E-05	4.5E-04
CMJ042C	129.2	3708.1	4.8	5.0E-05	4.5E-04
CMC158C	5.0	143.7	4.8	1.3E-03	6.4E-03
CMP193C	34.4	974.2	4.8	5.0E-05	4.5E-04
CMS309C	20.0	556.1	4.8	5.5E-04	3.3E-03
CMQ255C	4.2	115.0	4.8	5.0E-05	4.5E-04
CMN237C	37.8	1022.6	4.8	5.0E-05	4.5E-04
CMM188C	4.6	123.7	4.7	5.0E-05	4.5E-04
CMS031C	41.7	1114.6	4.7	5.0E-05	4.5E-04
CMG201C	21.4	558.6	4.7	5.0E-05	4.5E-04
CML205C	83.8	2155.7	4.7	5.0E-05	4.5E-04
CMA061C	21.5	549.8	4.7	5.0E-05	4.5E-04
CMJ212C	55.9	1428.4	4.7	5.0E-05	4.5E-04
CME180C	27.9	711.3	4.7	5.0E-05	4.5E-04
CMR109C	16.5	414.3	4.7	5.0E-05	4.5E-04
CMK114C	24.8	620.4	4.6	5.0E-05	4.5E-04
CMX001C	25.1	589.0	4.6	5.0E-05	4.5E-04
CMQ123C	35.2	822.0	4.5	5.0E-05	4.5E-04
CMQ113C	159.7	3721.3	4.5	5.0E-05	4.5E-04
CMK034C	8.2	172.4	4.4	5.0E-05	4.5E-04
CME172C	12.5	262.8	4.4	5.0E-05	4.5E-04
CME041C	93.9	1881.1	4.3	5.0E-05	4.5E-04
CMI076C	20.3	404.1	4.3	5.0E-05	4.5E-04
CMN022C	24.0	473.2	4.3	5.0E-05	4.5E-04
CMI172C	18.7	369.1	4.3	5.0E-05	4.5E-04
CML276C	27.4	532.6	4.3	5.0E-05	4.5E-04

continued on next page!

Table A.5 – continued from previous page

	FPKM values			Statistical cuffdiff values	
Gene ID	**BL(-)**	**BL (+)**	**$\log_2$ (fold change)**	**p value**	**q value**
CMN228C	13.0	250.7	4.3	5.0E-05	4.5E-04
CMB021C	155.0	2956.7	4.3	5.0E-05	4.5E-04
CMR441C	30.2	559.8	4.2	5.0E-05	4.5E-04
CMN074C	7.5	134.7	4.2	5.0E-05	4.5E-04
CMS136C	3.1	55.9	4.2	2.2E-03	9.9E-03
CMI233C	324.2	5809.1	4.2	5.0E-05	4.5E-04
CMM081C	7.9	134.2	4.1	5.0E-05	4.5E-04
CMQ270C	46.2	780.7	4.1	5.0E-05	4.5E-04
CMJ084C	13.5	224.5	4.1	5.0E-05	4.5E-04
CMJ225C	4.2	69.9	4.0	5.0E-05	4.5E-04
CMA085C	6.6	106.8	4.0	5.0E-05	4.5E-04
CMQ021C	23.0	367.1	4.0	5.0E-05	4.5E-04
CMO061C	3.1	49.1	4.0	1.6E-03	7.5E-03
CML299C	4.7	69.9	3.9	1.1E-03	5.8E-03
CMS248C	14.6	203.7	3.8	5.0E-05	4.5E-04
CMS209C	11.6	158.2	3.8	1.9E-03	8.8E-03
CMT193C	5.6	76.0	3.8	5.5E-04	3.3E-03
CML204C	22.0	292.1	3.7	5.0E-05	4.5E-04
CMV135C	13.5	178.9	3.7	5.0E-05	4.5E-04
CMN283C	10.7	140.8	3.7	1.6E-03	7.5E-03
CMR398C	5.8	75.2	3.7	1.0E-04	8.2E-04
CMJ298C	5.7	72.1	3.7	1.4E-03	6.7E-03
CMG021C	3.1	38.3	3.6	7.0E-04	4.0E-03
CMI185C	50.7	622.0	3.6	5.0E-05	4.5E-04
CML055C	15.1	184.7	3.6	5.0E-05	4.5E-04
CMR237C	95.8	1161.3	3.6	5.0E-05	4.5E-04

continued on next page!

Table A.5 – continued from previous page

	FPKM values			Statistical cuffdiff values	
Gene ID	**BL(-)**	**BL (+)**	**$\log_2$ (fold change)**	**p value**	**q value**
CMJ105C	55.6	673.4	3.6	5.0E-05	4.5E-04
CMG086C	22.3	263.2	3.6	5.0E-05	4.5E-04
CMJ142C	19.4	228.1	3.6	5.0E-05	4.5E-04
CMT558C	45.4	524.2	3.5	5.0E-05	4.5E-04
CMC157C	10.4	119.9	3.5	5.0E-05	4.5E-04
CMR479C	126.8	1442.4	3.5	5.0E-05	4.5E-04
CMT526C	67.0	759.8	3.5	5.0E-05	4.5E-04
CMN319C	17.2	191.7	3.5	5.0E-05	4.5E-04
CML178C	71.7	791.3	3.5	5.0E-05	4.5E-04
CML214C	13.0	142.3	3.5	5.0E-05	4.5E-04
CMP271C	26.5	289.8	3.4	5.0E-05	4.5E-04
CMM274C	11.2	121.2	3.4	5.0E-05	4.5E-04
CMQ044C	6.1	65.9	3.4	1.5E-04	1.2E-03
CMM013C	6.7	70.8	3.4	3.5E-04	2.3E-03
CMG188C	26.2	279.1	3.4	2.0E-04	1.5E-03
CMM058C	6.1	65.2	3.4	5.0E-05	4.5E-04
CMP304C	31.1	329.3	3.4	5.0E-05	4.5E-04
CMM334C	7.1	74.7	3.4	6.5E-04	3.8E-03
CMG189C	9.5	99.9	3.4	5.0E-05	4.5E-04
CMR165C	33.4	342.4	3.4	5.0E-05	4.5E-04
CMH197C	46.8	455.3	3.3	5.0E-05	4.5E-04
CMM286C	50.6	491.9	3.3	5.0E-05	4.5E-04
CMR493C	21.4	206.0	3.3	5.0E-05	4.5E-04
CMM169C	16.5	155.1	3.2	5.0E-05	4.5E-04
CMH019C	7.6	70.0	3.2	2.0E-04	1.5E-03
CMK174C	19.8	181.4	3.2	5.0E-05	4.5E-04

continued on next page!

Table A.5 – continued from previous page

	FPKM values			Statistical cuffdiff values	
Gene ID	**BL(-)**	**BL (+)**	**$\log_2$ (fold change)**	**p value**	**q value**
CMM167C	99.9	900.3	3.2	5.0E-05	4.5E-04
CMM051C	185.9	1674.1	3.2	5.0E-05	4.5E-04
CMV129C	261.5	2343.2	3.2	5.0E-05	4.5E-04
CMK086C	250.4	2210.1	3.1	5.0E-05	4.5E-04
CMT304C	16.0	139.6	3.1	5.0E-05	4.5E-04
CMT080C	16.5	143.1	3.1	5.0E-05	4.5E-04
CME194C	40.6	350.0	3.1	5.0E-05	4.5E-04
CMM191C	13.1	112.9	3.1	5.0E-05	4.5E-04
CMP227C	60.0	515.5	3.1	5.0E-05	4.5E-04
CMH183C	19.8	169.8	3.1	5.0E-05	4.5E-04
CMC135C	44.7	378.6	3.1	5.0E-05	4.5E-04
CMP046C	4.2	35.7	3.1	5.0E-05	4.5E-04
CMM166C	19.1	161.5	3.1	5.0E-05	4.5E-04
CMK085C	29.7	249.9	3.1	5.0E-05	4.5E-04
CMN291C	59.5	500.3	3.1	3.0E-04	2.0E-03
CMQ459C	3.3	28.0	3.1	5.0E-05	4.5E-04
CMB157C	133.0	1105.9	3.1	5.0E-05	4.5E-04
CMA122C	305.2	2526.5	3.0	5.0E-05	4.5E-04
CMV136C	9.3	76.0	3.0	5.0E-05	4.5E-04
CMN305C	11.4	93.2	3.0	6.5E-04	3.8E-03
CMI086C	13.7	111.9	3.0	5.0E-05	4.5E-04
CMS327C	29.0	235.6	3.0	5.0E-05	4.5E-04
CMG059C	376.4	3048.0	3.0	5.0E-05	4.5E-04
CMR158C	47.9	382.8	3.0	5.0E-05	4.5E-04
CMP052C	10.0	78.3	3.0	5.0E-05	4.5E-04
CMK232C	16.1	126.6	3.0	5.0E-05	4.5E-04

continued on next page!

Table A.5 – continued from previous page

	FPKM values			Statistical cuffdiff values	
Gene ID	**BL(-)**	**BL (+)**	**$\log_2$ (fold change)**	**p value**	**q value**
CMS159C	119.7	937.2	3.0	5.0E-05	4.5E-04
CMF138C	5.2	40.4	3.0	2.5E-04	1.8E-03
CMP003C	8.2	63.7	3.0	5.0E-05	4.5E-04
CMF147C	18.5	143.8	3.0	5.0E-05	4.5E-04
CMM145C	159.4	1196.8	2.9	5.0E-05	4.5E-04
CMT137C	90.8	680.6	2.9	5.0E-05	4.5E-04
CMS102C	38.3	284.5	2.9	5.0E-05	4.5E-04
CMI184C	16.7	123.7	2.9	1.3E-03	6.6E-03
CMQ053C	54.5	401.6	2.9	5.0E-05	4.5E-04
CML336C	19.2	140.9	2.9	5.0E-05	4.5E-04
CMN233C	67.4	492.2	2.9	5.0E-05	4.5E-04
CMQ012C	11.1	80.9	2.9	3.5E-04	2.3E-03
CMR014C	19.4	141.6	2.9	5.0E-05	4.5E-04
CMG015C	7.8	56.9	2.9	2.5E-04	1.8E-03
CMN258C	13.9	100.7	2.9	1.0E-04	8.2E-04
CMI087C	48.7	352.2	2.9	1.0E-04	8.2E-04
CMN306C	6.4	46.3	2.8	5.0E-05	4.5E-04
CMO012C	270.5	1929.8	2.8	5.0E-05	4.5E-04
CMS389C	91.7	652.2	2.8	5.0E-05	4.5E-04
CMM214C	25.7	182.8	2.8	5.0E-05	4.5E-04
CMD099C	6.4	45.2	2.8	7.5E-04	4.2E-03
CMI270C	35.2	246.4	2.8	5.0E-05	4.5E-04
CMC063C	23.2	162.6	2.8	5.0E-05	4.5E-04
CMR404C	108.6	758.6	2.8	5.5E-04	3.3E-03
CML213C	5.0	34.6	2.8	4.0E-04	2.6E-03
CMH052C	25.2	175.5	2.8	5.0E-05	4.5E-04

continued on next page!

Table A.5 – continued from previous page

	FPKM values			Statistical cuffdiff values	
Gene ID	**BL(-)**	**BL (+)**	**$\log_2$ (fold change)**	**p value**	**q value**
CMF024C	11.5	80.3	2.8	1.3E-03	6.4E-03
CMM162C	39.4	273.6	2.8	5.0E-05	4.5E-04
CMF070C	7.9	53.9	2.8	5.0E-05	4.5E-04
CMQ067C	8.0	54.5	2.8	5.0E-05	4.5E-04
CMJ296C	20.5	137.3	2.7	3.0E-04	2.0E-03
CMN263C	32.3	216.4	2.7	5.0E-05	4.5E-04
CMT611C	55.4	363.0	2.7	5.0E-05	4.5E-04
CMN017C	15.4	100.9	2.7	5.0E-05	4.5E-04
CME165C	31.7	207.0	2.7	5.0E-05	4.5E-04
CMQ397C	20.0	129.5	2.7	5.0E-05	4.5E-04
CMK192C	107.8	694.6	2.7	5.0E-05	4.5E-04
CMN129C	79.1	508.2	2.7	5.0E-05	4.5E-04
CMC152C	33.8	215.4	2.7	1.0E-04	8.2E-04
CMT100C	24.2	152.7	2.7	5.0E-05	4.5E-04
CMA030C	57.1	360.5	2.7	5.0E-05	4.5E-04
CMM072C	13.7	86.2	2.7	5.0E-05	4.5E-04
CMI123C	27.3	171.8	2.7	5.0E-05	4.5E-04
CMT204C	12.7	79.8	2.6	5.0E-05	4.5E-04
CMH145C	69.8	435.6	2.6	5.0E-05	4.5E-04
CMT416C	28.0	174.5	2.6	5.0E-05	4.5E-04
CMC021C	143.0	888.3	2.6	5.0E-05	4.5E-04
CMF055C	24.7	152.8	2.6	5.0E-05	4.5E-04
CMT577C	20.6	127.6	2.6	5.0E-05	4.5E-04
CMP155C	15.2	93.8	2.6	5.0E-05	4.5E-04
CMF033C	223.3	1373.1	2.6	5.0E-05	4.5E-04
CMB066C	7.7	46.9	2.6	5.0E-05	4.5E-04

continued on next page!

Table A.5 – continued from previous page

Gene ID	FPKM values		$\log_2$ (fold change)	Statistical cuffdiff values	
	BL(-)	BL (+)		p value	q value
CMJ276C	37.5	229.4	2.6	5.0E-05	4.5E-04
CMM044C	18.0	109.9	2.6	5.0E-05	4.5E-04
CMM031C	6.4	38.8	2.6	7.5E-04	4.2E-03
CMH107C	13.7	82.8	2.6	7.5E-04	4.2E-03
CMR256C	29.7	178.4	2.6	5.0E-05	4.5E-04
CMQ391C	52.6	315.8	2.6	5.0E-05	4.5E-04
CMT079C	14.5	87.2	2.6	5.0E-05	4.5E-04
CMN219C	149.2	888.2	2.6	5.0E-05	4.5E-04
CMS188C	417.3	2475.0	2.6	5.0E-05	4.5E-04
CMM228C	16.6	98.3	2.6	5.0E-05	4.5E-04
CMP303C	6.6	38.9	2.6	4.0E-04	2.6E-03
CMT453C	12.4	72.5	2.5	5.0E-05	4.5E-04
CMQ215C	15.2	88.6	2.5	5.0E-05	4.5E-04
CMQ222C	51.9	301.8	2.5	5.0E-05	4.5E-04
CMR198C	23.9	138.9	2.5	5.0E-05	4.5E-04
CMD024C	8.2	47.7	2.5	4.0E-04	2.6E-03
CMJ233C	19.2	111.2	2.5	5.0E-05	4.5E-04
CMO139C	121.1	696.7	2.5	5.0E-05	4.5E-04
CMV082C	13.7	78.7	2.5	1.6E-03	7.7E-03
CMO291C	124.1	711.0	2.5	5.0E-05	4.5E-04
CMT175C	142.9	817.6	2.5	5.0E-05	4.5E-04
CMT192C	54.3	308.5	2.5	5.0E-05	4.5E-04
CMM292C	26.2	148.4	2.5	5.0E-05	4.5E-04
CMM150C	5.9	33.5	2.5	5.0E-05	4.5E-04
CMN048C	41.6	234.4	2.5	5.0E-05	4.5E-04
CMC057C	8.8	49.4	2.5	3.5E-04	2.3E-03

continued on next page!

Table A.5 – continued from previous page

	FPKM values			Statistical cuffdiff values	
Gene ID	**BL(-)**	**BL (+)**	**$\log_2$ (fold change)**	**p value**	**q value**
CMF178C	24.3	134.9	2.5	5.0E-05	4.5E-04
CMQ191C	40.3	222.4	2.5	5.0E-05	4.5E-04
CMC043C	75.1	412.2	2.5	5.0E-05	4.5E-04
CMT058C	15.1	82.9	2.5	5.0E-04	3.1E-03
CMQ281C	76.8	420.8	2.5	5.0E-05	4.5E-04
CMS247C	21.5	117.5	2.5	5.0E-05	4.5E-04
CMS496C	4.4	24.3	2.4	5.0E-05	4.5E-04
CMT063C	236.0	1286.6	2.4	5.0E-05	4.5E-04
CMR488C	18.1	98.8	2.4	1.5E-04	1.2E-03
CML273C	42.1	227.7	2.4	5.0E-05	4.5E-04
CMO171C	157.3	848.1	2.4	1.5E-04	1.2E-03
CML110C	160.5	865.2	2.4	5.0E-05	4.5E-04
CMH187C	12.6	67.7	2.4	5.0E-05	4.5E-04
CMB158C	20.9	112.4	2.4	5.0E-05	4.5E-04
CMR108C	30.8	164.8	2.4	5.0E-05	4.5E-04
CMN290C	162.9	861.3	2.4	5.0E-05	4.5E-04
CMT412C	25.3	133.6	2.4	5.0E-05	4.5E-04
CMG170C	43.4	228.7	2.4	5.0E-05	4.5E-04
CMB043C	7.5	39.6	2.4	5.0E-05	4.5E-04
CMS045C	23.8	125.1	2.4	5.0E-05	4.5E-04
CMQ136C	30.4	159.3	2.4	5.0E-05	4.5E-04
CML267C	13.6	71.0	2.4	5.0E-05	4.5E-04
CMR240C	67.5	353.2	2.4	5.0E-05	4.5E-04
CMT252C	153.4	797.9	2.4	5.0E-05	4.5E-04
CMT561C	56.8	295.4	2.4	5.0E-05	4.5E-04
CMT330C	49.9	257.7	2.4	5.0E-05	4.5E-04

continued on next page!

Table A.5 – continued from previous page

Gene ID	FPKM values		$\log_2$ (fold change)	Statistical cuffdiff values	
	BL(-)	BL (+)		p value	q value
CMR267C	22.6	116.7	2.4	5.0E-05	4.5E-04
CMQ224C	416.8	2122.8	2.3	5.0E-04	3.1E-03
CMK237C	16.9	86.2	2.3	5.0E-05	4.5E-04
CMK187C	122.2	615.3	2.3	5.0E-05	4.5E-04
CMN227C	280.8	1409.8	2.3	5.0E-05	4.5E-04
CMV133C	145.6	726.7	2.3	1.3E-03	6.6E-03
CMT432C	62.5	311.5	2.3	5.0E-05	4.5E-04
CMI177C	8.9	44.5	2.3	1.8E-03	8.3E-03
CMD165C	554.0	2746.2	2.3	5.0E-05	4.5E-04
CMH038C	163.7	810.3	2.3	5.0E-05	4.5E-04
CMN109C	208.7	1028.1	2.3	5.0E-05	4.5E-04
CMQ190C	262.4	1290.2	2.3	5.0E-05	4.5E-04
CMP091C	13.1	64.3	2.3	3.5E-04	2.3E-03
CMI042C	56.3	273.5	2.3	5.0E-05	4.5E-04
CMO323C	8.4	40.5	2.3	1.0E-04	8.2E-04
CMO257C	59.4	285.0	2.3	5.0E-05	4.5E-04
CMO170C	85.3	407.4	2.3	5.0E-05	4.5E-04
CMP145C	534.4	2551.4	2.3	2.2E-03	9.9E-03
CMM323C	40.2	191.5	2.3	5.0E-05	4.5E-04
CMO268C	28.0	132.5	2.2	5.0E-05	4.5E-04
CME192C	21.2	100.2	2.2	5.0E-05	4.5E-04
CMG185C	151.5	716.4	2.2	5.0E-05	4.5E-04
CMS307C	10.8	51.0	2.2	5.0E-04	3.1E-03
CMH137C	20.3	95.2	2.2	1.0E-04	8.2E-04
CMT423C	246.4	1154.2	2.2	5.0E-05	4.5E-04
CMK175C	34.8	162.9	2.2	5.0E-05	4.5E-04

continued on next page!

Table A.5 – continued from previous page

	FPKM values			Statistical cuffdiff values	
Gene ID	**BL(-)**	**BL (+)**	**$\log_2$ (fold change)**	**p value**	**q value**
CMK291C	103.7	484.3	2.2	5.0E-05	4.5E-04
CMQ172C	267.5	1246.4	2.2	5.0E-05	4.5E-04
CMN023C	728.5	3393.2	2.2	1.0E-04	8.2E-04
CMR121C	324.1	1503.7	2.2	5.0E-05	4.5E-04
CML285C	122.1	564.4	2.2	5.0E-05	4.5E-04
CMN304C	32.4	149.0	2.2	5.0E-05	4.5E-04
CMJ083C	5.2	23.6	2.2	5.0E-05	4.5E-04
CMI162C	39.1	176.9	2.2	5.0E-05	4.5E-04
CMP010C	47.1	211.7	2.2	5.0E-05	4.5E-04
CML030C	216.0	969.3	2.2	5.0E-05	4.5E-04
CMM068C	26.3	117.8	2.2	5.0E-05	4.5E-04
CMM212C	190.7	854.6	2.2	5.0E-05	4.5E-04
CMM019C	562.7	2505.3	2.2	5.5E-04	3.3E-03
CMQ241C	276.4	1229.0	2.2	5.0E-05	4.5E-04
CME113C	38.8	172.5	2.2	5.0E-05	4.5E-04
CMR368C	25.8	114.5	2.1	7.0E-04	4.0E-03
CMM078C	163.6	723.5	2.1	5.0E-05	4.5E-04
CMR255C	191.2	844.2	2.1	5.0E-05	4.5E-04
CMR276C	9.7	43.0	2.1	1.4E-03	6.9E-03
CML190C	17.0	75.0	2.1	5.0E-05	4.5E-04
CMS272C	20.5	90.2	2.1	5.0E-05	4.5E-04
CMJ099C	8.3	36.2	2.1	2.5E-04	1.8E-03
CMM276C	70.3	304.3	2.1	5.0E-05	4.5E-04
CMQ026C	63.7	275.1	2.1	5.0E-05	4.5E-04
CMS390C	48.2	207.5	2.1	5.0E-05	4.5E-04
CMG080C	59.3	254.0	2.1	5.0E-05	4.5E-04

continued on next page!

Table A.5 – continued from previous page

	FPKM values			Statistical cuffdiff values	
Gene ID	**BL(-)**	**BL (+)**	**$\log_2$ (fold change)**	**p value**	**q value**
CMP042C	16.4	70.3	2.1	5.0E-05	4.5E-04
CMN084C	1154.9	4934.1	2.1	1.4E-03	6.9E-03
CMO317C	27.0	115.1	2.1	5.0E-05	4.5E-04
CMR061C	10.2	43.3	2.1	5.0E-05	4.5E-04
CMK001C	31.1	132.6	2.1	5.0E-05	4.5E-04
CMM098C	22.1	94.2	2.1	5.0E-05	4.5E-04
CMO270C	28.1	119.5	2.1	5.0E-05	4.5E-04
CMT165C	16.6	70.5	2.1	5.0E-05	4.5E-04
CML240C	13.5	57.2	2.1	5.0E-05	4.5E-04
CMH276C	59.4	252.1	2.1	1.0E-04	8.2E-04
CMS351C	502.0	2125.5	2.1	5.0E-05	4.5E-04
CMM317C	20.9	87.9	2.1	5.0E-05	4.5E-04
CMS372C	184.5	774.2	2.1	5.0E-05	4.5E-04
CMM074C	38.2	160.3	2.1	5.0E-05	4.5E-04
CMO192C	29.9	125.3	2.1	5.0E-05	4.5E-04
CMS416C	36.8	153.6	2.1	5.0E-05	4.5E-04
CMQ010C	40.2	167.2	2.1	5.0E-05	4.5E-04
CMJ016C	288.0	1191.1	2.0	1.0E-04	8.2E-04
CMT493C	9.5	39.3	2.0	7.0E-04	4.0E-03
CMS299C	104.9	431.7	2.0	5.0E-05	4.5E-04
CMK131C	457.3	1878.3	2.0	5.5E-04	3.3E-03
CMJ246C	45.3	185.8	2.0	5.0E-05	4.5E-04
CMR271C	18.8	77.1	2.0	5.0E-05	4.5E-04
CMS333C	26.2	107.1	2.0	5.0E-05	4.5E-04
CME080C	95.3	389.7	2.0	5.0E-05	4.5E-04
CMJ201C	13.6	55.5	2.0	5.5E-04	3.3E-03

continued on next page!

Table A.5 – continued from previous page

	FPKM values			Statistical cuffdiff values	
Gene ID	**BL(-)**	**BL (+)**	**$\log_2$ (fold change)**	**p value**	**q value**
CMM028C	9.8	39.8	2.0	5.0E-05	4.5E-04
CML012C	12.8	52.0	2.0	4.5E-04	2.8E-03
CMT083C	20.8	84.3	2.0	1.0E-04	8.2E-04
CMF094C	73.6	296.7	2.0	5.0E-05	4.5E-04
CMJ129C	39.4	157.9	2.0	5.0E-05	4.5E-04
CMM299C	62.8	251.8	2.0	5.0E-05	4.5E-04
CMQ120C	295.1	1181.6	2.0	4.0E-04	2.6E-03
CMP058C	101.7	405.8	2.0	5.0E-05	4.5E-04
CMH097C	21.7	86.3	2.0	5.0E-05	4.5E-04
CMS202C	21.5	85.5	2.0	5.0E-05	4.5E-04
CMT329C	77.1	304.4	2.0	5.0E-05	4.5E-04
CMS453C	22.5	88.4	2.0	5.0E-05	4.5E-04
CMR067C	25.2	98.5	2.0	5.0E-05	4.5E-04
CMT534C	102.0	398.8	2.0	5.0E-05	4.5E-04
CMH091C	16.5	64.4	2.0	1.3E-03	6.6E-03
CMT477C	51.2	199.3	2.0	5.0E-05	4.5E-04
CMJ081C	315.9	1225.0	2.0	1.5E-04	1.2E-03
CML088C	38.1	147.8	2.0	5.0E-05	4.5E-04
CMS155C	53.2	206.0	2.0	5.0E-05	4.5E-04
CMG171C	91.6	354.6	2.0	5.0E-05	4.5E-04
CMJ086C	46.7	180.9	2.0	5.0E-05	4.5E-04
CMK284C	8.0	31.0	1.9	1.3E-03	6.6E-03
CMH006C	165.1	634.5	1.9	5.0E-05	4.5E-04
CMM076C	52.2	200.1	1.9	5.0E-05	4.5E-04
CMT114C	29.1	111.4	1.9	2.5E-04	1.8E-03
CMM222C	52.4	199.5	1.9	5.0E-05	4.5E-04

continued on next page!

Table A.5 – continued from previous page

	FPKM values			Statistical cuffdiff values	
Gene ID	**BL(-)**	**BL (+)**	**$\log_2$ (fold change)**	**p value**	**q value**
CMP182C	23.6	89.4	1.9	5.0E-05	4.5E-04
CMQ427C	43.6	165.2	1.9	5.0E-05	4.5E-04
CMO029C	103.7	393.1	1.9	5.0E-05	4.5E-04
CML167C	30.1	113.8	1.9	5.0E-05	4.5E-04
CMQ246C	102.3	385.1	1.9	2.0E-04	1.5E-03
CMT267C	25.5	96.1	1.9	1.0E-04	8.2E-04
CMI192C	30.0	113.0	1.9	5.0E-05	4.5E-04
CMK150C	271.4	1020.1	1.9	1.2E-03	6.0E-03
CMI040C	448.7	1685.9	1.9	1.1E-03	5.5E-03
CMT381C	109.8	412.1	1.9	5.0E-05	4.5E-04
CMQ054C	246.6	926.0	1.9	3.0E-04	2.0E-03
CMN108C	65.1	244.2	1.9	5.0E-05	4.5E-04
CMB116C	52.3	195.9	1.9	9.0E-04	4.9E-03
CMV081C	35.3	132.4	1.9	4.5E-04	2.8E-03
CMB086C	48.8	182.6	1.9	3.0E-04	2.0E-03
CMK028C	761.4	2847.6	1.9	1.6E-03	7.7E-03
CMC037C	39.3	146.5	1.9	5.0E-05	4.5E-04
CMP106C	254.9	950.8	1.9	5.0E-05	4.5E-04
CMM270C	41.2	152.3	1.9	5.0E-05	4.5E-04
CMI112C	531.6	1966.1	1.9	5.0E-05	4.5E-04
CMQ064C	121.3	447.6	1.9	5.0E-05	4.5E-04
CMS315C	69.7	256.8	1.9	5.0E-05	4.5E-04
CMG043C	15.5	56.8	1.9	1.2E-03	6.2E-03
CMJ202C	21.6	79.2	1.9	5.0E-05	4.5E-04
CMT215C	30.9	113.2	1.9	5.0E-05	4.5E-04
CMI047C	9.9	36.3	1.9	1.5E-04	1.2E-03

continued on next page!

Table A.5 – continued from previous page

	FPKM values			Statistical cuffdiff values	
Gene ID	**BL(-)**	**BL (+)**	**$\log_2$ (fold change)**	**p value**	**q value**
CMM052C	84.2	307.8	1.9	5.0E-05	4.5E-04
CMR497C	21.0	76.7	1.9	5.0E-05	4.5E-04
CMO220C	14.1	51.3	1.9	1.5E-03	7.3E-03
CMO183C	474.8	1726.1	1.9	5.0E-05	4.5E-04
CMK008C	56.3	204.5	1.9	5.0E-05	4.5E-04
CMP216C	34.3	124.4	1.9	5.0E-05	4.5E-04
CMS090C	199.8	725.5	1.9	5.0E-05	4.5E-04
CMQ170C	29.6	107.2	1.9	5.0E-05	4.5E-04
CMO178C	56.2	203.5	1.9	5.0E-05	4.5E-04
CMX010C	39.3	141.9	1.9	5.0E-05	4.5E-04
CMS361C	45.2	163.1	1.9	5.0E-05	4.5E-04
CMN063C	37.6	135.6	1.9	5.0E-05	4.5E-04
CMH042C	41.0	147.1	1.8	5.0E-05	4.5E-04
CMQ382C	120.9	434.1	1.8	5.0E-05	4.5E-04
CMT492C	47.9	171.7	1.8	5.0E-05	4.5E-04
CMJ294C	59.8	214.5	1.8	5.0E-05	4.5E-04
CMT620C	20.8	74.4	1.8	5.0E-05	4.5E-04
CML098C	234.0	836.4	1.8	5.0E-05	4.5E-04
CMF062C	69.8	248.0	1.8	5.0E-05	4.5E-04
CMR373C	54.4	193.0	1.8	5.0E-05	4.5E-04
CMS500C	28.7	101.7	1.8	2.5E-04	1.8E-03
CMA029C	27.2	96.2	1.8	5.0E-05	4.5E-04
CMT510C	30.9	108.9	1.8	5.0E-05	4.5E-04
CMT610C	113.2	398.5	1.8	5.0E-05	4.5E-04
CMQ336C	38.8	136.5	1.8	5.0E-05	4.5E-04
CMF031C	6.5	22.9	1.8	1.4E-03	6.9E-03

continued on next page!

Table A.5 – continued from previous page

	FPKM values			Statistical cuffdiff values	
Gene ID	**BL(-)**	**BL (+)**	**$\log_2$ (fold change)**	**p value**	**q value**
CMK044C	177.5	622.8	1.8	2.0E-04	1.5E-03
CMH250C	39.6	138.7	1.8	5.0E-05	4.5E-04
CMC156C	20.1	70.3	1.8	2.5E-04	1.8E-03
CMV212C	44.5	155.0	1.8	1.5E-04	1.2E-03
CMA124C	23.7	82.5	1.8	5.0E-05	4.5E-04
CME103C	13.5	46.9	1.8	5.0E-05	4.5E-04
CMT600C	24.4	84.4	1.8	1.0E-04	8.2E-04
CMQ111C	33.7	115.8	1.8	5.0E-05	4.5E-04
CMQ101C	10.7	36.7	1.8	3.5E-04	2.3E-03
CML155C	546.3	1866.4	1.8	1.5E-04	1.2E-03
CMS073C	110.0	375.6	1.8	5.0E-05	4.5E-04
CMB087C	25.0	85.2	1.8	5.0E-05	4.5E-04
CMJ250C	19.2	65.3	1.8	1.5E-03	7.1E-03
CMT359C	37.4	126.8	1.8	5.0E-05	4.5E-04
CMG050C	82.6	280.5	1.8	5.0E-05	4.5E-04
CME179C	32.4	109.8	1.8	1.0E-04	8.2E-04
CMS385C	28.5	96.4	1.8	1.0E-04	8.2E-04
CMT172C	725.7	2446.3	1.8	1.3E-03	6.6E-03
CML320C	37.4	126.0	1.8	2.5E-04	1.8E-03
CMP345C	29.6	99.2	1.7	5.0E-05	4.5E-04
CML177C	47.5	159.5	1.7	1.5E-04	1.2E-03
CMP128C	64.6	216.5	1.7	5.0E-05	4.5E-04
CMR017C	163.1	546.0	1.7	5.0E-05	4.5E-04
CML047C	94.3	315.1	1.7	5.0E-05	4.5E-04
CMO300C	385.4	1287.7	1.7	5.0E-05	4.5E-04
CMI294C	104.2	346.7	1.7	1.5E-04	1.2E-03

continued on next page!

Table A.5 – continued from previous page

	FPKM values			Statistical cuffdiff values	
Gene ID	**BL(-)**	**BL (+)**	**$\log_2$ (fold change)**	**p value**	**q value**
CMH144C	135.1	447.6	1.7	5.0E-05	4.5E-04
CMR137C	87.7	290.6	1.7	5.0E-05	4.5E-04
CMR052C	811.8	2686.8	1.7	1.4E-03	6.7E-03
CMK282C	49.1	162.5	1.7	5.0E-05	4.5E-04
CMA114C	561.2	1854.3	1.7	5.0E-05	4.5E-04
CMI108C	22.4	73.8	1.7	4.0E-04	2.6E-03
CMS343C	78.4	256.2	1.7	5.0E-05	4.5E-04
CMM060C	87.3	285.1	1.7	5.0E-05	4.5E-04
CME134C	24.6	80.3	1.7	5.0E-05	4.5E-04
CMM014C	20.9	68.1	1.7	5.0E-05	4.5E-04
CMJ143C	71.5	232.7	1.7	5.0E-05	4.5E-04
CMK178C	146.3	475.9	1.7	5.0E-05	4.5E-04
CMD122C	133.9	434.1	1.7	5.0E-05	4.5E-04
CML079C	28.8	92.6	1.7	5.0E-05	4.5E-04
CMT633C	272.7	875.9	1.7	5.0E-05	4.5E-04
CMS232C	82.0	263.3	1.7	1.0E-04	8.2E-04
CMM273C	63.7	203.6	1.7	5.0E-05	4.5E-04
CMP117C	20.8	66.5	1.7	5.0E-05	4.5E-04
CMR272C	411.2	1308.5	1.7	1.0E-04	8.2E-04
CMG220C	17.1	54.5	1.7	2.0E-04	1.5E-03
CMT598C	57.0	180.6	1.7	5.0E-05	4.5E-04
CMJ149C	69.3	218.5	1.7	5.0E-05	4.5E-04
CME092C	22.3	70.2	1.7	5.0E-05	4.5E-04
CMP297C	28.0	88.0	1.7	5.0E-05	4.5E-04
CMS127C	42.2	132.6	1.7	5.0E-05	4.5E-04
CML249C	26.1	81.9	1.6	1.5E-04	1.2E-03

continued on next page!

Table A.5 – continued from previous page

	FPKM values			Statistical cuffdiff values	
Gene ID	**BL(-)**	**BL (+)**	**$\log_2$ (fold change)**	**p value**	**q value**
CMR044C	96.5	302.6	1.6	1.0E-04	8.2E-04
CMM190C	540.8	1690.5	1.6	1.5E-04	1.2E-03
CMK041C	80.3	250.3	1.6	5.0E-05	4.5E-04
CMN252C	201.5	622.4	1.6	5.0E-05	4.5E-04
CMI035C	59.5	182.9	1.6	1.5E-04	1.2E-03
CMS463C	25.8	78.9	1.6	3.5E-04	2.3E-03
CMN334C	24.8	75.4	1.6	8.5E-04	4.7E-03
CMQ121C	47.1	143.0	1.6	1.7E-03	7.9E-03
CMC181C	282.7	855.6	1.6	6.0E-04	3.6E-03
CMK092C	115.1	347.9	1.6	5.0E-05	4.5E-04
CMI253C	71.8	216.5	1.6	2.5E-04	1.8E-03
CMP289C	30.7	92.4	1.6	5.0E-05	4.5E-04
CMT050C	30.0	89.9	1.6	5.0E-05	4.5E-04
CMQ024C	82.2	245.9	1.6	5.0E-05	4.5E-04
CMJ277C	35.2	105.4	1.6	5.0E-05	4.5E-04
CMI264C	52.6	156.6	1.6	5.0E-05	4.5E-04
CMP113C	16.3	48.4	1.6	5.0E-05	4.5E-04
CME081C	31.4	93.4	1.6	4.5E-04	2.8E-03
CMI255C	168.3	499.6	1.6	1.4E-03	6.9E-03
CMI017C	28.2	83.4	1.6	2.0E-03	9.2E-03
CMT061C	26.3	77.7	1.6	1.0E-04	8.2E-04
CMT471C	18.5	54.8	1.6	5.5E-04	3.3E-03
CMJ144C	64.4	190.4	1.6	3.0E-04	2.0E-03
CMK151C	36.5	107.7	1.6	5.0E-05	4.5E-04
CMI055C	70.3	207.6	1.6	5.0E-05	4.5E-04
CMM229C	159.1	469.5	1.6	5.0E-05	4.5E-04

continued on next page!

Table A.5 – continued from previous page

	FPKM values			Statistical cuffdiff values	
Gene ID	**BL(-)**	**BL (+)**	**$\log_2$ (fold change)**	**p value**	**q value**
CMT497C	52.8	155.7	1.6	5.0E-05	4.5E-04
CMS270C	180.8	532.4	1.6	5.0E-05	4.5E-04
CMT119C	78.5	230.8	1.6	5.0E-05	4.5E-04
CMS231C	542.8	1590.5	1.6	3.5E-04	2.3E-03
CMS199C	19.2	55.9	1.5	5.0E-05	4.5E-04
CMC180C	209.7	610.0	1.5	5.0E-04	3.1E-03
CMC064C	224.4	651.7	1.5	3.0E-04	2.0E-03
CMQ051C	507.9	1472.7	1.5	5.0E-05	4.5E-04
CMJ218C	113.7	329.6	1.5	5.0E-05	4.5E-04
CMT424C	27.7	80.0	1.5	5.0E-05	4.5E-04
CMM287C	35.7	103.2	1.5	5.0E-05	4.5E-04
CMS489C	49.7	143.6	1.5	1.0E-04	8.2E-04
CMI062C	61.4	177.1	1.5	5.0E-05	4.5E-04
CMJ087C	189.1	544.6	1.5	2.0E-04	1.5E-03
CME195C	26.4	76.1	1.5	5.0E-05	4.5E-04
CMR123C	97.2	278.9	1.5	5.0E-05	4.5E-04
CMK089C	84.2	240.6	1.5	5.0E-04	3.1E-03
CMJ162C	135.8	388.0	1.5	5.0E-05	4.5E-04
CMK106C	52.1	148.7	1.5	2.1E-03	9.4E-03
CMO314C	139.6	398.1	1.5	5.0E-05	4.5E-04
CMD100C	74.2	211.7	1.5	5.0E-05	4.5E-04
CMM256C	109.9	313.3	1.5	1.0E-04	8.2E-04
CMQ174C	86.1	245.3	1.5	5.0E-05	4.5E-04
CMT231C	122.8	349.7	1.5	5.0E-05	4.5E-04
CMK191C	79.4	226.0	1.5	5.0E-05	4.5E-04
CMT331C	37.6	106.7	1.5	5.0E-05	4.5E-04

continued on next page!

Table A.5 – continued from previous page

Gene ID	FPKM values		$\log_2$ (fold change)	Statistical cuffdiff values	
	BL(-)	BL (+)		p value	q value
CME175C	1451.1	4110.4	1.5	5.0E-05	4.5E-04
CMT527C	153.6	434.3	1.5	5.0E-05	4.5E-04
CMQ011C	21.8	61.7	1.5	5.0E-05	4.5E-04
CMI122C	80.5	227.2	1.5	4.5E-04	2.8E-03
CMK272C	15.7	44.3	1.5	5.0E-05	4.5E-04
CMH192C	250.4	704.7	1.5	7.0E-04	4.0E-03
CMR284C	27.1	76.0	1.5	5.0E-05	4.5E-04
CMI061C	20.3	56.9	1.5	5.0E-05	4.5E-04
CMJ185C	57.7	161.6	1.5	5.0E-05	4.5E-04
CMM057C	39.2	109.8	1.5	5.0E-05	4.5E-04
CMO334C	24.5	68.7	1.5	2.5E-04	1.8E-03
CMR238C	110.8	310.0	1.5	5.0E-05	4.5E-04
CMP075C	64.4	179.9	1.5	5.0E-05	4.5E-04
CMS264C	95.0	264.8	1.5	5.0E-05	4.5E-04
CMQ342C	145.1	403.3	1.5	2.1E-03	9.5E-03
CMH135C	61.1	169.5	1.5	1.5E-04	1.2E-03
CME150C	26.6	73.8	1.5	1.9E-03	8.6E-03
CMQ313C	124.8	345.6	1.5	4.0E-04	2.6E-03
CMR178C	325.7	901.0	1.5	1.3E-03	6.4E-03
CMT318C	113.9	313.3	1.5	5.0E-05	4.5E-04
CMB050C	74.2	204.1	1.5	1.0E-04	8.2E-04
CMC140C	16.2	44.6	1.5	5.0E-04	3.1E-03
CMS060C	62.6	171.6	1.5	2.0E-04	1.5E-03
CMN027C	21.4	58.7	1.5	5.0E-05	4.5E-04
CMO193C	22.7	62.0	1.5	5.0E-05	4.5E-04
CMC054C	66.5	181.8	1.5	2.0E-04	1.5E-03

continued on next page!

Table A.5 – continued from previous page

	FPKM values			Statistical cuffdiff values	
Gene ID	**BL(-)**	**BL (+)**	**$\log_2$ (fold change)**	**p value**	**q value**
CMT159C	381.0	1041.6	1.5	5.0E-05	4.5E-04
CMT465C	109.5	298.8	1.4	5.0E-05	4.5E-04
CMF129C	222.5	605.1	1.4	1.5E-03	7.3E-03
CMS407C	105.1	285.4	1.4	3.5E-04	2.3E-03
CMN075C	31.7	85.7	1.4	4.0E-04	2.6E-03
CMH261C	46.8	126.5	1.4	5.0E-05	4.5E-04
CMV047C	116.1	313.0	1.4	1.9E-03	8.8E-03
CMM235C	132.2	356.2	1.4	5.0E-05	4.5E-04
CMM020C	94.0	252.9	1.4	1.5E-04	1.2E-03
CME094C	22.4	60.1	1.4	1.7E-03	8.1E-03
CMQ464C	58.2	156.1	1.4	9.5E-04	5.1E-03
CMP292C	53.3	142.3	1.4	5.0E-05	4.5E-04
CML043C	40.3	107.5	1.4	5.0E-05	4.5E-04
CMI227C	58.3	155.4	1.4	1.5E-04	1.2E-03
CMP129C	215.2	573.3	1.4	2.0E-04	1.5E-03
CMR266C	133.6	356.0	1.4	4.0E-04	2.6E-03
CMM067C	14.7	39.0	1.4	2.2E-03	9.9E-03
CMT176C	45.2	120.1	1.4	7.0E-04	4.0E-03
CMQ185C	129.1	343.0	1.4	2.0E-04	1.5E-03
CML049C	55.3	146.7	1.4	5.0E-05	4.5E-04
CMQ102C	41.7	110.6	1.4	5.5E-04	3.3E-03
CMS488C	62.3	164.6	1.4	5.0E-05	4.5E-04
CML087C	42.1	111.0	1.4	5.0E-05	4.5E-04
CME142C	14.0	36.9	1.4	6.0E-04	3.6E-03
CMH055C	13.4	35.1	1.4	5.0E-05	4.5E-04
CMK035C	59.4	155.0	1.4	5.0E-05	4.5E-04

continued on next page!

Table A.5 – continued from previous page

	FPKM values			Statistical cuffdiff values	
Gene ID	**BL(-)**	**BL (+)**	**$\log_2$ (fold change)**	**p value**	**q value**
CMF086C	201.9	525.9	1.4	5.0E-04	3.1E-03
CMN254C	58.9	153.3	1.4	1.5E-04	1.2E-03
CMT590C	26.0	67.4	1.4	1.0E-04	8.2E-04
CMC144C	74.9	194.1	1.4	1.5E-04	1.2E-03
CMS286C	96.6	250.0	1.4	5.0E-05	4.5E-04
CMA031C	100.5	260.1	1.4	5.0E-05	4.5E-04
CMH241C	40.5	104.8	1.4	5.0E-05	4.5E-04
CMS119C	15.0	38.7	1.4	7.5E-04	4.2E-03
CMF059C	107.4	277.1	1.4	3.0E-04	2.0E-03
CMT156C	156.3	402.5	1.4	5.0E-05	4.5E-04
CMP142C	42.3	108.4	1.4	5.0E-05	4.5E-04
CMG172C	20.9	53.5	1.4	4.5E-04	2.8E-03
CMH039C	389.1	996.7	1.4	1.3E-03	6.4E-03
CMA116C	13.6	34.9	1.4	1.5E-03	7.3E-03
CMT317C	70.9	181.4	1.4	5.0E-05	4.5E-04
CMA036C	40.4	103.3	1.4	1.7E-03	8.1E-03
CMO245C	337.6	862.6	1.4	9.0E-04	4.9E-03
CMR317C	46.6	119.0	1.4	1.0E-04	8.2E-04
CML202C	291.6	744.3	1.4	5.0E-05	4.5E-04
CMP070C	273.2	696.5	1.4	8.5E-04	4.7E-03
CMS191C	179.0	456.2	1.3	5.0E-05	4.5E-04
CMT323C	43.0	109.5	1.3	5.0E-05	4.5E-04
CMS334C	13.4	34.1	1.3	3.0E-04	2.0E-03
CMN081C	70.6	179.4	1.3	1.3E-03	6.6E-03
CMS338C	40.5	102.9	1.3	2.0E-04	1.5E-03
CMT595C	165.8	420.8	1.3	1.0E-04	8.2E-04

continued on next page!

Table A.5 – continued from previous page

	FPKM values			Statistical cuffdiff values	
Gene ID	**BL(-)**	**BL (+)**	**$\log_2$ (fold change)**	**p value**	**q value**
CMR440C	159.8	405.1	1.3	9.0E-04	4.9E-03
CMT409C	29.3	73.9	1.3	5.5E-04	3.3E-03
CMJ169C	87.6	221.1	1.3	1.0E-04	8.2E-04
CMR396C	49.1	123.4	1.3	1.0E-04	8.2E-04
CMJ096C	766.0	1925.3	1.3	5.0E-05	4.5E-04
CMJ139C	53.2	133.2	1.3	1.5E-04	1.2E-03
CMD049C	63.5	158.9	1.3	1.5E-04	1.2E-03
CMQ068C	43.8	109.4	1.3	5.0E-05	4.5E-04
CML209C	146.7	366.5	1.3	1.2E-03	6.0E-03
CMI088C	37.9	94.2	1.3	1.5E-04	1.2E-03
CMJ244C	34.4	85.2	1.3	5.0E-05	4.5E-04
CMJ178C	35.3	87.6	1.3	3.0E-04	2.0E-03
CMQ249C	64.7	160.2	1.3	5.0E-05	4.5E-04
CMV208C	261.6	647.1	1.3	1.0E-04	8.2E-04
CMK278C	85.4	211.3	1.3	2.5E-04	1.8E-03
CMT627C	480.5	1188.4	1.3	2.0E-04	1.5E-03
CMJ036C	157.0	387.7	1.3	1.4E-03	6.7E-03
CMT220C	45.5	111.9	1.3	4.0E-04	2.6E-03
CMB059C	48.8	120.0	1.3	1.5E-04	1.2E-03
CML113C	133.3	327.5	1.3	5.0E-05	4.5E-04
CMT476C	114.9	281.7	1.3	5.0E-05	4.5E-04
CMQ283C	55.1	134.9	1.3	2.5E-04	1.8E-03
CMG179C	16.7	40.8	1.3	5.0E-05	4.5E-04
CMI221C	84.3	205.6	1.3	5.0E-05	4.5E-04
CMI054C	58.5	142.5	1.3	5.0E-05	4.5E-04
CMP260C	75.9	184.7	1.3	5.0E-05	4.5E-04

continued on next page!

Table A.5 – continued from previous page

Gene ID	FPKM values		$\log_2$ (fold change)	Statistical cuffdiff values	
	BL(-)	BL (+)		p value	q value
CMQ331C	26.4	64.1	1.3	5.0E-05	4.5E-04
CMT205C	40.0	97.2	1.3	1.8E-03	8.4E-03
CMG165C	25.3	61.2	1.3	5.0E-05	4.5E-04
CMS291C	195.3	471.8	1.3	1.7E-03	7.9E-03
CMJ130C	34.7	83.8	1.3	1.0E-04	8.2E-04
CMP123C	31.2	75.0	1.3	4.5E-04	2.8E-03
CMP205C	100.6	241.3	1.3	2.1E-03	9.4E-03
CMH242C	19.2	46.1	1.3	5.0E-05	4.5E-04
CMM090C	58.0	138.1	1.3	1.0E-04	8.2E-04
CML032C	90.7	215.5	1.2	5.0E-05	4.5E-04
CMS508C	118.3	280.7	1.2	7.0E-04	4.0E-03
CMI298C	136.1	323.0	1.2	5.0E-05	4.5E-04
CMG164C	31.6	75.0	1.2	4.5E-04	2.8E-03
CMI194C	300.1	711.2	1.2	2.0E-03	9.2E-03
CMT472C	76.9	182.2	1.2	1.4E-03	6.7E-03
CMD006C	24.1	57.0	1.2	2.2E-03	9.7E-03
CMS004C	107.3	253.1	1.2	1.5E-04	1.2E-03
CMQ029C	40.3	95.1	1.2	1.5E-04	1.2E-03
CMD175C	72.9	171.9	1.2	5.0E-05	4.5E-04
CMJ188C	91.9	216.5	1.2	1.5E-04	1.2E-03
CMI209C	57.2	134.5	1.2	1.5E-04	1.2E-03
CMS211C	78.4	184.5	1.2	8.5E-04	4.7E-03
CMH236C	41.0	96.4	1.2	2.1E-03	9.5E-03
CML210C	64.1	150.3	1.2	1.0E-04	8.2E-04
CMP219C	15.6	36.6	1.2	7.0E-04	4.0E-03
CMJ055C	119.8	279.9	1.2	1.0E-04	8.2E-04

continued on next page!

Table A.5 – continued from previous page

	FPKM values			Statistical cuffdiff values	
Gene ID	**BL(-)**	**BL (+)**	**$\log_2$ (fold change)**	**p value**	**q value**
CMS035C	124.6	290.8	1.2	1.0E-04	8.2E-04
CMQ030C	70.5	164.5	1.2	2.5E-04	1.8E-03
CMT321C	695.8	1617.9	1.2	1.0E-04	8.2E-04
CMT131C	35.3	82.1	1.2	2.0E-04	1.5E-03
CMR057C	142.2	329.9	1.2	1.3E-03	6.6E-03
CMJ272C	45.5	105.5	1.2	2.0E-04	1.5E-03
CME123C	19.7	45.6	1.2	8.0E-04	4.5E-03
CMI023C	59.2	137.2	1.2	3.0E-04	2.0E-03
CMQ232C	186.0	430.6	1.2	1.1E-03	5.5E-03
CMR244C	235.2	544.3	1.2	1.1E-03	5.5E-03
CME176C	42.4	98.1	1.2	1.2E-03	6.2E-03
CME089C	86.4	199.5	1.2	5.0E-04	3.1E-03
CMR177C	153.6	353.6	1.2	2.0E-04	1.5E-03
CMT115C	17.3	39.7	1.2	1.0E-04	8.2E-04
CMX011C	491.0	1125.6	1.2	1.4E-03	6.9E-03
CMO269C	262.4	601.2	1.2	2.1E-03	9.4E-03
CMN210C	127.8	292.1	1.2	1.0E-04	8.2E-04
CMG200C	50.3	114.9	1.2	5.0E-05	4.5E-04
CMR341C	41.4	94.4	1.2	1.3E-03	6.4E-03
CMT528C	23.1	52.6	1.2	2.0E-03	9.2E-03
CMD028C	61.8	140.0	1.2	1.9E-03	8.8E-03
CMF015C	292.5	661.2	1.2	1.5E-04	1.2E-03
CMK097C	56.5	127.7	1.2	1.0E-04	8.2E-04
CMH177C	125.6	283.7	1.2	1.0E-04	8.2E-04
CMS078C	166.6	375.9	1.2	1.5E-03	7.3E-03
CME004C	802.2	1807.8	1.2	5.0E-05	4.5E-04

continued on next page!

Table A.5 – continued from previous page

	FPKM values			Statistical cuffdiff values	
Gene ID	**BL(-)**	**BL (+)**	**$\log_2$ (fold change)**	**p value**	**q value**
CMP329C	47.4	106.6	1.2	2.1E-03	9.4E-03
CMR053C	49.8	111.9	1.2	3.5E-04	2.3E-03
CMH252C	44.9	101.0	1.2	5.0E-05	4.5E-04
CMJ279C	106.2	237.6	1.2	1.5E-04	1.2E-03
CML314C	50.1	111.7	1.2	7.5E-04	4.2E-03
CMN260C	317.4	707.0	1.2	8.0E-04	4.5E-03
CMT420C	181.8	404.7	1.2	5.0E-04	3.1E-03
CMS328C	96.8	214.6	1.1	1.5E-04	1.2E-03
CMS024C	88.5	195.0	1.1	1.0E-04	8.2E-04
CMT571C	90.6	199.5	1.1	7.5E-04	4.2E-03
CMR030C	86.1	189.6	1.1	2.0E-04	1.5E-03
CMT207C	145.9	320.1	1.1	2.0E-03	9.0E-03
CMP064C	114.9	251.5	1.1	3.5E-04	2.3E-03
CMD154C	40.1	87.7	1.1	4.0E-04	2.6E-03
CML332C	145.1	315.6	1.1	2.0E-04	1.5E-03
CMO025C	87.9	191.0	1.1	2.1E-03	9.5E-03
CMN202C	63.5	137.8	1.1	5.0E-04	3.1E-03
CMF176C	88.0	191.0	1.1	6.0E-04	3.6E-03
CMJ012C	37.5	81.3	1.1	2.2E-03	9.9E-03
CMT433C	51.3	111.3	1.1	3.5E-04	2.3E-03
CMD058C	45.1	97.6	1.1	4.0E-04	2.6E-03
CMF107C	39.6	85.5	1.1	5.0E-04	3.1E-03
CMQ013C	124.6	268.3	1.1	1.6E-03	7.5E-03
CMK235C	37.6	80.9	1.1	6.5E-04	3.8E-03
CMO104C	29.0	62.5	1.1	6.5E-04	3.8E-03
CME044C	36.1	77.4	1.1	3.0E-04	2.0E-03

continued on next page!

Table A.5 – continued from previous page

	FPKM values			Statistical cuffdiff values	
Gene ID	**BL(-)**	**BL (+)**	**$\log_2$ (fold change)**	**p value**	**q value**
CMM079C	111.2	238.2	1.1	4.5E-04	2.8E-03
CMA048C	104.5	223.7	1.1	2.5E-04	1.8E-03
CMT227C	31.3	66.9	1.1	1.9E-03	8.8E-03
CMI197C	131.0	280.5	1.1	6.0E-04	3.6E-03
CMI091C	94.2	201.5	1.1	4.5E-04	2.8E-03
CMP036C	60.5	129.5	1.1	4.0E-04	2.6E-03
CMT041C	71.2	152.3	1.1	6.0E-04	3.6E-03
CMD030C	188.5	402.4	1.1	2.5E-04	1.8E-03
CMI130C	32.0	68.3	1.1	1.4E-03	6.9E-03
CMH090C	52.0	110.7	1.1	3.0E-04	2.0E-03
CMT530C	291.9	621.3	1.1	6.5E-04	3.8E-03
CMS294C	75.6	160.8	1.1	5.5E-04	3.3E-03
CMM048C	22.8	48.5	1.1	2.1E-03	9.4E-03
CMO244C	73.8	156.7	1.1	2.0E-03	9.0E-03
CMI142C	108.3	229.6	1.1	7.5E-04	4.2E-03
CMR179C	129.0	273.0	1.1	5.0E-04	3.1E-03
CMS276C	34.9	73.5	1.1	3.0E-04	2.0E-03
CMQ389C	68.7	144.3	1.1	1.3E-03	6.4E-03
CMS195C	168.2	353.1	1.1	1.3E-03	6.6E-03
CMD011C	191.0	399.8	1.1	3.5E-04	2.3E-03
CMQ124C	157.3	328.9	1.1	1.1E-03	5.8E-03
CMS088C	66.4	138.6	1.1	6.0E-04	3.6E-03
CMA106C	54.5	113.7	1.1	6.0E-04	3.6E-03
CME133C	104.7	218.6	1.1	6.5E-04	3.8E-03
CMH032C	27.2	56.8	1.1	9.5E-04	5.1E-03
CMP067C	146.1	304.5	1.1	6.0E-04	3.6E-03

continued on next page!

Table A.5 – continued from previous page

Gene ID	FPKM values		$\log_2$ (fold change)	Statistical cuffdiff values	
	BL(-)	BL (+)		p value	q value
CMR203C	39.6	82.4	1.1	1.1E-03	5.5E-03
CMN019C	102.4	212.7	1.1	7.5E-04	4.2E-03
CMR468C	27.9	57.7	1.1	1.9E-03	8.6E-03
CMT336C	40.9	84.5	1.0	1.0E-03	5.3E-03
CMK194C	114.8	236.9	1.0	7.0E-04	4.0E-03
CMB094C	93.4	192.8	1.0	7.0E-04	4.0E-03
CMQ035C	60.8	124.7	1.0	7.0E-04	4.0E-03
CMT190C	127.9	262.3	1.0	1.2E-03	6.2E-03
CMJ027C	142.0	291.0	1.0	1.1E-03	5.8E-03
CMA056C	29.4	60.2	1.0	9.0E-04	4.9E-03
CMI140C	970.6	1986.4	1.0	1.8E-03	8.4E-03
CMS208C	46.8	95.8	1.0	7.5E-04	4.2E-03
CMC098C	91.6	187.1	1.0	6.0E-04	3.6E-03
CMO278C	65.3	133.5	1.0	1.6E-03	7.5E-03
CMS289C	81.2	166.0	1.0	2.1E-03	9.5E-03
CMB009C	29.7	60.6	1.0	1.8E-03	8.4E-03
CME130C	127.8	260.5	1.0	6.5E-04	3.8E-03
CMO305C	84.5	172.3	1.0	1.0E-03	5.3E-03
CMO197C	98.3	200.2	1.0	1.5E-03	7.1E-03
CMF121C	22.3	45.3	1.0	9.5E-04	5.1E-03
CMG083C	28.5	58.1	1.0	6.0E-04	3.6E-03
CMN153C	113.0	229.2	1.0	1.6E-03	7.7E-03
CMN315C	1009.6	2047.2	1.0	6.0E-04	3.6E-03
CMM111C	88.3	178.7	1.0	9.0E-04	4.9E-03
CML103C	21.5	43.6	1.0	6.5E-04	3.8E-03
CML115C	214.8	432.9	1.0	1.0E-03	5.3E-03

continued on next page!

Table A.5 – continued from previous page

	FPKM values			Statistical cuffdiff values	
Gene ID	**BL(-)**	**BL (+)**	**$\log_2$ (fold change)**	**p value**	**q value**
CMK285C	72.9	146.9	1.0	1.3E-03	6.6E-03
CMJ080C	96.9	195.1	1.0	1.2E-03	6.0E-03
CMT541C	62.5	125.2	1.0	1.7E-03	7.9E-03
CMH047C	62.0	124.0	1.0	2.1E-03	9.4E-03
CMN050C	324.3	647.5	1.0	1.4E-03	6.7E-03
CMM215C	88.2	44.1	-1.0	2.2E-03	9.7E-03
CMQ091C	326.2	163.0	-1.0	9.5E-04	5.1E-03
CMM069C	121.1	60.5	-1.0	1.3E-03	6.6E-03
CMB038C	99.7	49.7	-1.0	6.0E-04	3.6E-03
CMC034C	139.0	69.3	-1.0	7.5E-04	4.2E-03
CMG117C	90.1	44.8	-1.0	1.2E-03	6.2E-03
CMP164C	136.9	68.0	-1.0	9.0E-04	4.9E-03
CMK243C	236.6	117.4	-1.0	7.0E-04	4.0E-03
CMS122C	143.5	71.1	-1.0	5.0E-04	3.1E-03
CMP192C	247.8	122.5	-1.0	7.5E-04	4.2E-03
CMG145C	222.9	109.9	-1.0	9.5E-04	5.1E-03
CMQ206C	116.3	57.3	-1.0	9.0E-04	4.9E-03
CMK069C	98.8	48.6	-1.0	1.2E-03	6.2E-03
CML126C	210.7	103.6	-1.0	1.2E-03	6.2E-03
CMT291C	264.6	130.1	-1.0	6.5E-04	3.8E-03
CMO055C	150.3	73.8	-1.0	1.3E-03	6.4E-03
CMB042C	205.5	100.8	-1.0	8.0E-04	4.5E-03
CMC111C	109.4	53.7	-1.0	6.5E-04	3.8E-03
CMB039C	154.9	75.9	-1.0	1.1E-03	5.8E-03
CMD181C	89.9	43.9	-1.0	1.8E-03	8.4E-03
CMP005C	213.0	103.6	-1.0	5.0E-04	3.1E-03

continued on next page!

Table A.5 – continued from previous page

	FPKM values			Statistical cuffdiff values	
Gene ID	**BL(-)**	**BL (+)**	**$\log_2$ (fold change)**	**p value**	**q value**
CMI299C	240.1	116.7	-1.0	1.1E-03	5.8E-03
CMR033C	159.1	77.2	-1.0	5.5E-04	3.3E-03
CMC114C	250.1	121.4	-1.0	5.5E-04	3.3E-03
CMJ300C	162.5	78.8	-1.0	7.0E-04	4.0E-03
CMI234C	179.5	87.1	-1.0	6.0E-04	3.6E-03
CMS432C	372.9	180.3	-1.0	1.4E-03	6.9E-03
CMP061C	146.1	70.5	-1.1	1.7E-03	8.1E-03
CMT268C	372.1	179.5	-1.1	1.5E-03	7.3E-03
CMQ020C	1007.6	485.9	-1.1	1.0E-03	5.3E-03
CMC067C	564.1	272.0	-1.1	3.5E-04	2.3E-03
CMT460C	364.4	174.7	-1.1	5.5E-04	3.3E-03
CMS097C	120.2	57.5	-1.1	5.5E-04	3.3E-03
CMR470C	85.7	41.0	-1.1	5.0E-04	3.1E-03
CMR355C	96.6	46.2	-1.1	1.4E-03	6.7E-03
CMH266C	112.6	53.8	-1.1	4.5E-04	2.8E-03
CMP332C	879.0	419.0	-1.1	1.9E-03	8.8E-03
CMR032C	132.3	63.0	-1.1	4.5E-04	2.8E-03
CMD034C	241.8	115.0	-1.1	1.3E-03	6.4E-03
CMP149C	233.0	110.7	-1.1	9.5E-04	5.1E-03
CML100C	131.4	62.4	-1.1	6.0E-04	3.6E-03
CMK181C	279.0	132.3	-1.1	5.0E-04	3.1E-03
CMD137C	197.9	93.8	-1.1	3.5E-04	2.3E-03
CMC110C	113.3	53.6	-1.1	3.0E-04	2.0E-03
CMO285C	194.7	91.9	-1.1	9.5E-04	5.1E-03
CMO015C	129.4	61.0	-1.1	4.0E-04	2.6E-03
CMN134C	126.1	59.5	-1.1	2.0E-03	9.0E-03

continued on next page!

Table A.5 – continued from previous page

	FPKM values			Statistical cuffdiff values	
Gene ID	**BL(-)**	**BL (+)**	**$\log_2$ (fold change)**	**p value**	**q value**
CMG079C	178.1	83.8	-1.1	5.0E-04	3.1E-03
CMM087C	225.8	106.0	-1.1	3.0E-04	2.0E-03
CMR384C	95.2	44.7	-1.1	1.7E-03	7.9E-03
CMB029C	152.5	71.6	-1.1	9.5E-04	5.1E-03
CMC105C	111.6	52.3	-1.1	2.1E-03	9.4E-03
CML326C	157.5	73.7	-1.1	3.5E-04	2.3E-03
CME138C	117.2	54.8	-1.1	3.0E-04	2.0E-03
CMO032C	276.6	129.3	-1.1	2.5E-04	1.8E-03
CMK146C	65.6	30.6	-1.1	3.0E-04	2.0E-03
CMS150C	141.5	66.0	-1.1	9.0E-04	4.9E-03
CMM002C	257.2	119.8	-1.1	3.0E-04	2.0E-03
CMP162C	156.6	72.9	-1.1	8.0E-04	4.5E-03
CMQ073C	263.3	122.5	-1.1	8.0E-04	4.5E-03
CMH231C	98.3	45.6	-1.1	1.5E-04	1.2E-03
CMI201C	187.7	87.0	-1.1	2.5E-04	1.8E-03
CMQ204C	123.0	57.0	-1.1	8.5E-04	4.7E-03
CMQ195C	81.7	37.8	-1.1	1.5E-03	7.1E-03
CMR077C	102.1	47.2	-1.1	1.5E-03	7.1E-03
CMT181C	167.4	77.1	-1.1	1.4E-03	6.9E-03
CMB155C	738.7	340.5	-1.1	1.1E-03	5.5E-03
CMN100C	130.9	60.3	-1.1	1.1E-03	5.8E-03
CMK140C	136.7	62.8	-1.1	1.1E-03	5.5E-03
CMR360C	324.6	148.8	-1.1	1.5E-03	7.3E-03
CMR427C	99.5	45.6	-1.1	2.5E-04	1.8E-03
CMR234C	107.3	49.1	-1.1	3.5E-04	2.3E-03
CMP140C	115.5	52.8	-1.1	3.0E-04	2.0E-03

continued on next page!

Table A.5 – continued from previous page

	FPKM values			Statistical cuffdiff values	
Gene ID	**BL(-)**	**BL (+)**	**$\log_2$ (fold change)**	**p value**	**q value**
CMS249C	144.1	65.8	-1.1	2.0E-04	1.5E-03
CMN029C	100.3	45.8	-1.1	4.5E-04	2.8E-03
CMI065C	145.5	66.4	-1.1	2.0E-04	1.5E-03
CMP210C	132.7	60.5	-1.1	2.1E-03	9.4E-03
CMR318C	1170.2	533.3	-1.1	4.5E-04	2.8E-03
CMI288C	66.4	30.3	-1.1	9.0E-04	4.9E-03
CMK163C	812.8	370.2	-1.1	7.0E-04	4.0E-03
CMQ358C	341.0	155.3	-1.1	3.0E-04	2.0E-03
CMS449C	228.2	103.9	-1.1	1.3E-03	6.4E-03
CMF155C	59.1	26.9	-1.1	6.0E-04	3.6E-03
CMT077C	88.2	40.1	-1.1	1.9E-03	8.8E-03
CMH049C	238.4	108.3	-1.1	2.0E-04	1.5E-03
CMA019C	93.1	42.3	-1.1	3.0E-04	2.0E-03
CMH255C	204.7	92.9	-1.1	1.0E-04	8.2E-04
CMI096C	188.0	85.1	-1.1	1.0E-03	5.3E-03
CML201C	2169.5	980.5	-1.1	3.5E-04	2.3E-03
CMF007C	136.1	61.4	-1.1	2.5E-04	1.8E-03
CMF128C	176.0	79.4	-1.1	1.5E-04	1.2E-03
CMP015C	93.1	42.0	-1.1	4.0E-04	2.6E-03
CMC172C	114.5	51.5	-1.2	2.0E-04	1.5E-03
CMI092C	140.6	63.1	-1.2	3.0E-04	2.0E-03
CMT445C	95.8	43.0	-1.2	1.5E-04	1.2E-03
CMS332C	306.5	136.9	-1.2	4.0E-04	2.6E-03
CMR010C	421.6	187.9	-1.2	5.0E-04	3.1E-03
CMM311C	119.4	53.2	-1.2	3.0E-04	2.0E-03
CMG142C	568.0	253.0	-1.2	2.2E-03	9.7E-03

continued on next page!

Table A.5 – continued from previous page

	FPKM values			Statistical cuffdiff values	
Gene ID	**BL(-)**	**BL (+)**	**$\log_2$ (fold change)**	**p value**	**q value**
CMJ072C	213.5	94.9	-1.2	2.5E-04	1.8E-03
CMT616C	218.3	97.0	-1.2	2.0E-04	1.5E-03
CMM153C	179.1	79.4	-1.2	5.0E-05	4.5E-04
CMN131C	66.5	29.5	-1.2	2.2E-03	9.7E-03
CMJ061C	133.7	59.2	-1.2	1.0E-04	8.2E-04
CMD125C	101.0	44.7	-1.2	1.3E-03	6.4E-03
CME031C	379.4	167.9	-1.2	3.5E-04	2.3E-03
CMA028C	391.0	172.6	-1.2	6.0E-04	3.6E-03
CMS115C	112.5	49.6	-1.2	1.5E-04	1.2E-03
CMO028C	192.1	84.7	-1.2	3.5E-04	2.3E-03
CMK139C	176.9	78.0	-1.2	3.5E-04	2.3E-03
CML186C	317.9	139.6	-1.2	2.0E-04	1.5E-03
CMB141C	272.1	119.5	-1.2	4.0E-04	2.6E-03
CMN211C	230.6	101.1	-1.2	5.0E-05	4.5E-04
CMR472C	412.5	180.8	-1.2	2.1E-03	9.4E-03
CMR400C	85.1	37.3	-1.2	1.5E-04	1.2E-03
CMB002C	120.5	52.5	-1.2	2.0E-04	1.5E-03
CMD053C	209.5	91.2	-1.2	3.0E-04	2.0E-03
CME071C	101.0	43.9	-1.2	2.1E-03	9.4E-03
CMC029C	219.4	95.2	-1.2	3.0E-04	2.0E-03
CMJ184C	153.5	66.5	-1.2	1.5E-04	1.2E-03
CMN143C	86.5	37.5	-1.2	1.7E-03	7.9E-03
CMS337C	156.4	67.7	-1.2	3.5E-04	2.3E-03
CMO102C	210.4	91.0	-1.2	4.0E-04	2.6E-03
CMS132C	95.6	41.2	-1.2	3.0E-04	2.0E-03
CMD074C	286.4	123.3	-1.2	2.0E-04	1.5E-03

continued on next page!

Table A.5 – continued from previous page

	FPKM values			Statistical cuffdiff values	
Gene ID	**BL(-)**	**BL (+)**	**$\log_2$ (fold change)**	**p value**	**q value**
CMG212C	164.0	70.3	-1.2	1.0E-04	8.2E-04
CMS282C	100.9	43.3	-1.2	3.0E-04	2.0E-03
CMD112C	331.6	141.7	-1.2	1.5E-04	1.2E-03
CMN062C	193.1	82.3	-1.2	5.0E-05	4.5E-04
CMQ182C	334.0	142.3	-1.2	3.5E-04	2.3E-03
CMQ271C	158.3	67.1	-1.2	2.0E-04	1.5E-03
CMH264C	74.8	31.7	-1.2	1.0E-04	8.2E-04
CMS062C	33.5	14.2	-1.2	8.5E-04	4.7E-03
CMJ295C	138.7	58.6	-1.2	1.6E-03	7.5E-03
CMQ447C	513.8	216.8	-1.2	1.7E-03	7.9E-03
CMF017C	613.0	258.2	-1.2	1.1E-03	5.5E-03
CMK197C	335.7	141.3	-1.2	1.5E-04	1.2E-03
CMJ046C	166.0	69.8	-1.3	3.0E-04	2.0E-03
CMG152C	394.7	165.5	-1.3	4.5E-04	2.8E-03
CMT122C	120.3	50.4	-1.3	5.0E-05	4.5E-04
CMT088C	102.8	42.9	-1.3	1.5E-04	1.2E-03
CMM147C	139.0	58.1	-1.3	1.5E-04	1.2E-03
CMM141C	120.5	50.0	-1.3	5.0E-05	4.5E-04
CMD118C	274.4	113.6	-1.3	1.5E-04	1.2E-03
CMK031C	718.0	297.1	-1.3	1.5E-04	1.2E-03
CMQ139C	42.8	17.7	-1.3	6.0E-04	3.6E-03
CMT191C	132.3	54.5	-1.3	5.0E-05	4.5E-04
CMK118C	1946.7	800.3	-1.3	7.0E-04	4.0E-03
CMM236C	185.8	76.3	-1.3	2.0E-04	1.5E-03
CMO266C	67.6	27.7	-1.3	9.0E-04	4.9E-03
CMM206C	82.0	33.6	-1.3	1.1E-03	5.8E-03

continued on next page!

Table A.5 – continued from previous page

	FPKM values			Statistical cuffdiff values	
Gene ID	**BL(-)**	**BL (+)**	**$\log_2$ (fold change)**	**p value**	**q value**
CMO173C	106.1	43.4	-1.3	5.0E-05	4.5E-04
CMC123C	241.9	98.7	-1.3	4.5E-04	2.8E-03
CMB114C	671.2	273.3	-1.3	5.0E-05	4.5E-04
CMD105C	200.8	81.7	-1.3	5.0E-05	4.5E-04
CMA070C	1068.0	434.5	-1.3	2.0E-04	1.5E-03
CML300C	203.2	82.4	-1.3	1.5E-04	1.2E-03
CMF022C	220.9	89.5	-1.3	1.0E-04	8.2E-04
CMB121C	240.9	97.6	-1.3	7.5E-04	4.2E-03
CMQ399C	317.3	128.4	-1.3	5.0E-05	4.5E-04
CMB075C	259.0	104.8	-1.3	5.0E-05	4.5E-04
CMS036C	130.3	52.7	-1.3	5.0E-05	4.5E-04
CMN146C	443.5	179.2	-1.3	5.0E-05	4.5E-04
CMC088C	267.6	108.0	-1.3	1.0E-04	8.2E-04
CMP278C	2958.4	1193.8	-1.3	5.0E-05	4.5E-04
CMH100C	45.6	18.4	-1.3	7.5E-04	4.2E-03
CMH210C	421.2	169.4	-1.3	3.5E-04	2.3E-03
CMM295C	259.7	104.2	-1.3	5.0E-05	4.5E-04
CMM260C	206.0	82.6	-1.3	5.0E-05	4.5E-04
CMC020C	232.9	93.3	-1.3	5.0E-05	4.5E-04
CMR112C	187.8	75.2	-1.3	1.5E-04	1.2E-03
CMG088C	195.1	78.0	-1.3	5.0E-05	4.5E-04
CMA093C	78.4	31.4	-1.3	2.5E-04	1.8E-03
CMF039C	504.3	201.6	-1.3	5.0E-05	4.5E-04
CMT178C	163.5	65.3	-1.3	2.0E-04	1.5E-03
CMH172C	272.5	108.6	-1.3	5.0E-05	4.5E-04
CMJ215C	212.1	84.4	-1.3	4.5E-04	2.8E-03

continued on next page!

Table A.5 – continued from previous page

	FPKM values			Statistical cuffdiff values	
Gene ID	**BL(-)**	**BL (+)**	**$\log_2$ (fold change)**	**p value**	**q value**
CMI119C	153.3	61.0	-1.3	2.5E-04	1.8E-03
CMN128C	222.9	88.5	-1.3	5.0E-05	4.5E-04
CML290C	263.1	104.4	-1.3	5.0E-05	4.5E-04
CML097C	71.8	28.5	-1.3	5.0E-05	4.5E-04
CML068C	145.5	57.6	-1.3	1.5E-04	1.2E-03
CMI014C	137.2	54.3	-1.3	5.0E-05	4.5E-04
CMR174C	221.2	87.3	-1.3	5.0E-05	4.5E-04
CMQ375C	171.8	67.8	-1.3	5.0E-05	4.5E-04
CMQ065C	431.9	169.6	-1.3	5.0E-05	4.5E-04
CMM314C	163.8	64.3	-1.3	2.0E-04	1.5E-03
CMS194C	541.0	212.4	-1.3	2.0E-04	1.5E-03
CML176C	329.1	129.2	-1.3	3.0E-04	2.0E-03
CMB098C	836.1	327.3	-1.4	5.0E-05	4.5E-04
CMA040C	190.8	74.7	-1.4	5.0E-05	4.5E-04
CMK161C	102.6	40.1	-1.4	5.0E-05	4.5E-04
CMT437C	381.7	149.3	-1.4	5.0E-05	4.5E-04
CMT625C	81.7	31.9	-1.4	5.0E-05	4.5E-04
CMP280C	650.4	254.2	-1.4	2.5E-04	1.8E-03
CMS047C	519.6	202.9	-1.4	5.0E-05	4.5E-04
CMB115C	130.4	50.9	-1.4	2.5E-04	1.8E-03
CMS040C	186.7	72.8	-1.4	5.0E-05	4.5E-04
CMF116C	117.1	45.6	-1.4	4.5E-04	2.8E-03
CMT009C	164.2	63.8	-1.4	5.0E-05	4.5E-04
CMK042C	402.8	156.6	-1.4	5.5E-04	3.3E-03
CMO319C	174.9	67.9	-1.4	5.0E-05	4.5E-04
CMM250C	2273.3	881.3	-1.4	8.0E-04	4.5E-03

continued on next page!

Table A.5 – continued from previous page

	FPKM values			Statistical cuffdiff values	
Gene ID	**BL(-)**	**BL (+)**	**$\log_2$ (fold change)**	**p value**	**q value**
CMK147C	357.2	138.5	-1.4	5.0E-05	4.5E-04
CMP356C	46.7	18.1	-1.4	5.0E-05	4.5E-04
CMS490C	911.6	353.0	-1.4	5.5E-04	3.3E-03
CMA007C	464.8	179.7	-1.4	1.0E-04	8.2E-04
CMQ081C	100.4	38.7	-1.4	1.4E-03	6.7E-03
CMK079C	76.6	29.5	-1.4	1.0E-03	5.3E-03
CML157C	291.7	112.1	-1.4	1.5E-04	1.2E-03
CMM258C	270.3	103.7	-1.4	5.0E-05	4.5E-04
CMM026C	187.8	71.9	-1.4	4.5E-04	2.8E-03
CMN286C	288.4	110.3	-1.4	3.5E-04	2.3E-03
CMI064C	100.2	38.2	-1.4	5.0E-05	4.5E-04
CMJ064C	135.4	51.6	-1.4	5.0E-05	4.5E-04
CMM037C	283.8	108.1	-1.4	1.5E-03	7.3E-03
CMO083C	166.4	63.2	-1.4	5.0E-05	4.5E-04
CMM217C	4091.3	1551.8	-1.4	6.5E-04	3.8E-03
CME082C	47.2	17.9	-1.4	1.7E-03	8.1E-03
CMH227C	268.8	101.7	-1.4	5.0E-05	4.5E-04
CME012C	222.0	83.7	-1.4	5.0E-05	4.5E-04
CMS495C	58.4	22.0	-1.4	4.0E-04	2.6E-03
CMQ278C	105.5	39.8	-1.4	5.0E-05	4.5E-04
CMS281C	128.0	48.2	-1.4	5.0E-05	4.5E-04
CMA107C	93.2	34.9	-1.4	5.0E-05	4.5E-04
CMQ040C	101.1	37.8	-1.4	5.0E-05	4.5E-04
CMT489C	276.5	103.2	-1.4	3.0E-04	2.0E-03
CMS093C	69.8	26.0	-1.4	5.0E-05	4.5E-04
CMS348C	313.0	116.3	-1.4	5.0E-05	4.5E-04

continued on next page!

Table A.5 – continued from previous page

	FPKM values			Statistical cuffdiff values	
Gene ID	**BL(-)**	**BL (+)**	**$\log_2$ (fold change)**	**p value**	**q value**
CMQ456C	170.5	63.3	-1.4	5.0E-05	4.5E-04
CMS283C	324.2	120.1	-1.4	5.0E-05	4.5E-04
CMJ050C	227.3	84.0	-1.4	5.0E-05	4.5E-04
CMP168C	247.6	91.4	-1.4	5.0E-05	4.5E-04
CMS371C	701.2	258.3	-1.4	1.2E-03	6.0E-03
CMO071C	172.7	63.6	-1.4	6.5E-04	3.8E-03
CMB078C	153.2	56.3	-1.4	5.0E-05	4.5E-04
CMM233C	32.4	11.9	-1.4	3.5E-04	2.3E-03
CMJ257C	111.6	41.0	-1.4	5.0E-05	4.5E-04
CMD142C	266.5	97.8	-1.4	5.0E-05	4.5E-04
CMS441C	267.6	98.1	-1.4	5.0E-05	4.5E-04
CMT121C	105.3	38.6	-1.4	4.5E-04	2.8E-03
CMJ033C	510.3	186.6	-1.5	1.0E-04	8.2E-04
CMT459C	234.7	85.8	-1.5	2.5E-04	1.8E-03
CMT452C	183.1	66.9	-1.5	5.0E-05	4.5E-04
CMN257C	55.3	20.2	-1.5	9.0E-04	4.9E-03
CMS067C	280.4	101.3	-1.5	5.0E-05	4.5E-04
CMT260C	322.9	116.6	-1.5	5.0E-05	4.5E-04
CMI211C	2137.5	770.2	-1.5	7.5E-04	4.2E-03
CMT021C	97.2	34.8	-1.5	5.0E-05	4.5E-04
CMQ031C	626.8	224.4	-1.5	5.0E-05	4.5E-04
CMS380C	311.0	111.3	-1.5	2.0E-03	9.2E-03
CML073C	477.2	170.7	-1.5	5.0E-05	4.5E-04
CMJ013C	166.8	59.3	-1.5	5.0E-05	4.5E-04
CMN160C	104.7	36.9	-1.5	2.0E-04	1.5E-03
CMQ221C	233.1	82.2	-1.5	5.0E-05	4.5E-04

continued on next page!

Table A.5 – continued from previous page

	FPKM values			Statistical cuffdiff values	
Gene ID	**BL(-)**	**BL (+)**	**$\log_2$ (fold change)**	**p value**	**q value**
CMQ412C	456.9	160.5	-1.5	3.5E-04	2.3E-03
CMR065C	181.5	63.6	-1.5	3.5E-04	2.3E-03
CMP308C	573.4	200.3	-1.5	5.0E-05	4.5E-04
CMM061C	1137.4	397.3	-1.5	7.5E-04	4.2E-03
CMP087C	717.9	250.4	-1.5	2.0E-03	9.2E-03
CMO125C	212.7	74.2	-1.5	5.0E-05	4.5E-04
CMS498C	423.9	147.6	-1.5	5.0E-05	4.5E-04
CMJ070C	994.3	345.9	-1.5	4.5E-04	2.8E-03
CMM326C	209.3	72.8	-1.5	1.5E-04	1.2E-03
CMK009C	275.7	95.7	-1.5	1.5E-04	1.2E-03
CMP159C	460.9	157.9	-1.5	4.5E-04	2.8E-03
CMR257C	88.8	30.3	-1.6	5.0E-05	4.5E-04
CMR066C	223.7	76.0	-1.6	5.0E-05	4.5E-04
CMM179C	114.5	38.8	-1.6	5.0E-05	4.5E-04

Table A.6: List of differentially expressed genes under red light in *C. merolae* (q-value < 0.01 and the absolute value of $|\log_2$ fold change$| \geq 1$).

	FPKM values			**Statistical cuffdiff values**	
Gene ID	**RL(-)**	**RL (+)**	**$\log_2$ (fold change)**	**p value**	**q value**
CMO111C	7.0	341.1	5.6	3.50E-04	2.31E-03
CMN022C	6.2	300.8	5.6	2.00E-04	1.46E-03
CMO306C	4.2	189.3	5.5	1.25E-03	6.36E-03
CMN019C	5.4	188.7	5.1	5.00E-05	4.50E-04
CMS308C	15.4	511.6	5.1	5.00E-05	4.50E-04
CMT305C	6.1	191.7	5.0	5.00E-05	4.50E-04
CMK291C	4.7	139.4	4.9	5.00E-05	4.50E-04
CMS159C	9.2	259.3	4.8	5.00E-05	4.50E-04
CMN235C	21.0	570.7	4.8	5.00E-05	4.50E-04
CMV158C	18.2	466.5	4.7	8.00E-04	4.46E-03
CMV159C	18.7	453.3	4.6	6.50E-04	3.79E-03
CMK188C	9.2	220.4	4.6	5.00E-05	4.50E-04
CMR237C	12.1	285.9	4.6	5.00E-05	4.50E-04
CMV208C	42.7	979.4	4.5	5.00E-05	4.50E-04
CMM162C	5.3	115.2	4.5	1.00E-04	8.17E-04
CMV209C	90.2	1949.2	4.4	5.00E-05	4.50E-04
CMQ233C	3.4	72.5	4.4	7.50E-04	4.24E-03
CMN237C	13.8	278.3	4.3	5.00E-05	4.50E-04
CMK063C	4.3	85.6	4.3	1.90E-03	8.83E-03
CMV207C	48.1	932.5	4.3	5.00E-05	4.50E-04
CMJ101C	256.2	4783.5	4.2	1.60E-03	7.70E-03
CMS311C	45.4	838.0	4.2	5.00E-05	4.50E-04
CMD051C	24.5	444.0	4.2	5.00E-05	4.50E-04

continued on next page!

Table A.6 – continued from previous page

	FPKM values			Statistical cuffdiff values	
Gene ID	**RL(-)**	**RL (+)**	**$\log_2$ (fold change)**	**p value**	**q value**
CMQ397C	9.8	171.6	4.1	5.00E-05	4.50E-04
CMM134C	40.9	662.1	4.0	1.95E-03	9.01E-03
CMA122C	35.2	561.9	4.0	5.00E-05	4.50E-04
CMQ113C	46.8	737.9	4.0	5.00E-05	4.50E-04
CMJ105C	11.3	172.1	3.9	5.00E-05	4.50E-04
CMN227C	21.1	282.1	3.7	5.00E-05	4.50E-04
CMG201C	10.0	131.2	3.7	5.00E-05	4.50E-04
CMT183C	133.8	1725.0	3.7	5.00E-05	4.50E-04
CMN234C	133.2	1714.4	3.7	5.00E-05	4.50E-04
CMB155C	95.1	1219.0	3.7	5.00E-05	4.50E-04
CMJ042C	75.3	918.6	3.6	4.00E-04	2.57E-03
CMJ265C	11.5	135.6	3.6	8.00E-04	4.46E-03
CMN109C	27.5	317.4	3.5	5.00E-05	4.50E-04
CMT162C	18.7	213.3	3.5	5.00E-05	4.50E-04
CMI233C	179.3	2000.1	3.5	5.00E-05	4.50E-04
CMR109C	17.0	185.2	3.4	5.00E-05	4.50E-04
CMK232C	3.8	40.2	3.4	1.65E-03	7.90E-03
CMQ051C	70.1	735.9	3.4	1.00E-04	8.17E-04
CMS351C	64.9	666.8	3.4	5.00E-05	4.50E-04
CMP012C	24.7	247.9	3.3	7.50E-04	4.24E-03
CMG086C	29.9	299.7	3.3	5.00E-05	4.50E-04
CMT329C	11.3	111.5	3.3	5.00E-05	4.50E-04
CMB157C	29.9	287.9	3.3	5.00E-05	4.50E-04
CMI140C	96.1	912.1	3.2	5.00E-05	4.50E-04
CMV129C	137.8	1305.7	3.2	5.00E-05	4.50E-04
CML276C	22.7	213.5	3.2	5.00E-05	4.50E-04

continued on next page!

Table A.6 – continued from previous page

Gene ID	FPKM values		$\log_2$ (fold change)	Statistical cuffdiff values	
	RL(-)	RL (+)		p value	q value
CMC157C	2.7	24.8	3.2	5.00E-04	3.07E-03
CMO139C	31.0	287.7	3.2	5.00E-05	4.50E-04
CMF098C	79.7	730.5	3.2	5.00E-05	4.50E-04
CMG188C	19.0	173.3	3.2	6.50E-04	3.79E-03
CMS189C	32.3	294.7	3.2	5.00E-05	4.50E-04
CMS031C	34.2	312.0	3.2	5.00E-05	4.50E-04
CMT304C	4.4	40.2	3.2	1.45E-03	7.14E-03
CMP086C	105.1	896.9	3.1	5.00E-05	4.50E-04
CMN084C	153.4	1281.8	3.1	1.00E-04	8.17E-04
CMQ270C	158.7	1295.0	3.0	5.00E-05	4.50E-04
CML196C	44.6	359.0	3.0	5.00E-05	4.50E-04
CMJ276C	14.5	116.5	3.0	9.00E-04	4.90E-03
CMQ191C	8.0	62.2	3.0	1.50E-04	1.15E-03
CME180C	31.2	241.2	2.9	5.00E-05	4.50E-04
CMF070C	3.0	23.2	2.9	2.50E-04	1.75E-03
CMS309C	40.9	307.1	2.9	3.50E-04	2.31E-03
CMQ123C	29.6	221.4	2.9	5.00E-05	4.50E-04
CMV135C	20.9	153.7	2.9	5.00E-05	4.50E-04
CMT627C	62.9	451.3	2.8	5.00E-05	4.50E-04
CMO291C	30.2	214.2	2.8	5.00E-05	4.50E-04
CME023C	58.0	406.5	2.8	5.00E-05	4.50E-04
CMT159C	45.4	316.7	2.8	5.00E-05	4.50E-04
CMK273C	45.0	308.6	2.8	2.00E-04	1.46E-03
CMG059C	176.8	1209.9	2.8	5.00E-05	4.50E-04
CMM145C	45.7	311.5	2.8	2.50E-04	1.75E-03
CMR346C	37.4	254.3	2.8	5.00E-05	4.50E-04

continued on next page!

Table A.6 – continued from previous page

	FPKM values			Statistical cuffdiff values	
Gene ID	**RL(-)**	**RL (+)**	**$\log_2$ (fold change)**	**p value**	**q value**
CMM060C	24.6	167.2	2.8	5.00E-05	4.50E-04
CMP106C	64.0	429.1	2.7	5.00E-05	4.50E-04
CMN290C	39.0	256.1	2.7	5.00E-05	4.50E-04
CMK174C	16.7	109.5	2.7	2.00E-04	1.46E-03
CMQ436C	54.5	356.1	2.7	5.00E-05	4.50E-04
CMJ154C	44.1	282.9	2.7	5.00E-05	4.50E-04
CMS102C	18.7	119.8	2.7	5.00E-05	4.50E-04
CMP354C	10.8	68.3	2.7	5.00E-05	4.50E-04
CMM052C	18.9	119.5	2.7	5.00E-05	4.50E-04
CMT611C	20.4	128.7	2.7	5.00E-05	4.50E-04
CMJ170C	134.7	846.4	2.7	1.05E-03	5.55E-03
CMT526C	129.4	803.5	2.6	5.00E-05	4.50E-04
CMS043C	4.2	25.8	2.6	1.15E-03	5.96E-03
CMP252C	45.5	274.8	2.6	5.00E-05	4.50E-04
CMP193C	59.3	358.2	2.6	5.00E-05	4.50E-04
CMJ142C	19.2	115.0	2.6	5.00E-05	4.50E-04
CMS361C	6.2	37.3	2.6	2.05E-03	9.36E-03
CMI162C	17.6	104.9	2.6	5.00E-05	4.50E-04
CMV241C	11.3	67.3	2.6	5.00E-05	4.50E-04
CMO012C	113.5	673.8	2.6	5.00E-05	4.50E-04
CMJ086C	44.0	259.2	2.6	5.00E-05	4.50E-04
CMT530C	79.4	458.1	2.5	5.00E-05	4.50E-04
CMA114C	120.1	692.8	2.5	5.00E-05	4.50E-04
CMV136C	10.7	61.6	2.5	5.00E-05	4.50E-04
CMR442C	44.2	251.9	2.5	5.00E-04	3.07E-03
CMI270C	19.8	111.9	2.5	5.00E-05	4.50E-04

continued on next page!

Table A.6 – continued from previous page

	FPKM values			Statistical cuffdiff values	
Gene ID	**RL(-)**	**RL (+)**	**$\log_2$ (fold change)**	**p value**	**q value**
CMN023C	225.8	1277.9	2.5	5.00E-05	4.50E-04
CMQ222C	41.8	233.6	2.5	5.00E-05	4.50E-04
CMA106C	62.2	347.2	2.5	5.00E-05	4.50E-04
CMS425C	77.6	432.4	2.5	5.00E-05	4.50E-04
CMI185C	42.1	233.8	2.5	5.00E-05	4.50E-04
CMJ305C	119.7	658.1	2.5	1.00E-04	8.17E-04
CME194C	28.2	154.7	2.5	5.00E-05	4.50E-04
CMA041C	38.8	211.4	2.4	5.00E-05	4.50E-04
CMQ246C	55.3	300.3	2.4	5.50E-04	3.32E-03
CML110C	54.9	296.9	2.4	1.00E-04	8.17E-04
CMT558C	53.2	286.7	2.4	5.00E-05	4.50E-04
CMJ201C	8.8	47.3	2.4	5.00E-04	3.07E-03
CME041C	82.1	436.4	2.4	9.50E-04	5.11E-03
CMK114C	42.8	227.0	2.4	5.00E-05	4.50E-04
CMB151C	13.8	72.9	2.4	1.60E-03	7.70E-03
CMP323C	24.4	128.1	2.4	5.00E-05	4.50E-04
CMN319C	10.1	52.8	2.4	5.00E-05	4.50E-04
CMV097C	388.0	1983.2	2.4	5.00E-05	4.50E-04
CMT410C	65.9	336.6	2.4	5.00E-05	4.50E-04
CMS429C	347.3	1757.2	2.3	1.50E-04	1.15E-03
CMR479C	60.9	308.3	2.3	5.50E-04	3.32E-03
CMS306C	329.0	1652.8	2.3	5.00E-05	4.50E-04
CML055C	12.6	63.2	2.3	5.00E-05	4.50E-04
CMT192C	19.0	95.5	2.3	5.00E-05	4.50E-04
CMG058C	44.9	225.2	2.3	5.00E-05	4.50E-04
CMM167C	56.1	278.3	2.3	5.00E-05	4.50E-04

continued on next page!

Table A.6 – continued from previous page

	FPKM values			Statistical cuffdiff values	
Gene ID	**RL(-)**	**RL (+)**	**$\log_2$ (fold change)**	**p value**	**q value**
CMS327C	16.0	79.1	2.3	5.00E-05	4.50E-04
CMG162C	400.4	1973.9	2.3	5.00E-05	4.50E-04
CMH065C	98.6	485.8	2.3	5.00E-05	4.50E-04
CML178C	89.6	441.4	2.3	5.00E-05	4.50E-04
CMI112C	121.7	599.1	2.3	5.00E-05	4.50E-04
CMK075C	20.9	102.7	2.3	1.00E-04	8.17E-04
CMT434C	49.1	240.0	2.3	5.00E-05	4.50E-04
CMM081C	23.1	112.7	2.3	5.00E-05	4.50E-04
CMV096C	740.9	3610.0	2.3	5.00E-05	4.50E-04
CMS372C	90.7	441.6	2.3	5.00E-05	4.50E-04
CMG171C	40.1	194.2	2.3	5.00E-05	4.50E-04
CMG015C	7.8	37.7	2.3	1.10E-03	5.75E-03
CMG189C	8.8	42.2	2.3	5.00E-05	4.50E-04
CMJ148C	645.3	3066.0	2.2	5.00E-05	4.50E-04
CMR317C	27.0	127.7	2.2	5.00E-05	4.50E-04
CMT172C	755.9	3569.4	2.2	1.00E-03	5.34E-03
CMK278C	25.6	120.2	2.2	5.00E-05	4.50E-04
CML079C	15.7	73.4	2.2	5.00E-05	4.50E-04
CMT330C	34.9	162.6	2.2	5.00E-05	4.50E-04
CMT137C	62.8	291.6	2.2	5.00E-05	4.50E-04
CMV155C	36.8	170.4	2.2	5.00E-05	4.50E-04
CMO212C	19.2	88.6	2.2	5.00E-05	4.50E-04
CMK131C	111.5	510.5	2.2	2.05E-03	9.36E-03
CMF094C	71.5	326.4	2.2	5.00E-05	4.50E-04
CMJ169C	33.8	153.3	2.2	5.00E-05	4.50E-04
CMC125C	18.3	82.3	2.2	5.00E-05	4.50E-04

continued on next page!

Table A.6 – continued from previous page

	FPKM values			Statistical cuffdiff values	
Gene ID	**RL(-)**	**RL (+)**	**$\log_2$ (fold change)**	**p value**	**q value**
CMR158C	35.2	158.1	2.2	5.00E-05	4.50E-04
CMM158C	456.2	2041.7	2.2	1.50E-04	1.15E-03
CME120C	80.1	357.9	2.2	5.00E-05	4.50E-04
CMP304C	26.1	116.3	2.2	5.00E-05	4.50E-04
CMF033C	86.9	384.8	2.1	1.55E-03	7.51E-03
CMR373C	89.3	394.7	2.1	5.00E-05	4.50E-04
CMH052C	12.3	53.4	2.1	5.00E-05	4.50E-04
CMN263C	14.7	63.5	2.1	5.00E-05	4.50E-04
CMQ120C	83.5	360.6	2.1	5.50E-04	3.32E-03
CMN125C	66.4	284.3	2.1	1.00E-04	8.17E-04
CMJ084C	20.0	84.7	2.1	5.00E-05	4.50E-04
CMT465C	29.4	124.5	2.1	5.00E-05	4.50E-04
CMQ255C	12.6	53.1	2.1	5.00E-05	4.50E-04
CMC063C	20.2	85.3	2.1	1.30E-03	6.56E-03
CMP227C	63.0	263.9	2.1	5.00E-05	4.50E-04
CMS232C	17.4	72.6	2.1	1.00E-04	8.17E-04
CMF178C	12.1	50.3	2.1	5.00E-05	4.50E-04
CME175C	376.7	1567.2	2.1	5.00E-05	4.50E-04
CMT453C	13.4	55.4	2.0	5.00E-05	4.50E-04
CMK085C	26.6	109.1	2.0	5.00E-05	4.50E-04
CMT412C	9.7	38.9	2.0	1.45E-03	7.14E-03
CMT538C	8.0	32.1	2.0	1.00E-04	8.17E-04
CMM276C	49.2	196.7	2.0	5.00E-05	4.50E-04
CMR004C	30.4	121.1	2.0	8.00E-04	4.46E-03
CMM214C	36.0	142.8	2.0	5.00E-05	4.50E-04
CMH047C	62.8	245.6	2.0	5.00E-05	4.50E-04

continued on next page!

Table A.6 – continued from previous page

	FPKM values			Statistical cuffdiff values	
Gene ID	**RL(-)**	**RL (+)**	**$\log_2$ (fold change)**	**p value**	**q value**
CMQ190C	405.3	1574.0	2.0	5.00E-05	4.50E-04
CMQ427C	41.0	158.9	2.0	5.00E-05	4.50E-04
CMM299C	49.0	188.9	1.9	5.00E-05	4.50E-04
CMS326C	21.5	82.3	1.9	7.50E-04	4.24E-03
CMM273C	32.5	123.9	1.9	5.00E-05	4.50E-04
CMO121C	44.3	168.7	1.9	5.00E-05	4.50E-04
CMS333C	14.4	55.0	1.9	5.00E-05	4.50E-04
CML285C	150.2	570.9	1.9	5.00E-05	4.50E-04
CMT154C	81.8	310.7	1.9	5.00E-05	4.50E-04
CMJ188C	70.0	265.0	1.9	5.00E-05	4.50E-04
CMP080C	16.4	61.9	1.9	7.50E-04	4.24E-03
CMD058C	18.4	69.6	1.9	5.00E-05	4.50E-04
CMJ233C	13.0	48.6	1.9	1.50E-03	7.33E-03
CMB050C	55.0	205.8	1.9	5.00E-05	4.50E-04
CMB018C	66.9	249.9	1.9	5.00E-05	4.50E-04
CMQ053C	44.2	164.2	1.9	5.00E-05	4.50E-04
CMQ241C	103.8	383.7	1.9	1.00E-04	8.17E-04
CMN228C	30.8	113.3	1.9	5.00E-05	4.50E-04
CMT119C	32.5	119.6	1.9	5.00E-05	4.50E-04
CMS231C	188.1	688.7	1.9	5.00E-05	4.50E-04
CMI227C	18.0	65.8	1.9	4.00E-04	2.57E-03
CMR014C	13.6	49.5	1.9	5.00E-05	4.50E-04
CMR012C	61.1	221.3	1.9	5.00E-05	4.50E-04
CME172C	22.6	81.7	1.9	5.00E-05	4.50E-04
CMH071C	68.1	246.8	1.9	1.00E-04	8.17E-04
CMQ142C	314.8	1139.5	1.9	5.00E-05	4.50E-04

continued on next page!

Table A.6 – continued from previous page

	FPKM values			Statistical cuffdiff values	
Gene ID	**RL(-)**	**RL (+)**	**$\log_2$ (fold change)**	**p value**	**q value**
CMS389C	89.8	324.4	1.9	5.00E-05	4.50E-04
CMM306C	21.2	76.3	1.8	8.00E-04	4.46E-03
CME095C	38.8	139.2	1.8	5.00E-05	4.50E-04
CMT541C	12.3	44.2	1.8	6.50E-04	3.79E-03
CMH276C	44.0	157.8	1.8	3.50E-04	2.31E-03
CML177C	37.3	133.1	1.8	1.00E-04	8.17E-04
CMP007C	137.5	490.7	1.8	5.00E-05	4.50E-04
CML339C	129.0	459.4	1.8	1.00E-04	8.17E-04
CMM212C	75.0	263.4	1.8	5.00E-05	4.50E-04
CMK151C	23.0	80.3	1.8	5.00E-05	4.50E-04
CMP271C	23.3	80.6	1.8	4.50E-04	2.83E-03
CMR052C	282.7	978.4	1.8	1.45E-03	7.14E-03
CMB094C	25.9	88.9	1.8	5.00E-05	4.50E-04
CMI248C	569.2	1957.1	1.8	5.00E-05	4.50E-04
CMG018C	9.9	33.9	1.8	7.50E-04	4.24E-03
CMQ382C	117.7	402.0	1.8	5.00E-05	4.50E-04
CMT252C	100.1	335.9	1.7	1.00E-04	8.17E-04
CMJ289C	160.7	538.5	1.7	5.00E-05	4.50E-04
CMC091C	13.0	43.5	1.7	2.00E-03	9.20E-03
CMS109C	76.2	253.6	1.7	5.00E-05	4.50E-04
CMP129C	76.9	255.9	1.7	5.00E-05	4.50E-04
CMA085C	11.0	36.4	1.7	9.50E-04	5.11E-03
CMI294C	29.4	97.5	1.7	1.40E-03	6.94E-03
CME133C	42.9	141.2	1.7	5.00E-05	4.50E-04
CMS155C	19.2	62.8	1.7	5.00E-04	3.07E-03
CMO250C	1089.2	3570.1	1.7	5.00E-05	4.50E-04

continued on next page!

Table A.6 – continued from previous page

	FPKM values			Statistical cuffdiff values	
Gene ID	**RL(-)**	**RL (+)**	**$\log_2$ (fold change)**	**p value**	**q value**
CMR238C	60.3	197.2	1.7	5.00E-05	4.50E-04
CML098C	122.8	401.5	1.7	5.00E-05	4.50E-04
CMR368C	35.0	114.2	1.7	7.00E-04	4.02E-03
CMR255C	93.8	305.8	1.7	5.00E-04	3.07E-03
CMQ172C	111.0	356.8	1.7	9.00E-04	4.90E-03
CMQ064C	64.4	206.9	1.7	5.00E-05	4.50E-04
CMM292C	13.1	41.9	1.7	3.50E-04	2.31E-03
CMA082C	128.2	408.0	1.7	1.00E-04	8.17E-04
CMM257C	81.9	258.8	1.7	1.50E-03	7.33E-03
CMR441C	62.5	197.1	1.7	1.50E-04	1.15E-03
CMR319C	109.4	344.3	1.7	5.00E-05	4.50E-04
CML202C	99.3	312.3	1.7	5.00E-05	4.50E-04
CMV132C	821.2	2579.6	1.7	5.00E-05	4.50E-04
CMT570C	98.9	310.3	1.6	5.00E-05	4.50E-04
CMG164C	13.5	42.1	1.6	3.50E-04	2.31E-03
CMH254C	452.0	1404.0	1.6	5.00E-05	4.50E-04
CMC180C	62.4	193.7	1.6	6.50E-04	3.79E-03
CMH197C	42.8	132.9	1.6	3.50E-04	2.31E-03
CMQ111C	15.9	49.2	1.6	6.50E-04	3.79E-03
CML267C	19.5	60.4	1.6	5.00E-05	4.50E-04
CMQ463C	109.6	338.9	1.6	4.00E-04	2.57E-03
CMI196C	262.9	810.3	1.6	2.50E-04	1.75E-03
CMO197C	48.3	148.7	1.6	1.00E-04	8.17E-04
CMT028C	31.5	96.9	1.6	2.50E-04	1.75E-03
CML049C	41.7	128.3	1.6	5.00E-05	4.50E-04
CMR469C	42.0	129.1	1.6	8.00E-04	4.46E-03

continued on next page!

Table A.6 – continued from previous page

	FPKM values			Statistical cuffdiff values	
Gene ID	**RL(-)**	**RL (+)**	**$\log_2$ (fold change)**	**p value**	**q value**
CMM190C	245.9	754.9	1.6	5.00E-05	4.50E-04
CMF117C	230.6	707.5	1.6	1.35E-03	6.75E-03
CMD047C	21.3	65.2	1.6	5.00E-05	4.50E-04
CMN202C	19.7	60.3	1.6	3.00E-04	2.04E-03
CMN048C	32.1	97.7	1.6	5.00E-05	4.50E-04
CME179C	63.5	190.8	1.6	5.00E-05	4.50E-04
CMR108C	54.4	163.3	1.6	5.00E-05	4.50E-04
CMJ129C	63.7	190.8	1.6	5.00E-05	4.50E-04
CMM078C	82.7	247.6	1.6	5.00E-05	4.50E-04
CML204C	56.8	169.9	1.6	5.00E-05	4.50E-04
CMV154C	24.0	71.6	1.6	2.10E-03	9.54E-03
CMT477C	53.0	158.3	1.6	1.00E-04	8.17E-04
CMV060C	19.4	57.9	1.6	5.00E-05	4.50E-04
CMK060C	119.1	353.6	1.6	5.00E-05	4.50E-04
CMX011C	157.2	466.1	1.6	5.00E-05	4.50E-04
CMT231C	63.7	188.7	1.6	5.00E-05	4.50E-04
CMI087C	83.6	247.5	1.6	1.20E-03	6.17E-03
CMI298C	61.1	179.2	1.6	5.00E-05	4.50E-04
CMS090C	128.2	375.4	1.5	5.00E-05	4.50E-04
CMH039C	141.4	413.6	1.5	6.50E-04	3.79E-03
CMH042C	55.8	163.1	1.5	5.00E-05	4.50E-04
CMM072C	15.3	44.6	1.5	1.50E-04	1.15E-03
CMT175C	169.9	494.9	1.5	5.00E-05	4.50E-04
CMF138C	33.3	96.6	1.5	5.00E-05	4.50E-04
CMJ107C	71.2	206.6	1.5	5.00E-05	4.50E-04
CMA091C	21.3	61.7	1.5	5.00E-05	4.50E-04

continued on next page!

Table A.6 – continued from previous page

	FPKM values			Statistical cuffdiff values	
Gene ID	**RL(-)**	**RL (+)**	**$\log_2$ (fold change)**	**p value**	**q value**
CMM256C	58.3	168.0	1.5	5.00E-05	4.50E-04
CMG170C	35.5	102.0	1.5	5.00E-05	4.50E-04
CMK292C	76.4	217.6	1.5	5.00E-05	4.50E-04
CMN081C	57.4	163.0	1.5	5.00E-04	3.07E-03
CMA061C	155.7	441.9	1.5	2.50E-04	1.75E-03
CMO317C	18.6	52.5	1.5	1.45E-03	7.14E-03
CMT204C	21.6	61.0	1.5	5.00E-05	4.50E-04
CMJ081C	143.8	406.3	1.5	1.30E-03	6.56E-03
CML047C	87.3	246.1	1.5	5.00E-05	4.50E-04
CMP179C	214.3	604.1	1.5	4.00E-04	2.57E-03
CMH046C	134.1	375.6	1.5	3.00E-04	2.04E-03
CMT236C	71.6	199.9	1.5	6.50E-04	3.79E-03
CMG157C	144.5	402.9	1.5	3.00E-04	2.04E-03
CMO249C	35.2	97.2	1.5	4.00E-04	2.57E-03
CMN224C	40.6	111.8	1.5	5.00E-05	4.50E-04
CMR440C	79.8	219.2	1.5	1.00E-04	8.17E-04
CMO270C	20.9	57.1	1.5	5.00E-05	4.50E-04
CMP064C	120.9	330.6	1.5	5.00E-05	4.50E-04
CMT381C	68.7	185.3	1.4	5.00E-05	4.50E-04
CMM317C	11.2	30.1	1.4	3.50E-04	2.31E-03
CMT207C	71.1	190.5	1.4	5.00E-05	4.50E-04
CMP285C	132.4	354.9	1.4	6.00E-04	3.55E-03
CMJ246C	46.5	124.3	1.4	5.00E-05	4.50E-04
CMI062C	53.5	143.0	1.4	5.00E-05	4.50E-04
CMD028C	50.2	133.1	1.4	6.00E-04	3.55E-03
CMC133C	202.6	537.6	1.4	5.00E-05	4.50E-04

continued on next page!

Table A.6 – continued from previous page

	FPKM values			Statistical cuffdiff values	
Gene ID	**RL(-)**	**RL (+)**	**$\log_2$ (fold change)**	**p value**	**q value**
CMA030C	56.7	150.3	1.4	2.00E-04	1.46E-03
CMS299C	57.1	151.1	1.4	8.50E-04	4.68E-03
CMK092C	88.3	233.5	1.4	5.00E-05	4.50E-04
CMP092C	103.7	274.0	1.4	1.50E-04	1.15E-03
CMC043C	58.6	154.9	1.4	8.50E-04	4.68E-03
CMR296C	135.0	356.4	1.4	5.00E-05	4.50E-04
CML030C	337.3	889.3	1.4	7.50E-04	4.24E-03
CMM274C	15.0	39.4	1.4	1.15E-03	5.96E-03
CMR272C	208.5	548.5	1.4	7.50E-04	4.24E-03
CMT527C	119.0	312.8	1.4	5.00E-05	4.50E-04
CMK178C	109.9	287.5	1.4	2.00E-04	1.46E-03
CMK192C	117.5	307.3	1.4	9.50E-04	5.11E-03
CMN252C	93.5	243.8	1.4	5.00E-05	4.50E-04
CMF086C	103.2	268.6	1.4	1.50E-04	1.15E-03
CMQ067C	12.5	32.4	1.4	1.65E-03	7.90E-03
CMD049C	34.8	90.2	1.4	5.00E-05	4.50E-04
CMQ281C	101.2	261.5	1.4	5.00E-05	4.50E-04
CMQ031C	85.9	220.9	1.4	9.50E-04	5.11E-03
CMP346C	285.8	731.5	1.4	5.00E-04	3.07E-03
CMD140C	189.8	484.0	1.4	1.00E-04	8.17E-04
CMN332C	148.6	377.9	1.3	1.50E-04	1.15E-03
CMD152C	619.9	1575.1	1.3	1.00E-04	8.17E-04
CMJ087C	87.4	221.6	1.3	5.50E-04	3.32E-03
CMJ121C	588.1	1486.0	1.3	5.00E-05	4.50E-04
CMJ179C	59.6	150.5	1.3	1.00E-04	8.17E-04
CMK262C	301.9	758.0	1.3	5.00E-05	4.50E-04

continued on next page!

Table A.6 – continued from previous page

	FPKM values			Statistical cuffdiff values	
Gene ID	**RL(-)**	**RL (+)**	**$\log_2$ (fold change)**	**p value**	**q value**
CMK175C	51.9	129.4	1.3	2.00E-04	1.46E-03
CMR244C	227.2	565.3	1.3	2.00E-04	1.46E-03
CMN137C	103.3	255.5	1.3	2.00E-04	1.46E-03
CMM323C	40.9	100.6	1.3	5.00E-05	4.50E-04
CMS453C	27.6	67.7	1.3	7.50E-04	4.24E-03
CMR256C	32.3	78.7	1.3	1.70E-03	8.08E-03
CMT271C	155.8	377.9	1.3	8.00E-04	4.46E-03
CMJ185C	54.8	132.8	1.3	5.00E-05	4.50E-04
CMP117C	13.8	33.5	1.3	1.50E-03	7.33E-03
CMO269C	161.0	389.3	1.3	4.00E-04	2.57E-03
CMC037C	27.8	67.1	1.3	2.00E-04	1.46E-03
CMT610C	82.7	199.5	1.3	8.00E-04	4.46E-03
CML087C	25.4	61.0	1.3	1.90E-03	8.83E-03
CMR396C	40.3	96.4	1.3	3.00E-04	2.04E-03
CMG118C	241.6	577.8	1.3	2.50E-04	1.75E-03
CMF089C	40.2	95.9	1.3	1.45E-03	7.14E-03
CMS286C	82.6	196.9	1.3	5.00E-05	4.50E-04
CMM169C	32.6	77.1	1.2	6.50E-04	3.79E-03
CMH016C	90.4	213.2	1.2	2.00E-04	1.46E-03
CMF067C	172.5	406.7	1.2	1.90E-03	8.83E-03
CMK237C	42.8	100.3	1.2	5.00E-05	4.50E-04
CMT388C	186.6	436.2	1.2	9.50E-04	5.11E-03
CMM119C	118.2	275.8	1.2	5.00E-05	4.50E-04
CMR421C	208.4	484.7	1.2	8.50E-04	4.68E-03
CMS202C	40.1	92.9	1.2	1.00E-04	8.17E-04
CMQ253C	145.2	334.8	1.2	1.90E-03	8.83E-03

continued on next page!

Table A.6 – continued from previous page

Gene ID	FPKM values		$\log_2$ (fold change)	Statistical cuffdiff values	
	RL(-)	RL (+)		p value	q value
CMR240C	65.6	151.0	1.2	1.10E-03	5.75E-03
CML088C	42.1	96.7	1.2	7.00E-04	4.02E-03
CMF062C	58.2	133.0	1.2	2.50E-04	1.75E-03
CMT083C	26.4	60.3	1.2	2.05E-03	9.36E-03
CMT476C	211.8	478.2	1.2	1.30E-03	6.56E-03
CMN210C	47.9	108.1	1.2	1.80E-03	8.44E-03
CMK224C	92.2	205.2	1.2	4.50E-04	2.83E-03
CMQ174C	55.1	122.6	1.2	1.40E-03	6.94E-03
CMM098C	32.4	72.0	1.1	5.50E-04	3.32E-03
CMJ078C	156.8	347.0	1.1	1.45E-03	7.14E-03
CMS328C	99.6	220.5	1.1	5.00E-05	4.50E-04
CMK207C	276.5	609.1	1.1	9.50E-04	5.11E-03
CMO278C	57.5	125.4	1.1	2.00E-04	1.46E-03
CMP070C	248.3	539.9	1.1	1.20E-03	6.17E-03
CMF055C	49.1	106.6	1.1	2.20E-03	9.91E-03
CMM126C	98.4	212.1	1.1	2.00E-04	1.46E-03
CMO226C	36.2	77.8	1.1	3.50E-04	2.31E-03
CMD067C	249.6	535.3	1.1	8.00E-04	4.46E-03
CMD100C	72.9	156.2	1.1	2.50E-04	1.75E-03
CMB077C	183.0	391.2	1.1	3.50E-04	2.31E-03
CMJ182C	47.5	101.4	1.1	1.75E-03	8.27E-03
CMC064C	145.2	309.7	1.1	1.25E-03	6.36E-03
CMK206C	36.1	77.1	1.1	2.05E-03	9.36E-03
CMN260C	142.6	304.0	1.1	8.50E-04	4.68E-03
CME134C	30.2	64.4	1.1	2.15E-03	9.73E-03
CMH038C	250.0	532.3	1.1	5.50E-04	3.32E-03

continued on next page!

Table A.6 – continued from previous page

	FPKM values			Statistical cuffdiff values	
Gene ID	**RL(-)**	**RL (+)**	**$\log_2$ (fold change)**	**p value**	**q value**
CMP067C	81.2	172.8	1.1	9.50E-04	5.11E-03
CMJ055C	62.0	131.5	1.1	5.50E-04	3.32E-03
CMF147C	54.6	115.6	1.1	2.10E-03	9.54E-03
CMH177C	137.2	289.9	1.1	2.00E-04	1.46E-03
CMQ355C	139.8	294.9	1.1	1.05E-03	5.55E-03
CMJ126C	150.6	316.3	1.1	6.00E-04	3.55E-03
CMT620C	22.3	46.8	1.1	4.00E-04	2.57E-03
CMS125C	97.6	202.8	1.1	2.00E-04	1.46E-03
CMG051C	60.2	124.1	1.0	2.00E-04	1.46E-03
CMI204C	107.3	221.4	1.0	9.50E-04	5.11E-03
CMR067C	42.9	87.9	1.0	1.75E-03	8.27E-03
CMQ389C	103.8	212.8	1.0	6.50E-04	3.79E-03
CMB118C	39.8	81.6	1.0	1.10E-03	5.75E-03
CMK088C	81.2	166.2	1.0	1.70E-03	8.08E-03
CMP142C	34.8	71.1	1.0	2.15E-03	9.73E-03
CMM277C	102.4	209.2	1.0	7.50E-04	4.24E-03
CMF133C	49.8	101.5	1.0	6.50E-04	3.79E-03
CMT317C	49.3	99.7	1.0	1.35E-03	6.75E-03
CMC039C	90.0	180.7	1.0	2.15E-03	9.73E-03
CMQ194C	205.3	102.7	-1.0	1.30E-03	6.56E-03
CMS040C	259.2	129.5	-1.0	5.00E-04	3.07E-03
CMT121C	186.8	93.3	-1.0	8.50E-04	4.68E-03
CMS105C	181.0	90.3	-1.0	1.80E-03	8.44E-03
CME126C	143.4	71.5	-1.0	5.50E-04	3.32E-03
CMQ063C	497.5	247.9	-1.0	1.45E-03	7.14E-03
CMB013C	23.6	11.7	-1.0	1.80E-03	8.44E-03

continued on next page!

Table A.6 – continued from previous page

	FPKM values			Statistical cuffdiff values	
Gene ID	**RL(-)**	**RL (+)**	**$\log_2$ (fold change)**	**p value**	**q value**
CMT437C	409.4	203.5	-1.0	6.50E-04	3.79E-03
CMP099C	300.6	149.3	-1.0	3.00E-04	2.04E-03
CMG190C	298.1	148.1	-1.0	1.25E-03	6.36E-03
CMI201C	405.1	200.9	-1.0	1.25E-03	6.36E-03
CMA140C	80.9	40.1	-1.0	3.50E-04	2.31E-03
CMM252C	153.2	75.9	-1.0	1.85E-03	8.64E-03
CMI249C	267.9	132.6	-1.0	5.50E-04	3.32E-03
CMT180C	277.8	137.5	-1.0	9.00E-04	4.90E-03
CMC172C	164.3	81.3	-1.0	2.50E-04	1.75E-03
CMM153C	272.5	134.6	-1.0	7.00E-04	4.02E-03
CMN215C	199.9	98.6	-1.0	1.50E-04	1.15E-03
CMG211C	182.8	90.2	-1.0	3.50E-04	2.31E-03
CMP223C	379.5	187.2	-1.0	7.00E-04	4.02E-03
CMP054C	56.0	27.6	-1.0	4.50E-04	2.83E-03
CMA130C	87.2	42.9	-1.0	1.40E-03	6.94E-03
CMN029C	60.9	30.0	-1.0	1.85E-03	8.64E-03
CMQ456C	208.9	102.8	-1.0	5.50E-04	3.32E-03
CMC077C	218.4	107.5	-1.0	4.00E-04	2.57E-03
CMR474C	113.8	56.0	-1.0	6.50E-04	3.79E-03
CMB120C	184.8	90.9	-1.0	5.50E-04	3.32E-03
CMI032C	300.5	147.6	-1.0	4.00E-04	2.57E-03
CMT433C	189.4	93.0	-1.0	8.50E-04	4.68E-03
CML130C	131.7	64.7	-1.0	1.60E-03	7.70E-03
CMM290C	389.0	190.9	-1.0	4.00E-04	2.57E-03
CMA013C	506.6	248.6	-1.0	6.50E-04	3.79E-03
CMM016C	50.0	24.5	-1.0	8.00E-04	4.46E-03

continued on next page!

Table A.6 – continued from previous page

	FPKM values			Statistical cuffdiff values	
Gene ID	**RL(-)**	**RL (+)**	**$\log_2$ (fold change)**	**p value**	**q value**
CME162C	192.4	94.3	-1.0	1.25E-03	6.36E-03
CMJ232C	85.1	41.7	-1.0	1.15E-03	5.96E-03
CMS114C	80.4	39.4	-1.0	2.50E-04	1.75E-03
CMK288C	223.2	109.4	-1.0	2.10E-03	9.54E-03
CMN157C	223.6	109.6	-1.0	7.00E-04	4.02E-03
CML293C	122.5	59.9	-1.0	1.00E-04	8.17E-04
CMI299C	402.7	197.1	-1.0	1.40E-03	6.94E-03
CML069C	103.2	50.4	-1.0	1.50E-04	1.15E-03
CMM006C	229.5	112.2	-1.0	2.50E-04	1.75E-03
CMI217C	160.7	78.4	-1.0	1.40E-03	6.94E-03
CMO161C	302.8	147.7	-1.0	2.50E-04	1.75E-03
CMR081C	27.3	13.3	-1.0	8.50E-04	4.68E-03
CMQ097C	98.6	48.1	-1.0	3.00E-04	2.04E-03
CMK119C	88.7	43.2	-1.0	5.50E-04	3.32E-03
CMH204C	155.5	75.8	-1.0	4.50E-04	2.83E-03
CMO232C	294.3	143.4	-1.0	2.50E-04	1.75E-03
CMT447C	9725.1	4733.7	-1.0	7.00E-04	4.02E-03
CMC027C	251.8	122.5	-1.0	3.50E-04	2.31E-03
CMM087C	338.1	164.5	-1.0	3.50E-04	2.31E-03
CMA025C	328.3	159.6	-1.0	8.50E-04	4.68E-03
CMK012C	769.4	373.2	-1.0	1.85E-03	8.64E-03
CML128C	105.4	51.1	-1.0	2.50E-04	1.75E-03
CMM320C	152.0	73.7	-1.0	2.50E-04	1.75E-03
CMS192C	221.1	107.1	-1.0	1.10E-03	5.75E-03
CML126C	231.8	112.3	-1.0	2.50E-04	1.75E-03
CMS494C	339.3	164.3	-1.0	1.55E-03	7.51E-03

continued on next page!

Table A.6 – continued from previous page

	FPKM values			Statistical cuffdiff values	
Gene ID	**RL(-)**	**RL (+)**	**$\log_2$ (fold change)**	**p value**	**q value**
CMT297C	151.0	73.0	-1.0	1.50E-04	1.15E-03
CMH073C	121.4	58.7	-1.0	1.15E-03	5.96E-03
CMS015C	551.4	266.4	-1.0	1.90E-03	8.83E-03
CMR041C	141.0	68.1	-1.0	4.50E-04	2.83E-03
CMB042C	188.2	90.9	-1.1	3.50E-04	2.31E-03
CMM220C	142.7	68.9	-1.1	1.00E-04	8.17E-04
CME111C	596.5	287.5	-1.1	9.50E-04	5.11E-03
CMI278C	85.5	41.2	-1.1	3.50E-04	2.31E-03
CMS484C	96.8	46.6	-1.1	2.50E-04	1.75E-03
CMT281C	106.9	51.5	-1.1	1.50E-04	1.15E-03
CMT130C	101.0	48.6	-1.1	2.00E-04	1.46E-03
CMD007C	137.1	66.0	-1.1	5.50E-04	3.32E-03
CML102C	256.4	123.2	-1.1	5.00E-04	3.07E-03
CMR174C	434.6	208.9	-1.1	5.50E-04	3.32E-03
CMQ429C	160.3	77.0	-1.1	2.15E-03	9.73E-03
CMR226C	409.9	196.8	-1.1	2.50E-04	1.75E-03
CMS152C	33.3	16.0	-1.1	1.00E-04	8.17E-04
CMS486C	125.9	60.4	-1.1	2.00E-04	1.46E-03
CMC020C	293.7	140.9	-1.1	1.75E-03	8.27E-03
CMP274C	164.1	78.6	-1.1	1.50E-04	1.15E-03
CMB070C	142.6	68.3	-1.1	9.00E-04	4.90E-03
CMR210C	264.2	126.2	-1.1	1.50E-04	1.15E-03
CMS469C	53.2	25.4	-1.1	3.50E-04	2.31E-03
CMH158C	237.1	113.1	-1.1	5.00E-05	4.50E-04
CMB029C	175.6	83.7	-1.1	6.00E-04	3.55E-03
CMK109C	138.8	66.1	-1.1	7.50E-04	4.24E-03

continued on next page!

Table A.6 – continued from previous page

	FPKM values			Statistical cuffdiff values	
Gene ID	**RL(-)**	**RL (+)**	**$\log_2$ (fold change)**	**p value**	**q value**
CMO181C	555.7	264.3	-1.1	9.50E-04	5.11E-03
CMK185C	218.5	103.9	-1.1	6.00E-04	3.55E-03
CMH049C	252.6	120.1	-1.1	3.00E-04	2.04E-03
CMM002C	295.3	140.3	-1.1	1.00E-04	8.17E-04
CMH237C	334.2	158.8	-1.1	4.00E-04	2.57E-03
CMT529C	131.3	62.4	-1.1	5.00E-05	4.50E-04
CMG016C	50.1	23.8	-1.1	1.00E-04	8.17E-04
CMS236C	137.4	65.2	-1.1	3.50E-04	2.31E-03
CMR159C	249.5	118.3	-1.1	8.00E-04	4.46E-03
CMR309C	257.7	122.1	-1.1	2.00E-04	1.46E-03
CMB074C	323.9	153.4	-1.1	1.15E-03	5.96E-03
CMT548C	140.3	66.4	-1.1	2.50E-04	1.75E-03
CMO058C	188.9	89.4	-1.1	1.50E-04	1.15E-03
CMB039C	126.9	60.0	-1.1	3.50E-04	2.31E-03
CMQ343C	78.9	37.3	-1.1	5.00E-04	3.07E-03
CMT333C	201.2	94.9	-1.1	1.10E-03	5.75E-03
CMT090C	111.0	52.2	-1.1	1.00E-04	8.17E-04
CMM201C	141.3	66.4	-1.1	1.00E-04	8.17E-04
CMN288C	142.7	67.0	-1.1	1.50E-04	1.15E-03
CMR168C	293.1	137.5	-1.1	5.50E-04	3.32E-03
CMM325C	167.2	78.4	-1.1	1.00E-04	8.17E-04
CMF022C	296.7	139.1	-1.1	5.00E-05	4.50E-04
CMS041C	140.7	65.9	-1.1	4.00E-04	2.57E-03
CMS330C	193.1	90.4	-1.1	4.50E-04	2.83E-03
CMJ136C	66.2	31.0	-1.1	2.00E-04	1.46E-03
CMI229C	37.7	17.7	-1.1	4.00E-04	2.57E-03

continued on next page!

Table A.6 – continued from previous page

	FPKM values			Statistical cuffdiff values	
Gene ID	**RL(-)**	**RL (+)**	**$\log_2$ (fold change)**	**p value**	**q value**
CMD137C	330.9	154.9	-1.1	6.50E-04	3.79E-03
CMH111C	231.9	108.5	-1.1	2.50E-04	1.75E-03
CMS344C	193.7	90.6	-1.1	5.00E-05	4.50E-04
CMH195C	48.9	22.9	-1.1	2.00E-04	1.46E-03
CMM147C	257.7	120.5	-1.1	5.00E-05	4.50E-04
CMP288C	81.7	38.2	-1.1	5.50E-04	3.32E-03
CMI207C	150.4	70.3	-1.1	2.50E-04	1.75E-03
CMR468C	63.9	29.8	-1.1	1.00E-04	8.17E-04
CMS401C	231.0	107.8	-1.1	5.00E-05	4.50E-04
CMI029C	241.9	112.9	-1.1	1.50E-04	1.15E-03
CMS150C	162.9	75.9	-1.1	1.00E-04	8.17E-04
CMT160C	324.6	151.1	-1.1	2.00E-04	1.46E-03
CMO283C	60.9	28.3	-1.1	2.00E-04	1.46E-03
CMT134C	93.5	43.5	-1.1	1.00E-04	8.17E-04
CMT566C	57.2	26.6	-1.1	2.00E-04	1.46E-03
CMG036C	267.6	124.2	-1.1	1.25E-03	6.36E-03
CMH157C	84.5	39.2	-1.1	2.00E-03	9.20E-03
CMS034C	165.9	76.9	-1.1	2.50E-04	1.75E-03
CMG124C	234.6	108.5	-1.1	5.00E-05	4.50E-04
CMN167C	198.8	91.9	-1.1	3.00E-04	2.04E-03
CMT199C	341.6	157.9	-1.1	2.50E-04	1.75E-03
CMS178C	47.6	22.0	-1.1	2.50E-04	1.75E-03
CMG108C	348.0	160.5	-1.1	5.50E-04	3.32E-03
CMM177C	119.3	55.0	-1.1	2.00E-04	1.46E-03
CMT169C	166.7	76.8	-1.1	5.00E-05	4.50E-04
CMI288C	57.7	26.5	-1.1	4.00E-04	2.57E-03

continued on next page!

Table A.6 – continued from previous page

	FPKM values			Statistical cuffdiff values	
Gene ID	**RL(-)**	**RL (+)**	**$\log_2$ (fold change)**	**p value**	**q value**
CMD181C	187.8	86.3	-1.1	5.00E-05	4.50E-04
CMT325C	229.2	105.2	-1.1	1.00E-04	8.17E-04
CMK134C	219.9	100.8	-1.1	4.00E-04	2.57E-03
CMR203C	91.0	41.7	-1.1	5.00E-04	3.07E-03
CMS273C	372.3	170.5	-1.1	3.50E-04	2.31E-03
CMT078C	92.9	42.5	-1.1	1.50E-04	1.15E-03
CMN096C	84.2	38.6	-1.1	5.00E-05	4.50E-04
CMP309C	49.1	22.4	-1.1	2.50E-04	1.75E-03
CMF084C	354.9	162.2	-1.1	2.10E-03	9.54E-03
CMN212C	24.0	11.0	-1.1	1.60E-03	7.70E-03
CMS067C	264.1	120.6	-1.1	5.00E-05	4.50E-04
CMS493C	199.2	90.9	-1.1	2.00E-04	1.46E-03
CMS120C	195.3	89.0	-1.1	6.50E-04	3.79E-03
CMP210C	312.3	142.4	-1.1	5.00E-05	4.50E-04
CMA011C	79.4	36.2	-1.1	1.50E-04	1.15E-03
CMT522C	156.9	71.5	-1.1	1.00E-04	8.17E-04
CMR064C	97.7	44.5	-1.1	2.50E-04	1.75E-03
CMC051C	252.8	114.9	-1.1	8.00E-04	4.46E-03
CMT563C	137.8	62.6	-1.1	2.50E-04	1.75E-03
CMM245C	31.9	14.5	-1.1	1.00E-04	8.17E-04
CMN131C	174.6	79.2	-1.1	1.00E-04	8.17E-04
CMT489C	261.7	118.6	-1.1	9.50E-04	5.11E-03
CMN162C	228.3	103.1	-1.1	1.00E-04	8.17E-04
CMG103C	408.9	184.6	-1.1	1.70E-03	8.08E-03
CMS194C	585.3	264.3	-1.1	4.00E-04	2.57E-03
CMH174C	86.6	39.0	-1.1	5.00E-05	4.50E-04

continued on next page!

Table A.6 – continued from previous page

	FPKM values			Statistical cuffdiff values	
Gene ID	**RL(-)**	**RL (+)**	**$\log_2$ (fold change)**	**p value**	**q value**
CMB082C	44.1	19.9	-1.2	4.00E-04	2.57E-03
CMI152C	404.5	182.1	-1.2	5.00E-05	4.50E-04
CMM335C	206.9	93.2	-1.2	3.00E-04	2.04E-03
CMO347C	249.8	112.4	-1.2	5.50E-04	3.32E-03
CMM108C	338.0	151.3	-1.2	1.80E-03	8.44E-03
CML100C	279.0	124.9	-1.2	4.50E-04	2.83E-03
CML095C	50.6	22.6	-1.2	6.50E-04	3.79E-03
CMP096C	473.6	211.9	-1.2	5.50E-04	3.32E-03
CMQ103C	353.2	158.0	-1.2	6.50E-04	3.79E-03
CMK122C	321.9	143.9	-1.2	5.00E-05	4.50E-04
CMF035C	166.0	74.2	-1.2	4.50E-04	2.83E-03
CMB142C	205.1	91.6	-1.2	2.00E-04	1.46E-03
CMG027C	108.2	48.3	-1.2	7.00E-04	4.02E-03
CMM103C	123.4	55.0	-1.2	2.00E-04	1.46E-03
CMI065C	224.7	100.2	-1.2	1.50E-04	1.15E-03
CMN179C	121.3	54.1	-1.2	1.50E-04	1.15E-03
CMJ030C	28.7	12.8	-1.2	1.35E-03	6.75E-03
CMT537C	271.8	121.1	-1.2	1.00E-04	8.17E-04
CMC070C	105.9	47.1	-1.2	5.00E-05	4.50E-04
CMR484C	42.8	19.0	-1.2	4.50E-04	2.83E-03
CMM170C	116.0	51.5	-1.2	5.00E-04	3.07E-03
CMS079C	353.2	156.7	-1.2	5.00E-05	4.50E-04
CMT104C	160.5	71.2	-1.2	5.00E-05	4.50E-04
CMQ279C	259.3	114.9	-1.2	5.00E-05	4.50E-04
CMH264C	58.0	25.7	-1.2	5.00E-05	4.50E-04
CMS076C	189.9	83.9	-1.2	5.00E-05	4.50E-04

continued on next page!

Table A.6 – continued from previous page

	FPKM values			Statistical cuffdiff values	
Gene ID	**RL(-)**	**RL (+)**	**$\log_2$ (fold change)**	**p value**	**q value**
CMJ015C	149.3	65.9	-1.2	5.00E-05	4.50E-04
CMF179C	80.2	35.3	-1.2	1.50E-04	1.15E-03
CMS193C	262.4	115.6	-1.2	5.00E-05	4.50E-04
CMS456C	305.9	134.7	-1.2	1.50E-04	1.15E-03
CMO238C	105.8	46.6	-1.2	5.00E-05	4.50E-04
CMD034C	256.5	112.9	-1.2	2.00E-04	1.46E-03
CMO044C	125.7	55.3	-1.2	5.00E-05	4.50E-04
CMN222C	223.8	98.4	-1.2	5.50E-04	3.32E-03
CMT147C	199.0	87.5	-1.2	5.00E-05	4.50E-04
CMQ073C	350.1	153.6	-1.2	9.50E-04	5.11E-03
CMQ347C	120.5	52.9	-1.2	5.00E-05	4.50E-04
CMI030C	61.2	26.8	-1.2	1.00E-04	8.17E-04
CME112C	176.5	77.3	-1.2	5.00E-05	4.50E-04
CMA093C	80.1	35.0	-1.2	1.00E-04	8.17E-04
CMT373C	295.0	129.0	-1.2	4.00E-04	2.57E-03
CMS180C	362.3	158.3	-1.2	9.00E-04	4.90E-03
CMO037C	102.9	44.9	-1.2	5.00E-05	4.50E-04
CMP149C	400.1	174.8	-1.2	5.00E-04	3.07E-03
CMP118C	220.3	96.1	-1.2	6.00E-04	3.55E-03
CMT278C	155.3	67.6	-1.2	5.00E-05	4.50E-04
CMG006C	103.0	44.8	-1.2	1.50E-04	1.15E-03
CML323C	516.0	224.2	-1.2	1.50E-03	7.33E-03
CMS054C	244.9	106.4	-1.2	5.00E-05	4.50E-04
CMN062C	296.8	128.8	-1.2	5.00E-05	4.50E-04
CMH165C	27.0	11.7	-1.2	1.55E-03	7.51E-03
CMT511C	76.8	33.2	-1.2	5.00E-05	4.50E-04

continued on next page!

Table A.6 – continued from previous page

	FPKM values			Statistical cuffdiff values	
Gene ID	**RL(-)**	**RL (+)**	**$\log_2$ (fold change)**	**p value**	**q value**
CMD010C	177.2	76.7	-1.2	2.50E-04	1.75E-03
CMC102C	96.9	41.9	-1.2	5.00E-05	4.50E-04
CML211C	521.2	224.9	-1.2	2.00E-03	9.20E-03
CMG063C	166.3	71.8	-1.2	1.00E-04	8.17E-04
CMS281C	263.9	113.8	-1.2	1.00E-04	8.17E-04
CMR399C	130.1	56.0	-1.2	7.00E-04	4.02E-03
CML068C	252.8	108.7	-1.2	5.00E-05	4.50E-04
CMN143C	201.3	86.5	-1.2	5.00E-05	4.50E-04
CMN118C	223.9	96.2	-1.2	2.00E-04	1.46E-03
CMG210C	536.3	230.4	-1.2	5.00E-05	4.50E-04
CMQ334C	197.9	85.0	-1.2	5.00E-05	4.50E-04
CMB027C	113.5	48.7	-1.2	1.00E-04	8.17E-04
CMN206C	120.1	51.5	-1.2	5.00E-05	4.50E-04
CMG203C	189.5	81.2	-1.2	1.50E-04	1.15E-03
CMG044C	80.2	34.3	-1.2	5.00E-05	4.50E-04
CMN286C	478.3	204.6	-1.2	1.70E-03	8.08E-03
CMT191C	187.4	80.1	-1.2	5.00E-05	4.50E-04
CMH034C	216.2	92.4	-1.2	3.00E-04	2.04E-03
CMT195C	320.7	137.1	-1.2	4.00E-04	2.57E-03
CMQ393C	129.5	55.3	-1.2	1.00E-04	8.17E-04
CMJ160C	1161.1	496.0	-1.2	2.50E-04	1.75E-03
CMK297C	160.6	68.6	-1.2	5.00E-05	4.50E-04
CMH268C	163.0	69.6	-1.2	8.50E-04	4.68E-03
CMS168C	166.9	71.2	-1.2	4.00E-04	2.57E-03
CMP294C	277.3	118.3	-1.2	5.00E-05	4.50E-04
CMB113C	75.3	32.1	-1.2	5.00E-05	4.50E-04

continued on next page!

Table A.6 – continued from previous page

	FPKM values			Statistical cuffdiff values	
Gene ID	**RL(-)**	**RL (+)**	**$\log_2$ (fold change)**	**p value**	**q value**
CMM179C	245.1	104.5	-1.2	5.00E-04	3.07E-03
CMQ462C	309.5	131.8	-1.2	5.00E-05	4.50E-04
CMI179C	110.6	47.1	-1.2	5.00E-05	4.50E-04
CMM241C	316.8	134.9	-1.2	1.50E-04	1.15E-03
CMH242C	52.7	22.4	-1.2	5.00E-05	4.50E-04
CMS303C	127.4	54.2	-1.2	5.00E-05	4.50E-04
CMF092C	514.7	218.5	-1.2	8.50E-04	4.68E-03
CMC017C	75.0	31.8	-1.2	5.00E-05	4.50E-04
CMK110C	149.8	63.5	-1.2	5.00E-05	4.50E-04
CMJ196C	91.7	38.8	-1.2	5.00E-05	4.50E-04
CMS179C	686.3	290.1	-1.2	5.00E-04	3.07E-03
CMT501C	134.7	56.9	-1.2	5.00E-05	4.50E-04
CMP110C	752.3	317.4	-1.2	1.25E-03	6.36E-03
CMN139C	175.5	74.0	-1.2	1.00E-04	8.17E-04
CMC182C	25.4	10.7	-1.2	5.00E-05	4.50E-04
CMO214C	60.3	25.3	-1.2	1.00E-04	8.17E-04
CMO056C	297.1	124.9	-1.2	5.00E-04	3.07E-03
CMR253C	97.6	40.9	-1.3	5.00E-05	4.50E-04
CMA054C	196.6	82.4	-1.3	1.50E-04	1.15E-03
CMS218C	215.7	90.3	-1.3	1.00E-04	8.17E-04
CMB092C	140.8	59.0	-1.3	5.00E-05	4.50E-04
CMA068C	311.3	130.3	-1.3	5.00E-05	4.50E-04
CMT616C	280.7	117.4	-1.3	5.00E-05	4.50E-04
CMR349C	92.8	38.7	-1.3	5.00E-05	4.50E-04
CMI301C	185.4	77.2	-1.3	5.00E-05	4.50E-04
CMH156C	236.8	98.5	-1.3	5.00E-05	4.50E-04

continued on next page!

Table A.6 – continued from previous page

	FPKM values			Statistical cuffdiff values	
Gene ID	**RL(-)**	**RL (+)**	**$\log_2$ (fold change)**	**p value**	**q value**
CMH110C	30.4	12.6	-1.3	5.00E-04	3.07E-03
CMR428C	199.3	82.8	-1.3	1.00E-04	8.17E-04
CMP325C	58.9	24.5	-1.3	5.00E-05	4.50E-04
CMG056C	146.9	60.9	-1.3	5.00E-05	4.50E-04
CMO265C	123.4	51.0	-1.3	2.00E-04	1.46E-03
CMO285C	322.8	133.5	-1.3	4.00E-04	2.57E-03
CMR472C	377.4	156.1	-1.3	1.50E-04	1.15E-03
CMA053C	33.3	13.8	-1.3	1.00E-04	8.17E-04
CMD057C	403.3	166.7	-1.3	5.00E-05	4.50E-04
CML136C	83.5	34.5	-1.3	5.00E-05	4.50E-04
CMO152C	314.2	129.6	-1.3	5.00E-05	4.50E-04
CMO186C	414.4	171.0	-1.3	5.00E-05	4.50E-04
CMI096C	198.0	81.7	-1.3	2.50E-04	1.75E-03
CMS187C	362.2	149.3	-1.3	1.50E-04	1.15E-03
CMA023C	781.1	321.9	-1.3	1.50E-03	7.33E-03
CMT550C	101.8	41.9	-1.3	3.00E-04	2.04E-03
CMI300C	359.0	147.8	-1.3	5.00E-05	4.50E-04
CMI007C	106.4	43.8	-1.3	5.00E-05	4.50E-04
CMN279C	801.2	329.7	-1.3	5.00E-05	4.50E-04
CMQ418C	381.4	156.9	-1.3	7.50E-04	4.24E-03
CMF017C	1981.0	812.5	-1.3	1.00E-04	8.17E-04
CMP188C	98.3	40.2	-1.3	8.50E-04	4.68E-03
CMS297C	52.5	21.4	-1.3	5.00E-05	4.50E-04
CMM331C	178.9	73.0	-1.3	5.00E-05	4.50E-04
CMP100C	98.5	40.2	-1.3	2.00E-04	1.46E-03
CMG010C	270.9	110.4	-1.3	5.00E-05	4.50E-04

continued on next page!

Table A.6 – continued from previous page

	FPKM values			Statistical cuffdiff values	
Gene ID	**RL(-)**	**RL (+)**	**$\log_2$ (fold change)**	**p value**	**q value**
CMO203C	77.1	31.4	-1.3	5.00E-05	4.50E-04
CMB037C	39.6	16.1	-1.3	5.00E-05	4.50E-04
CMS490C	851.3	346.4	-1.3	7.00E-04	4.02E-03
CMC074C	535.8	217.8	-1.3	1.55E-03	7.51E-03
CML160C	577.1	234.5	-1.3	5.00E-05	4.50E-04
CML176C	578.3	234.9	-1.3	5.50E-04	3.32E-03
CMQ324C	56.8	23.1	-1.3	5.00E-05	4.50E-04
CML289C	130.6	53.0	-1.3	5.00E-05	4.50E-04
CML226C	466.1	188.7	-1.3	5.00E-04	3.07E-03
CMI250C	254.7	102.9	-1.3	5.00E-05	4.50E-04
CMC068C	975.3	394.1	-1.3	8.00E-04	4.46E-03
CME181C	506.7	204.5	-1.3	8.00E-04	4.46E-03
CMA017C	255.1	102.9	-1.3	5.00E-05	4.50E-04
CMN183C	787.6	316.3	-1.3	5.00E-05	4.50E-04
CMR173C	247.8	99.5	-1.3	5.00E-05	4.50E-04
CMK228C	48.3	19.4	-1.3	1.00E-04	8.17E-04
CMD080C	258.5	103.6	-1.3	1.50E-04	1.15E-03
CMF168C	173.6	69.5	-1.3	5.00E-05	4.50E-04
CMP273C	102.5	41.0	-1.3	2.00E-04	1.46E-03
CMR415C	49.4	19.8	-1.3	5.00E-05	4.50E-04
CMN204C	312.0	124.8	-1.3	1.00E-04	8.17E-04
CMF039C	613.8	245.3	-1.3	1.00E-04	8.17E-04
CME104C	75.8	30.3	-1.3	5.00E-05	4.50E-04
CMT046C	344.7	137.7	-1.3	4.00E-04	2.57E-03
CMG009C	118.8	47.4	-1.3	5.00E-05	4.50E-04
CMS441C	297.5	118.7	-1.3	5.00E-05	4.50E-04

continued on next page!

Table A.6 – continued from previous page

	FPKM values			Statistical cuffdiff values	
Gene ID	**RL(-)**	**RL (+)**	**$\log_2$ (fold change)**	**p value**	**q value**
CMJ064C	191.7	76.4	-1.3	1.50E-04	1.15E-03
CMQ399C	679.9	271.1	-1.3	2.00E-04	1.46E-03
CMQ352C	62.1	24.7	-1.3	5.00E-05	4.50E-04
CMH074C	247.2	98.5	-1.3	1.50E-04	1.15E-03
CMM311C	184.2	73.4	-1.3	5.00E-05	4.50E-04
CMK221C	122.4	48.7	-1.3	7.00E-04	4.02E-03
CMI044C	585.7	233.0	-1.3	5.00E-05	4.50E-04
CMA119C	114.1	45.4	-1.3	5.00E-05	4.50E-04
CMG193C	116.6	46.4	-1.3	2.50E-04	1.75E-03
CMH216C	461.0	183.0	-1.3	5.00E-04	3.07E-03
CMH231C	144.7	57.4	-1.3	5.00E-05	4.50E-04
CMH155C	175.1	69.4	-1.3	4.00E-04	2.57E-03
CMR344C	181.6	71.9	-1.3	5.00E-05	4.50E-04
CMG117C	192.6	76.3	-1.3	5.00E-05	4.50E-04
CML192C	80.2	31.7	-1.3	8.50E-04	4.68E-03
CMF182C	115.4	45.7	-1.3	5.00E-05	4.50E-04
CMQ028C	79.0	31.2	-1.3	5.00E-05	4.50E-04
CMS348C	671.1	265.1	-1.3	7.50E-04	4.24E-03
CMR032C	285.8	112.7	-1.3	5.00E-05	4.50E-04
CMS176C	290.4	114.5	-1.3	5.00E-05	4.50E-04
CML135C	346.0	136.2	-1.3	1.50E-04	1.15E-03
CMR470C	175.7	69.1	-1.3	1.00E-04	8.17E-04
CMM291C	168.8	66.4	-1.3	5.00E-05	4.50E-04
CMT185C	67.8	26.6	-1.4	5.00E-05	4.50E-04
CMK217C	297.6	116.5	-1.4	2.00E-04	1.46E-03
CMD055C	485.9	190.3	-1.4	2.50E-04	1.75E-03

continued on next page!

Table A.6 – continued from previous page

	FPKM values			Statistical cuffdiff values	
Gene ID	**RL(-)**	**RL (+)**	**$\log_2$ (fold change)**	**p value**	**q value**
CMH245C	198.7	77.8	-1.4	1.50E-04	1.15E-03
CMD144C	140.5	54.9	-1.4	5.00E-05	4.50E-04
CMI098C	111.2	43.4	-1.4	5.00E-05	4.50E-04
CMM024C	432.8	169.0	-1.4	5.00E-05	4.50E-04
CMK182C	420.2	164.0	-1.4	1.30E-03	6.56E-03
CMP267C	178.8	69.8	-1.4	5.00E-05	4.50E-04
CMQ441C	158.7	61.8	-1.4	5.00E-05	4.50E-04
CMC032C	175.2	68.1	-1.4	5.00E-05	4.50E-04
CMT461C	218.2	84.7	-1.4	5.00E-05	4.50E-04
CMR433C	68.1	26.4	-1.4	5.00E-05	4.50E-04
CMI106C	158.6	61.5	-1.4	5.00E-05	4.50E-04
CMJ050C	342.4	132.5	-1.4	2.00E-04	1.46E-03
CMH101C	116.5	45.0	-1.4	5.00E-05	4.50E-04
CMR018C	55.4	21.4	-1.4	5.00E-05	4.50E-04
CMS435C	169.5	65.2	-1.4	5.00E-05	4.50E-04
CMP021C	112.7	43.3	-1.4	5.00E-05	4.50E-04
CMF063C	172.0	66.1	-1.4	5.00E-05	4.50E-04
CMO097C	379.0	145.1	-1.4	5.00E-05	4.50E-04
CMN199C	142.3	54.4	-1.4	5.00E-05	4.50E-04
CMA045C	132.2	50.5	-1.4	5.00E-05	4.50E-04
CMR139C	52.9	20.2	-1.4	5.00E-05	4.50E-04
CMG153C	300.4	114.6	-1.4	5.00E-05	4.50E-04
CMT071C	520.9	198.5	-1.4	3.00E-04	2.04E-03
CMT291C	489.2	186.1	-1.4	5.00E-05	4.50E-04
CMR447C	99.2	37.7	-1.4	5.00E-05	4.50E-04
CMJ230C	112.5	42.8	-1.4	5.00E-05	4.50E-04

continued on next page!

Table A.6 – continued from previous page

	FPKM values			Statistical cuffdiff values	
Gene ID	**RL(-)**	**RL (+)**	**$\log_2$ (fold change)**	**p value**	**q value**
CMM102C	191.1	72.6	-1.4	1.50E-04	1.15E-03
CMN156C	819.8	311.4	-1.4	1.00E-03	5.34E-03
CMN058C	109.0	41.4	-1.4	5.00E-05	4.50E-04
CMF060C	34.2	13.0	-1.4	5.00E-05	4.50E-04
CMB038C	153.0	57.9	-1.4	5.00E-05	4.50E-04
CMH106C	33.5	12.7	-1.4	5.00E-05	4.50E-04
CMB095C	75.9	28.7	-1.4	5.00E-05	4.50E-04
CMG180C	40.8	15.4	-1.4	5.00E-05	4.50E-04
CMN046C	141.6	53.3	-1.4	1.00E-04	8.17E-04
CMD074C	510.5	191.6	-1.4	5.00E-05	4.50E-04
CMD125C	181.3	67.9	-1.4	5.00E-05	4.50E-04
CMS249C	298.7	111.8	-1.4	1.00E-04	8.17E-04
CMK157C	179.0	66.8	-1.4	5.00E-05	4.50E-04
CMQ040C	166.8	62.3	-1.4	5.00E-05	4.50E-04
CML058C	315.8	117.9	-1.4	2.00E-04	1.46E-03
CMT228C	45.7	17.0	-1.4	5.00E-05	4.50E-04
CMR183C	364.4	135.9	-1.4	8.50E-04	4.68E-03
CMN171C	539.0	200.8	-1.4	1.00E-04	8.17E-04
CMS009C	297.3	110.7	-1.4	5.00E-05	4.50E-04
CMP019C	106.0	39.5	-1.4	5.00E-05	4.50E-04
CME050C	1349.2	501.6	-1.4	1.85E-03	8.64E-03
CML302C	218.8	81.3	-1.4	5.00E-05	4.50E-04
CMI107C	164.5	61.0	-1.4	5.00E-05	4.50E-04
CMJ132C	231.3	85.7	-1.4	5.00E-05	4.50E-04
CMO008C	289.6	107.2	-1.4	1.00E-04	8.17E-04
CMN113C	137.4	50.8	-1.4	5.00E-05	4.50E-04

continued on next page!

Table A.6 – continued from previous page

	FPKM values			Statistical cuffdiff values	
Gene ID	**RL(-)**	**RL (+)**	**$\log_2$ (fold change)**	**p value**	**q value**
CMR432C	43.1	15.9	-1.4	5.00E-05	4.50E-04
CMR375C	223.8	82.6	-1.4	1.00E-04	8.17E-04
CML081C	93.0	34.3	-1.4	1.00E-04	8.17E-04
CMT459C	300.4	110.7	-1.4	1.00E-04	8.17E-04
CMS335C	456.7	168.2	-1.4	8.50E-04	4.68E-03
CMT246C	361.2	132.8	-1.4	5.00E-05	4.50E-04
CMO219C	41.9	15.4	-1.4	5.00E-05	4.50E-04
CMJ157C	322.6	118.6	-1.4	5.00E-05	4.50E-04
CMP269C	122.5	45.0	-1.4	5.00E-05	4.50E-04
CMB099C	757.1	276.8	-1.5	5.00E-05	4.50E-04
CMI064C	216.1	78.9	-1.5	5.00E-05	4.50E-04
CMQ301C	1834.2	669.0	-1.5	2.10E-03	9.54E-03
CMN024C	48.5	17.7	-1.5	5.00E-05	4.50E-04
CMR200C	57.2	20.8	-1.5	5.00E-05	4.50E-04
CMK161C	254.5	92.6	-1.5	5.00E-05	4.50E-04
CMM026C	106.3	38.6	-1.5	5.00E-05	4.50E-04
CMK079C	45.4	16.5	-1.5	1.50E-03	7.33E-03
CMN313C	90.3	32.8	-1.5	5.00E-05	4.50E-04
CMI052C	46.2	16.8	-1.5	2.00E-04	1.46E-03
CMQ077C	118.1	42.9	-1.5	5.00E-05	4.50E-04
CMP022C	291.8	105.8	-1.5	5.00E-05	4.50E-04
CMS095C	491.3	178.0	-1.5	5.00E-05	4.50E-04
CMH246C	49.0	17.8	-1.5	5.00E-05	4.50E-04
CML319C	171.6	62.1	-1.5	5.00E-05	4.50E-04
CMM206C	69.7	25.2	-1.5	1.50E-04	1.15E-03
CMT444C	93.3	33.7	-1.5	5.00E-05	4.50E-04

continued on next page!

Table A.6 – continued from previous page

	FPKM values			Statistical cuffdiff values	
Gene ID	**RL(-)**	**RL (+)**	**$\log_2$ (fold change)**	**p value**	**q value**
CMB121C	443.8	160.4	-1.5	1.50E-04	1.15E-03
CMM093C	142.7	51.6	-1.5	5.00E-05	4.50E-04
CMI218C	157.2	56.7	-1.5	5.00E-05	4.50E-04
CMG099C	629.4	227.1	-1.5	1.50E-04	1.15E-03
CMP114C	73.7	26.6	-1.5	5.00E-05	4.50E-04
CMB141C	292.5	105.4	-1.5	5.00E-05	4.50E-04
CMP261C	372.7	134.2	-1.5	3.00E-04	2.04E-03
CME012C	273.0	98.2	-1.5	5.00E-05	4.50E-04
CMS438C	77.1	27.7	-1.5	5.00E-05	4.50E-04
CMQ272C	106.7	38.3	-1.5	5.00E-05	4.50E-04
CMT009C	415.5	148.7	-1.5	5.00E-05	4.50E-04
CMN151C	178.8	64.0	-1.5	5.00E-05	4.50E-04
CMO055C	346.4	123.7	-1.5	5.00E-05	4.50E-04
CMK163C	2474.4	883.3	-1.5	1.50E-04	1.15E-03
CMP331C	217.2	77.5	-1.5	5.00E-05	4.50E-04
CMM202C	137.9	49.2	-1.5	5.00E-05	4.50E-04
CMF040C	373.3	133.0	-1.5	5.00E-05	4.50E-04
CMK168C	254.5	90.7	-1.5	5.00E-05	4.50E-04
CMP254C	147.2	52.4	-1.5	5.00E-05	4.50E-04
CMH179C	44.6	15.9	-1.5	5.00E-05	4.50E-04
CMN163C	156.9	55.8	-1.5	5.00E-05	4.50E-04
CMS163C	2562.4	910.9	-1.5	1.65E-03	7.90E-03
CMR427C	142.7	50.5	-1.5	5.00E-05	4.50E-04
CMT462C	97.8	34.6	-1.5	5.00E-05	4.50E-04
CMM056C	154.8	54.7	-1.5	5.00E-05	4.50E-04
CMI244C	915.3	323.5	-1.5	5.00E-04	3.07E-03

continued on next page!

Table A.6 – continued from previous page

	FPKM values			Statistical cuffdiff values	
Gene ID	**RL(-)**	**RL (+)**	**$\log_2$ (fold change)**	**p value**	**q value**
CMR066C	339.9	119.9	-1.5	5.00E-05	4.50E-04
CMK211C	79.2	27.9	-1.5	5.00E-05	4.50E-04
CML300C	265.0	93.4	-1.5	5.00E-05	4.50E-04
CMN326C	561.5	197.6	-1.5	1.20E-03	6.17E-03
CMR019C	74.7	26.3	-1.5	5.00E-05	4.50E-04
CMT283C	202.8	71.2	-1.5	5.00E-05	4.50E-04
CMI198C	183.5	64.4	-1.5	1.50E-04	1.15E-03
CMO319C	348.4	122.2	-1.5	1.00E-04	8.17E-04
CMQ204C	91.1	31.9	-1.5	5.00E-05	4.50E-04
CMA087C	246.3	86.3	-1.5	5.00E-05	4.50E-04
CMM130C	309.8	108.5	-1.5	5.00E-05	4.50E-04
CMS275C	335.2	117.1	-1.5	5.00E-05	4.50E-04
CMP162C	205.1	71.6	-1.5	5.00E-05	4.50E-04
CMS302C	185.8	64.9	-1.5	5.00E-05	4.50E-04
CMT203C	237.8	83.0	-1.5	5.00E-05	4.50E-04
CMK242C	156.6	54.5	-1.5	5.00E-05	4.50E-04
CMT488C	131.4	45.7	-1.5	5.00E-05	4.50E-04
CMH164C	49.7	17.3	-1.5	5.00E-05	4.50E-04
CMI051C	118.3	41.0	-1.5	5.00E-05	4.50E-04
CMB097C	200.8	69.4	-1.5	5.00E-05	4.50E-04
CMN085C	229.0	79.1	-1.5	5.00E-05	4.50E-04
CMS375C	143.5	49.5	-1.5	5.00E-05	4.50E-04
CMR078C	28.1	9.7	-1.5	5.00E-05	4.50E-04
CMM236C	365.1	125.8	-1.5	5.00E-05	4.50E-04
CMF162C	175.0	60.3	-1.5	1.50E-04	1.15E-03
CMI092C	141.5	48.7	-1.5	5.00E-05	4.50E-04

continued on next page!

Table A.6 – continued from previous page

	FPKM values			Statistical cuffdiff values	
Gene ID	**RL(-)**	**RL (+)**	**$\log_2$ (fold change)**	**p value**	**q value**
CMS483C	163.9	56.3	-1.5	5.00E-05	4.50E-04
CMT094C	95.7	32.9	-1.5	5.00E-05	4.50E-04
CMQ195C	110.5	37.9	-1.5	5.00E-05	4.50E-04
CMQ038C	523.6	179.7	-1.5	5.00E-05	4.50E-04
CMQ260C	247.9	84.6	-1.6	1.50E-04	1.15E-03
CMK069C	190.8	65.1	-1.6	5.00E-05	4.50E-04
CMM184C	94.0	32.0	-1.6	1.00E-04	8.17E-04
CMT353C	42.2	14.4	-1.6	5.00E-05	4.50E-04
CMT443C	160.1	54.5	-1.6	5.00E-05	4.50E-04
CMR400C	208.7	70.9	-1.6	5.00E-05	4.50E-04
CMG177C	178.5	60.6	-1.6	5.00E-05	4.50E-04
CMM231C	121.0	40.9	-1.6	5.00E-05	4.50E-04
CMN273C	23.8	8.0	-1.6	5.00E-05	4.50E-04
CMO108C	531.2	179.4	-1.6	5.00E-05	4.50E-04
CMS358C	164.8	55.6	-1.6	1.00E-04	8.17E-04
CMS360C	33.1	11.2	-1.6	5.00E-05	4.50E-04
CMO255C	299.7	101.0	-1.6	1.00E-04	8.17E-04
CMM280C	403.8	135.9	-1.6	5.00E-05	4.50E-04
CMI013C	194.9	65.6	-1.6	5.00E-05	4.50E-04
CMC169C	145.5	48.9	-1.6	5.00E-05	4.50E-04
CMT363C	237.7	79.8	-1.6	5.00E-05	4.50E-04
CMJ049C	303.4	101.6	-1.6	5.00E-05	4.50E-04
CMS418C	811.3	271.7	-1.6	5.00E-05	4.50E-04
CME117C	196.4	65.8	-1.6	5.00E-05	4.50E-04
CMT622C	59.0	19.8	-1.6	5.00E-05	4.50E-04
CMH266C	109.7	36.6	-1.6	5.00E-05	4.50E-04

continued on next page!

Table A.6 – continued from previous page

	FPKM values			Statistical cuffdiff values	
Gene ID	**RL(-)**	**RL (+)**	**$\log_2$ (fold change)**	**p value**	**q value**
CMH109C	40.1	13.3	-1.6	5.00E-05	4.50E-04
CME138C	168.9	56.1	-1.6	5.00E-05	4.50E-04
CMP246C	95.5	31.7	-1.6	5.00E-05	4.50E-04
CML152C	121.9	40.4	-1.6	5.00E-05	4.50E-04
CMQ081C	209.4	69.3	-1.6	5.00E-05	4.50E-04
CMP343C	236.4	78.1	-1.6	5.00E-05	4.50E-04
CMO173C	227.6	75.1	-1.6	5.00E-05	4.50E-04
CMT405C	176.8	58.2	-1.6	5.00E-05	4.50E-04
CMO096C	74.7	24.5	-1.6	5.00E-05	4.50E-04
CME108C	464.5	152.1	-1.6	2.50E-04	1.75E-03
CMR112C	212.7	69.6	-1.6	5.00E-05	4.50E-04
CMT074C	98.5	32.2	-1.6	2.00E-04	1.46E-03
CMF101C	723.2	236.4	-1.6	4.50E-04	2.83E-03
CMH168C	33.1	10.8	-1.6	5.00E-05	4.50E-04
CMQ079C	320.6	104.7	-1.6	5.00E-05	4.50E-04
CMA118C	102.2	33.3	-1.6	5.00E-05	4.50E-04
CMR454C	243.8	79.5	-1.6	5.00E-05	4.50E-04
CMG008C	1136.4	370.5	-1.6	5.00E-05	4.50E-04
CMO352C	97.5	31.7	-1.6	5.00E-05	4.50E-04
CMP160C	188.0	61.1	-1.6	5.00E-05	4.50E-04
CMH229C	69.0	22.4	-1.6	5.00E-05	4.50E-04
CML025C	115.7	37.6	-1.6	5.00E-05	4.50E-04
CMR124C	511.4	165.9	-1.6	5.00E-05	4.50E-04
CMR374C	122.0	39.5	-1.6	5.00E-05	4.50E-04
CMR049C	102.9	33.3	-1.6	5.00E-05	4.50E-04
CMD151C	139.8	45.2	-1.6	5.00E-05	4.50E-04

continued on next page!

Table A.6 – continued from previous page

	FPKM values			Statistical cuffdiff values	
Gene ID	**RL(-)**	**RL (+)**	**$\log_2$ (fold change)**	**p value**	**q value**
CMI125C	76.4	24.7	-1.6	5.00E-05	4.50E-04
CME090C	154.1	49.8	-1.6	5.00E-05	4.50E-04
CMT559C	231.4	74.7	-1.6	5.00E-05	4.50E-04
CMA010C	110.0	35.5	-1.6	5.00E-05	4.50E-04
CML326C	283.0	91.0	-1.6	5.00E-05	4.50E-04
CMT120C	287.1	92.2	-1.6	5.00E-05	4.50E-04
CMS430C	733.9	233.9	-1.6	1.50E-04	1.15E-03
CMJ133C	398.9	127.1	-1.7	5.00E-05	4.50E-04
CMS371C	555.4	176.2	-1.7	5.00E-05	4.50E-04
CMR417C	226.4	71.8	-1.7	5.00E-05	4.50E-04
CMR077C	157.7	50.0	-1.7	5.00E-05	4.50E-04
CMS437C	437.0	138.5	-1.7	5.00E-05	4.50E-04
CMI276C	81.7	25.9	-1.7	5.00E-05	4.50E-04
CMS206C	119.5	37.8	-1.7	5.00E-05	4.50E-04
CMP015C	164.4	51.8	-1.7	5.00E-05	4.50E-04
CMR487C	43.1	13.6	-1.7	5.00E-05	4.50E-04
CMT415C	218.5	68.8	-1.7	5.00E-05	4.50E-04
CMI014C	106.7	33.6	-1.7	5.00E-05	4.50E-04
CMT088C	176.8	55.6	-1.7	5.00E-05	4.50E-04
CMP176C	123.9	38.9	-1.7	5.00E-05	4.50E-04
CMI119C	145.1	45.6	-1.7	5.00E-05	4.50E-04
CMJ215C	156.4	49.0	-1.7	5.00E-05	4.50E-04
CMM316C	141.4	44.3	-1.7	5.00E-05	4.50E-04
CMS056C	193.9	60.6	-1.7	5.00E-05	4.50E-04
CMR248C	130.8	40.8	-1.7	5.00E-05	4.50E-04
CMF116C	240.7	75.0	-1.7	5.00E-05	4.50E-04

continued on next page!

Table A.6 – continued from previous page

	FPKM values			Statistical cuffdiff values	
Gene ID	**RL(-)**	**RL (+)**	**$\log_2$ (fold change)**	**p value**	**q value**
CMT311C	36.6	11.4	-1.7	1.00E-04	8.17E-04
CMD117C	110.9	34.4	-1.7	5.00E-05	4.50E-04
CMK029C	272.8	84.4	-1.7	7.50E-04	4.24E-03
CMQ426C	27.8	8.6	-1.7	1.50E-04	1.15E-03
CMJ034C	987.4	304.9	-1.7	3.00E-04	2.04E-03
CME029C	74.5	22.9	-1.7	5.00E-05	4.50E-04
CMO015C	163.3	50.2	-1.7	5.00E-05	4.50E-04
CMN317C	81.5	25.0	-1.7	5.00E-05	4.50E-04
CMD005C	77.7	23.8	-1.7	5.00E-05	4.50E-04
CMF159C	152.4	46.6	-1.7	5.00E-05	4.50E-04
CMD092C	272.6	83.3	-1.7	5.00E-05	4.50E-04
CMS495C	158.4	48.1	-1.7	5.00E-05	4.50E-04
CMF026C	217.4	66.0	-1.7	5.00E-05	4.50E-04
CMR356C	142.1	43.0	-1.7	5.00E-05	4.50E-04
CMN123C	74.8	22.6	-1.7	5.00E-05	4.50E-04
CMH069C	312.4	93.7	-1.7	5.00E-05	4.50E-04
CML168C	147.2	44.1	-1.7	5.00E-05	4.50E-04
CMR355C	106.3	31.7	-1.7	5.00E-05	4.50E-04
CMJ135C	208.7	62.2	-1.7	5.00E-05	4.50E-04
CMG191C	315.3	93.9	-1.7	5.00E-05	4.50E-04
CMI018C	161.3	47.8	-1.8	5.00E-05	4.50E-04
CMT452C	247.3	73.2	-1.8	5.00E-05	4.50E-04
CME022C	50.9	15.0	-1.8	5.00E-05	4.50E-04
CMO355C	62.2	18.4	-1.8	5.00E-05	4.50E-04
CMI026C	294.8	87.1	-1.8	5.00E-05	4.50E-04
CML097C	99.6	29.4	-1.8	5.00E-05	4.50E-04

continued on next page!

Table A.6 – continued from previous page

	FPKM values			Statistical cuffdiff values	
Gene ID	**RL(-)**	**RL (+)**	**$\log_2$ (fold change)**	**p value**	**q value**
CMQ380C	75.8	22.3	-1.8	5.00E-05	4.50E-04
CMI136C	488.2	143.8	-1.8	5.00E-05	4.50E-04
CMT312C	389.4	114.3	-1.8	5.00E-05	4.50E-04
CMN160C	80.2	23.5	-1.8	5.00E-05	4.50E-04
CMK183C	193.3	56.6	-1.8	5.00E-05	4.50E-04
CMF155C	120.4	35.1	-1.8	5.00E-05	4.50E-04
CMN146C	957.9	279.1	-1.8	5.00E-05	4.50E-04
CML146C	295.9	86.0	-1.8	5.00E-05	4.50E-04
CMT494C	1080.6	313.8	-1.8	5.00E-05	4.50E-04
CMS036C	140.1	40.4	-1.8	5.00E-05	4.50E-04
CMD135C	934.6	269.3	-1.8	2.00E-04	1.46E-03
CMP358C	33.5	9.6	-1.8	1.00E-04	8.17E-04
CMS472C	43.2	12.4	-1.8	5.00E-05	4.50E-04
CMS403C	195.9	56.1	-1.8	5.00E-05	4.50E-04